Styles of continental margin sedimentation: comparing glaciated and non-glaciated slope systems using case studies on the southeast Canadian and northern Argentine and Uruguay continental slope

Dissertation
zur Erlangung des Doktorgrades der Naturwissenschaften
am Fachbereich Geowissenschaften
der Universität Bremen

vorgelegt von
Tammo Jan Huppertz
Bremen, April 2011

Gutachter:
Prof. Dr. Rüdiger Henrich
Prof. Dr. David Piper

0. Abstract

Continental slope sedimentation is in generally highly driven by hinterland climate and the oceanographic setting along a margin. This study compares slope architecture of the glaciated Scotian Slope on the southeast Canadian continental margin to the non-glaciated northern Argentine and Uruguay continental slope, where sedimentation is driven by the complex oceanic circulation due to the Brazil Malvinas Confluence zone and the fluvial discharge of the La Plata Rivers within the Rio de la Plata estuary.

On the Scotian Slope, a new slope-wide seismic stratigraphy was developed to identify patterns of slope sedimentation. The Early Quaternary sequence (older than 500 ka) is characterized by few large mass transport deposits (MTDs) and deposition occurs at the lower slope. The mode of deposition changes greatly towards the younger sequence, when different types of MTDs characterize the slope system. This observation could be used to define 8 different morpho-sedimentary slope zones alongslope. Each zone is characterized by the interaction of hemipelagic sedimentation with different types of MTDs.

During times in the Mid- to Late Quaternary, when ice sheets terminated at the shelf break, mass wasting is much more voluminous and affects larger areas on the slope compared to the Early Quaternary sedimentary sequence. Additionally, each zone is characterized by different types of MTDs having different volumes, erosive character or changing nature in pinch-out character. The change in character and frequency of MTDs within a section could be used to improve the understanding of ice sheet dynamics on the shelf. The dynamics of shelf-break ice sheets have a severe impact on styles of slope sedimentation, e.g. the drainage pathways of meltwater may be linked to frequency of slope canyons or fast flowing ice streams supply much greater sediment volumes resulting in more frequent failures affecting larger areas.

The Argentine Continental Slope is characterized by several marine terraces, of which the Ewing Terrace in 1200 m water depth is the most pronounced one. Using core and to a limited extent Parasound data, processes of slope deposition along the northern Argentine and Uruguay Slope could be defined and used to understand variations in slope deposition over the last few glacial cycles. On a regional scale, the northern Argentine and Uruguay continental slope changes styles of sedimentation in the area of the Rio de la Plata estuary at ~37°S, when slope terraces, typical for the Argentine Slope, terminate abruptly northwards. This was used to classify the slope into 5 different zones: each zone is characterized by specific slope processes driven by either oceanic circulation or gravity processes. To the south of 37°S, slope deposition is driven by oceanic circulation and to a lesser extent gravity driven. Shelf break overspilling supplies at times sediment to the Ewing Terrace. Similarly, at times sediment is exported downslope to the lower slope and the abyssal plain, termed Argentine Basin, which is generally characterized by contour current processes from the

Antarctic Bottom Water. To the north of 37°S, turbidites and debris flows characterize slope deposition, whereas the lowermost slope is either constructed by turbidite lobes or possibly by contourite sheets. Mode of deposition changes on small spatial scales (km-scales) to the north of 37°S rapidly, highly dependent on core positions in relationship to canyons and other slope depressions.

In a more local study, the sediments on the northernmost Ewing Terrace could be dated and characterized sedimentologically using a range of methods including x-radiographs and grain size data. Age control, given by $\delta^{18}O$ data, suggests relatively low sedimentation rates: 5-6 m long sediment cores reach back into Marine Isotope Stage 3. The slope system is generally sediment-starved: during intense Pleistocene storm events, sediments may be supplied to the terrace as wave-supported gravity flows, which are then reworked to different extents by the Antarctic-sourced ocean currents.

By comparing the two climatically different slope systems, the Scotian and northern Argentine and Uruguay Slope, more general ideas of continental slope deposition could be achieved. Glaciations have an intense impact on slope systems compared to non-glaciated margins and compared to glaciated slopes during pre-glacial times in the Early Quaternary. Furthermore, the process and overall dynamics are very similar in glacial and non-glacial slope systems, as during glacial stages increased mass wasting occurs compared to the interglacial stages. The alongslope variability of sedimentation can be easily achieved by slope system zoning, where each zone is characterized by specific sedimentary and seismic character, which is directly linked to certain processes of slope deposition.

0.1 Zusammenfassung

Im Allgemeinen ist die Sedimentation am Kontinentalhang stark durch klimatische Variationen im Hinterland und die ozeanographische Zirkulation der Region gesteuert. Diese Dissertation vergleicht die Architektur von zwei verschiedenen Kontinentalhängen während des Quatärs. Diese sind der ehemals vergletscherte Scotian Slope am südöstlichen Kontinentalhang von Kanada und der unvergletscherte Kontinentalhang vor Nord-Argentinien und Uruguay, wo Sedimentationsprozesse stark durch die komplexe ozeanische Zirkulation der Brasil-Malvinas Konfluenzzone und den fluvialen Export der La Plata Flüsse in der Rio de la Plata-Mündung beeinflusst werden.

Am Scotian Slope wurde eine neue, hangweite seismische Stratigraphie entwickelt, um Variationen von Hangsedimentation zu identifizieren. Die Früh-Quartären Sequenzen (älter als 500 000 Jahre) schließen nur wenige große Hanginstabilitäten (Massentransport Ablagerungen: in Englischen mit MTDs abgekürzt) ein; die Ablagerung erfolgte zumeist am unteren Hang. Jüngere sedimentäre Sequenzen zeigen sigifikante Veränderungen in der Sedimentation, da zu dieser Zeit verschiedene Typen von MTDs das Hangsystem charakterisieren. Diese Beobachtung konnte verwendet werden, um 8 verschiedene morpho-sedimentäre Hangzonen entlang des Kontinentalhanges zu definieren. Jede Zone ist durch das Zusammenspiel von hemipelagischer Sedimentation mit verschiedenen Typen von MTDs gekennzeichnet.

Im mittleren bis späten Quartär, als Eisschilde an der Schelfkante terminierten, werden die Massenbewegungen am Hang wesentlich voluminöser und beeinflussen größere Flächen am Hang im Vergleich zu den Früh-Quartären sedimentären Sequenzen. Darüber hinaus ist jede Zone durch verschiedene Typen von MTDs gekennzeichnet. Diese Unterscheide zeigen sich in deren basalen erosiven Charakter oder deren Art der Termination zum Beispiel durch sogenannten „pinch-out“ Charakter, also die Art und Weise wie der Schuttstrom (Schlammgeröllstrom) ausläuft. Die Veränderung der Art und der Häufigkeit von MTDs innerhalb jeder Hangzone konnte benutzt werden, um das Verständnis der Dynamik von Eissschilden auf dem Schelf signifikant zu verbessern. Die Dynamik der Eisschilde an der Schelfkante hat gravierende Auswirkungen auf den Typus von Hangsedimentation, beispielsweise sind Entwässerungswege von Schmelzwässern bestimmend für die Anlage von Schluchtstrukturen (Canyons und kleinere Kanäle) am Hang. Zudem ist die Schuttfracht und der Eintrag von unsortiertem Schutt in Regionen, gekennzeichnet durch schnell fließendes Eis (Eisströme), wesentlich höher als im Vergleich zu Regionen entlang der Schelfkante, die nicht durch schnell fließendes Eis gekennzeichnet sind.

Der Argentinische Kontinentalhang ist durch mehrere marine Terrassen gekennzeichnet. Die Ewing Terrasse in 1200 m Wassertiefe ist die am besten ausgeprägteste. Sedimentdaten von Schwerelot Sedimentkernen und einige wenige

Parasound Schnitte wurden verwendet, um Prozesse der Hangsedimentation entlang des nördlichen Argentinischen und Uruguayanischen Hanges zu identifizieren und dessen Dynamik zu kennzeichnen. Diese Ergebnisse konnten benutzt werden, um Variationen in den Sedimentationsmustern über einige spätquatäre Eiszeitzyklen zu rekonstruireren. Regional verändert sich der Stil der Sedimentation am nördlichen Argentinischen und Uruguayanischen Kontinentalhang im Bereich der Rio de la Plata-Mündung bei etwa 37° S, wo die Hangterrassen, die typisch für den argentinischen Hang sind, abrupt nach Norden hin terminieren. Diese Beobachtung konnte verwendet werden, um den Kontinentalhang in 5 verschiedene morphologische und sedimentäre Zonen einzuteilen. Jede Zone ist durch spezifische Hangneigungen und Ablagerungsprozesse, die entweder durch ozeanische Zirkulation oder hangabwärts gerichtete Prozesse gesteuert werden, charakterisiert. Südlich von 37° S wird die Hangsedimentation von der ozeanographischen Zirkulation und in geringerem Maße durch gravitative Prozesse gesteuert. Sediment, welches über die Schelfkante transportiert wird, liefert zeitweise Material auf die Ewing Terrasse. Zu bestimmten Zeiten kann es auch zum Sedimenteintrag von der Terasse auf den unteren Hang kommen. Solches Material kann dann sogar bis in die Tiefseeebene transportiert werden. Sedimentation ist in diesem Bereich meist durch Kontourit-Aktivität, gesteuert durch das Antarktischen Bodenwasser, gekennzeichnet. Nördlich von 37° S charakterisieren Turbidite und Schlammgeröllströme die Sedimentation, während der unterste Teil des Hanges entweder durch Turbiditsande oder durch Kontouritloben geformt wird. Das Ablagerungsmilieu ändert sich rasch auf kleinen räumlichen Skalen (km-Skalen) und ist stark abhängig von der Lage zu Hangschluchten und anderen Hangsenken.

In einer Lokalstudie auf dem nördlichsten Teil der Ewing Terrasse konnten die dort liegenden Sedimente datiert und sedimentologisch charakterisiert werden, unter anderem durch Radiographieaufnahmen und durch Daten zur Korngrößenbestimmung. Die Altersmodelle der untersuchten Sedimentkerne beruhen auf $\delta^{18}O$ Isotopen Daten von benthischen Foraminiferen. Es weden für Kontouritsedimente vergleichsweise niedrige Sedimentationsraten registriert. 5-6 m lange Kerne reichen zurück bis in das Marine Isotopenstadium 3. Daher ist im Allgemeinen die Terrasse durch geringe Sedimentationsraten gekennzeichnet. Allerdings wird während außergewöhnlicher pleistozäner Sturmereignisse pulsartig Sediment auf die Terrasse durch Wellen-induzierte gravitative Sedimentströme geschüttet, das anschließend durch die Antarktischen Ozeanischen Strömungen stark aufgearbeitet wird.

Anhand des Vergleichs der beiden klimatisch recht unterschiedlichen Hangsysteme, des Scotian Slopes und des nördlichen Argentinischen und Uruguayanischen Hanges, konnten mehrere allgemein gültige Modelle für Massentransporte an Kontinentalhängen erarbeitet werden. Kontinentalhänge, welche stark durch die Ausbreitung von Eisschilden auf dem Schelf beeinflusst werden, zeigen generell häufiger und voluminösere Hangrutschungskörper auf, als solche, die nicht vergletschert gewesen sind. Für die von wesentlich geringeren Eisausdehnungen auf den Schelfen beeinflussten Schelf/Kontinentalhang Konfigurationen der frühen Quartärs ergibt sich ein intermediäres Bild, mit Phänomenen, die zwischen den ober erwähnten liegen. Dennoch sind die Prozesse und die allgemeine Dynamik vergletscherter und eisfreier Kontinentalhängen recht ähnlich. Beispielsweise treten in beiden Typen von Hängen während der Kaltzeiten vergleichsweise vermehrt Massentransporte auf und es wird eine vermehrte Turbiditaktivität beobachtet. Anhand der Variabilität von Sedimentationsprozessen am Hang können verscheidene characteristische Zonen der Sedimentdynamik ausgewiesen werden. Jede dieser Zonen ist durch spezielle Sedimentationsphänomene charakterisiert, zum Beispiel duch das Volumen oder die Typen von MTDs, durch die Frequenz und die Ausbreitung von Turbiditen oder durch vorherrschende hemipelagische Sedimentation.

Contents

1. Introduction

The style of Late Quaternary sedimentation on mid latitude glaciated and un-glaciated continental margins is extremely variable. Controls on sedimentation are mainly governed by (1) sediment availability, (2) shelf and slope morphology and geometry, (3) the oceanic circulation pattern and (4) slope angle and depth of shelf break. These four factors are further influenced by the local climate setting and related sea level drops during Pleistocene glaciations.

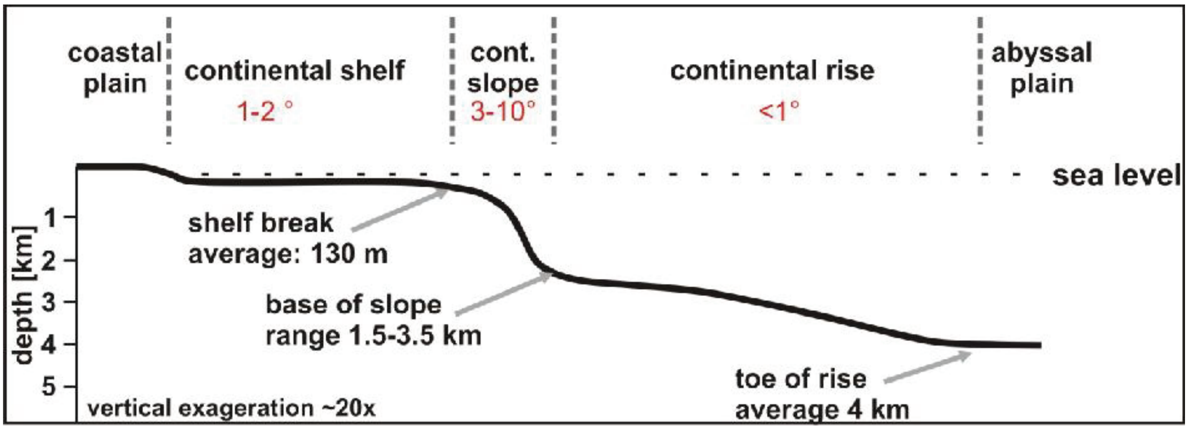

Fig. 1.1: Continental margin morphology showing terminology used in this study (after Brink et al., 1992), red colored numbers indicate general dipping angles for the shelf slope and rise areas.

Continental margins can generally be divided into the shallow shelf area (water depth generally ~100 m) and slope area, separated by the shelf break (Fig. 1.1). Today, the average depth of the shelf break occurs at ~130 m water depth (Gross, 1972). Nevertheless, this is only the case during sea level highstands as observed during the Holocene and marine isotope stage (MIS) 5 (Fig. 1.2). During most other glacial stages since the mid-Quaternary (MIS 12) (Maslin and Ridgwell, 2005), sea level was much lower than today (up to 120 m) due to ice sheet build-up on continental Europe, North America, northern Asia and Antarctica (Clark and Mix, 2002). This resulted in a seaward migration of the coastline and thus the water depth of the shelf break was shallower (Schaaf, 1996; Nittrouer et al., 2007; Piper and Normark, 2009).

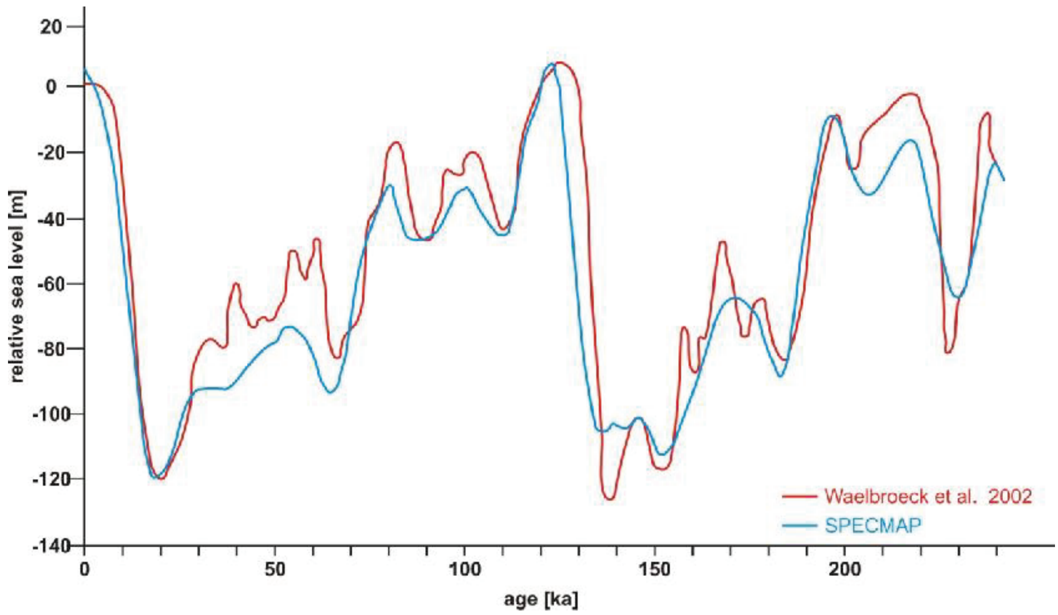

Fig: 1.2: Sea level changes over the last 250 ka [kilo years] (modified after Waelbroeck et al., 2002 as cited in; Antonioli et al., 2004)

Shelf areas are generally characterized by low morphological features and low slope angles (1-2°, Fig. 1.1) (Schaaf, 1996). At the shelf break, seabed slope angles change significantly (up to 10°, Fig. 1.1) towards the uppermost slope. This is the critical interface along all continental margins (Vanney and Stanley, 1983), where the upper slope starts. The overall slope morphology is generally concave (Pratson and Haxby, 1996) and has its steepest area just below the shelf break, where local slope angle be as high as 15° - in canyon areas much higher angles are possible (Fig. 1.3) (Prior and Doyle, 1985; Schlager and Camber, 1986; Adams and Schlager, 2000; Popescu et al., 2004).

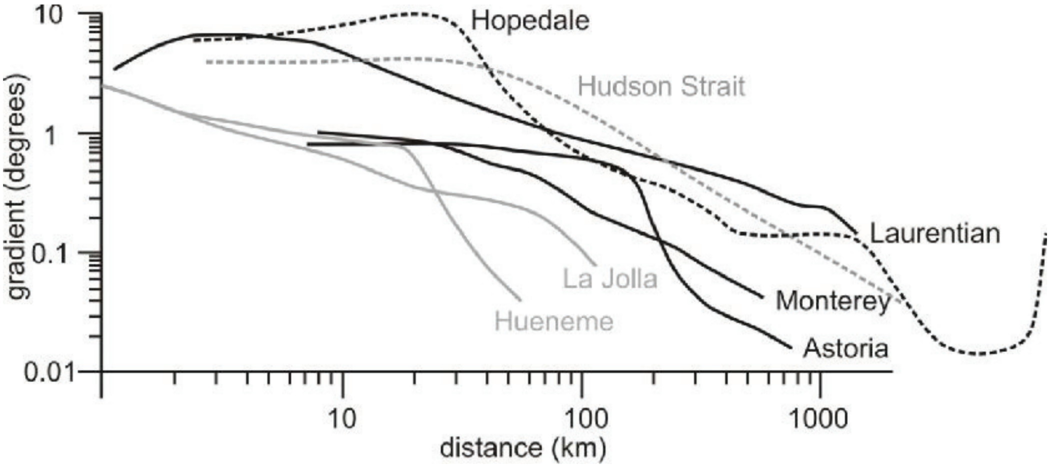

Fig. 1.3: Slope angles of various fan systems on glaciated and non-glaciated continental margins (modified after Piper and Normark, 2009)

Slope areas can be grouped morphologically into areas often dissected by canyons (Smith, 2004; Jenner et al., 2007; Pratson et al., 2007; Piper and Normark, 2009) and areas with few sediment conduits as canyons and smaller scale gullies (also termed the open slope) (Campbell, 2000; Piper and Normark, 2001; Puig et al., 2003). Sediment is transported to both areas, but in canyon areas, the sediment crossing the shelf break is trapped within canyon heads just below the shelf break, where it transforms during times of triggering events into turbidity currents within the canyons (Piper and Normark, 2009), whereas in areas away from canyons, upper slope sands are formed and may be preserved and winnowed over longer time scales (Mulder and Moran, 1995; Viana and Faugères, 1998; Rodriguez and Anderson, 2004; Jenner et al., 2007).

1.1. General styles of sedimentation on continental slopes

Various types of sediment transfer processes have been identified on continental slopes. Generally, two main groups can be established: (1) processes driven by gravitation and (2) processes driven by currents following the bathymetry (contour currents). Both processes can be observed on glaciated and non-glaciated continental margins (Laberg and Vorren, 1995; Piper and Normark, 2001; Bryn et al., 2005a; Laberg and Andreassen, 2007; Piper et al., 2007; Huppertz and Piper, 2010). The processes leading to similarly appearing deposits may vary on glaciated and non-glaciated continental margins: glaciated margins show due to the presence of ice sheets generally higher rates of erosion and are characterized by the frequent dumping of poorly sorted sediment from ice sheets with different flow dynamics and/or from melting icebergs resulting in plume sedimentation as tidewater glacier fronts (Fig. 1.4) (Anderson et al., 1980; Vorren et al., 1998; Taylor et al., 2000; Piper and Normark, 2001; Dowdeswell et al., 2004; Piper, 2005), compared to the non-glaciated margins, where frequently lower sediment flux to the shelf break decreases overall slope dynamics (Syvitski et al., 1996a). Nevertheless, at large river mouths, e.g. at the Amazon (Piper et al., 1997; Piper and Normark, 2001) or the Mississippi slope (Reynolds, 2000; Wright and Friedrichs, 2006), similarly high sedimentation rates can be reached during flooding events with high fluvial sediment discharge (Mulder et al., 2003). Furthermore, when studying slope processes, the shelf environment cannot be ignored, especially when taking times of sea level lowstands during glaciations into account (Schaaf, 1996), which changes the local oceanographic and geomorphological setting completely.

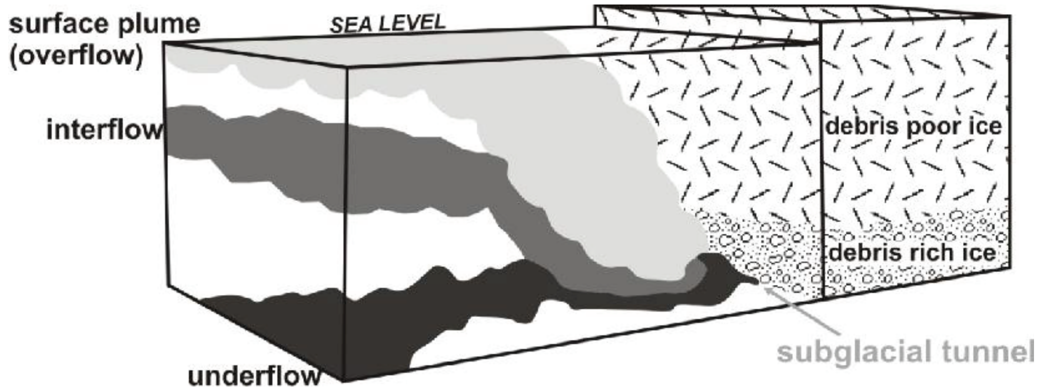

Fig. 1.4: Different types of sediment laden plumes and their generation in a glacial setting, similarly these processes work seawards of river mouths (after Powell and Molnia, 1989; Lemmen, 1990; Hesse et al., 1999)

1.1.1. Styles of sedimentation on glaciated continental slopes

Glaciated continental margins are characterized by the huge sediment supply from hinterland ice sheet (Taylor et al., 2002; Piper, 2005). Quaternary type examples are the eastern Canadian Margin (Piper, 2005), the Norwegian-Barents Sea Margin (Henrich et al., 1989, 1995; Vorren and Laberg, 1997; Solheim et al., 1998; Taylor et al., 2002), the Greenland Margin (Solheim et al., 1998; Vorren et al., 1998) or the margin surrounding Antarctica (Domack et al., 1999; Dowdeswell et al., 2004). The ice sheet configurations on the shelf and at the shelf break results in areas affected differently by the ice sheet dynamics:

(1) ***Stagnant ice sheets*** may result in the formation of large glacial marine till deposits and little basal erosion occurs below the ice sheet. These till tongues are typically observed on the upper slope (King and Fader, 1986; King, 1993). The overall slope is characterized by well-laminated plume sediment fallout from ice sheet related plumes (**Fig. 1.4**). Plumes are generated by influx of sediment-laden fresh water from glaciers. Different types of plumes can be distinguished: overflow-, interflow or underflow turbid plumes (**Fig. 1.4**). All three types may generate small-scale seabed failures resulting in turbidity currents (Powell and Molnia, 1989; Lemmen, 1990; Hesse et al., 1999), or lead to very high sedimentation rates (Piper et al., 2007). Nevertheless, their erosive character is minor compared to areas of fast flowing ice. At the seawards side of till tongues (**Fig. 1.5**), small debris flows can be generated by the flow behavior of the till and its transformation to debris flows (Mosher et al., 2004; Piper, 2005). This is highly dependent on the slope angle and the dynamics of till tongue deposition.

(2) ***Slow flowing ice sheets*** with basal erosion result in few small slope failures. Some of these smaller failures may be redirected into canyon structures starting in mid slope areas (Pratson and Coakley, 1996; Pratson et al., 2007). Such canyons starting at mid-slope can be created by a range of processes, including erosional potential of sediment gravity flows (Pratson et al., 1994), large-scale slumping events (Dingle and

Robson, 1985), or along deeper-rooted weak structures as fault systems (Shepard, 1981). Repeated retrogressive and sidewall failures deepens such morphological structures (Pratson and Coakley, 1996; Piper and Normark, 2009). Canyon heads are filled in by sand and, due to various processes including sediment over-steepening. Formation of elevated pore pressure gradients or sea level changes related to Pleistocene glaciations (Piper et al., 2003; Campbell et al., 2004; Huppertz and Piper, 2010) can lead to failure generating turbidity currents within the canyons. Therefore, in these areas seawards of slow flowing ice, upper slope erosion is small and areas between canyons usually show a continuous stratigraphic record (Campbell, 2000). Nevertheless, feeding of slope canyons may result in high canyon activity with stacked mass transport deposits and sandy or muddy turbidite beds on canyon floors. The canyon activity may further trigger wall failures (Sultan et al., 2004; Sultan et al., 2007). These flows bypass most of the canyons and deposit their bed load only on the rise and abyssal plain (Piper and Hundert, 2002).

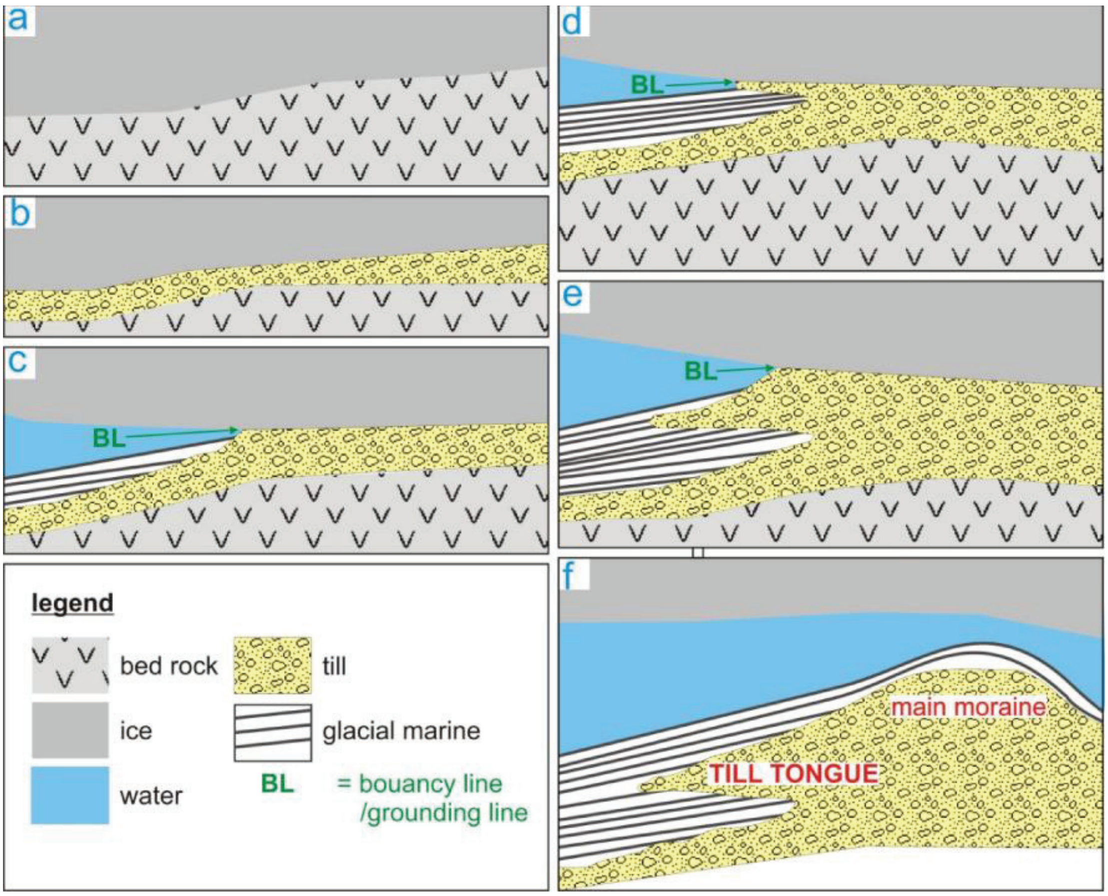

Fig. 1.5: Till tongue formation: (a) ice sheet over bed rock/ shelf area, (b) development of basal till, (c) floating ice sheet with glacial-marine sedimentation, (d) seaward movement of grounding line, (e) retreat of grounding line and deposition of glacial marine sediments over till tongue, (f) total ice shelf development (after King and Fader, 1986; King et al., 1991).

Seaward of trough mouth fans (TMFs), little stratigraphic record is preserved due to the high sediment supply by (3) ***fast flowing ice*** (Vorren and Laberg, 1997; Piper, 2001). The seabed is characterized by various types of mass transport deposits and turbidite beds. The most common indicator for high impact of ice sheets on the slope are glacigenic debris flows (King et al., 1998) initiated directly by the adjacent ice sheet.

In all three areas, with (1) stagnant ice sheets, (2) slow flowing ice sheets and (3) fast flowing ice streams, random sediment failures may additionally be induced by (i) high sediment supply resulting in over-steepening, (ii) retrogressive failures, (iii) sediment failures by icebergs scouring sea bed or dumping large amounts of poorly sorted sediments, and (iv) rare passive margin seismicity especially related to ice sheet dynamics (Normark and Piper, 1991; Piper et al., 1999; Piper, 2005; Huppertz, 2007; Niedoroda et al., 2007).

Sediments which are distal to ice sheets still show the glacial influence. Such glaciomarine sedimentation is frequently characterized by well-laminated plume sediments with drop stones of various size throughout (Hesse et al., 1999). In the Norwegian-Greenland Sea, the sudden collapse of the ice sheet close to the shelf break with extensive meltwater fronts, is manifested by an extensive release of glacial-marine debris from armadas of drifting icebergs, resulting in the deposition of glacial-marine iceberg deposits, e.g. diamictons, which may be traced far offshore into the basin and abyssal plain (Henrich et al., 1989, 1991, 1995). Such ice rafted debris originates from icebergs transported to the area by ocean currents (Dowdeswell and Murray, 1990; Syvitski et al., 1996b; Matsumoto, 1997). Over longer time spans such material may be redistributed by turbidity currents and slumping events depending highly on morphology (Syvitski et al., 1996b).

Additionally, plume sedimentation may affect areas several 10s of kilometers from the source when generating hyperpycnal flows (Piper et al., 2011) which may still show erosive potential in distal settings (Piper et al., 2011). This is especially true when the ice sheet does not terminate at the shelf break but in mid-shelf positions. In such a setting meltwater crosses the outer shelf first (Huppertz and Piper, 2009).

The preserved long-term sedimentary record (on a Quaternary scale) on glacial slope systems remains due to erosion mostly incomplete as most of the supplied sediment is eventually eroded and deposited only on the lower rise or abyssal plain forming large debris lobes (Piper and Hundert, 2002; Taylor et al., 2002; Piper and Ingram, 2003).

1.1.2. Styles of sedimentation on non-glaciated continental slopes

Un-glaciated continental margins are margins where calving ice sheets have never been present. Nevertheless, glaciations have imprinted on these margins as well by changing climate in the hinterland and sea level at the margins (Nittrouer et al., 2007). Well studied type examples could be the California (Nittrouer et al., 2007) and

New Jersey continental margin (Nittrouer et al., 2007), the New Zealand margin (Pierson, 1981; Friedrichs, 2004; Rose and Kuehl, 2010) or the Brazilian margin (Piper et al., 1997; Viana and Faugères, 1998; Viana et al., 1998a). Most of the sediment present on these margins is supplied by fluvial systems and continental runoff, which may vary over glacial (and interglacial) cycles when climate changed in the hinterland (Mulder and Syvitski, 1995).

Large submarine fans (e.g. Nile Fan (Ducassou et al., 2008), Amazon Fan (Piper and Deptuck, 1997; Piper et al., 1997; Piper and Normark, 2001) or Congo Fan (Coward et al., 1999; Vittori et al., 2000)) are constructed seawards of several major river mouths. Some of these fan systems (e.g. the Congo, Nile and Amazon fan) are found due to margin morphology in deep water and are mainly constructed by mass transport deposits and sandy or muddy turbidity current deposits (Loncke et al., 2009; Migeon et al., 2010). Other fan systems, which are in areas of e.g. broad shelves, may be subject to wave-induced reworking (Prior et al., 1979; Hart et al., 1992), especially during lowered sea level in the Pleistocene due to a seaward shift of the coastline (Schaaf, 1996; Blum and Törnqvist, 2000). The sediment from the fan front fails and is transported to the lower slope and rise (Piper and Normark, 2001).

Seawards of large rivers with high sediment bed load, hyperpycnal flows are initiated by highly sediment laden fresh water plumes (Mulder and Syvitski, 1995). The influx of the fresh water forms a freshwater plume similar as in the glacial setting offshore ice sheets (Fig. 1.4) inducing seabed erosion. When these sediment-laden plumes reach the shelf break (Mulder et al., 2001), they can initiate turbidity currents or lead to other types of seabed failure (Mulder et al., 2003; Ducassou et al., 2008).

Storm events can also result in sediment-laden water, which can travel across large parts of the shelf (Traykovski et al., 2000) and possibly reach the shelf break (Wright and Friedrichs, 2006). Such flows are very efficient to transport fine-grainsed sediment (mostly muds) to the upper slope. Additionally, turbidity within the water column may result in hyperpycnal flows which are capable of failures (Mulder et al., 2003).

On non-glaciated continental margins, slope sediment failures are most commonly initiated by hyperpycnal flows (Mulder et al., 2003), storm event reworking (Héquette and Hill, 1995; Héquette et al., 2001), rare passive margin seismicity (Husebyea and Mäntyniemib, 2005) or gas hydrate release (Maslin et al., 2004).

Similar to the setting on glaciated slopes, slope instabilities (e.g. turbidity current activity) are common in areas where gullies and canyon structures are present (Henrich et al., 2010), whereas away from such conduits on the open slope, fewer failures are observed but may develop huge mass flow deposits (slides, debris flows) at certain periods (Henrich et al., 2008, Förster et al. 2010).

1.2. Processes and products: sediment movement and deposition on shelves and slopes

Sedimentary models display simplified-idealistic sedimentary sequences resulting from end-member depositional processes. Such sedimentary models are generally considered dynamic, meaning that improvements can be made when new structures are repeatedly observed by ongoing research activities. Additionally, such sedimentary models have been applied globally on a huge variety of deposits in various continental margin systems. Furthermore, each facies model not only envisions a specific depositional process but also suggests a certain environment. As an example, the Bouma sequence (Bouma, 1962) is formed by low density turbidity currents creating a sequence of normal graded units with small and large scale cross bedding and implies a turbulent environment during deposition and supply of source material covering a wide grain size spectrum (clay to coarse sand).

In addition, there are facies models which describe shelf processes, e.g. the tempestite facies model (Einsele and Seilacher, 1991; Einsele, 1996) or the hyperpycnal sequence (Mulder et al., 2003), and those describing slope depositional processes as the turbidite (Bouma, 1962; Blatt et al., 1980) or contourite facies model (Faugères et al., 1984).

Some shelf facies models may show very similar sedimentary structures compared to slope facies models (Fig. 1.6). As an example, the contourite facies model (Faugères et al., 1984) shows several graded sequences with bioturbation. Such units are also observed in the tempestite facies model (Einsele and Seilacher, 1991). Nevertheless, described upper slope shallow sands have been mostly linked to contourite deposition (e.g. Viana and Faugères, 1998; Viana et al., 1998a). However, reworked storm deposits have generally not been considered in their discussions. Due to large Pleistocene sea level changes (up to 120 m (Lambeck and Chappell, 2001)), upper slope sands should not be prematurely linked to a specific depositional models, but be studied in detail and compared to all available shelf depositional models to identify possible similarities. Such improved understanding may ease the identification of the depositional process and sediment transfer across the shelf break.

Generally, there are three main facies models used to express depositional styles of slope and abyssal plain sedimentation (Fig. 1.6). The Bouma Sequence (Bouma, 1962; Middleton and Hampton, 1976; Blatt et al., 1980), describes the depositional sequence of (1) low density sandy turbidity current flows. Since defining this initial facies model, several new sedimentation models of closely related flows have been defined, including high and low density currents (Lowe, 1982), flows closely related to debris flows (hybrid event beds) (Haughton et al., 2009) or turbidite models considering top and base cutout sequences (Stow and Piper, 1984). On high-resolution seismic data, turbidite beds can be identified by showing thin (approximately one seismic cycle) chaotic appearing units with minor basal erosion. Seaward thinning of such beds is typical (Aksu and Hiscott, 1989; Howe, 1995; Beaubouef and Friedmann, 2000; Hieke, 2000; Piper, 2005; Tripsanas et al., 2008).

(2) Fine grained turbidite beds have been described from several study areas, e.g. the southeast Canadian continental margin (Hill, 1984a), the Congo Fan (van Weering and van Iperen, 1984) or the continental margin around Antarctica (Porebski et al., 1991). Such deposits are characterized by thin bedded very fine sands and silts with high clay percentages throughout (Piper, 1978). They generally show very few sedimentary structures and can either show faint grading (Huppertz and Piper, 2010) or laminated silty sequences (Stow and Piper, 1984). In core data, muddy turbidites may resemble hemipelagic sedimentation and a detailed study using high resolution bed-by-bed visual core description, grain size data, x-radiographies and sedimentary structures is needed to detect the presence of muddy turbidites in core data (Stow, 1979; Hill, 1984b). Seismically, it is not possible to define the deposits, as they are laminated similarly as hemipelagic sedimentation; in such cases ground truthing with core data is needed to define the character in a certain study area (Stow and Piper, 1984; Stow and Wetzel, 1990).

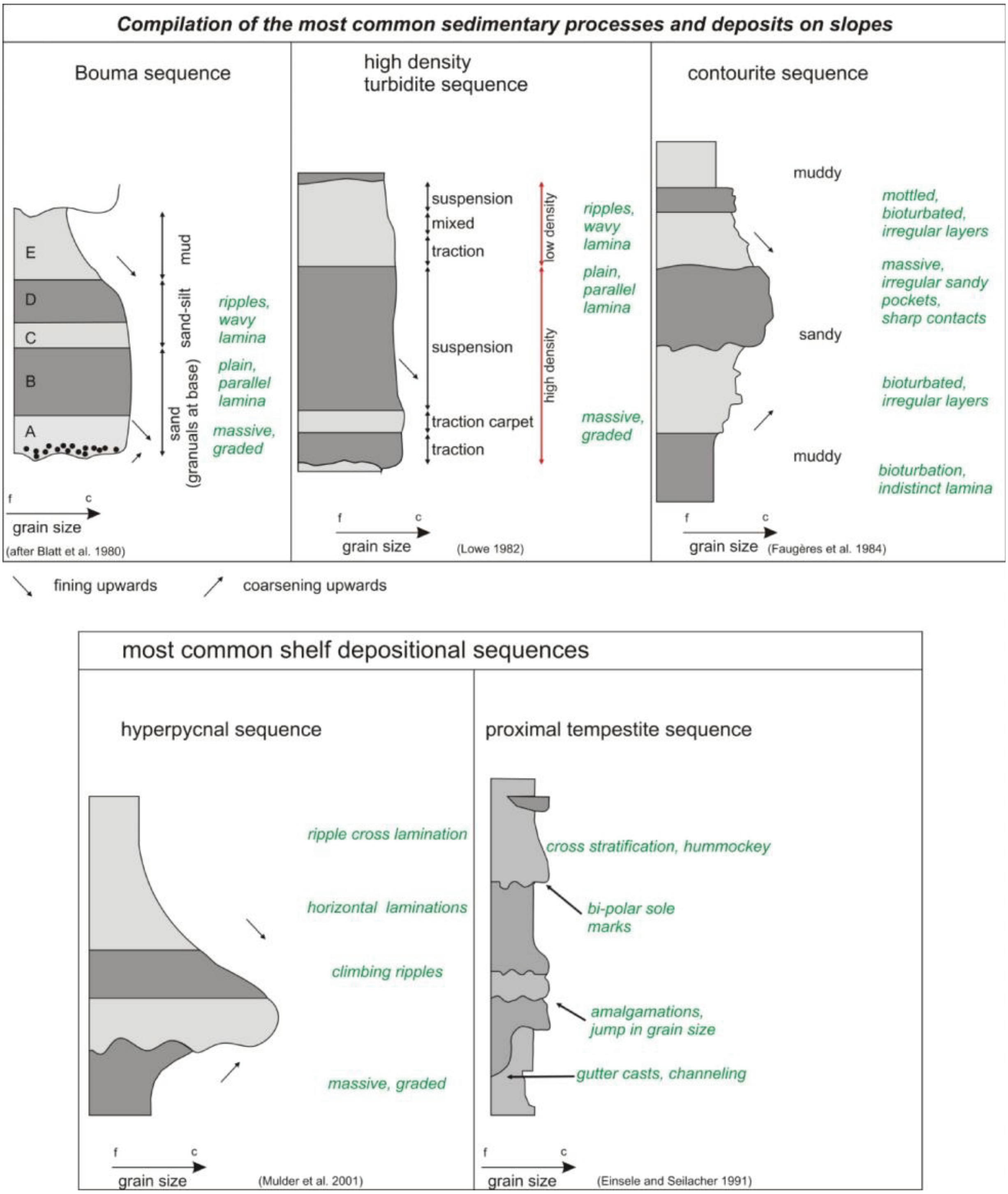

Fig. 1.6: Compilation of the most commonly observed deposits of sedimentary processes in continental margin systems. Green colored text indicates major observed sedimentary structures (Blatt et al., 1980; Lowe, 1982; Faugères et al., 1984; Einsele and Seilacher, 1991; Mulder et al., 2003), color shading only for contrast of units, Bouma sequence units numbered following standard notations (e.g. Blatt et al., 1980).

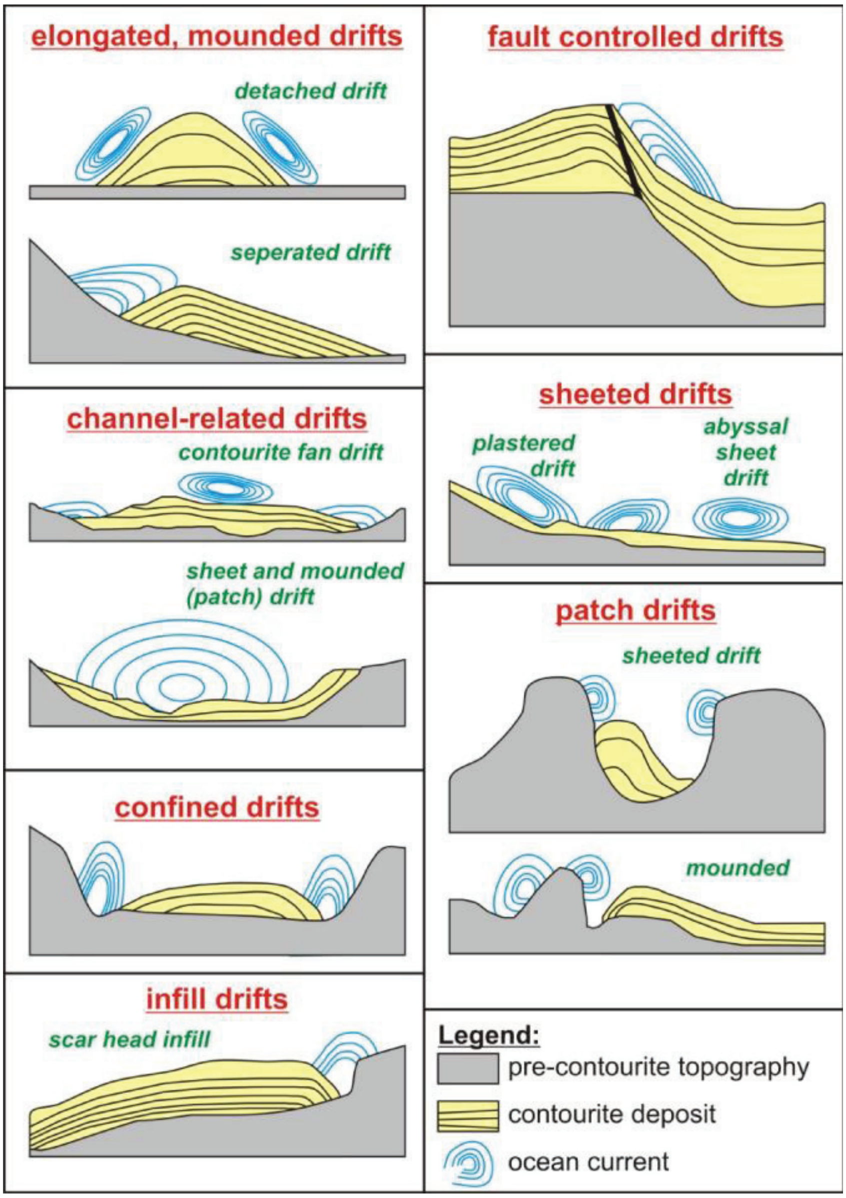

Fig. 1.7: Sketch of different contourite drift types along continental margins (modified after Hernández-Molina et al., 2008b)

Oceanic circulation is closely related to slope morphology as small changes in morphology may change speed and flow direction of a water mass (Stow, 1982; Faugères et al., 1993). It can easily winnow sediment below the ocean currents without forming drift bodies (Shanmugam and Moiola, 1982). Nevertheless, long-term (1000s of years) sediment transport within an ocean current leads frequently to the construction of (3) contourite depositional sequences (Figs. 1.6 and 1.7) (McCave, 1985). These deposits are generally directly linked to a specific ocean current, that has not changed significantly over long time scales (several 1000 years) (Stow et al., 2002; Stow et al., 2008). The original contourite facies model is characterized by a thick and highly bioturbated inverse graded units overlain by massive sands and normally graded bioturbated units (Fig. 1.6) (Faugères et al., 1984).

Sandy contourites are generally well-sorted deposits with little mud, which would have been winnowed out by the current. Observed grain size variability reflects waning of ocean currents and adjustment to the new flow pattern (Fig. 1.6). Various characteristics have been used to distinguish these deposits from turbidite. The contourite deposits should be well sorted, show possibly a gravel lag, have units that are highly bioturbated and show no regular sequence of sedimentary structures (Stow et al., 2002). On high-resolution seismic data, few erosional surfaces and large-scale (km-scale) sediment waves are typically observed in contourite sheets (Stow et al., 2002; Huppertz and Piper, 2010).

Muddy contourites are fine-grained mud dominated sediments with few sedimentary structures or may even be structureless (Stow, 1985; Faugères and Stow, 1993). They are highly bioturbated and thus lack sedimentary structures indicative of contourite deposition (Faugères and Stow, 1993): biogenic debris is the main constituent (Stow and Holbrook, 1984). Such fine grained contourites have mostly been observed in either shallow water areas (Sivkov et al., 2002; Verdicchio and Trincardi, 2008), or on abyssal plains where some were linked to nepheolid layers (Stow and Lovell, 1979; Martín-Chivelet et al., 2008). The distinction between muddy contourites, pelagic sedimentation and muddy turbidites has not been resolved yet, unless the setting can be used to exclude either process (Stanley, 1981; Stow and Wetzel, 1990; Faugères and Stow, 1993).

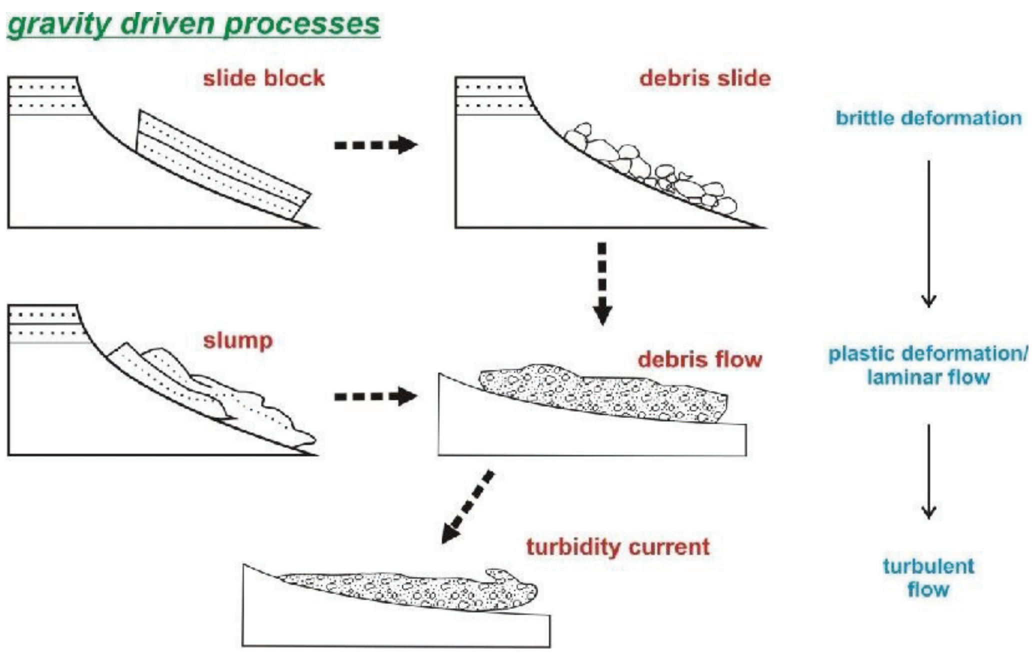

Fig. 1.8: Summary diagram showing main gravity driven processes and how they interact and transform into each other (after McHugh et al., 2002)

Gravity driven processes can also result in (4) mass transport deposits (MTDs) described initially by Takahashi (1981) and recognized globally on continental margins (**Fig. 1.8**) (Taylor et al., 2000; Taylor et al., 2002; Piper, 2005; Owen et al., 2007). A wide range of flow types has been observed and linked to different triggering processes (Hampton et al., 1996): nevertheless it is generally very challenging to link a specific failure deposit to a triggering process as the resultant deposit has always the same appearance (Hampton et al., 1996) . The main characteristics of debris flows are their chaotic character with mud clasts throughout. In few cases, the mud clasts can be aligned in flow direction (Piper et al., 2003; Jenner et al., 2007; Tripsanas et al., 2008). Seismic data shows chaotic appearance with varying amount of basal erosion (Niedoroda et al., 2006; Niedoroda et al., 2007; Huppertz and Piper, 2009).

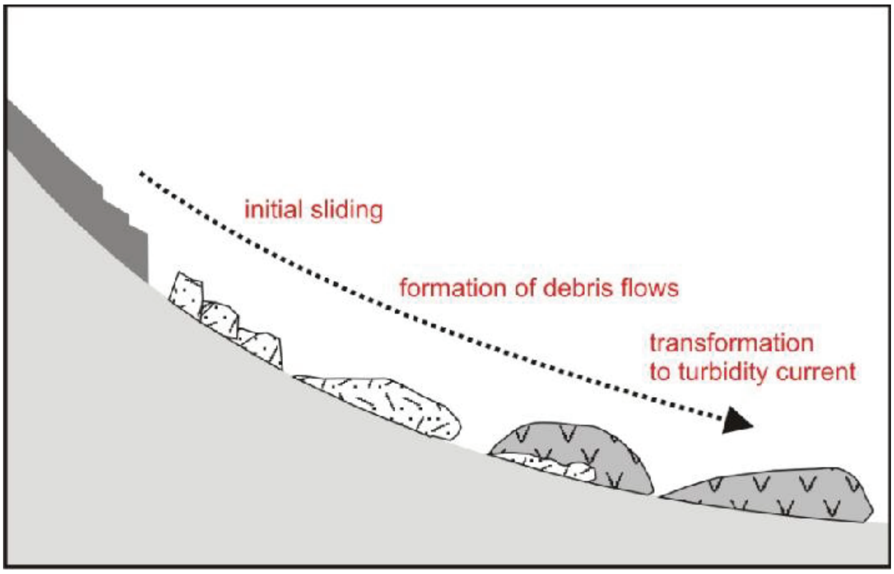

Fig. 1.9: Schematic diagram showing transformation of gravity flows downslope (after Bryn et al., 2005b)

1.2.1. Outer shelf processes: a short overview

The continental shelf is a highly dynamic system landwards from the shelf break (**Fig. 1.1**). Sedimentary processes acting in the shelf environment can result in deposits very similar to the slope depositional models as already outlined. Thus, the sedimentary sequence of these shelf deposits must be considered, especially when interpreting upper slope sediments. The main depositional models of the shelf environment are the (1) storm or tempestite sequence (Einsele and Seilacher, 1991; Einsele, 1996; Myrow and Southard, 1996), and the (2) hyperpycnal sequence (Mulder et al., 2003) (Fig. 1.6). Especially during Pleistocene sea level low stands (Schaaf, 1996), these shelf processes have acted either close to the shelf break or even on the continental slope itself. Therefore, a new effort will be needed to look especially at the interaction of shelf and slope processes at the shelf break.

1.3. Geological setting of the two study areas

During this study, the geographical focus was on two areas: the Scotian Slope representing a glaciated continental margin and the Argentine Slope being the non-glaciated representative. Both study areas are found along the western Atlantic passive continental margin (**Fig. 1.10**). The margins were formed during initial rifting (Uliana et al., 1989; Wade and MacLean, 1990).

Fig. 1.10: Geographic position of the two study areas: Scotian Slope and the northern Argentine and Uruguay Slope (map from National Geographic Society; Cartographic Division, 1990)

These two margins were chosen, as both are characterized by high sediment discharge, the Scotian Slope due to intense glaciations since isotope stage 12 (Piper et al., 1994; Piper, 2005), the Argentine and Uruguayan slope due to the complex interaction of ocean currents and the discharge of the La Plata rivers (Paraná and Uruguay rivers) (Martins and Willwock, 1987; Framinan and Brown, 1996; Piola and Matano, 2001). Thus both slopes are subject to high sediment discharge affecting slope deposition.

1.3.1. Nova Scotian Continental Slope

The Nova Scotian continental margin is located on the southeast Canadian continental margin between Northeast Fan and the Laurentian Channel (**Fig. 1.11**). The shelf break occurs in 200 m water depth (Campbell et al., 2004), the base of rise is below 4900 m water depth where the Sohm Abyssal Plain continues (Horn et al., 1971).

Sedimentation on the Scotian Slope is strongly influenced by ice sheet dynamics of the Pleistocene ice sheets since marine isotope stage 12 when ice sheets first reached the shelf break (Piper et al., 1994). Since then, the ice sheets have supplied a vast amount of sediment to the margin and initiated sediment failures on different scales depending on how far they crossed the shelf and how long they were stagnant at the shelf break (Piper, 2001; Piper, 2005).

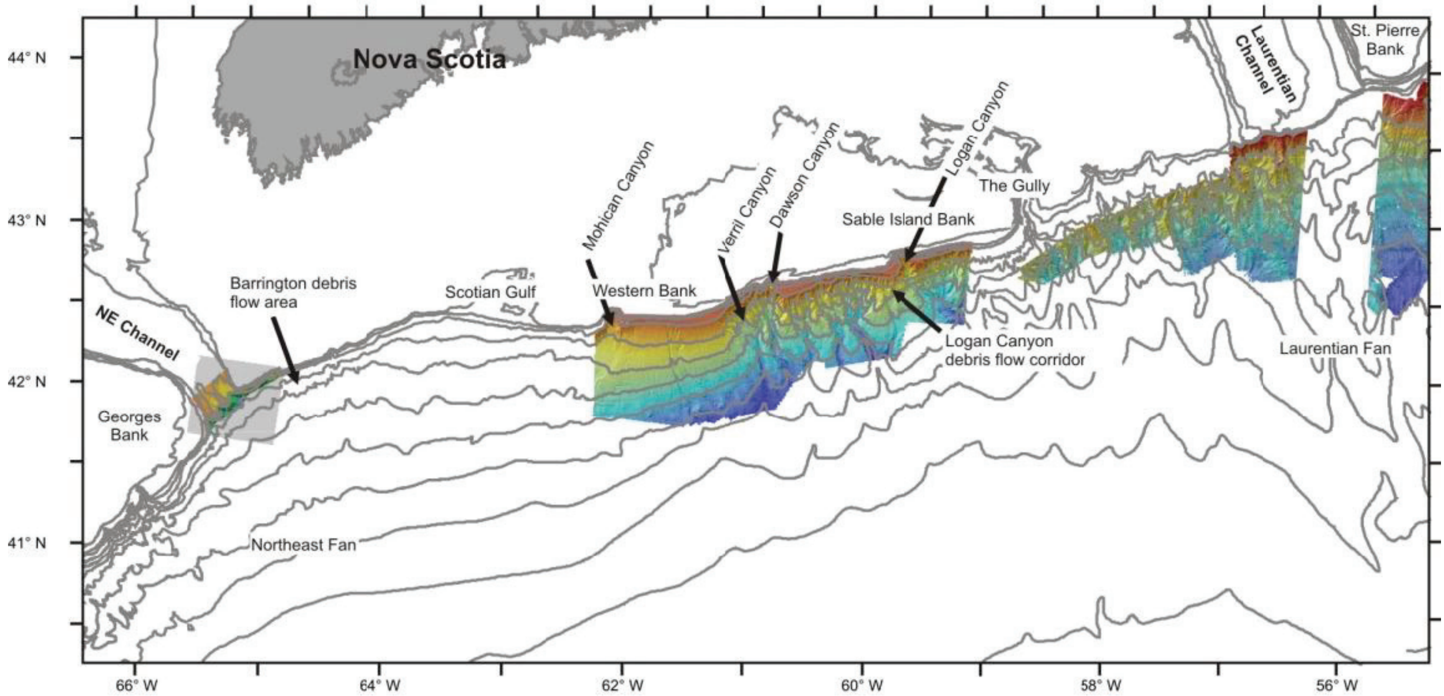

Fig. 1.11: Overview map of the Scotian Slope along the southeast Canadian continental margin, bathymetry spacing is 500 m on the slope, and 100 m above 500 m water depth (modified after Huppertz et al., 2009).

The evolution of these dynamic ice sheets has resulted in a very complex margin setting: the central Scotian Slope shows well stratified sequences with little erosional surfaces present (Campbell, 2000; Campbell and MacDonald, 2006), whereas towards the west and east major slope failures are characteristic for the sequence (Hughes Clarke et al., 1992; Jenner et al., 2007; Hundert and Piper, 2008).

The central, well-stratified area has the longest and mostly complete stratigraphic record, and is characterized by plume sedimentation (Campbell, 2000). Few turbidite beds are found (Campbell, 2000). Till tongues on the shelf break indicate little ice sheet dynamics (Piper and Brunt, 2006). Plume sedimentation occurred from meltwater flux originating either out of the Laurentian Channel or from Hudson Strait in Labrador (Hesse and Khodabakhsh, 2006; Piper et al., 2011). The sediments originating from the Laurentian Channel are reddish colored and reflect the Carboniferous-Permian red beds outcropping in the Gulf of St. Laurence (Stea et al., 1998). Plumes originating from Hudson strait deposit light gray colored sediments and are transported to the area by the

Labrador Current. Sediment originating off Nova Scotia has dark gray colors (Stea et al., 1998; Piper and DeWolfe, 2003). Additionally, icebergs within these meltwater plumes supplied ice rafted debris to the slope (Piper and Campbell, 2002; Piper and Brunt, 2006).

The eastern Scotian Slope and Rise is characterized by large-scale sediment failures just west of the Laurentian Fan (Piper and Ingram, 2003). The Laurentian Fan was a major ice stream during glacial stages when ice reached large parts of the shelf break (Shaw et al., 2006). The fan is constructed by stacked turbidites of various age and volume. Few debris flows are present and if, they are thin and have small volumes (Skene and Piper, 2003; Skene and Piper, 2006; Piper et al., 2007). This observation is likely linked to the high slope angles on the Laurentian Fan resulting in sediment bypassing as it was observed during the 1929 Grand Banks earthquake (Piper, 2005; Mosher and Piper, 2007; Piper et al., 2007).

The western Scotian Slope is characterized by the trough mouth fan seawards of the Scotian Gulf (Hill, 1984b) and the fan offshore Northeast Channel (Hundert and Piper, 2008). In the Scotian Gulf, stacked mass transport deposits characterize the unit, very little stratified sediments remain (Hill, 1983; Berry and Piper, 1993). Northeast Fan is characterized by turbidite beds and few debris flows. Similarly to the Laurentian Channel, bypassing is the likely cause for this observation. Several channels have been mapped to the rise (Hughes Clarke et al., 1992), where they feed the Sohm Abyssal Plain.

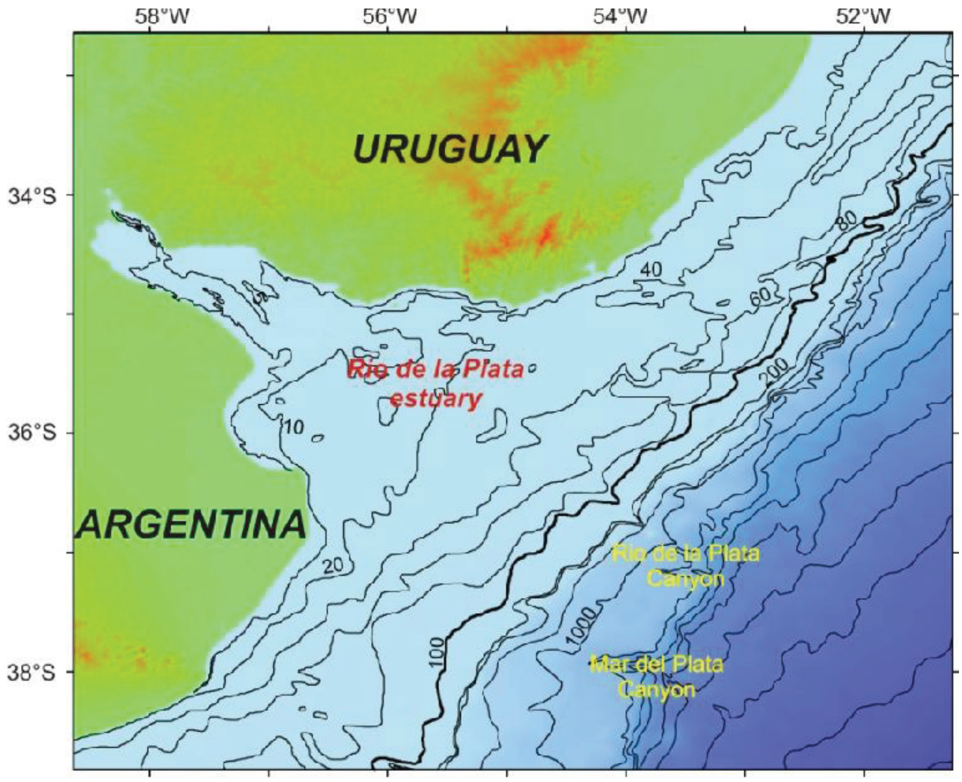

Fig. 1.12: Overview map of the Argentine Slope (slope bathymetry after Martins and Correa (1996), slope bathymetry from Gebco 2003 [www.gebco.net])

1.3.2. Northern Argentine and Uruguay Continental Margin

The northern Argentine and Uruguay continental margin (**Figs. 1.10 and 1.12**) is located just seawards of the Rio de la Plata estuary, where the Paraná and Uruguay (La Plata) rivers drain (Parker et al., 1994; Framinan and Brown, 1996; Parker et al., 1997). These two rivers drain the second largest basin in South America and discharge up to 80-130 million tons of mostly silty and finer grained sediments to the southwestern Atlantic Ocean (Depetris and Griffin, 1968; Gilberto et al., 2004). Recent studies suggest that most of the discharged sediment remains within the estuary and is not being exported to the outer shelf areas (Violante and Parker, 2004). Sediments on the mid and outer shelf are considered relictic sediments from the Pleistocene, when large parts of the shelf were exposed (Martins et al., 2005c). These include gravelly sand bars and several marine terraces interpreted as former sea level lowstands (Urien and Ewing, 1974).

The Quaternary sequence of the Uruguay and northern Argentine slope has been little studied, even though a large number of sediment cores have been collected since the 1970. Most studies in the area have focused either on oceanographic or climate-related topics (Piola and Matano, 2001; Chiessi et al., 2008; Chiessi et al., 2010) or have worked within the Argentine Basin (Ewing et al., 1964; Ewing, 1965; Flood et al., 1993), the abyssal plain seawards of the Argentine Slope. On the southern Argentine Slope some pollen studies have been used to date few major shallow seismic horizons (Groot and Groot, 1966; Groot et al., 1967).

Several contourite sequences have been described from the southern Argentine Slope and mapped out regionally (**Fig. 1.13**) (Hernández-Molina et al., 2009). Nevertheless, the used datasets were mostly low-resolution single- and multi-channel seismic airgun data (Hernández-Molina et al., 2009).

The northern Argentine Slope is characterized by few large canyon structures (**Fig. 1.13**) (Urien and Ewing, 1974), which may have been fed by the Rio de la Plata Rivers during lower sea level (Wells and Daborn, 1997). Most of these canyons do not incise into the shelf break, but start at the Ewing terrace, a slope basin, at ~1200 m water depth (Urien and Ewing, 1974; Hernández-Molina et al., 2009). Several studies have mapped out canyons feeding the terrace during sea level lowstands (Wells and Daborn, 1997; Martins et al., 2005a), but no seismic or core data has yet been presented to support this interpretation. On the Uruguayan margin, large mass transport deposits have been described and linked to several scarps observed throughout the slope. Slope oversteepening and pore-water pressures have been used to interpret sediment failures (Antobreh, 2005). Passive margin seismicity has also been observed in this part of the margin and may be a cause of large scale failures along the Uruguayan and northernmost Argentine slope (Assumpcao, 1998; Benavídez Sosa, 1998), nevertheless no reliable paleo-seismic record exists currently from the margin.

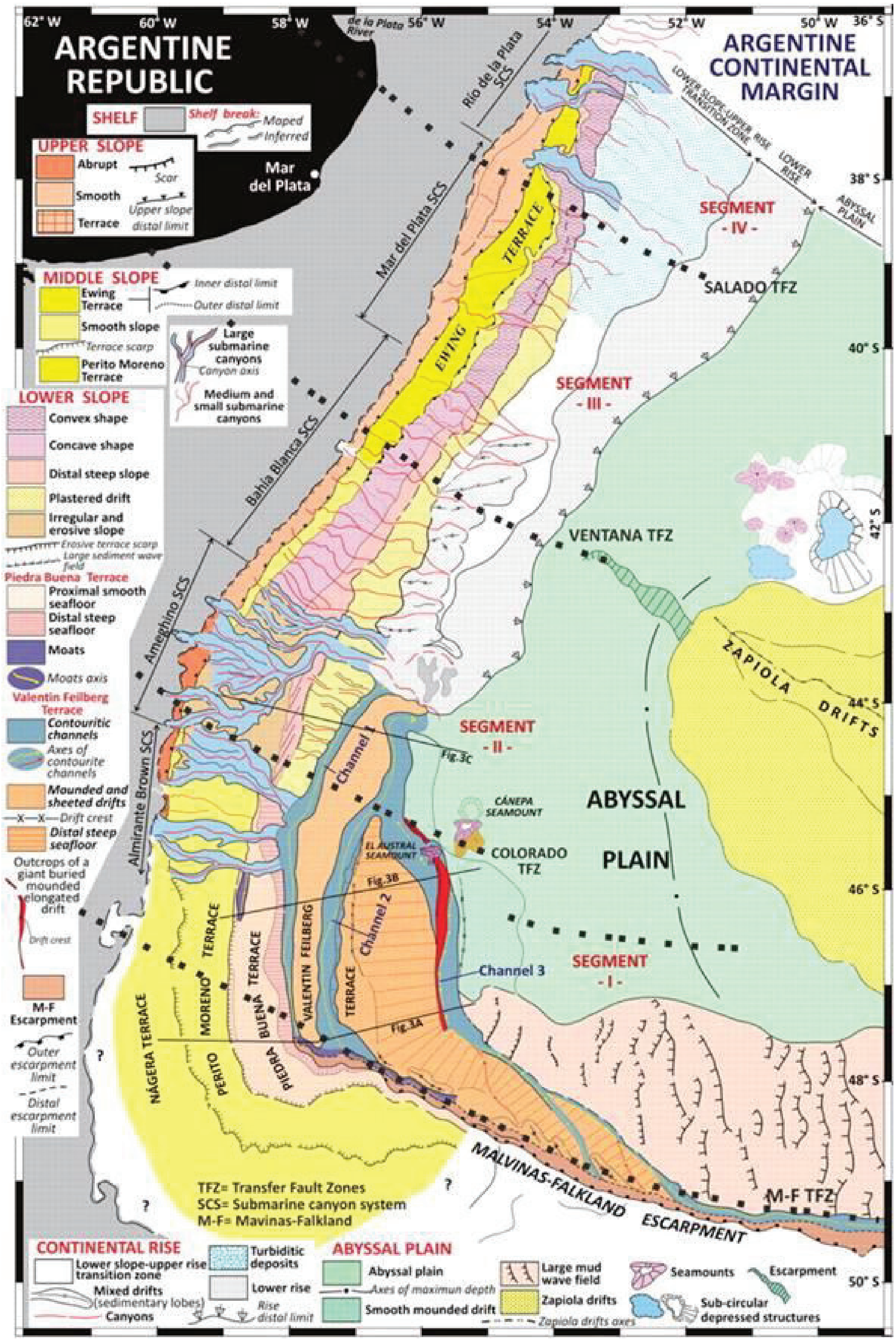

Fig. 1.13: Overview map of the slope system on the Argentine Slope (from Hernández-Molina et al., 2009); TFZ=transform fault Zone, SCS=submarine canyon system, Figures referenced on this map refer to the Geology paper figures (Hernández-Molina et al., 2009) and should thus be ignored for this work.

1.3.2.1. Brief overview of the oceanographic setting in the southern SW Atlantic Ocean

Due to the presence of contourites throughout the Argentine Slope (Hernández-Molina et al., 2009; 2010), the ocean circulation plays a much more important role on the Argentine and Uruguayan Slope compared to the Scotian Slope, thus a brief description is given here.

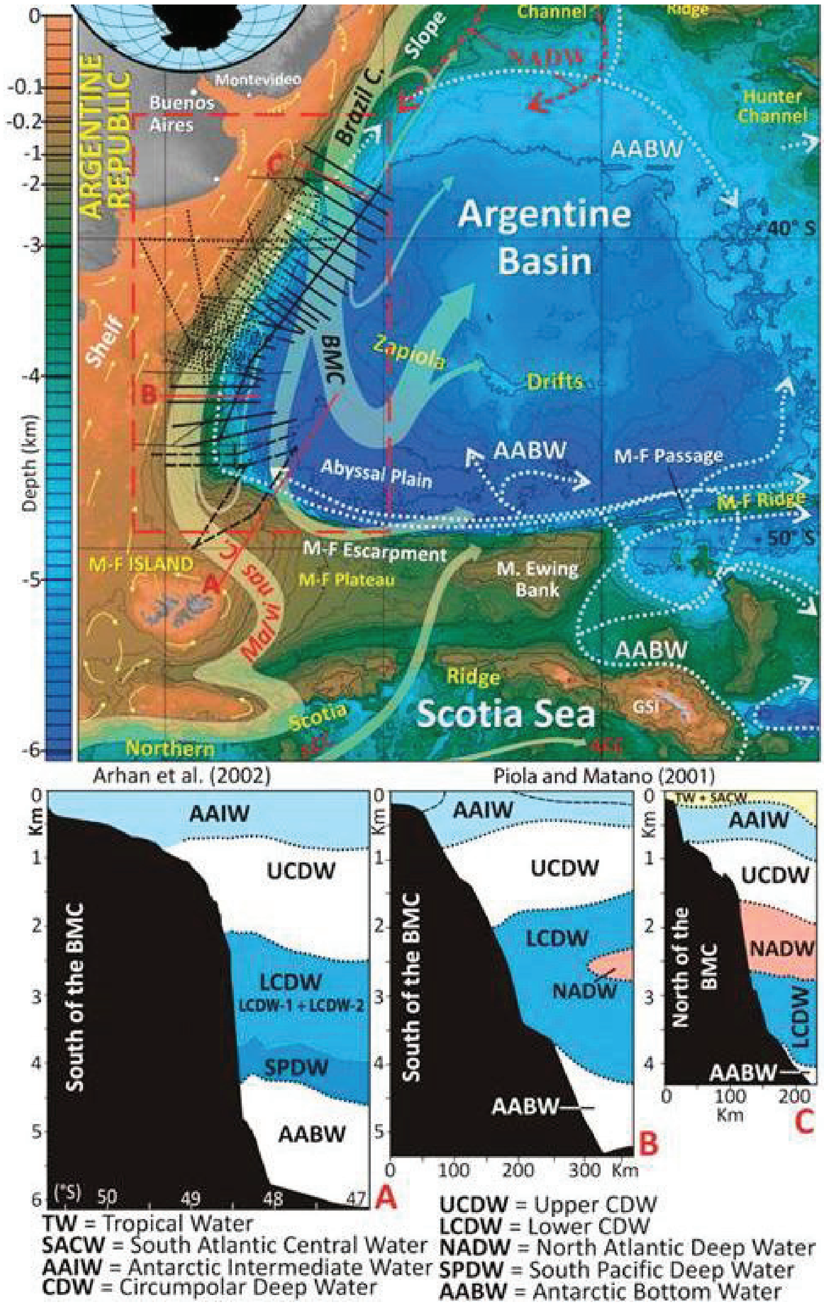

Fig. 1.14 on previous page: Simplified oceanography in the Argentine Basin modified after Hernández-Molina (2009) citing Piola and Matano (2001) and Arhan et al. (2002), see text for more details.BMC=Brazil Malvinas Confleunce

The main oceanographic feature in the area is the Brazil-Malvinas Confluence zone (**Fig. 1.14**), where tropical and Antarctic sourced water masses collide, resulting in the detachment of some from the currents from the continental margin (Stramma and England, 1999; Piola and Matano, 2001; Frenz et al., 2003). Within the upper 1000 m water column, the northwards directed Falkland/Malvinas Current and the southwards flowing Brazil Current collide. Each of these two currents is formed by two water masses (Stramma and England, 1999): the Falkland/Malvinas current by Subantarctic Waters and Antarctic Intermediate Water, the Brazil current by Tropical Waters and recirculated Antarctic Intermediate Water (Stramma and England, 1999; Piola and Matano, 2001; Frenz et al., 2003). The recirculation of the Antarctic Intermediate Water occurs within the South Atlantic Gyre, after the Antarctic Intermediate Water detaches from the margin (Schmid et al., 2000).

Below this shallow circulation, the northwards flowing Circumpolar Deep Water is split vertically by the southward directed North Atlantic Deep Water. South of the confluence, the North Atlantic Deep Water also detaches from the slope at ~ 40°S (Frenz et al., 2003) and flows into the Argentine Basin (von Lom-Keil et al., 2003). The split Circumpolar Deep Water continues northwards along the Brazilian Slope (Piola and Matano, 2001; Hernández-Molina et al., 2009). Below 4000 m water depth, the Antarctic Bottom Water flows clockwise through the Argentine Basin. Seaward of the La Plata estuary it splits and parts of it flow basinwards whereas other parts continue along the to of the slope (Coles et al., 1996).

1.4. Approach and scope

The main scientific approach was very similar in both study areas. A general geological review of previous work was required to define where good starting points were at, to aim at achieving new insights into continental margin architecture. The general understanding of both study areas is very different, the Scotian slope has been studied for more than 40 years and a vast amount of knowledge exist on several small areas on the slope: the main aim here was to understand how all these different areas connect to each other and how the different processes acting in the different areas are related to each other in a stratigraphic way.

This is in strong contrast to the northern Argentine slope, where only few studies have focused on the slope so far. Therefore, the overall depositional sequence had to first be established to generate a general architectural setting. Questions included what sediments are present on this margin and which processes can we see and is there any stratigraphic change visible and if so of what nature is this change?

Therefore, each study area had first of all its own questions and anticipated results, before larger scale questions about margin architecture could be addressed. The main questions on the Scotian Slope were:

I. How do glaciations influence slope sedimentation and can we see ice sheet dynamics imprinted onto the slope?
II. Are the slope-wide described mass transport deposits all the same or do different mass transport deposits characterize the slope not only at different times but also in different areas during similar times?
III. When does slope building take place and at what times is the slope eroded?
IV. How does the slope evolve over several glacial cycles and how long does material reside on the slope before being transported to the abyssal plain?
V. Can we quantify short-term (10 ka) and long-term (100 ka) slope erosion and when do the slope building and slope-eroding processes take place?

The main scopes of the Argentine margin were:

I. Contourites have been described from Airgun data in the area: are these contourites still active and can we use these as climate records?
II. What sediments are present on the continental slope offshore the Rio de la Plata and what impact does the fluvial discharge have on sedimentation.
III. Where does the sediment building the contourites come from and can we establish a specific water masses responsible for the transport?

1.5. General methodology

During this study, generally three datasets have been used: (a) sediment core data from gravity and piston cores, (b) high resolution seismic data (Parasound data and Huntec deep towed seismic data) and (3) airgun data. The combined use of all three datasets guaranteed a thorough understanding of the continental slope architecture.

On the Scotian Slope, the main focus was on establishing a slope-wide seismic stratigraphy by using high resolution Huntec data for the upper few 100s meters, whereas the lower sequence to the base of the Quaternary used airgun data. Core data was only used to a very limited extent, mainly for establishing age control on the Huntec seismic stratigraphy and to estimate slope-wide sediment fluxes (Jenner et al., 2010). Published exploration well data was used to establish the age model of the airgun stratigraphy (e.g. Mosher et al., 2004). The link to upper slope till tongues further supported the established reflection ages.

The studies on the northern Argentine slope were mainly relying on core data. Two studies were done on this margin, a more regional study on overall slope architecture and a more local study on the interaction of along and downslope processes on the northern Ewing terrace. The regional study used core descriptions, bathymetry data and surface seabed photography. For the more local study, high-resolution Parasound data was only used to establish the regional architectural context and to define major erosional events. Core data was mainly analyzed using a range of methods including grain size data, x-radiography and component analysis data. Age control could not be established from radiocarbon dates due to low carbonate content in cores, but oxygen isotope data ($\delta^{18}O$) supplied age control.

1.6. Objectives of thesis:

The main objectives of the thesis were to try answering the following questions:

- What are the controlling mechanisms of continental margin evolution and how strong is the impact of glaciations on continental margin sedimentation compared to a non-glaciated margin?
- Do the processes differ on margins in different climatic settings?

1.7. Why study the Scotian Slope and the northern Argentine and Uruguay Slope?

Sedimentary slope processes have been thoroughly studied on the Scotian Slope. Therefore, the main processes were known acting on large parts of the margin. Therefore, it seemed being a prime area to target in on some of the questions stated above. Especially trying to aim at regional slope evolution on this well studied margin seemed to be very promising for these questions.

The previously described contourites on the Argentine margin were not very well understood. Therefore the aims at understanding slope evolution in this area highly influenced by contourite deposition seemed to be very promising for improving the understanding of contourite deposition processes and their interaction with downslope driven processes.

1.8. Data quality and availability

In both areas, very similar datasets were available: high- and low-resolution seismic data and sediment cores. Nevertheless, the amounts and availability of data differed strongly in the two study areas. 1000s of line-km and a large number of cores characterize the Scotian slope. This is in contrast to the northern Argentine slope, where only few cores and seismic data are available. Slope processes have only been inferred from low-resolution seismic data so far and few ideas on age exist within the area. During 2009, a Meteor cruise (M78/3) aimed at this study area to collect new cores and seismic data. During this cruise, where the author was a participant, most of the cores used in the local aiming study on the Argentine Slope were collected. Additionally new Parasound data running through the core positions were also collected as was the used multibeam data.

Therefore, the data coverage was different in both study areas, but the quality of data used in the study was generally very good. Few old seismic lined were considered on the Scotian slope, but the poorer quality data did not affect interpretation significantly as generally newer data close by could be used as a substitute.

1.9. Organization of thesis

The central chapters of this thesis are published papers or submitted manuscripts. Two research papers were established for each of the two study areas; additionally a process-oriented review paper was written for the Argentine and Uruguay continental margin. All the research, ideas and interpretation were carried out by the student, T. J. Huppertz, but the supervisors, D. J. W. Piper and R. Henrich, helped to guide the research and improve the manuscripts. Some papers have more co-authors, who the author had fruitful discussion with. Nevertheless, the presented ideas were mostly developed by the author himself.

Chapters 2 and 3 describe the geological findings established during this study from the Scotian Slope, chapter 4 is a review paper on the Argentine Shelf and Slope and the chapters 5 and 6 display the new findings of slope architecture on the northern Argentine and Uruguayan Slope. The last chapter summarized the main findings in the two study areas and sets them into context. It reflects on the stated objectives and evaluates their approach.

1.10. References

Adams, E.A. and Schlager, W., 2000. Basic types of submarine slope curvature. Journal of Sedimentary Geology, 70(4): 814-828.
Aksu, A.E. and Hiscott, R.N., 1989. Slides and debris flows on the high-latitude continental slopes of Baffin Bay. Geology, 17(10): 885-888.
Anderson, J.B., Kurtz, D.D., Domack, E.W. and Balshaw, K.M., 1980. Glacial and glacial marine sediments of the Antarctic continental shelf. Journal of Geology, 88(4): 399-414.

Antobreh, A.A., 2005. Channelised and open-slope processes of mass sediment transport: their morphological and seismic characterisation from selected Atlantic high productivity regions. Ph. D. Thesis, University of Bremen, Bremen, 130 pp.
Antonioli, F., Bard, E., Potter, E.-K., Silenzi, S. and Improta, S., 2004. 215-ka History of sea-level oscillations from marine and continental layers in Argentarola Cave speleothems (Italy). Global and Planetary Change, 43(1-2): 57-78.
Arhan, M., Naveira Garabato, A.C., Heywood, K.J. and Stevens, D.P., 2002. The Antarctic Circumpolar Current between the Falkland Islands and South Georgia. Journal of physical Oceanography, 32(6): 1914–1931.
Assumpcao, M., 1998. Seismicity and stresses in the Brazilian passive margin. Bulletin of the Seismological Society of America, 88(1): 160-169.
Beaubouef, R.T. and Friedmann, S.J., 2000. High resolution seismic/sequence stratigraphic framework for the evolution of Pleistocene intra slope basins, western Gulf of Mexico: depositional models and reservoir analogs, GCSSEPM Foundation 20th Annual Research Conference: Deep Water reservoirs of the World, Houstan, TX, pp. 40-60.
Benavídez Sosa, A., 1998. Sismicidad y sismotectónica en Uruguay. Fisica de la Tierra, 10: 167-186.
Berry, J.A. and Piper, D.J.W., 1993. Seismic stratigraphy of the central Scotian rise: a record of continental margin glaciation. Geo-Marine Letters, 13(4): 197-206.
Blatt, H., Middleton, G. and Murry, R., 1980. Origin of sedimentary rocks. Prentice-Hall, Inc., Englewood Cliffs, New Jersey, 782 pp.
Blum, M.D. and Törnqvist, T.E., 2000. Fluvial responses to climate and sea-level change: a review and look forward. Sedimentology, 47: 2-48.
Bouma, A.H., 1962. Sedimentology of some flysch deposits. Elsevier Publishing Company, Amsterdam, 168 pp.
Brink, K.H., Bane, J.M., Church, T.M., Fairall, C.W., Geernaert, G.L., Hammond, D.E., Henrichs, S.M., Martens, C.S., Nittrouer, C.A., Rogers, D.P., Roman, M.R., Roughgarde, J.D., Smith, R.L., Wright, L.D. and Yoder, J.A., 1992. Coastal ocean processes: a science prospectus. Technical Report WHOI-92-18, Wood Hole Oceanographic Institute.
Bryn, P., Berg, K., Stoker, M.S., Haflidason, H. and Solheim, A., 2005a. Contourites and their relevance for mass wasting along the mid-Norwegian margin. Marine and Petroleum Geology, 22(1-2): 85-96.
Bryn, P., Berg, K., Forsberg, C.F., Solheim, A. and Kvalstad, T.J., 2005b. Explaining the Storegga Slide. Marine and Petroleum Geology, 22(1-2): 11-19.
Campbell, D.C., 2000. Relationship of sediment properties to failure horizons for a small area of the Scotian Slope. Current research 2000-D8, Geological Survey of Canada, Dartmouth.
Campbell, D.C., Shimeld, J.W., Mosher, D.C. and Piper, D.J.W., 2004. Relationships between sediment mass-failure modes and magnitudes in the evolution of the Scotian Slope, offshore Nova Scotia, Offshore Technology Conference, Houston, Texas, pp. OTC 16743.
Campbell, D.C. and MacDonald, A.W.A., 2006. Geohazard assessment of five deepwater pipeline scenarios on the Scotian Slope. Open File 5079, Geological Survey of Canada, Ottawa.

Chiessi, C.M., Mulitza, S., Paul, A., Pätzold, J., Groeneveld, J. and Wefer, G., 2008. South Atlantic interocean exchange as the trigger for the Bølling warm event. Geology, 36(12): 919-922.
Chiessi, C.M., Mulitza, S., Pätzold, J. and Wefer, G., 2010. How different proxies record precipitation variability over southeastern South America. IOP Conference Series: Earth and Environmental Science, 9: 012007.
Clark, P.U. and Mix, A.C., 2002. Ice sheets and sea level of the Last Glacial Maximum. Quaternary Science Reviews, 21(1-3): 1-7.
Coles, V.J., McCartney, M.S., Olson, D.B. and Smethie, W.M., 1996. Changes in Antarctic Bottom Water properties in the western South Atlantic in the late 1980s. Journal of Geophysical Research, 101(C4): 8957-8970.
Coward, M.P., Purdy, E.G., Ries, A.C. and Smith, D.G., 1999. The distribution of petroleum reserves in basins of the South Atlantic margins. In: N.R. Cameron, R.H. Bate and V.S. Clure (Editors), The oil and gas habitats of the South Atlantic. Geological Society, Special Publication 153, London, pp. 101-131.
Depetris, P.J. and Griffin, J.J., 1968. Suspended load in the Rio de la Plata drainage basin. Sedimentology, 11(1-2): 53-60.
Dingle, R.V. and Robson, S., 1985. Slumps, canyons and related features on the continental margin off East London, SE Africa (SW Indian Ocean). Marine Geology, 67(1-2): 37-54.
Domack, E.W., Jacobson, E.A., Shipp, S. and Anderson, J.B., 1999. Late Pleistocene–Holocene retreat of the West Antarctic Ice-Sheet system in the Ross Sea: Part 2—Sedimentologic and stratigraphic signature. Geological Society of America Bulletin, 111(10): 1517-1536.
Dowdeswell, J.A. and Murray, T., 1990. Modelling rates of sedimentation from icebergs. In: J.A. Dowdeswell and J.D. Scourse (Editors), Glacimarine Environments: Processes and Sediments. Geological Society, Special Publication 53, London, pp. 121-137.
Dowdeswell, J.A., Ó Cofaigh, C. and Pudsey, C.J., 2004. Continental slope morphology and sedimentary processes at the mouth of an Antarctic palaeo-ice stream. Marine Geology, 204(1-2): 203-214.
Ducassou, E., Mulder, T., Migeon, S., Gonthier, E., Murat, A., Revel, M., Capotondi, L., Bernasconi, S.M., Mascle, J. and Zaragosi, S., 2008. Nile floods recorded in deep Mediterranean sediments. Quaternary Research, 70(3): 382-391.
Einsele, G. and Seilacher, A., 1991. Distinction of tempestites and turbidites. In: G. Einsele, W. Ricken and A. Seilacher (Editors), Cycles and events in stratigraphy. Springer Verlag, Berlin, Heidelberg, New York, pp. 377-382.
Einsele, G., 1996. Event deposits: the role of sediment supply and relative sea-level changes - overview. Sedimentary Geology, 104(1-4): 11-37.
Ewing, M., Ludwig, W.J. and Ewing, J.I., 1964. Sediment distribution in the oceans: the Argentine Basin. Journal of Geophysical Research, 69(10): 2003-2032.
Ewing, M., 1965. The sediments of the Argentine Basin (Harold Jeffreys Lecture). Quarterly Journal of the Royal Astronomical Society, 6: 10-27.
Faugères, J.-C., Gonthier, E. and Stow, D.A.V., 1984. Contourite drift molded by deep Mediterranian outflow. Geology, 12(5): 296-300.
Faugères, J.-C. and Stow, D.A.V., 1993. Bottom-current-controlled sedimentation: a synthesis of the contourite problem. Sedimentary Geology, 82(1-4): 287-297.

Faugères, J.-C., Mézerais, M.L. and Stow, D.A.V., 1993. Contourite drift types and their distribution in the North and South Atlantic Ocean basins. Sedimentary Geology, 82(1-4): 189-203.
Flood, R.D., Shor, A. and Manley, P.L., 1993. Morphology of abyssal mudwaves at Project MUDWAVES sites in the Argentine Basin. Deep Sea Research Part II: Topical Studies in Oceanography, 40(4/5): 859-888.
Framinan, M.B. and Brown, O.B., 1996. Study of the Río de la Plata turbidity front, Part 1: spatial and temporal distribution. Continental Shelf Research, 16(10): 1259-1282.
Frenz, M., Höppner, R., Stuut, J.-B.W., Wagner, T. and Henrich, R., 2003. Surface sediment bulk geochemistry and grain size composition related to the oceanic circulation along the South American continental margin in the southwest Atlantic. In: G. Wefer, S. Mulitza and V. Ratmeyer (Editors), The South Atlantic in the Late Quaternary: reconstruction of material budgets and current systems. Springer Verlag, Berlin, Heidelberg, pp. 347-373.
Friedrichs, C.T., 2004. Gravity-driven sediment transport on the continental shelf: implications for equilibrium profiles near river mouths. Coastal Engineering, 51(8-9): 795-811.
Förster, A., R. Ellis, R. Henrich, S. Krastel and A.J. Kopf (2010) Geotechnical characterization and strain analyses of sediment in the Mauritania Slide Complex, NW-Africa. Marine and Petroleum Geology 27: 1175-1189.
Gilberto, D.A., Bremec, C.S., Acha, E.M. and Mianzán, H.W., 2004. Large-scale spatial patterns of benthic assemblages in the SW Atlantic: the Río de la Plata estuary and adjacent shelf waters. Estuarine, Coastal and Shelf Science, 61(1): 1-13.
Groot, J.J. and Groot, C.R., 1966. Pollen spectra from deep-sea sediments as indicators of climatic changes in southern South America. Marine Geology, 4(6): 525-537.
Groot, J.J., Groot, C.R., Ewing, M., Burckle, L. and Conolly, J.R., 1967. Spores, pollen, diatoms and provenance of the Argentine Basin sediments. In: M. Sears (Editor), Progress in Oceanography, Volume 4. Pergamon Press, pp. 179-217.
Gross, G.M., 1972. Oceanography: A View of the Earth. Prentice-Hall, Inc., Englewood Cliffs.
Hampton, M.A., Lee, H.J. and Locat, J., 1996. Submarine landslides. Reviews of Geophysics, 34(1): 33-59.
Hart, B.S., Prior, D.B., Barrie, J.V., Curry, R.G. and Luternauer, J.L., 1992. A river mouth submarine channel and failure complex, Fraser Delta, Canada. Sedimentary Geology, 81(1-2): 73-87.
Haughton, P.D.W., Davis, C., McCaffrey, W.D. and Barker, S., 2009. Hybrid sediment gravity flow deposits – Classification, origin and significance. Marine and Petroleum Geology, 26(10): 1900-1918.
Henrich, R., Kassens, H., Vogelsang, E. and Thiede, J. (1989): Sedimentary facies of glacial- interglacial cycles in the Norwegian Sea during the last 350 ka. - Mar. Geol., 86: 283-319.
Henrich, R. (1990): Cycles, rhythms, and events in Quaternary Arctic and Antarctic glaciomarine deposits. - In Bleil, U. & Thiede, J.(eds.): Geological history of the Polar Oceans: Arctic versus Antarctic.- Nato ASI Series C, Kluwer Acad. Publ., 213-244.

Henrich, R., Wagner, T., Goldschmidt, P. and K. Michels (1995): Depositional regimes in the Norwegian-Greenland Sea: the last two glacial to interglacial transitions.- Geol. Rdschau, 84: 28-48.
Henrich, R., Hanebuth, T.J.J., Krastel, S., Neubert, N. and Wynn, R.B., 2008. Architecture and sediment dynamics of the Mauritania Slide Complex. Marine and Petroleum Geology, 25(1): 17-33.
Henrich, R., Cherubini, Y. and Meggers, H., 2010. Climate and sea level induced turbidite activity in a canyon system offshore the hyperarid Western Sahara (Mauritania): the Timiris Canyon. Marine Geology, 275(1-4): 178-198.
Héquette, A. and Hill, P.R., 1995. Response of the seabed to storm-generated combined flows on a sandy Arctic shoreface, Canadian Beaufort Sea. Journal of Sedimentary Research, 65(3a): 461-471.
Héquette, A., Desrosiers, M., Hill, P.R. and Forbes, D.L., 2001. The influence of coastal morphology on shoreface sediment transport under storm-combined flows, Canadian Beaufort Sea. Journal of Coastal Research, 17(3): 507-516.
Hernández-Molina, F.J., Llave, E. and Stow, D.A.V., 2008. Continental slope contourites. In: M. Rebesco and A. Camerlenghi (Editors), Developments in Sedimentology 60. Elsevier, pp. 379-408.
Hernández-Molina, F.J., Paterlini, M., Violante, R.A., Marshall, P., de Isasi, M., Somoza, L. and Rebesco, M., 2009. Contourite depositional system on the Argentine slope: an exceptional record of the influence of Antarctic water masses. Geology, 37(6): 507-510.
Hernández-Molina, F.J., Paterlini, C.M., Somoza, L., Violante, R.A., Arecco, M.A., de Isasi, M., Rebesco, M., Uenzelmann-Neben, G. and Mashall, P., 2010. Giant mounded drifts in the Argentine Continental Margin: Origins, and global implications for the history of thermohaline circulation. Marine and Petroleum Geology, 27(7): 1508-1530.
Hesse, R., Klauck, I., Khodabakhsh, S. and Piper, D.J.W., 1999. Continental slope sedimentation adjacent to an ice margin. III. The upper Labrador Slope. Marine Geology, 155(3-4): 249-276.
Hesse, R. and Khodabakhsh, S., 2006. Significance of fine-grained sediment lofting from melt-water generated turbidity currents for the timing of glaciomarine sediment transport into the deep sea. Sedimentary Geology, 186(1-2): 1-11.
Hieke, W., 2000. Transparent layers in seismic reflection records from the central Ionian Sea (Mediterranean)—evidence for repeated catastrophic turbidite sedimentation during the Quaternary. Sedimentary Geology, 135(1-4): 89-98.
Hill, P.R., 1983. Detailed morphology of a small area on the Nova Scotian continental slope. Marine Geology, 53(1-2): 55-76.
Hill, P.R., 1984a. Facies and sequence analysis of Nova Scotian slope muds: turbidites vs 'hemipelagic' deposition. In: D.A.V. Stow and D.J.W. Piper (Editors), Fine grained sediments: deep water processes and facies. Geological Society, Special Publication 15, London, pp. 311-318.
Hill, P.R., 1984b. Sedimentary facies of the Nova Scotian upper and middle continental slope, offshore eastern Canada. Sedimentology, 31(3): 293-309.
Horn, D.R., Ewing, M., Horn, B.M. and Delach, M.N., 1971. Turbidites of the Hatteras and Sohm Abyssal Plains, western North Atlantic. Marine Geology, 11(5): 287-323.

Howe, J.A., 1995. Sedimentary processes and variations in slope-current activity during the last Glacial-Interglacial episode on the Hebrides Slope, northern Rockall Trough, North Atlantic Ocean. Sedimentary Geology, 96(3-4): 201-230.
Hughes Clarke, J.E., O'Leary, D.W. and Piper, D.J.W., 1992. The relative importance of mass wasting and deep boundary current activity on the continental rise off western Nova Scotia. In: C.W. Poag and P.C. de Graciansky (Editors), Geologic evolution of Atlantic continental rises. van Nostrand Reinhold, New York, pp. 266-281.
Hundert, T. and Piper, D.J.W., 2008. Late Quaternary sedimentation on the southwestern Scotian Slope, eastern Canada: relationship to glaciation. Canadian Journal of Earth Sciences, 45(3): 267-285.
Huppertz, T.J., 2007. Late Quaternary history of Flemish Pass, southeast Canadian continental margin. M.Sc. Thesis, Dalhousie University, Halifax, 124 pp.
Huppertz, T.J. and Piper, D.J.W., 2009. The influence of shelf-crossing glaciation on continental slope sedimentation, Flemish Pass, eastern Canadian continental margin. Marine Geology, 265(1-2): 67-85.
Huppertz, T.J., Piper, D.J.W., Mosher, D.C. and Jenner, K.A., 2009. The significance of mass transport deposits for the evolution of a proglacial continental slope. In: D.C. Mosher, C.R. Shipp, L. Moscardelli, J.D. Chaytor, C.D.P. Baxter, H.J. Lee and R. Urgeles (Editors), Submarine mass movements and their consequences IV. Springer Verlag, Dordrect, Heidelberg, London, New York, pp. 631-641.
Huppertz, T.J. and Piper, D.J.W., 2010. Interbedded Late Quaternary turbidites and contourites in Flemish Pass, off southeast Canada: their recognition, origin and temporal variation. Sedimentary Geology, 228(1-2): 46-60.
Husebyea, E.S. and Mäntyniemib, P., 2005. The Kaliningrad, West Russia earthquakes on the 21st of September 2004 - Surprise events in a very low-seismicity area. Physics of the Earth and Planetary Interiors, 153(4): 227-236.
Jenner, K.A., Piper, D.J.W., Campbell, D.C. and Mosher, D.C., 2007. Lithofacies and origin of Late Quaternary mass transport deposits in submarine canyons, central Scotian Slope, Canada. Sedimentology, 54(1): 19-38.
Jenner, K.A., Piper, D.J.W., Campbell, C.D. and Mosher, D.C., 2010. Piston cores and supporting high-resolution seismic data, Scotian Slope, Eastern Canada: data and interpretations. Open File 6558, Geological Survey of Canada, Ottawa.
King, E.L., Haflidason, H., Sejrup, H.P. and Løvlie, R., 1998. Glacigenic debris flows on the North Sea Trough Mouth Fan during ice stream maxima. Marine Geology, 152(1-3): 217-246.
King, L.H. and Fader, G.B.J., 1986. Wisconsin glaciation of the Atlantic continental shelf of southeast Canada. Bulletin 363, Geological Survey of Canada, Ottawa.
King, L.H., Rokoengen, K., Fader, G.B.J. and Gunleiksrud, T., 1991. Till-tongue stratigraphy. Geological Society of America Bulletin, 103(5): 637-659.
King, L.H., 1993. Till in the marine environment. Journal of Quaternary Science, 8(4): 347-358.
Laberg, J.S. and Vorren, T.O., 1995. Late Weichselian submarine debris flow deposits on the Bear Island Trough Mouth Fan. Marine Geology, 127(1-4): 45-72.
Laberg, J.S. and Andreassen, K., 2007. Submarine paleo-failure morphology on a glaciated continental margin from 3D seismic data. In: V. Lykousis, D. Sakellariou

and J. Locat (Editors), Submarine mass movements and their consequences. Springer Verlag, 3rd International Symposium, Dordrecht, pp. 11-18.
Lambeck, K. and Chappell, J., 2001. Sea level change through the last glacial cycle. Science, 292: 679-686.
Lemmen, D.S., 1990. Glaciomarine sedimentation in Disraeli Fiord, high Arctic Canada. Marine Geology, 94(1-2): 9-22.
Loncke, L., Gaullier, V., Droz, L., Ducassou, E., Migeon, S. and Mascle, J., 2009. Multi-scale slope instabilities along the Nile deep-sea fan, Egyptian margin: A general overview. Marine and Petroleum Geology, 26(5): 633-646.
Lowe, D.R., 1982. Sediment gravity flows: II. Depositional models with special reference to the deposits of high density turbidity currents. Journal of Sedimentary Petrology, 52(1): 279-297.
Martín-Chivelet, J., Fregenal-Martínez, M.A. and Chacón, B., 2008. Traction structures in contourites. In: M. Rebesco and A. Camerlenghi (Editors), Developments in Sedimentology 60. Elsevier, pp. 159-182.
Martins, L.R. and Willwock, J.A., 1987. Eastern South America Quaternary coastal and marine geology: a synthesis, Quaternary coastal geology of Western Africa and South America. Unesco Reports in Marine Sciences, 43, Dakar, pp. 28-96.
Martins, L.R. and Correa, I.C.S., 1996. Atlas morphology and sedimentology of the southwest Atlantic coastal zone and continental shelf from Cabo Frio (Brazil) and Peninsula Valdés (Argentina), Universidade Federal do Rio Grande do Sul, Rio Grande do Sul.
Martins, L.R., Urien, C.M. and Martins, I.R., 2005a. Gênese dos sedimentos da plataforma continental Atlântica entre o Rio Grande do Sul (Brasil) e Tierra del Fuego (Argentina). Gravel, 3: 85-102.
Martins, L.R., Martins, I.R. and Martins, R.R., 2005b. Utilização de testemunhador livre na região dos Poços de Lama. Gravel, 3: 1-8.
Maslin, M.A., Owen, M., Day, S. and Long, D., 2004. Linking continental-slope failures and climate change: Testing the clathrate gun hypothesis. Geology, 32(1): 53-56.
Maslin, M.A. and Ridgwell, A.J., 2005. Mid-Pleistocene revolution and the ‘eccentricity myth’. In: M.J. Head and P.L. Gibbard (Editors), Early-Middle Pleistocene transitions: the land-ocean evidence. Geological Society, Special Publication 247, London, pp. 19-34.
Matsumoto, K., 1997. Modeled glacial North Atlantic ice-rafted debris pattern and its sensitivity to various boundary conditions. Paleoceanography, 12(2): 271-280.
McCave, I.N., 1985. Sedimentology and stratigraphy of box cores from the HEBBLE site on the Nova Scotian continental rise. Marine Geology, 66(1-4): 59-89.
McHugh, C.M.G., Damuth, J.E. and Mountain, G.S., 2002. Cenozoic mass-transport facies and their correlation with relative sea-level change, New Jersey continental margin. Marine Geology, 184(3-4): 295-334.
Middleton, G.V. and Hampton, M.A., 1976. Subaqueous sediment transport and deposition by sediment gravity flows. In: D.J. Stanley and D.J.P. Swift (Editors), Marine sediment transport and environmental management. Wiley & sons, New York, London, Toronto, Sidney, pp. 197-218.
Migeon, S., Ducassou, E., Le Gonidec, Y., Rouillard, P., Mascle, J. and Revel-Rolland, M., 2010. Lobe construction and sand/mud segregation by turbidity currents and

debris flows on the western Nile deep-sea fan (Eastern Mediterranean). Sedimentary Geology, 229(3): 124-143.
Mosher, D.C., Piper, D.J.W., Campbell, D.C. and Jenner, K.A., 2004. Near-surface geology and sediment-failure geohazards of the central Scotian Slope. AAPG Bulletin, 88(6): 703-723.
Mosher, D.C. and Piper, D.J.W., 2007. Multibeam seafloor imagery of the Laurentian Fan and the 1929 Grand Banks landslide area. Open File 5638, Geological Survey of Canada, Ottawa.
Mulder, T. and Moran, K., 1995. Relationship among submarine instabilities, sea level variations, and the presence of an ice sheet on the continental shelf: An example from the Verrill Canyon Area, Scotian Shelf. Paleoceanography, 10(1): 137-154.
Mulder, T. and Syvitski, J.P.M., 1995. Turbidity currents generated at river mouths during exceptional discharges to the world oceans. Journal of Geology, 103(3): 285-299.
Mulder, T., Migeon, S., Savoye, B. and Faugères, J.-C., 2001. Inversely graded turbidite sequences in the deep Mediterranean: a record of deposits from flood-generated turbidity currents? Geo-Marine Letters, 21(2): 86-93.
Mulder, T., Syvitski, J.P.M., Migeon, S., Faugères, J.-C. and Savoye, B., 2003. Marine hyperpycnal flows: initiation, behavior and related deposits. A review. Marine and Petroleum Geology, 20(6-8): 861-882.
Myrow, P.M. and Southard, J.B., 1996. Tempestite deposition. Journal of Sedimentary Research, 66(5): 875-887.
National Geographic Society; Cartographic Division, 1990. World ocean floors [cartographic material] / produced by the Cartographic Division, National Geographic Society ; John B. Garver Jr., chief cartographer ; painting by Tibor G. Toth ; design, Allen Caroll. In: A. Carroll, J.B. Garver and T.G. Toth (Editors). The Society, Washington, D.C. .
Niedoroda, A.W., Reed, C., Das, H., Hatchett, L. and Perlet, A.B., 2006. Controls of the behaviour of marine debris flows. Norwegian Journal of Geology (Norsk Tidsskrift), 86(3): 256-274.
Niedoroda, A.W., Reed, C.W., Das, H. and Hatchett, L., 2007. The general behavior of mass gravity flows in the marine environment. In: V. Lykousis, D. Sakellariou and J. Locat (Editors), Submarine mass movements and their consequences. Springer Verlag, 3rd International Symposium, Dordrecht, pp. 111-118.
Nittrouer, C.A., Austin, J.A., Field, M.E., Kravitz, J.H., Syvitski, J.P.M. and Wiberg, P.L., 2007. Writing a Rosetta stone: insights into continental-margin sedimentary processes and strata. In: C.A. Nittrouer, J.A. Austin, M.E. Field, J.H. Kravitz, J.P.M. Syvitski and P.L. Wiberg (Editors), Continental margin sedimentation: from sediment transport to sequence stratigraphy. Blackwell Publishing, Oxford, UK, pp. 1-48.
Normark, W.R. and Piper, D.J.W., 1991. Initiation processes and flow evolution of turbidity currents: implications for the depositional record. SEPM Special Publication, 46: 207-230.
Owen, M., Day, S. and Maslin, M., 2007. Late Pleistocene submarine mass movements: occurrence and causes. Quaternary Science Reviews, 26(7-8): 958-978.
Parker, G., Paterlini, C.M. and Violante, R.A., 1994. Edad y génesis del Río de la Plata. Revista de la Asociación Geológica Argentina, 49(1-2): 11-18.

Parker, G., Paterlini, C.M. and Violante, R.A., 1997. El fondo marino. In: E. Boschi (Editor), El Mar Argentino y sus recursos pesqueros, Tomo 1: Antecedentes historicos de las exploraciones en el mar y las caracteristicas ambientaies. Instituto Nacional de Investigación y Desarrollo Pesquero Secretaría de Agricultura, Ganadería, Pesca y Allmentación, Mar del Plata, Argentina, pp. 65-87.
Pierson, T.C., 1981. Dominant particle support mechanisms in debris flows at Mt Thomas, New Zealand, and implications for flow mobility. Sedimentology, 28: 49-60.
Piola, A.R. and Matano, R.P., 2001. Brazil and Falklands (Malvinas) currents. In: J.H. Steele and S.A. Thorpe (Editors), Encyclopedia of Ocean Sciences. Academic Press, San Diego, pp. 340-349.
Piper, D.J.W., 1978. Turbidite muds and silts on deep sea fans and abyssal plains. In: D.J. Stanley and G. Kelling (Editors), Sedimentation in submarine canyons, fans and trenches. Dowden, Hutchinson & Ross, Inc., Stroudsburg, pp. 163-176.
Piper, D.J.W., Mudie, P.J., Aksu, A.E. and Skene, K.I., 1994. A 1 Ma record of sediment flux south of the Grand Banks used to infer the development of glaciation in southeastern Canada. Quaternary Science Reviews, 13(1): 23-37.
Piper, D.J.W. and Deptuck, M., 1997. 5. Fine-grained turbidites of the Amazon Fan: facies characterization and interpretation. In: R.D. Flood, D.J.W. Piper, A. Klaus and L.C. Peterson (Editors), Proceedings of the Ocean Drilling Program, Scientific Results, Volume 155. Ocean Drilling Program, College Station, TX, pp. 79-108.
Piper, D.J.W., Pirmez, C., Manley, P.L., Long, D., Flood, R.D., Normark, W.R. and Showers, W., 1997. 6. Mass transport deposits of the Amazon fan. In: R.D. Flood, D.J.W. Piper, A. Klaus and L.C. Peterson (Editors), Proceedings of the Ocean Drilling Program, Scientific Results, Volume 155, College Station, TX, pp. 109-146.
Piper, D.J.W., Skene, K.I. and Morash, N., 1999. History of major debris flows on the Scotian Rise, offshore Nova Scotia. Current research 1999-E, Geological Survey of Canada, Ottawa.
Piper, D.J.W., 2001. The geological framework of sediment instability on the Scotian Slope: studies to 1999. Open File 3920, Geological Survey of Canada, Ottawa.
Piper, D.J.W. and Normark, W.R., 2001. Sandy fans—from Amazon to Hueneme and beyond. AAPG Bulletin, 85(8): 1407-1438.
Piper, D.J.W. and Hundert, T., 2002. Provenance of distal Sohm Abyssal Plain sediments: history of supply from the Wisconsinan glaciation in eastern Canada. Geo-Marine Letters, 22(2): 75-85.
Piper, D.J.W. and Campbell, D.C., 2002. Surficial geology of the Scotian Slope, eastern Canada. Current Research 2002-E15, Geological Survey of Canada, Dartmouth.
Piper, D.J.W., Mosher, D.C., Gauley, B.-J., Jenner, K.A. and Campbell, D.C., 2003. The chronology and recurrence of submarine mass movements on the continental slope off southeastern Canada. In: J. Locat and J. Mienert (Editors), Submarine mass movements and their consequences: First international symposium. Kluwer Academic Publishers, pp. 299-306.

Piper, D.J.W. and Ingram, S., 2003. Major Quaternary sediment failures on the east Scotian Rise, eastern Canada. Current Research 2003-D1, Geological Survey of Canada (Atlantic), Dartmouth.
Piper, D.J.W. and DeWolfe, M., 2003. Petrographic evidence from the eastern Canadian margin of shelf-crossing glaciations. Quaternary International, 99-100: 99-113.
Piper, D.J.W., 2005. Late Cenozoic evolution of the continental margin of eastern Canada. Norwegian Journal of Geology (Norsk Tidsskrift), 85: 305-318.
Piper, D.J.W. and Brunt, R.A., 2006. High-resolution seismic transects of the upper continental slope off southeastern Canada. Open File 5310, Geological Survey of Canada, Ottawa.
Piper, D.J.W., Shaw, J. and Skene, K.I., 2007. Stratigraphic and sedimentological evidence for late Wisconsinan sub-glacial outburst floods to Laurentian Fan. Paleogeography, Paleoclimatology, Paleoecology, 246(1): 101-119.
Piper, D.J.W. and Normark, W.R., 2009. Processes that initiate turbidity currents and their influence on turbidites: a marine geology perspective. Journal of Sedimentary Research, 79(6): 347-362.
Piper, D.J.W., Deptuck, M., Mosher, D.C., Hughes Clarke, J.E. and Migeon, S., 2011. Erosional and depositional features of glacial meltwater discharges on the eastern Canadian continental margin, SEPM Special Publication
Popescu, I., Lericolais, G., Panin, N., Normand, A., Dinu, C. and Le Drezen, E., 2004. The Danube submarine canyon (Black Sea): morphology and sedimentary processes. Marine Geology, 206(1-4): 249-265
Porebski, S.J., Meischner, D. and Görlich, K., 1991. Quaternary mud turbidites from the South Shetland Trench (West Antarctica): recognition and implications for turbidite facies modelling. Sedimentology, 38(4): 691-715.
Powell, R.D. and Molnia, B.F., 1989. Glacimarine sedimentary processes, facies and morphology of the south-southeast Alaska shelf and fjords. Marine Geology, 85(2-4): 359-390.
Pratson, L.F., Ryan, W.B.F., Mountain, G.S. and Twichell, D.C., 1994. Submarine canyon initiation by downslope-eroding sediment flows: Evidence in late Cenozoic strata on the New Jersey continental slope. Geological Society of America Bulletin, 106(3): 395-412.
Pratson, L.F. and Coakley, B.J., 1996. A model for the headward erosion of submarine canyons induced by downslope-eroding sediment flows. Geological Society of America Bulletin, 108(2): 225-234.
Pratson, L.F. and Haxby, W.F., 1996. What is the slope of the U.S. continental slope? Geology, 24(1): 3-6.
Pratson, L.F., Nittrouer, C.A., Wiberg, P.L., Steckler, M.S., Swenson, J.B., Cacchione, D.A., Karson, J.A., Murray, A.B., Wolinsky, M.A., Gerber, T.P., Mullenbach, B.L., Spinelli, G.A., Fulthorpe, C.S., O'Grady, D.B., Parker, G., Driscoll, N.W., Burger, R.L., Paola, C., Orange, D.L., Field, M.E., Friedrichs, C.T. and Fedele, J.J., 2007. Seascape evolution on clastic continental shelves and slopes. In: C.A. Nittrouer, J.A. Austin, M.E. Field, J.H. Kravitz, J.P.M. Syvitski and P.L. Wiberg (Editors), Continental margin sedimentation: from sediment transport to sequence stratigraphy. Blackwell Publishing, Oxford, UK, pp. 339-380.

Prior, D.B., Coleman, J.L. and Garrison, L.E., 1979. Digitally acquired undistorted side-scan sonar images of submarine landslides, Mississippi River delta. Geology, 7(9): 423-425.
Prior, D.B. and Doyle, E.H., 1985. Intra-slope canyon morphology and its modification by rockfall processes, U.S. Atlantic continental margin. Marine Geology, 67(1-2): 177-196.
Puig, P., Ogston, A.S., Mullenbach, B.L., Nittrouer, C.A. and Sternberg, R.W., 2003. Shelf-to-canyon sediment-transport processes on the Eel continental margin (northern California). Marine Geology, 193(1-2): 129-149.
Reynolds, T., 2000. Reservoir architecture in the Mars field, deepwater Gulf of Mexico, USA: the implications of production, seismic, core and well-log data, GCSSEPM Foundation 20th Annual Research Conference: Deep Water reservoirs of the World, Houston, TX, pp. 877-893.
Rodriguez, A.N. and Anderson, J.B., 2004. Contourite origin for shelf and upper slope sand sheet, offshore Antarctica. Sedimentology, 51(4): 699-711.
Rose, L.E. and Kuehl, S.A., 2010. Recent sedimentation patterns and facies distribution on the Poverty Shelf, New Zealand. Marine Geology, 270(1-4): 160-174.
Schaaf, A., 1996. Sea level changes, continental shelf morphology, and global paleoecological constraints in the shallow benthic realm: a theoretical approach. Palaeogeography, Palaeoclimatology, Palaeoecology, 121(3-4): 259-271.
Schlager, W. and Camber, O., 1986. Submarine slope angles, drowning unconformities, and self-erosion of limestone escarpments. Geology, 14(9): 762-765.
Schmid, C., Siedler, G. and Zenk, W., 2000. Dynamics of Intermediate Water Circulation in the subtropical South Atlantic. Journal of Physical Oceanography, 30(12): 3191-3211.
Shanmugam, G. and Moiola, R.J., 1982. Eustatic control of turbidites and winnowed turbidites. Geology, 10(5): 231-235.
Shaw, J., Piper, D.J.W., Fader, G.B.J., King, E.L., Todd, B.J., Bell, T., Batterson, M.J. and Liverman, D.G.E., 2006. A conceptual model of the deglaciation of Atlantic Canada. Quaternary Science Reviews, 25(17-18): 2059-2081.
Shepard, F.P., 1981. Submarine canyons: multiple causes and long-time persistence. AAPG Bulletin, 65(6): 1062-1077.
Sivkov, V., Gorbatskiy, V., Kuleshov, A. and Zhurov, Y., 2002. Muddy contourites in the Baltic Sea: an example of a shallow-water contourite system. In: D.A.V. Stow, C.J. Pudsey, J.-C. Faugères and A.R. Viana (Editors), Deep-water contourite systems: modern drifts and ancient series, seismic and sedimentary characteristics. Geological Society, Memoir 22, London, pp. 121-136.
Skene, K.I. and Piper, D.J.W., 2003. Late Quaternary stratigraphy of Laurentian Fan: a record of events off the eastern Canadian continental margin during the last deglacial period. Quaternary International, 99-100: 135-152.
Skene, K.I. and Piper, D.J.W., 2006. Late Cenozoic evolution of Laurentian Fan: development of a glacially-fed submarine fan. Marine Geology, 227(1-2): 67-92.
Smith, R.U., 2004. Silled sub-basins to connected tortuous corridors: sediment distribution systems on topographically complex sub-aqueous slopes. In: S.A. Lomas and P. Joseph (Editors), Confined turbidite systems. Geological Society, London, Special Publication 222, London, pp. 23-43.

Solheim, A., Faleide, J.I., Andersen, E.S., Elverhøi, A., Forsberg, C.F., Vanneste, K., Uenzelmann-Neben, G. and Channell, J.E.T., 1998. Late Cenozoic seismic stratigraphy and glacial geological development of the East Greenland and Svalbard-Barents Sea continental margins. Quaternary Science Reviews, 17(1-3): 155-184.
Stanley, D.J., 1981. Unifites: structureless muds of gravity-flow origin in Mediterranean basins. Geo-Marine Letters, 1(2): 77-83.
Stea, R.R., Piper, D.J.W., Fader, G.B.J. and Boyd, R., 1998. Wisconsinan glacial and sea-level history of Maritime Canada and the adjacent continental shelf: A correlation of land and sea events. Geological Society of America Bulletin, 110(7): 821-845.
Stow, D.A.V. and Lovell, J.P.B., 1979. Contourites: their recognition in modern and ancient sediments. Earth-Science Reviews, 14(3): 251-291.
Stow, D.A.V., 1979. Distinguishing between fine-grained turbidites and contourites on the Nova Scotian deep water margin. Sedimentology, 26(3): 371-387.
Stow, D.A.V., 1982. Bottom currents and contourites in the North Atlantic. Bulletin de l'Institut de Geologie du Bassin d'Aquitaine, 31: 151-166.
Stow, D.A.V. and Piper, D.J.W., 1984. Deep-water fine-grained sediments: facies models. In: D.A.V. Stow and D.J.W. Piper (Editors), Fine grained sediments: deep water processes and facies. Geological Society, Special Publication 15, London, pp. 611-646.
Stow, D.A.V. and Holbrook, J.A., 1984. North Atlantic contourites: an overview. In: D.A.V. Stow and D.J.W. Piper (Editors), Fine grained sediments: deep water processes and facies. Geological Society, Special Publication 15, London, pp. 245-256.
Stow, D.A.V., 1985. Fine-grained sediments in deep water: An overview of processes and facies models. Geo-Marine Letters, 5(1): 17-23.
Stow, D.A.V. and Wetzel, A., 1990. Hemiturbidite: a new type of deep water sediment. In: J.R. Cochran and D.A.V. Stow (Editors), Proceedings Ocean Drilling Program Scientific Results, 116, College Station, TX, pp. 25-34.
Stow, D.A.V., Faugères, J.-C., Howe, J.A., Pudsey, C.J. and Viana, A.R., 2002. Bottom currents, contourites and deep-sea sediment drifts: current state of the art. In: D.A.V. Stow, C.J. Pudsey, J.A. Howe, J.-C. Faugères and A.R. Viana (Editors), Deep-water contourite systems: modern drifts and ancient series, seismic and sedimentary characteristics. The Geological Society, Memoir 22, London, pp. 7-20.
Stow, D.A.V., Hunter, S.E., Wilkinson, D. and Hernández-Molina, F.J., 2008. The nature of contourite deposition. In: M. Rebesco and A. Camerlenghi (Editors), Developments in Sedimentology 60. Elsevier, pp. 143-156.
Stramma, L. and England, M.H., 1999. On the water masses and mean circulation of the South Atlantic Ocean. Journal of Geophysical Research, 104(C9): 20863-20883.
Sultan, N., Cochonat, P., Canals, M., Cattaneo, A., Dennielou, B., Haflidason, H., Laberg, J.S., Long, D., Mienert, J., Trincardi, F., Urgeles, R., Vorren, T.O. and Wilson, C., 2004. Triggering mechanisms of slope instability processes and sediment failures on continental margins: a geotechnical approach. Marine Geology, 213(1-4): 291-321.

Sultan, N., Gaudin, M., Berne, S., Canals, M., Urgeles, R. and Lafuerza, S., 2007. Analysis of slope failures in submarine canyon heads: An example from the Gulf of Lions. Journal of Geophysical Research, 112: F01009.
Syvitski, J.P.M., Alexander, C.R., Field, M.E., Gardner, J.V., Orange, D.L. and Yun, J.W., 1996a. Continental-slope sedimentation: the view from northern California. Oceanography, 9(3): 163-167.
Syvitski, J.P.M., Andrews, J.T. and Dowdeswell, J.A., 1996b. Sediment deposition in an iceberg-dominated glacimarine environment, East Greenland: basin fill implications. Global and Planetary Change, 12(1-4): 251-270.
Takahashi, T., 1981. Debris flow. Annual Review of Fluid Mechanics, 13(1): 57-77.
Taylor, J., Dowdeswell, J.A., Kenyon, N.H., Whittington, R.J., van Weering, T.C.E. and Mienert, J., 2000. Morphology and Late Quaternary sedimentation on the North Faeroes slope and abyssal plain, North Atlantic. Marine Geology, 168(1-4): 1-24.
Taylor, J., Dowdeswell, J.A. and Siegert, M.J., 2002. Late Weichselian depositional processes, fuxes, and sediment volumes on the margins of the Norwegian Sea (62-75°N). Marine Geology, 188(1-2): 61-77.
Traykovski, P.A., Geyer, W.R., Irish, J.D. and Lynch, J.F., 2000. The role of wave-induced density-driven fluid mud flows for cross-shelf transport on the Eel River continental shelf. Continental Shelf Research, 20(16): 2113-2140.
Tripsanas, E.K., Piper, D.J.W. and Campbell, D.C., 2008. Evolution and depositional structure of earthquake-induced mass movements and gravity flows: southwest Orphan Basin, Labrador Sea. Marine and Petroleum Geology, 25(7): 645-662.
Uliana, M.A., Biddle, K.T. and Cerdan, J., 1989. Mesozoic extension and the formation of Argentine sedimentary basins. In: A.J. Tankard and H.R. Balkwill (Editors), Extensional tectonics and stratigraphy of the North Atlantic margins. American Association of Petroleum Geologists, AAPG Memoir 46, Tulsa, Oklahoma, pp. 599-614.
Urien, C.M. and Ewing, M., 1974. Recent sediments and environments of southern Brazil, Uruguay, Buenos Aires and Rio Negro continental shelf. In: C.A. Burke and C.L. Drake (Editors), The geology of continental margins. Springer Verlag, Berlin, pp. 157-177.
van Weering, T.C.E. and van Iperen, J., 1984. Fine-grained sediments of the Zaire deep-sea fan, southern Atlantic Ocean. In: D.A.V. Stow and D.J.W. Piper (Editors), Fine grained sediments: deep water processes and facies. Geological Society, Special Publication 15, London, pp. 95-113.
Vanney, J.-R. and Stanley, D.J., 1983. Shelf break physiography: an overview. In: D.J. Stanley and G.T. Moore (Editors), The Shelfbreak : critical interface on continental margins. Society of Economic Paleontologists and Mineralogists, Special Publication 33, Tulsa, pp. 1-24.
Verdicchio, G. and Trincardi, F., 2008. Mediterranean shelf-edge muddy contourites: examples from the Gela and South Adriatic basins. Geo-Marine Letters, 28(3): 137-151.
Viana, A.R., Faugères, J.-C. and Stow, D.A.V., 1998. Bottom-current-controlled sand deposits — a review of modern shallow- to deep-water environments. Sedimentary Geology, 115(1-4): 53-80.
Viana, A.R. and Faugères, J.-C., 1998. Upper slope sand deposits: the example of Campos Basin, a latest Pleistocene-Holocene record of the interaction between

alongslope and downslope currents. In: M.S. Stoker and D. Evans (Editors), Geological processes on continental margins: sedimentation, mass-wasting and stability. Geological Society, London, Special Publication 129, London, pp. 287-316.

Violante, R.A. and Parker, G., 2004. The post-last glacial maximum transgression in the de la Plata River and adjacent inner continental shelf, Argentina. Quaternary International, 114(1): 167-181.

Vittori, J., Morash, A., Savoye, B., Marsset, T., Lopez, M., Droz, L. and Cremer, M., 2000. The Quaternary Congo deep-sea fan: preliminary results on reservoir complexity in turbiditic systems using 2D high resolution seismic and multibeam data, GCSSEPM Foundation 20th Annual Research Conference: Deep Water reservoirs of the World, Houstan, TX, pp. 1045-1058.

von Lom-Keil, H., Schlacht, R. and Spieß, V., 2003. Bottom current influenced sedimentation in the Argentine Basin and on the Argentine continental margin reflected in high resolution seismic data, EGS-AGU-EUG Joint Assembly. European Geophysical Society, pp. 11459.

Vorren, T.O. and Laberg, J.S., 1997. Trough mouth fans — palaeoclimate and ice-sheet monitors. Quaternary Science Reviews, 16(8): 865-881.

Vorren, T.O., Laberg, J.S., Blaume, F., Dowdeswell, J.A., Kenyon, N.H., Mienert, J., Rumohr, J. and Werner, F., 1998. The Norwegian-Greenland Sea continental margins: morphology and late Quaternary sedimentary processes and environment. Quaternary Science Reviews, 17(1-3): 273-302.

Wade, J.A. and MacLean, B.C., 1990. The geology of the southeastern margin of Canada, Part 2: Aspects of the geology of the Scotian Basin from recent seismic and well data. In: M.J. Keen and G.L. Williams (Editors), Geology of the continental margin of eastern Canada. Geological Survey of Canada, Ottawa, pp. 190-238.

Waelbroeck, C., Labeyrie, L., Michel, E., Duplessy, J.-C., McManus, J.F., Lambeck, K., Balbon, E. and Labracherie, M., 2002. Sea level and deep water temperature changes derived from benthic foraminifera isotopic records. Quaternary Science Reviews, 21(1-3): 295-305.

Wells, P.G. and Daborn, G.R., 1997. The Rio de la Plata - an environmental overview. Dalhousie University, Halifax, 248 pp.

Wright, L.D. and Friedrichs, C.T., 2006. Gravity-driven sediment transport on continental shelves: A status report. Continental Shelf Research, 26(17-18): 2092-2107

2. The significance of mass transport deposits for the evolution of a proglacial continental slope

Tammo J. Huppertz[1] David J.W. Piper[2], D. C. Mosher[2], K. Jenner[2]

1 University of Bremen, Faculty of Geosciences, FB 5 Klagenfurter Strasse 28359 Bremen, Germany. huppertz@uni-bremen.de

2 Geological Survey of Canada, Natural Resources Canada Bedford Institute of Oceanography, 1 Challenger Drive, Dartmouth, Nova Scotia, B2Y 4A2, Canada

Citation: Huppertz, T.J., Piper, D.J.W., Mosher, D.C. and Jenner, K.A., 2009. The significance of mass transport deposits for the evolution of a proglacial continental slope. In: D.C. Mosher, C.R. Shipp, L. Moscardelli, J.D. Chaytor, C.D.P. Baxter, H.J. Lee and R. Urgeles (Editors), Submarine mass movements and their consequences IV. Springer Verlag, Dordrect, Heidelberg, London, New York, pp. 631-641.

Abstract

The continental slope off southeast Canada has been influenced by ice sheet fluctuations in the Pleistocene. These ice sheets have supplied the bulk of the sediment, which is the driving process for the observed slope architecture. Several studies with a more local scope have explored the Late Quaternary geological history of the Scotian slope and have used the sedimentary sequence including mass transport deposits to understand depositional processes on the slope over time. Using this existing understanding of the geological setting on the slope, a new slope-wide regional seismic stratigraphy was developed. This stratigraphy was used to understand variations of MTD deposition on a regional scale on the Scotian Margin. The spatial occurrence of different types of MTDs and their relationship to the regional morphology is used to establish different MTD zones. Mapping of the zones improved the understanding of slope stability and the importance of MTDs for continental margin evolution.

Keywords: mass transport deposits, mass-failure, geohazards, seafloor geomorphology, submarine canyon, submarine valley, slope classification, Scotian Slope

1. Introduction

Mass transport deposits (MTDs) are widely recognized along continental margins and record a component of the erosional history of continental margins. Regional studies have emphasized on the importance of mass wasting along glaciated continental margins (Canals et al. 2000, Piper 2005, Rise et al. 2005, Wilken and Mienert 2006).

1.1 Regional Geology

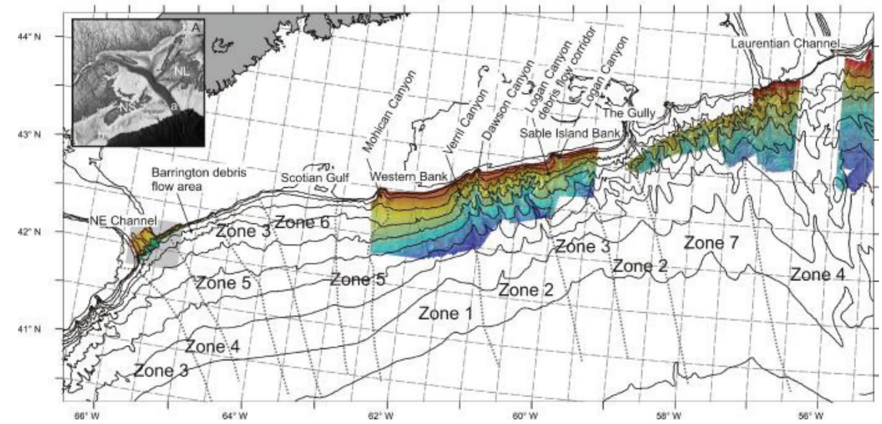

Fig. 1: Overview map of the Scotian Slope and its different MTD zones, for more details see results section; inset A shows the working area along the SE Canadian continental margin: NS: Nova Scotia, NF: Newfoundland, a: Laurentian Channel, b: Northeast Channel

The Scotian Slope (Fig. 1) is a mid-latitude margin, which has been influenced by advance and retreat of ice sheets since at least oxygen isotope stage 12, when high sedimentation rates in deeper water were first observed (Piper et al. 1994, Piper and Normark 1989). The ice sheets supplied large amounts of poorly sorted sediment to the shelf edge as till, together with suspended sand and mud in glacial outwash. Sedimentation rates on the slope are as high as 1–5 m/ka when glacial ice crossed the shelf. Major mass-transport flows were common in the late Quaternary of the Scotian Slope. Several studies with a more local approach have reported the stratigraphic and volumetric importance of such flow deposits along this margin (Berry and Piper 1993, Campbell et al. 2004, Gauley 2001, Mosher et al. 2004, Piper 2001, Piper et al. 1985, Shor and Piper 1989). Most of the flows were initiated during glacial stages, but a clear link between glaciation and MTD deposition could usually not be shown (Mosher et al. 2004). Some MTDs are related to retrogressive failure initiated on the lower rise by oversteepening by salt tectonic processes

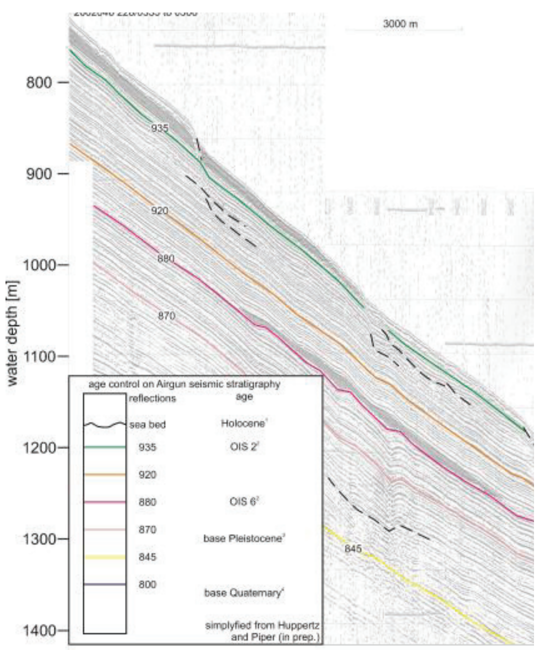

Figure 2: typical central Scotian slope Airgun seismic line from Zone 1 showing seismic reflectors and erosional planes (back dashed lines) and their relationship to MTDs. Deeper lying disturbances can have a pronounced impact on the upper sequence; the age control of the seismic reflections was taken from previous studies in the area: [1]Piper and Campbell (2000), [2]Piper and Sparkes (1990), [3]Piper (2001) and [4]Piper and Ingram (2003); area covered by stratigraphy box is a data gap.

and triggered by seismic shaking (Mosher and Piper 2007). Failure was probably favored by high rates of proglacial sedimentation on the continental slope (Piper 2005). Seaward of some transverse troughs, glacigenic debris flows formed by direct flow of till into deep water (Piper and Normark submitted). Large blocky failures resulted from failure along weak layers, as a result of erosion by canyons (Piper and Ingram 2003).

In contrast to previous studies that have focused on individual MTDs and have emphasized processes, the work reported here attempts a regional synthesis of MTDs throughout much of the Scotian margin, in order to place the formation of MTDs in a spatial and temporal context. It is based on a new Quaternary slope-wide seismic stratigraphy that was established from Huntec sparker and airgun seismic data. The stratigraphy was developed from previous studies (Campbell et al. 2004, Gauley 2001, Hundert and Piper 2008, Piper 2001) and jump-correlated (correlation based on character including presence of erosional surfaces, across canyons where no continuous sections exists) across canyons based on regional sedimentation rates and correlation using widespread MTDs (Huppertz and Piper submitted). Age control for the shallow sequence is given by published radiocarbon dates in piston cores (Piper 2001); the age of markers deeper in the stratigraphy was based on correlation with till tongues on the upper slope and ties to wells (Piper 2001, Piper and Brunt 2006). The reflectors shown in Figs. 2–4 have the following approximate ages: sea bed is usually Holocene (Piper and Campbell 2002), 935 = last glacial maximum (Piper and Sparkes 1990); 880 = marine isotope stage 6 (Piper and Sparkes 1990); 800 to 845 = early Quaternary (Piper 2001, Piper and Ingram 2003) . Shallow mass transport deposits along the Scotian slope have been identified using high resolution Huntec boomer and sparker systems, which can image the upper 100 m of sea bed at a vertical resolution of 1 m (Mosher and Simpkin 1999). Lower resolution airgun seismic data was used for the deeper sedimentary sequence from 100-500 m sub-bottom, at a resolution of tens of meters.

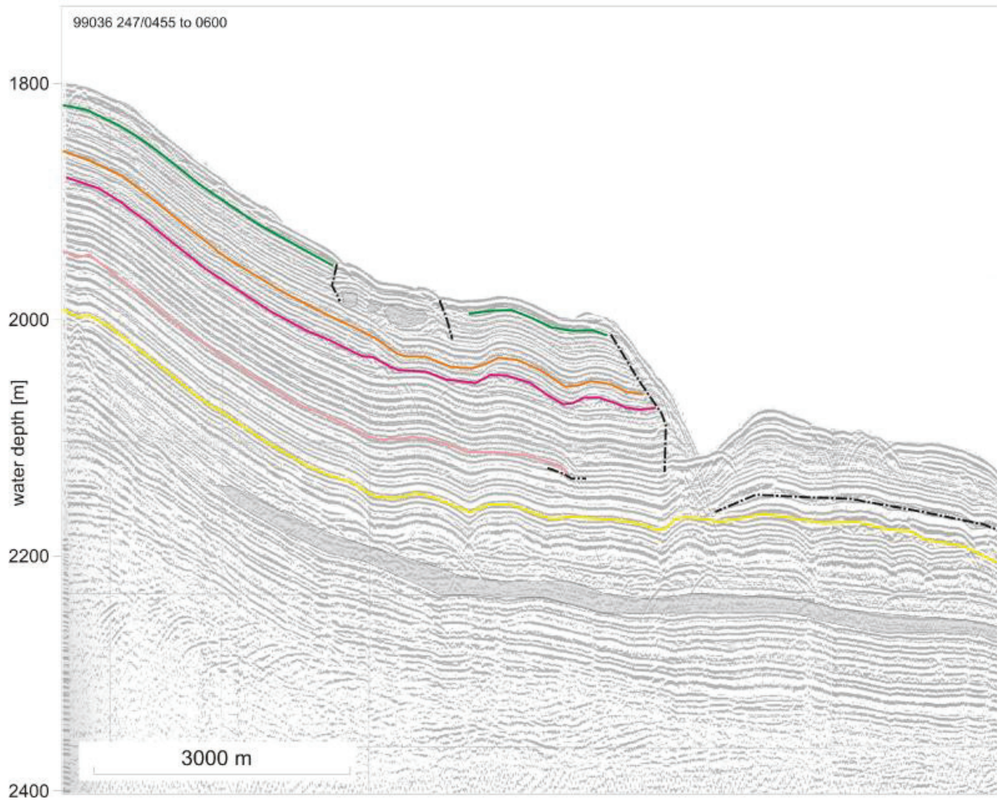

Figure 3: Airgun seismic profile showing the age control on the major scarp at ~ 2100 m water depth. The first continuous reflection under the scarp is close to the base of the Quaternary sequence. This profile is from area 1 and shows well stratified sediments with few erosional surfaces within the sequence; reflector colors as Fig. 2

2. Mass transport deposits and their distribution

Sediment failures occur throughout the slope area from the shelf break at ~500 m to the lower slope at 4500 m. No clear stratigraphic variability in failures can be resolved at the resolution of the seismic correlation, but the distribution of MTDs varies spatially. Those failures that are not related to canyons, e. g. off Western Bank (Campbell 2000), can be related to scarps and failure planes upslope from the deposit (Fig. 2). Within canyons, small MTDs are interbedded with turbidite sands and appear linked to failures on canyon walls and at the heads of the canyons (Jenner et al. 2007).

Head scarps are widely found along the Scotian margin and range from a few meters to 100s of meters high (Fig. 3), both at the seafloor and buried by younger sediment. Some scarps appear to be the result of repeated retrogressive failures (Mosher et al. 2004). The oldest scarp in the central area cuts back to at least oxygen isotope stage 6 (Fig. 3).

	slope character	erosion	slope gradient	type area
Zone 1	smooth slope, inter-canyon areas	few scarps	low	off western Bank
Zone 2	areas highly dissected by deeply incised canyons, small lensoid MTDs on canyon floors	in canyons very high, in areas between canyons low	variable	Verrill Canyon to Logan Canyon DF corridor
Zone 3	abundant lenticular MTDs on low angle slopes	locally, linked to MTDs	low to medium	west of Scotian Gulf
Zone 4	MTDs in areas with stable canyons off shelf troughs	in canyons and areas of overspill	low to high	NE Fan and Laurentian Fan
Zone 5	widespread failures, no well developed canyons	high erosion, widespread	medium	Albatross area, Barrington DF area
Zone 6	widespread debris flows and cut-and-fill morphology, little stratification	widespread	low to medium	Off Scotian Gulf
Zone 7	deeply incised old canyon systems with major wall failures, no canyons along shelf break	high to very high	high	easternmost Scotian Slope

Table 1: summary of MTD zones on the Scotian Slope; DF= debris flow, MTDs=mass transport deposits

In some cases, more than one MTD appears geometrically linked to particular failure planes and erosional surfaces upslope and downslope (Fig. 2), implying that once established, a failure surface might evolve and release several retrogressively failed MTDs. Downslope, MTDs are commonly thinner on the mid-slope and thicker on the rise, suggesting bypassing of sediment.

Spatially, the distribution of MTDs is closely related to the shelf and slope morphology (Huppertz and Piper in preparation), the prevailing ice sheet regime and the occurrence of older failures in the area. Variation in these parameters has been used to classify the slope into different zones, each with different distribution of MTDs (Fig 1, Table 1):

Zone 1 includes areas of smooth slope and inter-canyon areas characterized by thick, well stratified sediments with few erosional surfaces and related MTDs < 20 ms thick. The overall regional slope gradient is low and lacks deeply incised canyons. The outer shelf areas are characterized by shallow banks. The type area is the slope off Western Bank between Mohican Channel and Verrill Canyon (Table 1).

Zone 2 consists of areas highly dissected by canyons, with canyon floors covered by MTDs and turbidite sands (e.g. as described by Jenner et al. (2007)). Intercanyon highs between canyons are well stratified but show frequent erosional surfaces throughout, many of which terminate in arcuate headscarps. Zone 2 occurs in areas of higher regional gradient seaward of shallow banks that in many places show buried tunnel valleys (King 2001, Piper et al. 2007). The type area is the areas from Verrill Canyon to the area just west of the Logan Canyon debris flow corridor (Table 1).

Zone 3 is characterized by abundant, lenticular MTDs, which occur throughout the stratigraphic succession (Fig 4). Individual deposits are volumetrically small. The thin interbedded stratified sediments are of minor importance and frequently show erosion and cuts; they are usually highly discontinuous. The upper slope shows discontinuous sequences with frequent erosion (Table 1).

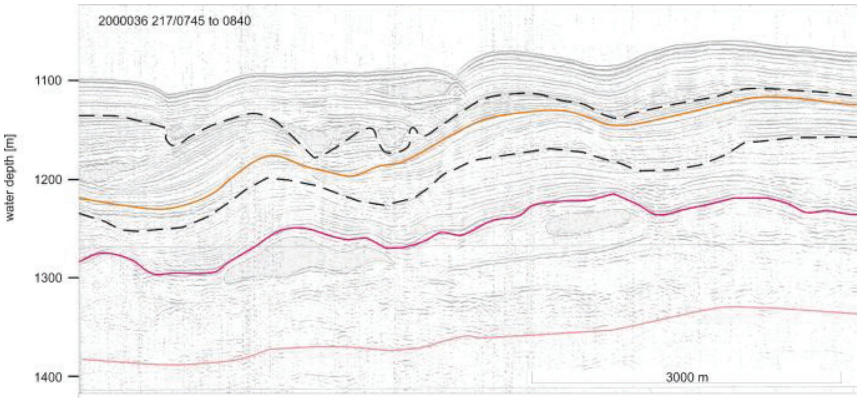

Figure 4: Airgun seismic slope-parallel transect between the Barrington Debris Flow area and the Scotian Gulf showing the sedimentary sequence in the western slope area with several small, lensoid-shaped MTDs. some of the stratified units may represent overspill deposits from turbidity activity. The black dashed lines are prominent erosional surfaces and may represent paleo-horizons.

Zone 4 is characterized by mass transport deposits in areas, where stable canyon systems off shelf troughs have been observed, e. g. off NE Fan (Robichaud 2006) and Laurentian Fan (Skene and Piper 2006). These areas are characterized by deeply incised, narrow canyons from the shelf break to almost 4000 m water depth with MTDs along the canyon floors in the case of NE Fan and on levees in the case of Laurentian Fan (Table 1).

Zone 5 is characterized by widespread failures with no morphologically well developed canyons. The head scarps of these failures are usually difficult to identify because retrogressive failures may have eroded older head scarps. The MTDs are sometimes related to shallow canyon systems and can cover large areas downslope. They may have infilled or eroded older canyon systems completely. The individual flows are several 10s of ms thick and frequently their thickness cannot be observed on the seismic data; most of the flows have a local source area and show short runout distances and blocky surfaces (Albatross area (Shor and Piper 1989) Barrington debris flow area (Mosher et al. this volume)) (Table 1).

Zone 6 is characterizes by widespread debris flows and cut-and-fill morphologies. This zone was only observed off the Scotian Gulf (Fig. 1), where almost no stratified sequences occur (Piper 2000). The lower slope is characterized by several small lobe-like structures built from few canyons on the slope (Table 1).

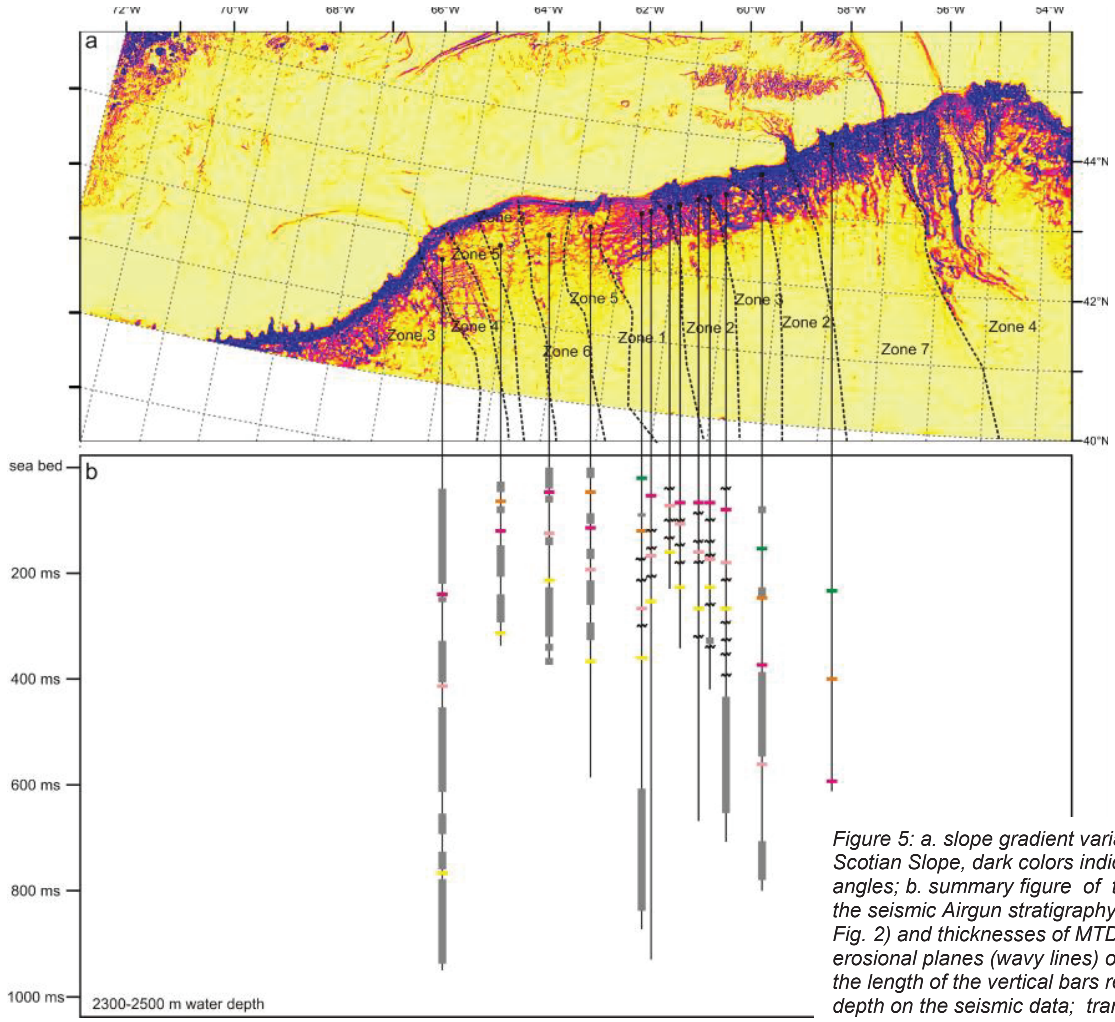

Figure 5: a. slope gradient variations along the Scotian Slope, dark colors indicate steep slope angles; b. summary figure of the spatial variation of the seismic Airgun stratigraphy (colored bars as in Fig. 2) and thicknesses of MTDs (gray bars) and erosional planes (wavy lines) on the Scotian Slope, the length of the vertical bars represents penetration depth on the seismic data; transect points between 2300 and 2500 m water depth.

Zone 7 is found on the easternmost Scotian Slope and is characterized by deeply incised canyons and major wall failures (Piper and Ingram 2003) which created to major MTDs on the rise and outer slope. The complete slope is characterized by MTDs of various sizes. No stratigraphic control was possible in this area (Table 1).

3. Discussion

There are several different types of MTDs found along the Scotian slope:

(a) Massive blocky MTDs , mostly found in Zone 5 are likely derived from deeply buried, consolidated sediment on the upper to mid slope (Barrington area: Mosher et al. this volume; Albatross area: (Shor and Piper 1989).

(b) Retrogressive failures like the 1929 failure. These are common in zone 1 and in intercanyon areas of zone 2. They may be favored by high sedimentation rates from plumes; triggering may be from retrogressive failure from salt tectonics on the lower slope or from steep canyon walls.

(c) Glacigenic debris flows. As argued by Piper and Normark (submitted), these are absent on the steep slopes off Laurentian Channel and Northeast Channel, probably because they have transformed to turbidity currents. They appear to be present off the Scotian Gulf in zone 6.

(d) Stacked small-scale lensoid-shaped MTDs. These flows are mostly found in areas with no canyons and a low slope gradient as the large parts of the western Scotian slope in zone 3. These flows were initiated by local failures due to cutting by melt water and retrogressive failures (Hill 1984) or from mud tectonics and related oversteepening (Piper and Sparkes 1987).

(e) Major slope-wide erosion in areas of deeply incised canyons where wall failures are frequently observed. These MTDs were only observed in zone 7 where the MTDs have eroded most of the slope sequence at least once and can be found down to the rise areas (Piper and Ingram 2003).

The observed distribution of different types of MTDs along the margin may indicate that the character of the initiated MTD is somehow related to the regional slope gradient and the processes along the slope break. The different zones have different slope gradients (Fig 5). Overall, slope and upper rise gradients are less west of Mohican Channel than in the east. Upper slope gradients are least in zones 1 and 6 whereas highest slope gradients are found in zone 7 and 5. Slope erosion is thus related to gradients: low MTD activity is found in Zones 1 and 2 which have low gradients, whereas steeper slopes are characterized by major slope failures (zones 5 and 7). An exception are the shelf troughs, where major sediment transfer to the shelf break occurs, especially off the Laurentian Channel (Shaw et al. 2006) and the NE Channel (Hundert and Piper 2008), where sediment from Scotian Shelf sources creates sediment failures and characterizes the areas seaward of the troughs.

In the case of slope failures, the failed sediment consists principally of blocks of variably consolidated slope sediment (Mosher et al. 2004). The role of sediment transported directly from the shelf, such as jökulhlaups at ice maxima (Tripsanas and Piper 2008) or by storms after ice has retreated (Piper 2005) in some cases erode only surficial sediments (Canals et al. 2006) but in the case of larger event will erode deeper lithified sediment along the canyon walls (Piper et al. 2007).

The extent and frequency of sediment failure appears related to the erosional history of an area. Most of sediment failures occur over time in the same areas (mainly zones 3, 4, 5, 6 and 7) whereas zones 1 and the local highs of zone 2 have been stable for most of the Quaternary (Figs. 1, 3 and 5). Therefore, sediment failure is likely related to processes, which occur again and again in the areas of observed sediment failures.

The presence of MTDs also enhances the possibility of more frequent failures in the same areas as failure can precondition for further failures (Fig. 5). Due to sediment failures, slope angle and stability are changed significantly and may promote retrogressive failure or change the pathways for turbidity currents flowing down the slope. Lobe areas, such as the area seaward of the Laurentian Channel, are only constructed in areas where frequent failures generate the lobe. Thus, over several glacial cycles, areas of failure are generally similar and can be used to predict future areas of geohazards by sediment failures (Fig 5). Isolated sediment failures within an area are more likely related to random slope failures which are not related to cyclic events as glaciation, but are more likely related to random initiating events such as passive margin seismicity.

4. Conclusions

Construction of the Quaternary Scotian Slope has been highly impacted by several different types of mass transport deposits. The distinct character of the different types of MTDs could be used to classify the slope into seven different MTD zones. These zones are (1) well stratified areas with few MTDs, (2) highly canyonized areas with mostly complete sequences in intercanyon areas, (3) areas of several small-scale lensoid MTDs, (4) MTDs on local highs and canyon floors in areas with stable canyons and shelf troughs, (5) area of widespread local failures on the mid-slope with few shallow channels, (6) large blocky debris flows and (7) areas of deeply incised canyons with slope-wide sediment failures. The spatial distribution of these different zones allows an assessment of the role of direct glacial supply, preconditioning by high sedimentation rates and older failures, and the effect of canyon erosion and regional gradient on the style of MTDs on the slope.

5. Acknowledgements

This is Natural Resources Canada Earth Sciences Sector Contribution No. 2009???. Work funded by the Geological Survey of Canada, the Natural Sciences and Engineering Research Council of Canada, and the Canada Program of Energy R & D; we would like to thank the two reviewers, Jan Laberg and John Andrews for the helpful comments.

6. References

Berry JA and Piper DJW, 1993. Seismic stratigraphy of the central Scotian rise: a record of continental margin glaciation. Geo-Mar Lett 13: 197-206

Campbell DC, 2000. Relationship of sediment properties to failure horizons for a small area of the Scotian Slope. Current research 2000-D8, Geol Surv Can

Campbell DC, Shimeld JW, Mosher DC and Piper DJW, 2004. Relationships between sediment mass-failure modes and magnitudes in the evolution of the Scotian Slope, offshore Nova Scotia, Offshore Technology Conference Houston Texas pp. OTC 16743

Canals M, Puig P and Durrieu de Madron X, 2006. Flushing submarine canyons. Nature 444: 354-357

Canals M, Urgeles R and Calafat AM, 2000. Deep sea-floor evidence of past ice streams off the Antarctic Peninsula. Geology 28: 31-34

Gauley B-JL, 2001. Lithostratigraphy and sediment failure on the central Scotian slope, Department of Earth Sciences. Dalhousie University, Halifax pp. 214.

Hill PR, 1984. Sedimentary facies of the Nova Scotian upper and middle continental slope, offshore eastern Canada. Sedimentology 31: 293-309.

Hundert T and Piper DJW, 2008. Late Quaternary sedimentation on the southwestern Scotian Slope, eastern Canada: relationship to glaciation. Can J Earth Sci 45: 267-285.

Huppertz TJ and Piper DJW, submitted. Scotian slope seismic stratigraphy and failure history. Mar Petrol Geol

Jenner KA, Piper DJW, Campbell DC and Mosher DC, 2007. Lithofacies and origin of late Quaternary mass transport deposits in submarine canyons, central Scotian Slope, Canada. Sedimentology, 54: 19-38.

King EL, 2001. A glacial origin for Sable Island: ice and sea-level fluctuations from seismic stratigraphy on Sable Island Bank, Scotian Shelf, offshore Nova Scotia. Current research 2001-D19, Geol Surv Can

Mosher DC and Piper DJW, 2007. Analysis of multibeam seafloor imagery of the Laurentian Fan and the 1929 Grand Banks landslide area. In: V Lykousis et al (eds), Submarine mass movements and their consequences. Springer The Netherlands pp. 77-88.

Mosher DC, Piper DJW, Campbell DC and Jenner KA, 2004. Near-surface geology and sediment-failure geohazards of the central Scotian Slope. AAPG Bull 88: 703-723.

Mosher DC and Simpkin PG, 1999. Environmental marine geosciences 1: status and trends of marine high-resolution seismic reflection profiling: data acquisition. Geosci Can 26: 174-188.

Piper DJW, 2000. Pleistocene ice outlets on the central Scotian Slope, offshore Nova Scotia. Current research 2000-D7, Geol Surv Can

Piper DJW, 2001. The geological framework of sediment instability on the Scotian Slope: studies to 1999. Open File 3920, Geol Surv Can

Piper DJW, 2005. Late Cenozoic evolution of the continental margin of eastern Canada. Nor J Geol 85: 305-318.

Piper DJW and Brunt RA, 2006. High-resolution seismic transects of the upper continental slope off southeastern Canada. Open File 5310, Geol Surv Can

Piper DJW and Campbell DC, 2002. Surficial geology of the Scotian Slope, eastern Canada. Current Research 2002-E15, Geol Surv Can

Piper DJW, Farre JA and Shor A, 1985. Late Quaternary slumps and debris flows on the Scotian Slope. Geol Soc of Am Bull 96: 1508–1517.

Piper DJW and Ingram S, 2003. Major Quaternary sediment failures on the east Scotian Rise, eastern Canada. Current Research 2003-D1, Geol Surv Can

Piper DJW, Mudie PJ, Aksu AE and Skene KI, 1994. A 1 Ma record of sediment flux south of the Grand Banks used to infer the development of glaciation in southeastern Canada. Quaternary Sci Rev 13: 23-37.
Piper DJW and Normark WR, 1989. Late Cenozoic sea-level changes and the onset of glaciation: impact on continental slope progradation off eastern Canada. Mar Petrol Geol 6: 336-347.
Piper DJW and Normark WR, submitted. Jour Sed Res
Piper DJW, Shaw J and Skene KI, 2007. Stratigraphic and sedimentological evidence for late Wisconsinan sub-glacial outburst floods to Laurentian Fan. Paleogeogr Paleoecl 246: 101-119.
Piper DJW and Sparkes R, 1987. Proglacial sediment instability features on the Scotian Slope at 63°W. Mar Geol 76: 15-31.
Piper DJW and Sparkes R, 1990. Pliocene - Quaternary geology of the central Scotian Slope. Open File 2233, Geol Surv Can
Rise L, Ottensen D, Berg K and Lundin E, 2005. Large-scale development of the mid-Norwegian margin during the last 3 million years. Mar Petrol Geol 22: 33-44.
Robichaud M, 2006. Late Quaternary evolution of the Northeast Fan, offshore Nova Scotia, Department of Earth Sciences. Dalhousie University, Halifax, pp. 98.
Shaw J, Piper DJW, Fader GBJ, King EL, Todd BJ, Bell T, Batterson MJ and Liverman DGE, 2006. A conceptual model of the deglaciation of Atlantic Canada. Quaternary Sci Rev 25: 2059-2081.
Shor A and Piper DJW, 1989. A large Late Pleistocene blocky debris flow on the central Scotian slope. Geo-Mar Lett 9: 153-160.
Skene KI and Piper DJW, 2006. Late Cenozoic evolution of Laurentian Fan: development of a glacially-fed submarine fan. Marine Geology, 227: 67-92.
Tripsanas EK and Piper DJW, 2008. Late Quaternary stratigraphy and sedimentology of Orphan Basin: implications for meltwater dispersal in the southern Labrador Sea. Paleogeography, Paleoclimatology, Paleoecology, 260: 521-539.
Wilken M and Mienert J, 2006. Submarine glacigenic debris flows, deep-sea channels and past ice-stream behaviour of the East Greenland continental margin. Quaternary Science Reviews, 25: 784-810.

3. Controls on the temporal and spatial variability of slope architecture on a glaciated margin: the southeast Canadian continental margin

Citation:
Huppertz, T.J. and Piper, D.J.W., submitted by mid-May 2011. Controls on the temporal and spatial variability of slope architecture on a glaciated margin: the southeast Canadian continental margin. Marine and Petroleum Geology.

3.0. Abstract

The Scotian Slope on the southeast Canadian continental margin is a passive margin highly influenced by glaciations since oxygen isotope stage 12 when ice first crossed the shelf. A new regional slope-wide seismic stratigraphy for high resolution Huntec and lower resolution airgun data has been established based on previous studies with a more local scope. The new seismic stratigraphy is used to improve the understanding of timing of sedimentation with a special focus on mass transport deposits (MTDs). Different types of MTDs characterize not only different areas over time, but during specific isochrones, different types of MTDs are found along the margin in different areas. The observed types of MTDs and deposition from meltwater plume sedimentation are directly related to the ice sheet behavior at the shelf edge. Till tongues and well stratified areas are linked to stagnant ice with little slope erosion, whereas seawards of shelf troughs either major MTDs characterize the slope or if slope angles are too high, sediment bypassing can be observed on parts of the slope. These observations in spatial and temporal variability of slope deposition resulted in a slope-sedimentation scheme: glaciated slopes can be classified into different zones characterized by specific shelf ice sheet behavior resulting in certain sedimentary processes on the slope and their resulting deposits.

3.1. Introduction and purpose

Glaciated mid-latitude margins are highly influenced by ice sheet fluctuations. The architecture of such continental margins is governed by the interplay of depositional and erosive processes. Most important depositional processes include meltwater plume-sediment fallout (Hesse et al., 1999; Tripsanas and Piper, 2008) and deposition from various types of mass transport processes and turbidity currents (Armishaw et al., 1998; Baltzer et al., 1998; Clausen, 1998; Mosher et al., 2004). Most of the sediment constructing the slope is transported to the area during times of deglaciation (Taylor et al., 2002; Piper, 2005; Shaw et al., 2006). Hemipelagic interstadial sedimentation is generally low (Piper, 2005). The upper slope areas are frequently characterized by tills and related sediment failures, which can affect large areas along the slope (Clausen, 1998; Mosher et al., 2004).

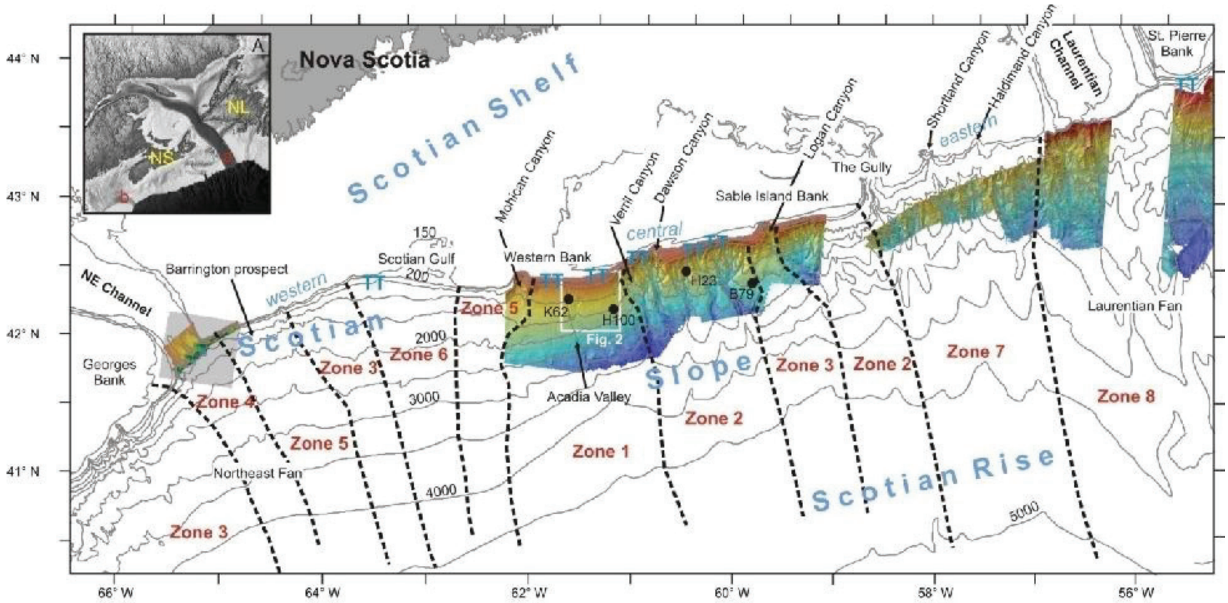

Figure 3.1: Map showing the setting of the Scotian Margin with the MTD zones (modified after Huppertz et al., 2009) and the areas of known till tongues (indicated by the blue TTs) (Piper and Brunt, 2006) along the shelf break. The bathymetry is in 500 m steps below 500 m, shallower lines are the 150 m and 200 m line. Areas of multibeam data are indicated. Major exploration wells are shown: D79-Balvenie, H23-Newburn, K62-Acadia, H100-Shubenacadie. Inset A shows the position of the margin along the southeast Canadian Margin: NS: Nova Scotia, NL: Newfoundland, a. Laurentian Channel, b. Northeast Channel.

The Scotian Slope is an excellent area to address questions about the architecture of mid-latitude glaciated margins because of its geographic and morphological setting (**Fig. 1**). Different ice sheet processes were active simultaneously along the margin, e.g. ice streams, stagnant ice or areas of calving ice (Piper and MacDonald, 2001; Piper et al., 2003; Mosher et al., 2004; Piper, 2005). Furthermore, the data availability and especially the spacing of the high-resolution sparker data allow imaging of shallow subsurface structures at high resolution. Hundreds of long piston cores (Jenner et al., 2010) provide detailed groundtruth and shallow chronology along this slope.

The purpose of this study was to determine: (i) how does sedimentation vary spatially along the margin at different time slices over glacial– interglacial cycles, (ii) how does the timing of ice advances influence the types and styles of sedimentation and (iii) how do sedimentation processes change and hence sedimentation patterns temporally and spatially on the margin, and (vi) why does the sedimentation pattern vary spatially.

3.2. Geological setting

3.2.1 Introduction

The passive continental margin off Nova Scotia was formed during initial rifting of the Atlantic in the early Mesozoic (Wade and MacLean, 1990). The morphology and geometry of the Scotian Slope has been greatly influenced by glaciations since oxygen isotope stage (OIS) 12 (Piper et al., 1994), when large amounts of sediment were transported to the continental margin. The entire slope from eastern Georges Bank slope to St Pierre slope has been influenced by various slope failures (Mosher et al., 2004; Huppertz et al., 2009; Mosher et al., 2009). The shelf break occurs in water depths between 100 and 400 m. The slope angle is highest just below the shelf break and decreases seawards towards the rise (**Fig. 1**).

3.2.2 Oceanography and Quaternary geology

The oceanic circulation is mainly influenced by the northeast flowing Gulf Stream and the southwestwards flowing continuation of the Labrador Current. The continental slope down to 2000 m is mainly influenced by the cold Labrador Current, which is pushed seawards by the Laurentian Channel outflow water and comes again inshore 200 km west of the Laurentian Channel (**Fig. 1**). The Scotian Rise is influenced by the southwestward flowing Western Boundary undercurrent shallower than 4000 m water depth and the Cold Filament Current at ~5000 m water depth (Hogg, 1983; McCave, 1985; Tucholke et al., 1985; Han, 2004).

Large parts of the slope are characterized by a thin (< 1 m) muddy Holocene sequence draping the underlying glacial sequence (Piper and Campbell, 2002) Glacial deposits dominate the sedimentary sequence on the Scotian Slope since OIS 12 (Piper et al., 1994) and glacial ice reached the shelf break several times. During the maximum ice extent on the shelf, the Scotian Shelf and upper slope was influenced by sediment input from ice streams in Laurentian Channel, the Scotian Gulf and Northeast Channel (Gauley, 2001; Piper and MacDonald, 2001; Robichaud, 2006; Hundert and Piper, 2008). Sediment failures were common off several areas along the slope, initiated by various ice sheet processes (Mulder and Moran, 1995; Mosher et al., 2004). The presence of ice at the shelf break has also been documented from till tongues (**Fig. 1**) (Piper and Brunt, 2006), from plume sedimentation (Piper and Skene, 1998) and deposits from subglacial meltwater (Piper, 2005; Shaw et al., 2006; Piper et al., 2007). Slope failures are common downslope from the stacked till tongues, which result in MTDs in deeper water (Pickerill et al., 2001; Piper and McCall, 2003; Piper, 2005).

During the last glacial cycle (OIS 2), the ice sheet receded along the western Scotian Shelf from the slope break by circa 19 cal ka (16 ka ^{14}C) (Shaw et al., 2006;

Hundert and Piper, 2008). Shelf basins landward of the central Scotian Slope (**Fig. 1**) were ice-free as early as 22.5 cal ka (17 ka ^{14}C) and open water conditions dominated by 16.3 cal ka (14 ka ^{14}C), shown in storm event deposits at this time (Gipp and Piper, 1989; Gipp, 1994); the inner shelf was ice-free by 13.8 cal ka (12 ka) (Piper and Fehr, 1991). The eastern outer Scotian Shelf and the mouth of the Laurentian Channel (**Fig. 1**) were not ice-free until 13.8-15.1 cal ka (12 to 13 ka ^{14}C) (King, 1996).

Various types of mass transport deposits have been recognized along all the Scotian Slope (Berry and Piper, 1993; Mosher et al., 1994; Piper and Ingram, 2003; Mosher et al., 2004; Piper et al., 2005; Huppertz et al., 2009; Mosher et al., 2009). These flows have been interpreted as mostly initiated during deglaciation by earthquakes, although variation in pore water pressure, canyon undercutting, current erosion or release of gas hydrates may all have played a role (Mosher et al., 2004; Jenner et al., 2007).

The morphology of the Scotian Slope is characterized by a variety of slope valleys (**Fig. 1**). Canyons are large structures cutting into older sedimentary strata and the larger canyons are connected to the shelf break. These canyons pass downslope to channels on the lower slope and rise and are conduits for coarse-grained sediments (e.g. turbidite flows and their deposits). Gullies are smaller valleys on the slope that in many cases lead to larger canyons or channels. Various processes, including retrogressive failure, erosion by turbidity currents, and erosion by hyperpycnal meltwater discharge have been interpreted as contributing to the formation of slope valleys (Piper, 2005).

3.2.3 Previous Quaternary seismic stratigraphy

The seismic stratigraphy on the Scotian Slope was developed from Huntec sparker and airgun seismic data and was dated using ^{14}C radiocarbon dating in cores (**Table 1**) and biostratigraphy from petroleum exploration wells (Fig. 1) (Piper and Sparkes, 1990; Mosher et al., 2004; Piper, 2005; Jenner et al., 2007). The airgun seismic stratigraphy was defined in a type section on the central Scotian Slope (Fig. 2) (Mosher et al., 1989; Piper and Sparkes, 1990). For age control links were established to the Shubenacadie H-100 and Acadia K-62 wells (**Fig. 1**) (Piper, 2001) and to till tongues off Western Bank (**Fig. 1**) (Mosher et al., 2004). They provide stratigraphic control for the entire Quaternary section.

Higher resolution seismic stratigraphy using the Huntec sparker data set was previously established in several local studies (Mosher et al., 1989; Baltzer et al., 1994; Gauley, 2001; Robichaud, 2006; Hundert and Piper, 2008) but most have not been previously correlated with each other. Huntec sparker data only rarely images as deep as the OIS 6 reflector.

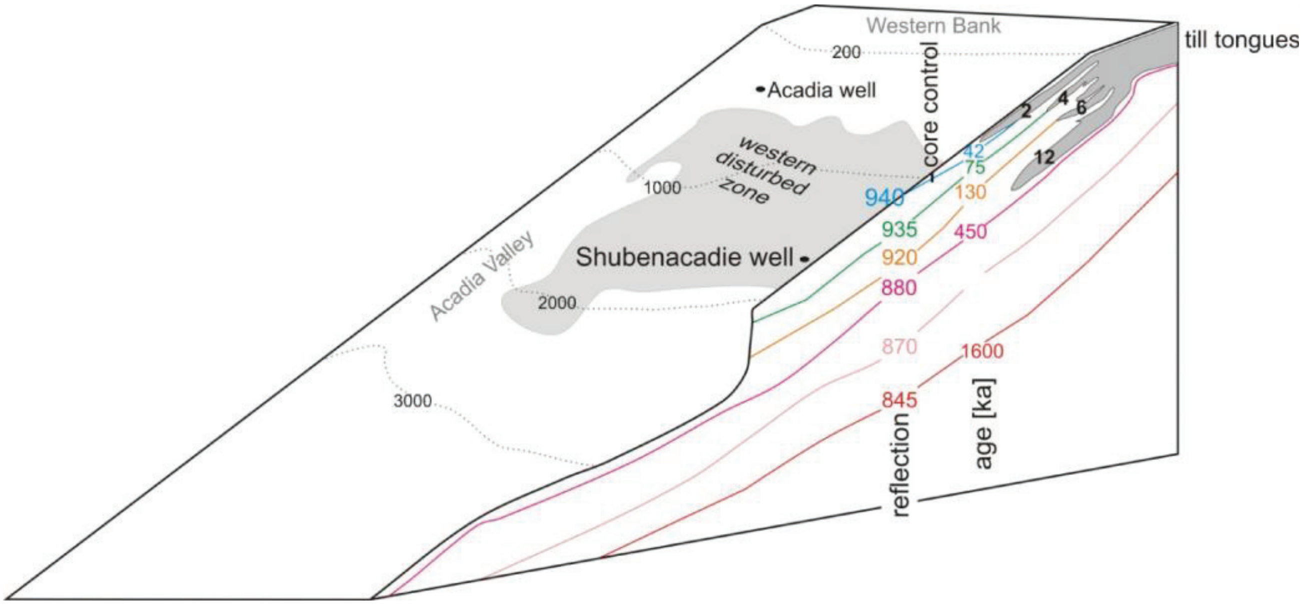

Figure 3.2: Schematic sketch of the airgun seismic stratigraphy in zone 1 based on Campbell (2000). Key airgun reflections are shown as 940, 935 etc. Reflection 940 is defined in this study in the Balvenie area (see also Fig. 5), reflections 935 and 920 are from Gauley (2001), reflections 880-845 are from Mosher et al (1989; 2004). Ages <50 ka are based on 14C chronology on cores (Table 1, Fig. 14); > 50 ka are based on ages inferred for till tongues from Mosher et al (1989; 2004).

Table 3-1: Radiocarbon dates used in this study to date the Huntec seismic reflections < 50 ka. All ^{14}C dates were calibrated using CALIB 6.0.

cruise	core	lab no.	depths [cm]	14 C age	std dev	reservoir corrected	calibrated	std dev cal
82004	2	Beta15245	659-660	18320	440	17870	19378	1022
83012	6	TO7747	445-448	36420	420	35970	39178	799
86034	40	Beta 20733	690-691	18700	300	18250	19869	687
86034	41	TO2387	623-624	16050	220	15600	17240	24
88010	18	TO8302	584-585	18390	130	17940	19446	321
99036	38	TO9547	863-875	23710	260	23260	26171	549
99036	39	TO10877	500-525	24130	1050	23680	26556	2097
99036	28	Beta139258	667-668	19040	50	18590	20283	205
99036	35	TO9548	258-261	18100	230	17650	19166	509
99036	12	TO8773	989-990	17620	160	17170	18154	128
2002046	33	OS39338	1085-1086	17800	95	17350	18858	279
2002046	40	OS39340	870-880	18600	120	18150	19734	448
2000Harrison	3	OS39342	450-460	18500	110	18050	19582	376
2000Harrison	8	TO9777	388-389	18040	280	17590	18962	762
2000Harrison	10	OS39341	253-254	17700	100	17250	18673	885
2000036	30	Beta149805	505-506	42100	1280	41650	43305	4475

3.3. Methods

3.3.1. Field and lab data acquisition

Large areas in the central and eastern parts of the Scotian Slope down to 2500 m water depth have been imaged with the Simrad EM300 and EM1002 multibeam systems (**Fig. 1**) (Pickerill et al., 2001; Mosher et al., 2004; Mosher and Piper, 2007). These previously published data provide a context for interpreting the Quaternary geology.

Airgun data collected since the early 1970s were used to image the upper 100-150 m of the sedimentary sequence, establishing a large dataset (several thousand line-km) especially in the central Scotian Slope (**Fig. 3**). The higher resolution Huntec sparker system, imaging the upper 50 m of sea bed at a resolution of 1 m and penetration of up to 150 m (Mosher and Simpkin, 1999), is available for large parts of the central Scotian Slope. To the east and west, fewer lines exist (**Fig. 3**).

Select piston cores (**Fig. 3**) were mainly used to provide chronology and ground-truth for lithofacies and thus sedimentation processes and were selected from the dataset reported by Jenner et al. (2010).

All radiocarbon dates were recalibrated using CALIB 6 (**Table 1**). A marine reservoir correction (Δ = 450 yr) was applied to all samples, as the potential variability in the reservoir effect during the early Holocene and late glacial (Bondevik et al., 2006; Cao et al., 2007) is not well enough known.

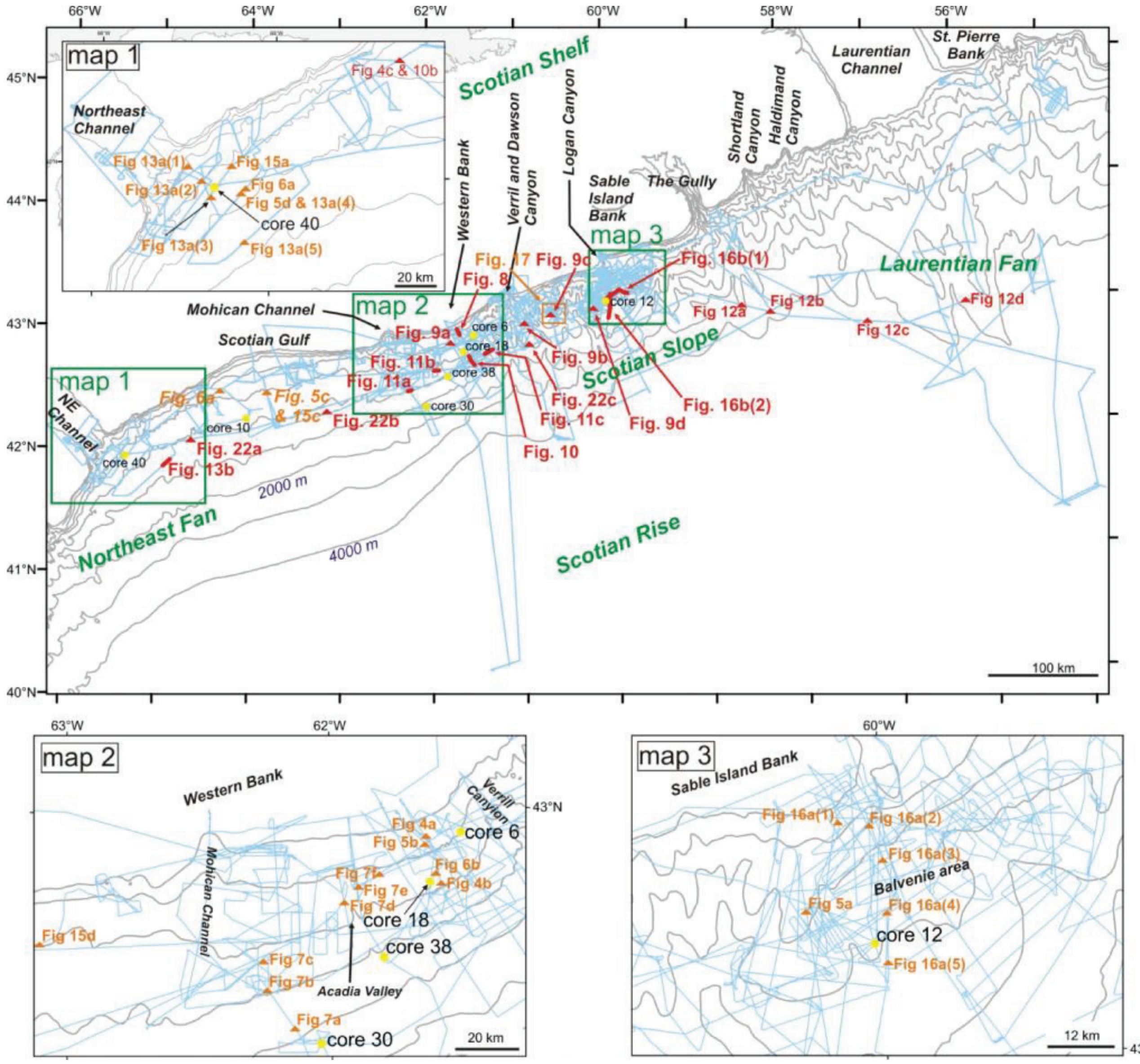

Figure 3.3: Map showing all used core and seismic data (blue lines) and the position of illustrated seismic data on the Scotian slope. Red colors indicates airgun seismic figures, orange colors are Huntec seismic figures: the triangles indicate seismic point sections, whereas lines show longer stretches of seismic data; maps 1-3 are shown in green on the main map, major key cores are shown as yellow dots.

3.3.2. Approach used in this study

The existing core and seismic data were correlated (**Fig. 3**) and published interpretations revisited and re-evaluated. Previous schemes for sediment facies and seismic stratigraphies were harmonized and correlated based on unpublished datasets. Furthermore, new jump-correlations and lithological correlations further refined the framework.

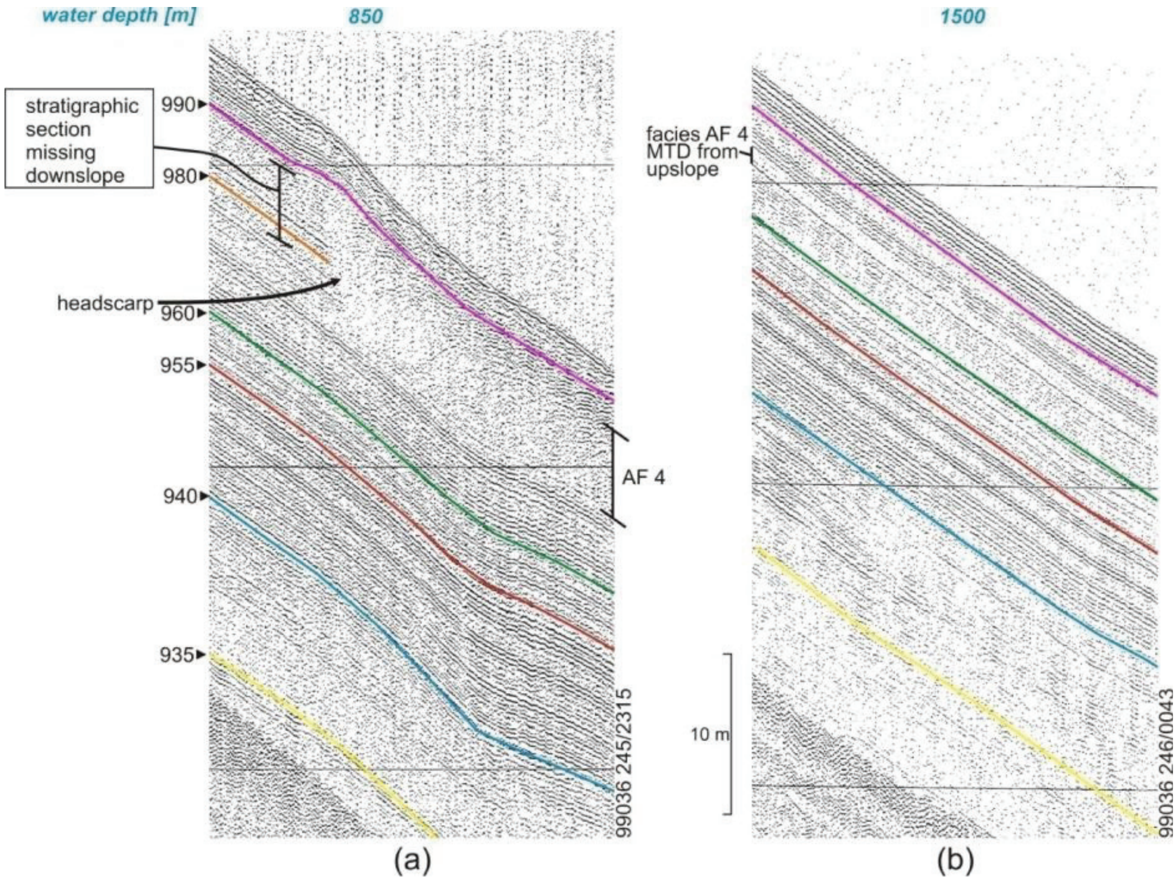

Figure 3.4: Sediment failure in the area of the type section of Mosher et al. (1989; 2004) and its continuation downslope. This thin failure had been overlooked in earlier studies; acoustic facies AF 4 is also indicated. (a) headscarp of failure, (b) downslope thinning of failure deposit.

3.4. Results

3.4.1. Seismic stratigraphy

The previously used Huntec type section on the Scotian Slope was defined by Mosher et al. (2004). It is incomplete due to a failure plane close to the seafloor (**Fig. 4**). Thus, a new seismic type section was defined close to the Balvenie B-79 exploration well (**Figs. 1, 3 and 5a**), where a continuous sedimentary record lacking mass failures was found. Six key Huntec seismic reflections were defined in this section and correlated to the Mosher et al. (2004) type section (**Figs. 5 and 6**). The seismic reflections were annotated calling seabed the topmost reflection, in this case SS 1000, and counting downwards. The key horizons can be traced for long distances and correspond in many places to changes in facies.

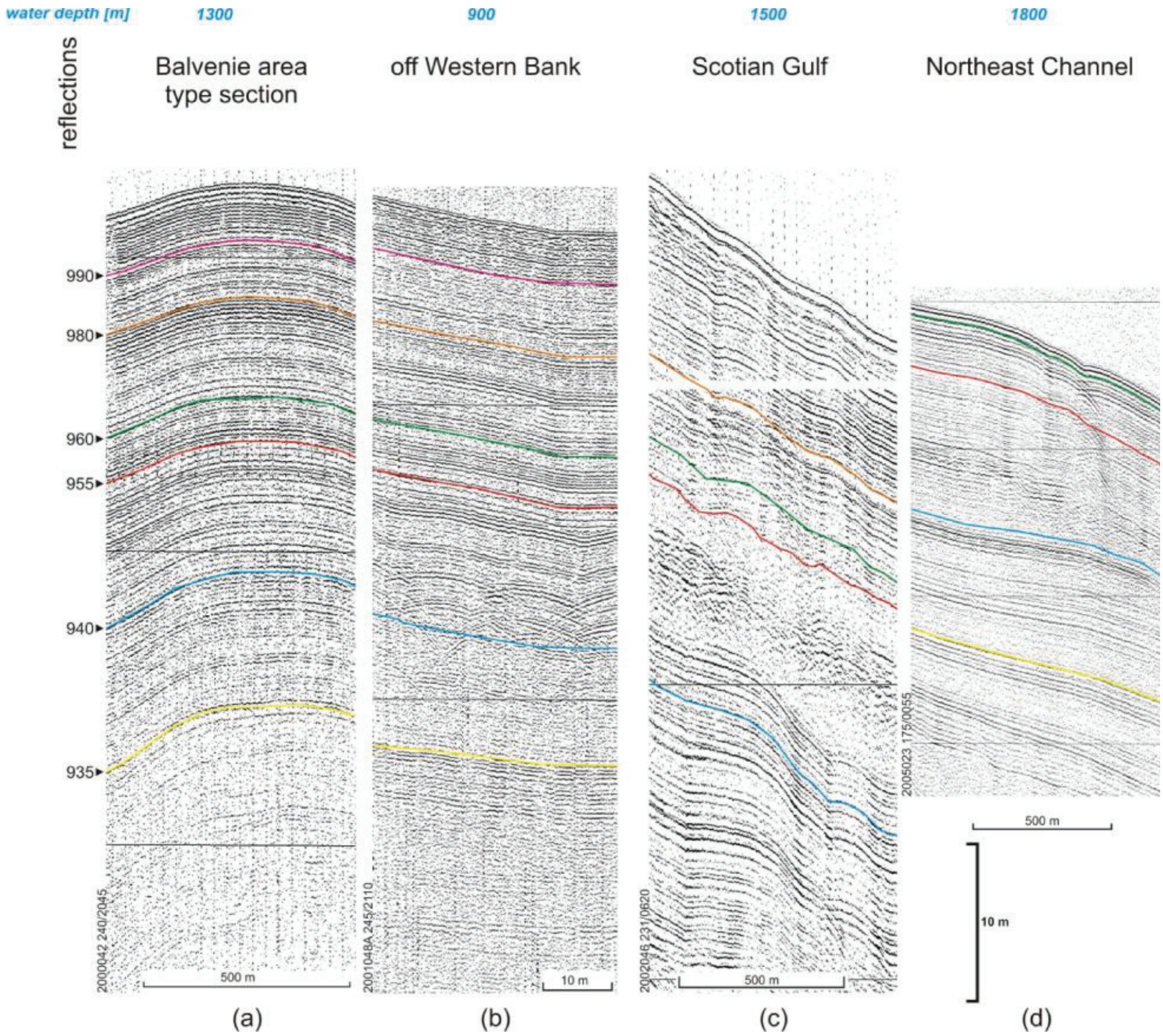

Figure 3.5: Huntec type section for seismic stratigraphy in Huntec seismic profiles near the Balvenie well and the correlation of the reflections along the Scotian Slope; please note differences in horizontal scales.

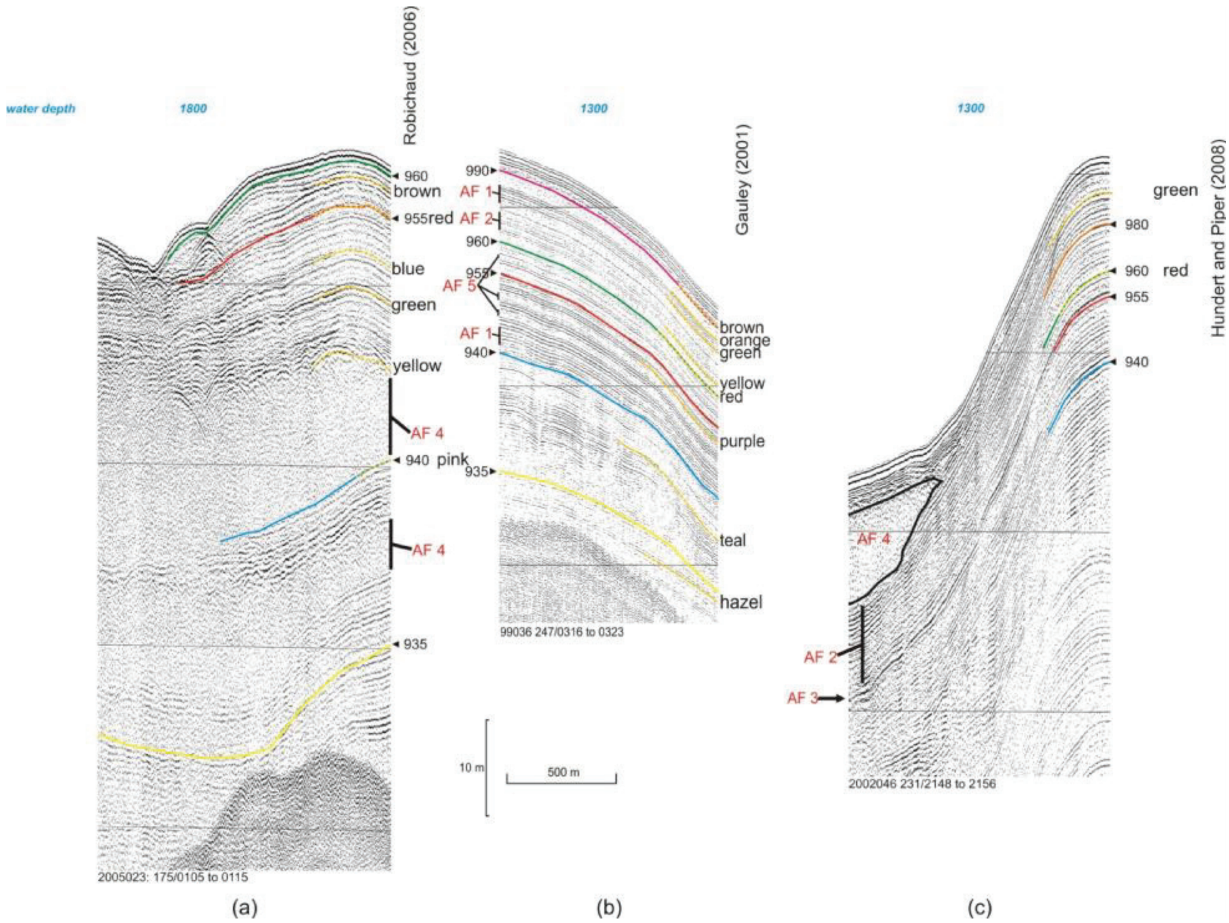

Figure 3.6: Correlation of the new Huntec seismic stratigraphy to previous local nomenclature schemes (Gauley, 2001; Robichaud, 2006; Hundert and Piper, 2008). Also shows examples of acoustic facies (AF) 1-5.

Direct tracing was rarely possible for more than 50 km along strike due to erosion and canyon incision (**Fig. 1**). Down-dip correlations were easier, as erosional scarps are less common. Such direct tracing shows gradual variation of seismic character on the slope. For example, the sections in **Fig. 7e and 7f** are almost in the same water depth and separated by 7 km. The 960 reflection occurs at the base of a distinctive packet of high-amplitude reflections and reflection 935 is at the top of another similar packet **(Fig. 7).** Reflection 960 occurs in Fig. **7c** below a MTD, a similar setting is observed in **Fig. 7a and d**, even though it is shown that these MTDs are not physically connected, but likely resulted from the same event. This procedure also showed gradual change in acoustic character both along strike (e.g. from **Fig. 7c to 7f**) and down dip.

Across canyons and major scarps, jump correlation was used. This correlation is based on matching the seismic character in similar water depths using ^{14}C ages in adjacent cores and erosional planes as a guide, assuming these erosional planes represent regional failures (**Figs. 5, 7 and 9**) (Piper, 2005).

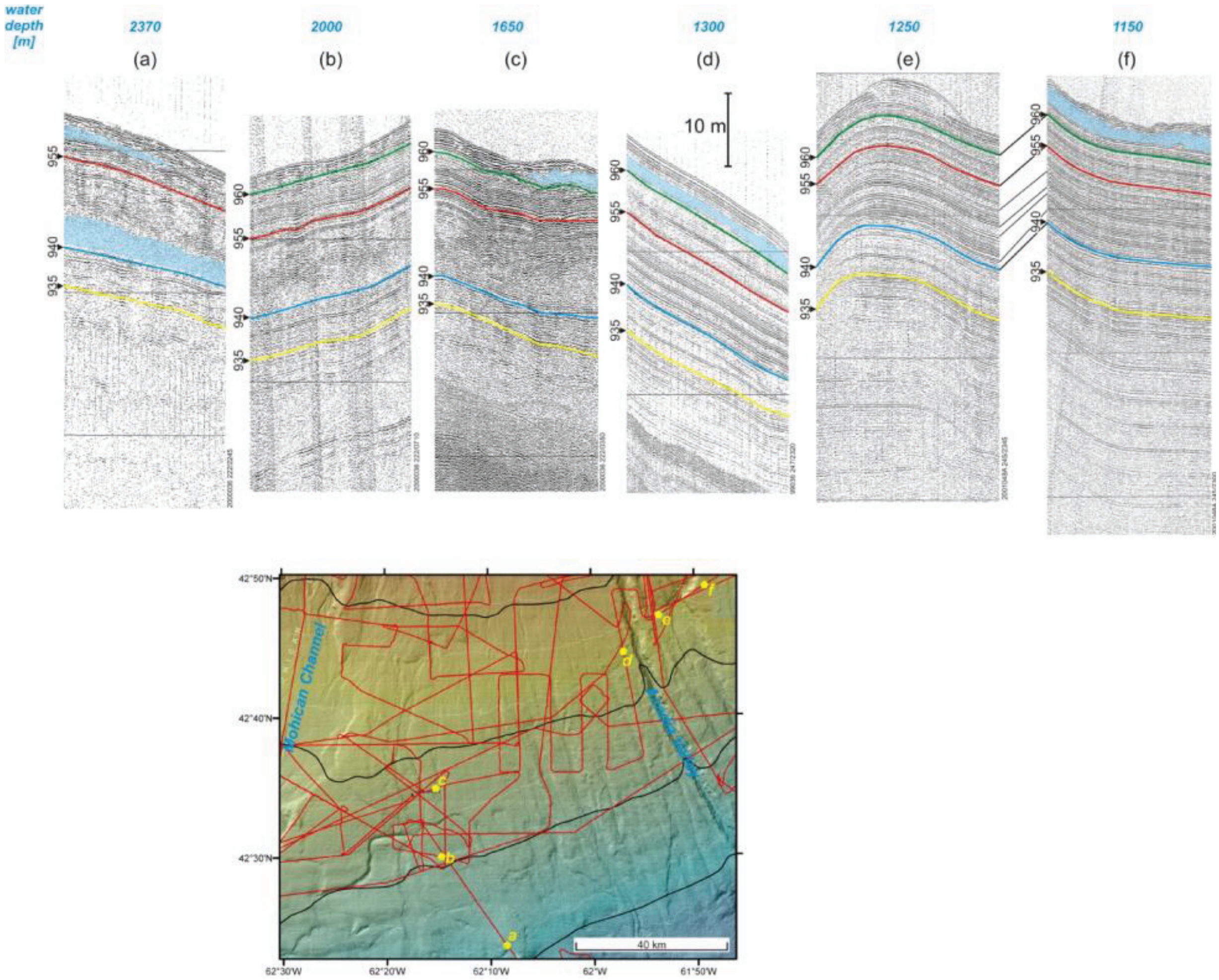

Figure 3.7 Example of an along-slope correlation east of Western Bank (map 2, Fig. 3). Jump correlation based on the seismic character, the occurrence of MTDs and major erosional surfaces was used to correlate these sections: an example is given between (e) and (f) where lines indicate equivalent horizons (see text for more detail); index map shows positions of the correlation east of Western Bank (see also Figure 3 for position).

A further check on validity of correlations is to check against correlations to till tongues (**Figs. 1 and 8**), based on the assumption that only maximum ice advances produce till tongues (King, 1993) that are regionally synchronous. Indeed, some authors have argued the pattern of till tongue extent can be used as a correlation tool on the uppermost slope (Piper et al., 2005).

Correlations were further checked against previous local correlations (Piper, 2001; Skene and Piper, 2003; Hundert and Piper, 2008) and were generally found to be consistent. In some cases, previous studies had misinterpreted the presence or extent of erosional hiatuses (e.g. **Fig. 4**).

In this way, a regional Huntec stratigraphy on the Scotian Slope was developed (**Fig. 5**). Other, more local Huntec stratigraphic schemes (Gauley, 2001; Robichaud, 2006; Hundert and Piper, 2008) were related to the new stratigraphic framework (**Fig. 6**).

The airgun seismic reflections traced in this study were taken from the type section defined by Mosher et al. (1989; 2004) off Western Bank (**Figs. 2, 3 and 8**). Key

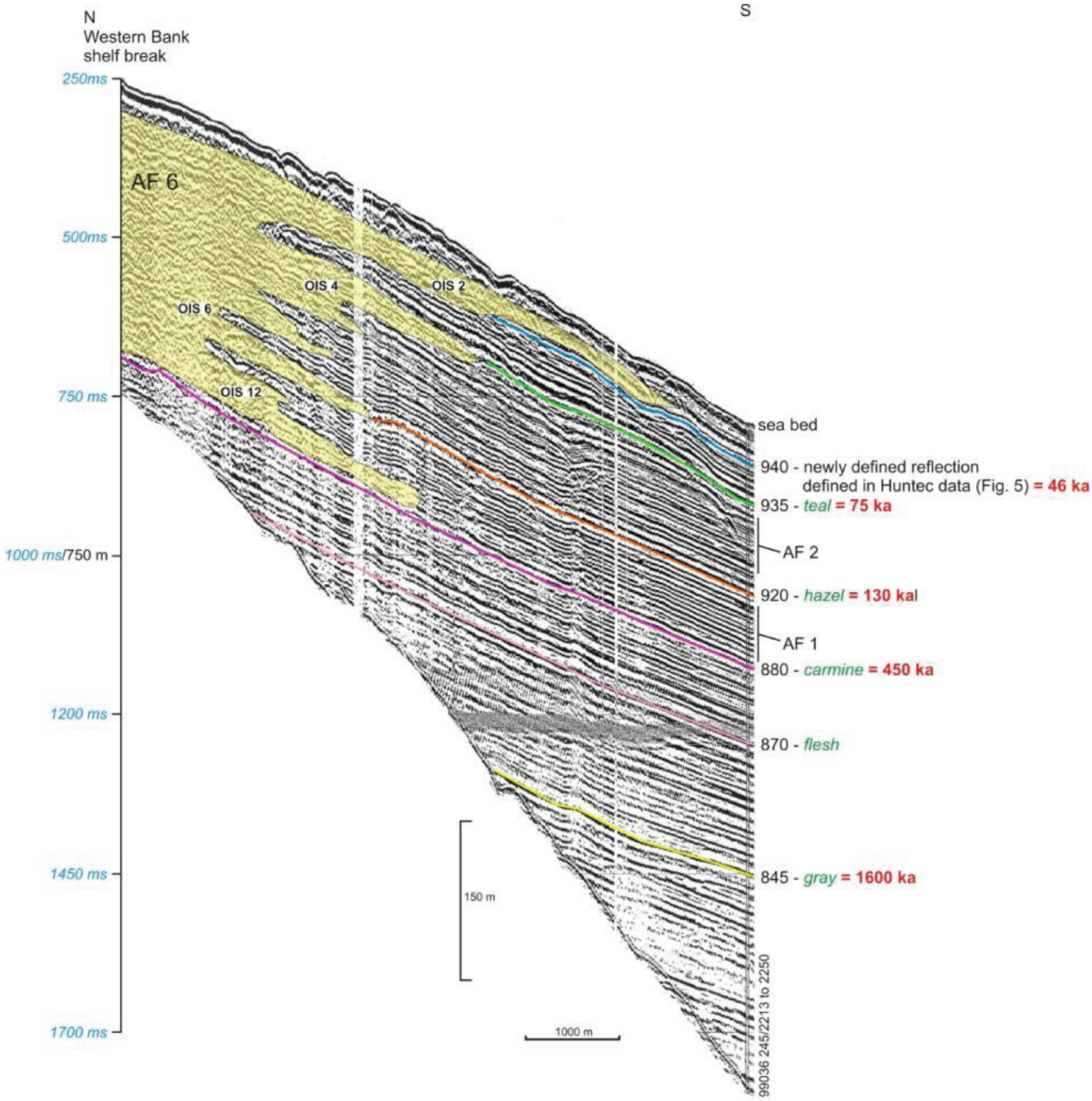

Figure 3.8: Airgun seismic data showing till tongues on the upper slope off Western Bank (see Fig. 3 main map for position) and its correlation to the Airgun seismic stratigraphy based on Mosher al. (2004) and Gauley (2001) (see also Fig. 2). Their reflection names and ages are indicated in green and red respectively. Also indicated is the acoustic character of AF 1, 2 and 6 on airgun seismic data.

areas were retraced to check previous correlations (**Fig. 9**) and jump correlations were made on seismic character across canyons, in a manner similar to that used for the Huntec data. In particular, seismic stratigraphy of the eastern Scotian Margin was correlated to the central Scotian Slope by jumping from just west of The Gully canyon to near the Balvenie B-79 well in 1500 m water depth (**Fig. 12**). The seismic reflections were thus correlated throughout the Scotian Slope from NE Channel to the Laurentian

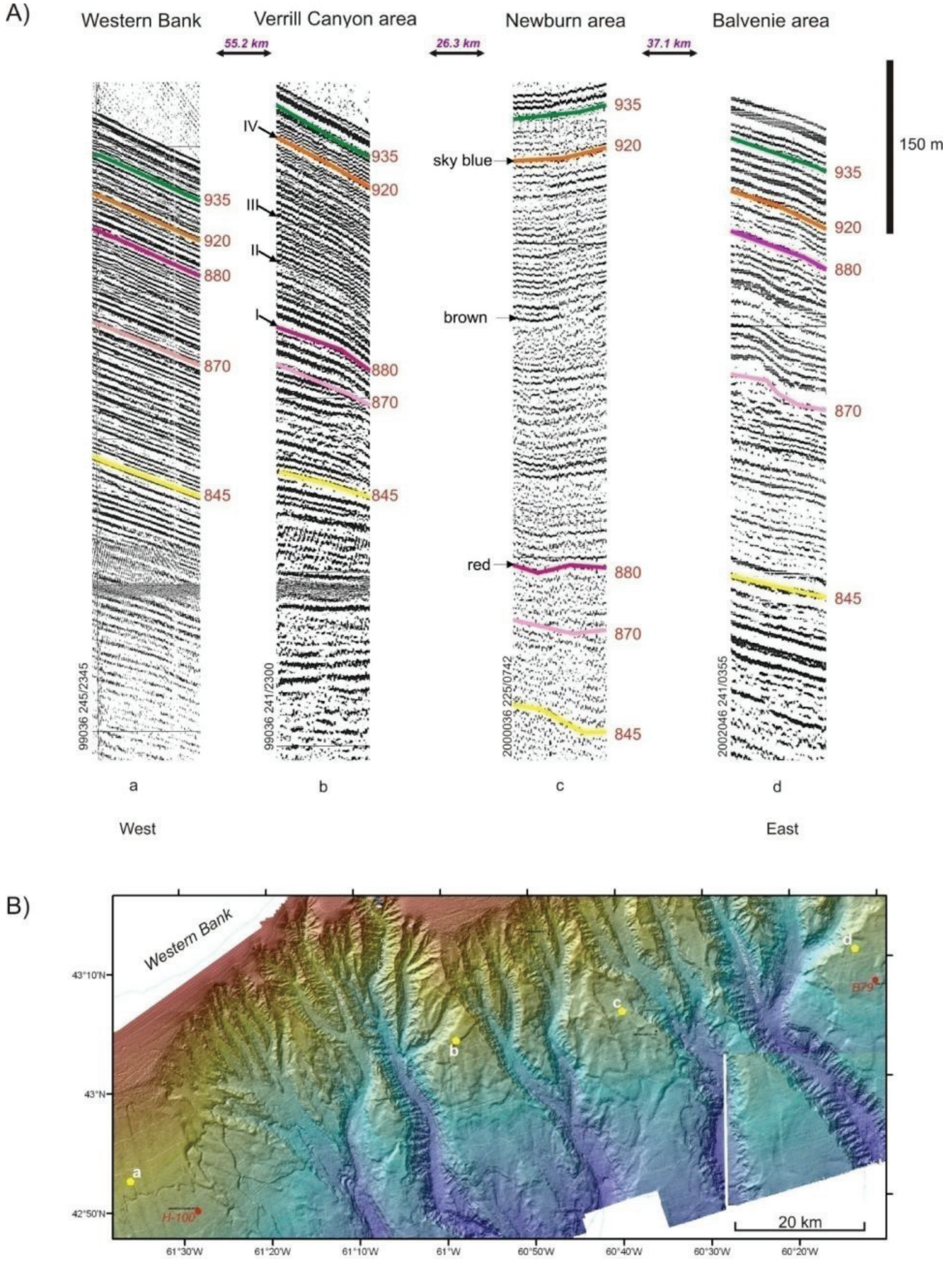

Figure 3.9 on previous page: A) Airgun seismic correlations alongslope from Western Bank (type section of Mosher et al. (2004)) to the new type section near the Balvenie well (see Fig 3 main map and B) map), distances in km between sections are also indicated. Correlations were achieved by jump correlating over major canyon systems east of Western Bank (Fig. 1). Reflections in (b) Verrill canyon area from Piper et al. (2002), reflections in (c) Newburn area from Chubbs (2003). B) Map showing position of seismic data from A along the central Scotian Slope, H-100 Shubenacadie well, B-79 Balvenie well.

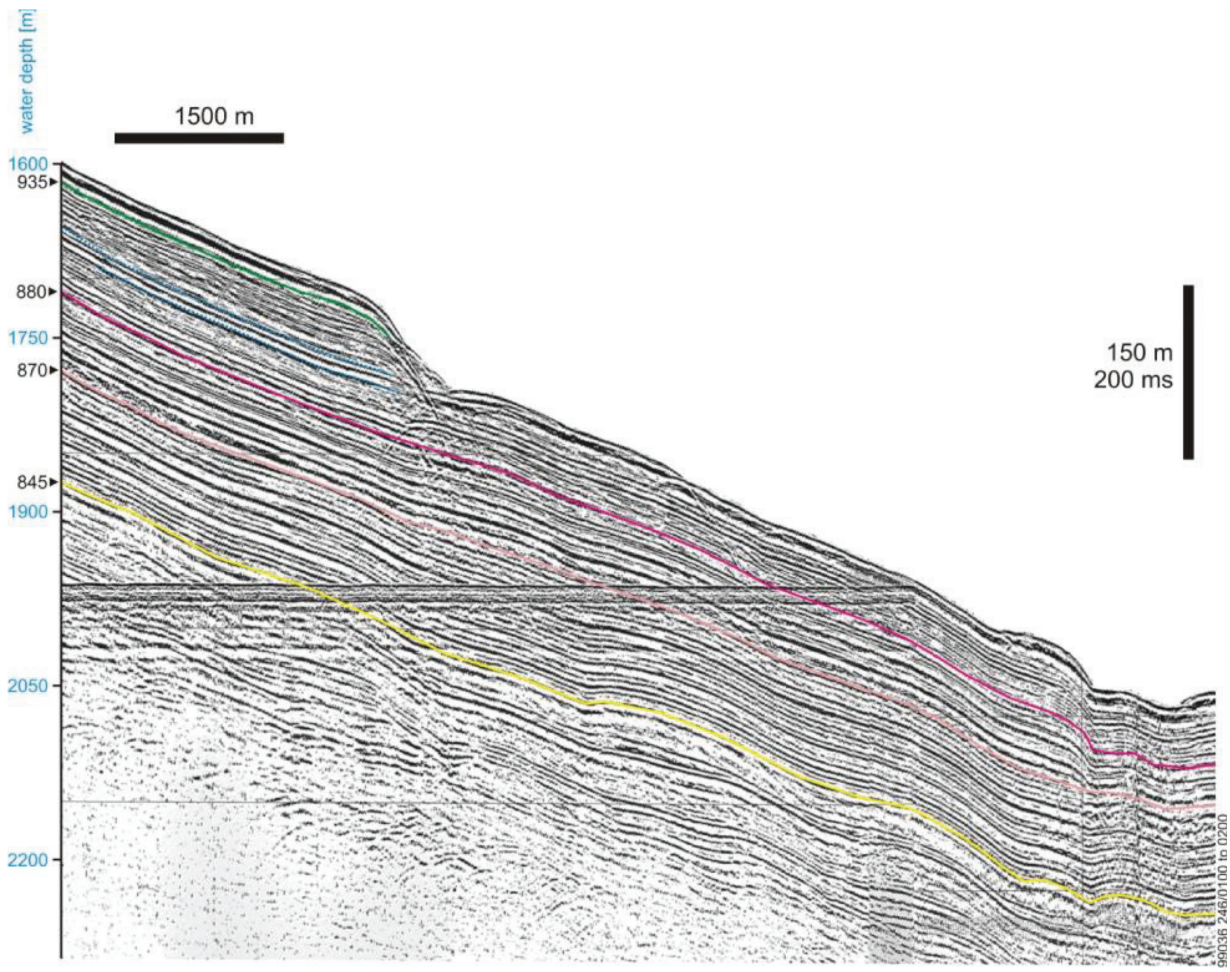

Figure 3.10: Downslope seismic airgun profile off Western Bank showing a major erosional scarp at ~2300 m water depth (Fig. 1 and 2), where almost the whole sequence since reflection 880 (~450 ka) has failed.

Channel down to water depths of ~3000 m. Farther downslope, data density is sparse and parts of the sequence are lost due to major failures and prominent slope-wide scarps (**Figs. 10 and 11c**). The deeper water seismic stratigraphy below 3000 m water depth (**Fig. 12**) was only correlated on the eastern Scotian Rise, between the Logan Canyon and Laurentian Fan (**Figs. 1 and 3**). Here it was tied to previous work on the Laurentian Fan (**Fig. 12c**) (Skene and Piper, 2006) and the seismic stratigraphy of the rise south of Shortland and Haldimand canyons (**Figs. 1, 3 and 12**) (Piper and Ingram, 2003). The seismic stratigraphy could not be extended into two areas: the upper slope in

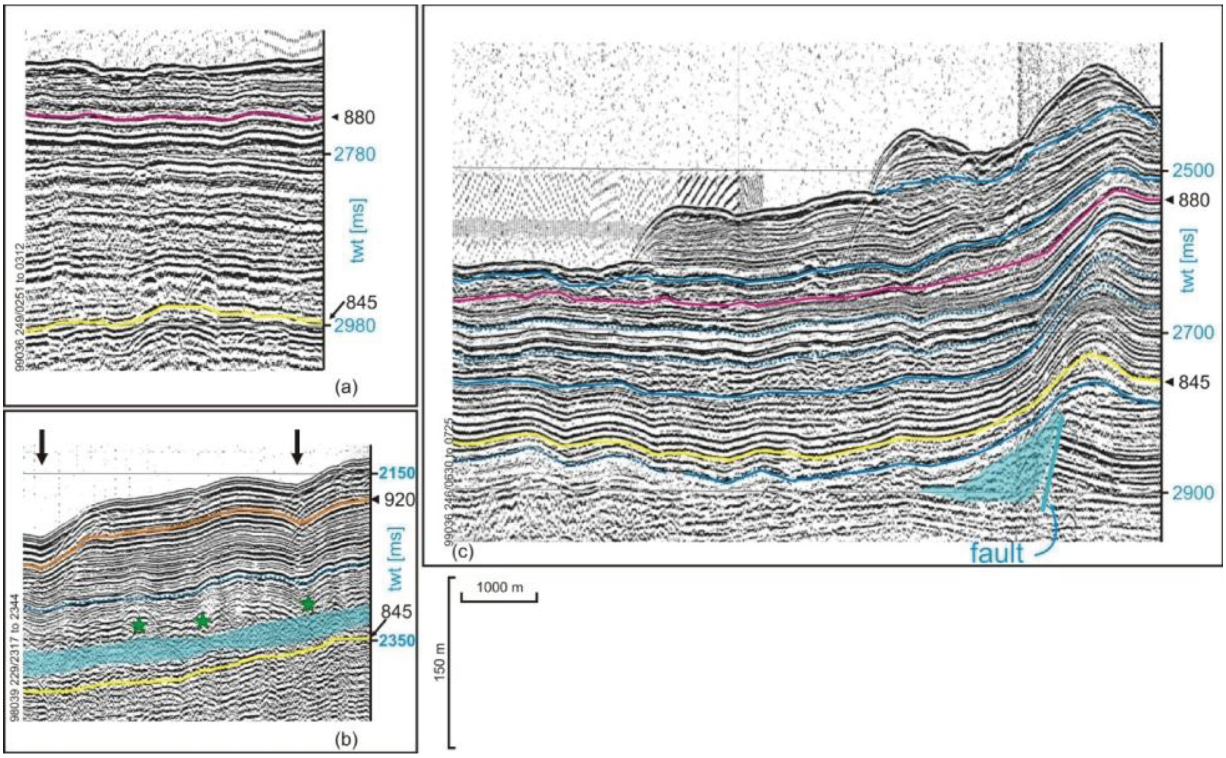

Figure 3.11: Examples of mid-slope architecture from Airgun seismic data at the same scale: (a) well stratified plume sedimentation with little erosion (comparable to Huntec data on Fig 5a and b). (b) Stratified plume sedimentation with few MTDs and small channels (arrows). The deeper sequence is characterized by MTDs and cut and fill morphology (green stars). (c) Laminated sediments with frequent erosional horizons and MTDs throughout the seqeunce. The blue lines indicate major erosional surfaces (dashed = no erosion occurring). This also shows nicely the downslope loss of sequence due to step-like morphology; a fault is shown in light blue.

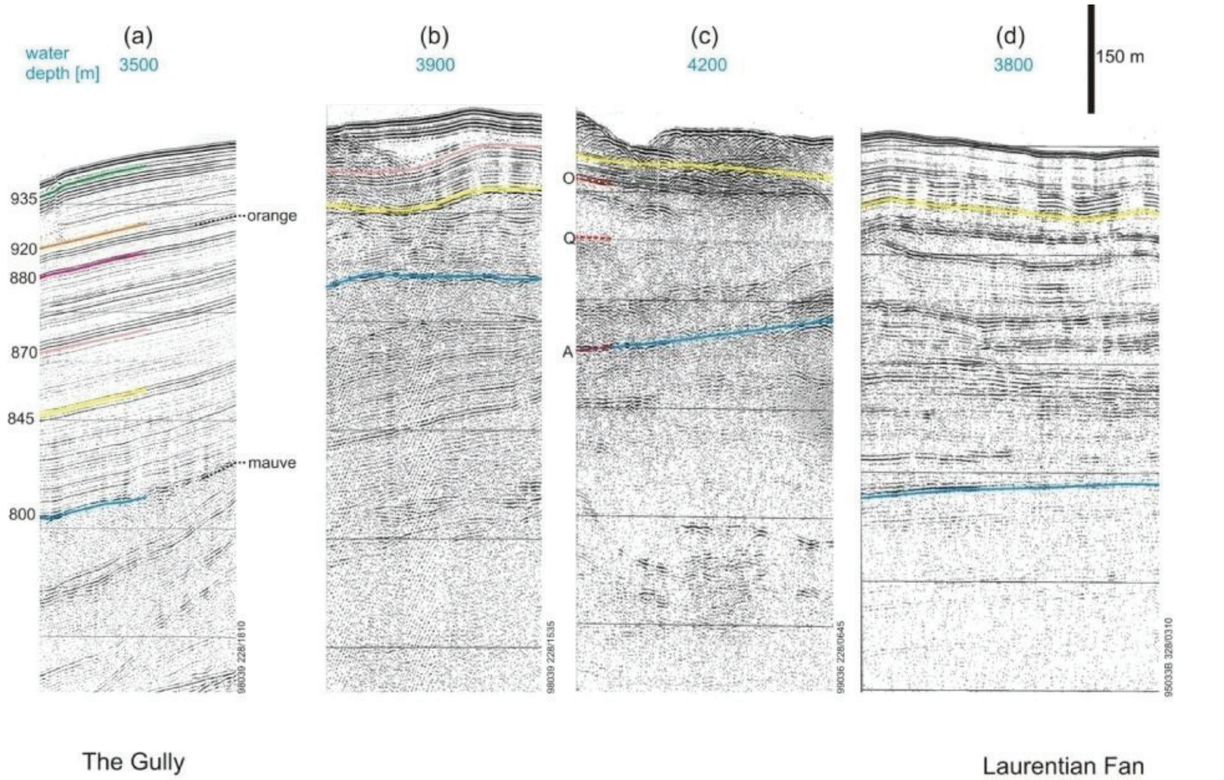

Figure 3.12: Airgun seismic profiles on the lower slope of the eastern Scotian Slope (Fig, 3 for positions) showing architecture and seismic jump correlation of the Airgun seismic stratigraphy to the Laurentian Fan. All reflections as in Figure 2 except for SS 800 which is defined on the basis of mauve from Piper and Ingram (2003) and used only on the lower slope. Reflections "orange" and "mauve" in (a) from Piper and Ingram (2003); reflections A, Q and O in (c) from Skene and Piper (2003).

the Shortland and Haldimand canyon area and the lower slope and rise area west of Logan Canyon to offshore Georges Bank. This is due to very limited seismic coverage in these areas and the frequent abundance of major MTDs, slope scars and deep canyons (**Fig. 1**).

3.4.2. Definition of acoustic facies

Several previous studies (King and Fader, 1986; Mosher et al., 1994; Piper, 2000; Hundert and Piper, 2008) used the Huntec sparker data to establish seismic facies on the slope and thus to characterize the depositional processes. Different authors had defined similar facies and matching interpretations for deposition of these facies in different areas along the slope.

These previous classifications were used to define seven new acoustic facies; the interpretation follows especially the studies of Piper (2000) and more recently Hundert and Piper (2008). These acoustic facies (AF) (**Table 2**) are the key elements for building the Scotian Slope. Where Huntec sparker data and lower resolution airgun data overlap, the acoustic character of the same facies can be defined in airgun data and are used to characterize the deeper sedimentary sequence along the Scotian Slope. Facies could

Table 3-2: Summary of acoustic facies (AF) used or defined in this study, and their interpretation and spatial occurrence on the Scotian Slope.

Facies	character	described by	interpretation	spatial extent	example
continuous draped facies (AF 1)	stacked parallel reflections, follow topography, high amplitude reflections	Facies D of Hundert and Piper (2008), Facies 1 of Piper (2000)	plume sedimentation*	upper and mid slope	Fig. 5, 6
mounded continuous facies (AF 2)	highly sinuous parallel reflections	Facies C of Hundert and Piper (2008), Facies 3 of Piper (2000)	erosion within plume sediments*	upper and mid slope	Figs. 5, 6, 13
strong continuous reflection facies (AF 3)	very strong double reflections related to erosional horizons	previously undescribed	erosional surfaces and failure planes	whole slope	Fig. 5
highly disturbed and chaotic facies (AF 4)	low amplitude and incoherent reflections, lensoid shapes common	Facies B of Hundert and Piper (2008), Facies 4 of Piper (2000)	mass transport deposits*	whole slope	Fig. 5
sheet-like poorly stratified facies (AF 5)	thin, poorly stratified lenses within other facies, frequenty observed within canyons and related to local highs	Facies E ? of Hundert and Piper (2008), Facies 5 ? of Piper (2000), Core control from Hill (1984) and Piper and Campbell (2002)	sandy turbidites*	whole slope, related to canyon settings	Fig. 5
highly reflective facies (AF 6)	high amplitude incoherent and irregular reflections	Facies A of Hundert and Piper (2008), Facies 5 of Piper (2000)	till tongues*	upper slope	Fig. 8
highly sinuous seabed facies (AF 7)	poorly stratified meter-scale waves	Pickerill et al. (2001)	sediment waves, current reworking*	upper slope, outer shelf	Fig. 1

* the interpretations are based on previous intrepretations and have not been revised

not be recognized on (i) some older poor-quality airgun data, (ii) in very thin layers, and in (iii) areas highly disturbed by sediment failures.

The continuous draped facies (AF 1) is characterized by several stacked sub-parallel to parallel reflections over large areas down- and alongslope (**Figs. 6 and 8**). It was mostly recognized in the shallowest sedimentary sequence between 200 and 2500 m water depth. The reflections run parallel over large areas along- and downslope. Thinning may occur on steep slopes. Few erosional cuts are observed, which are

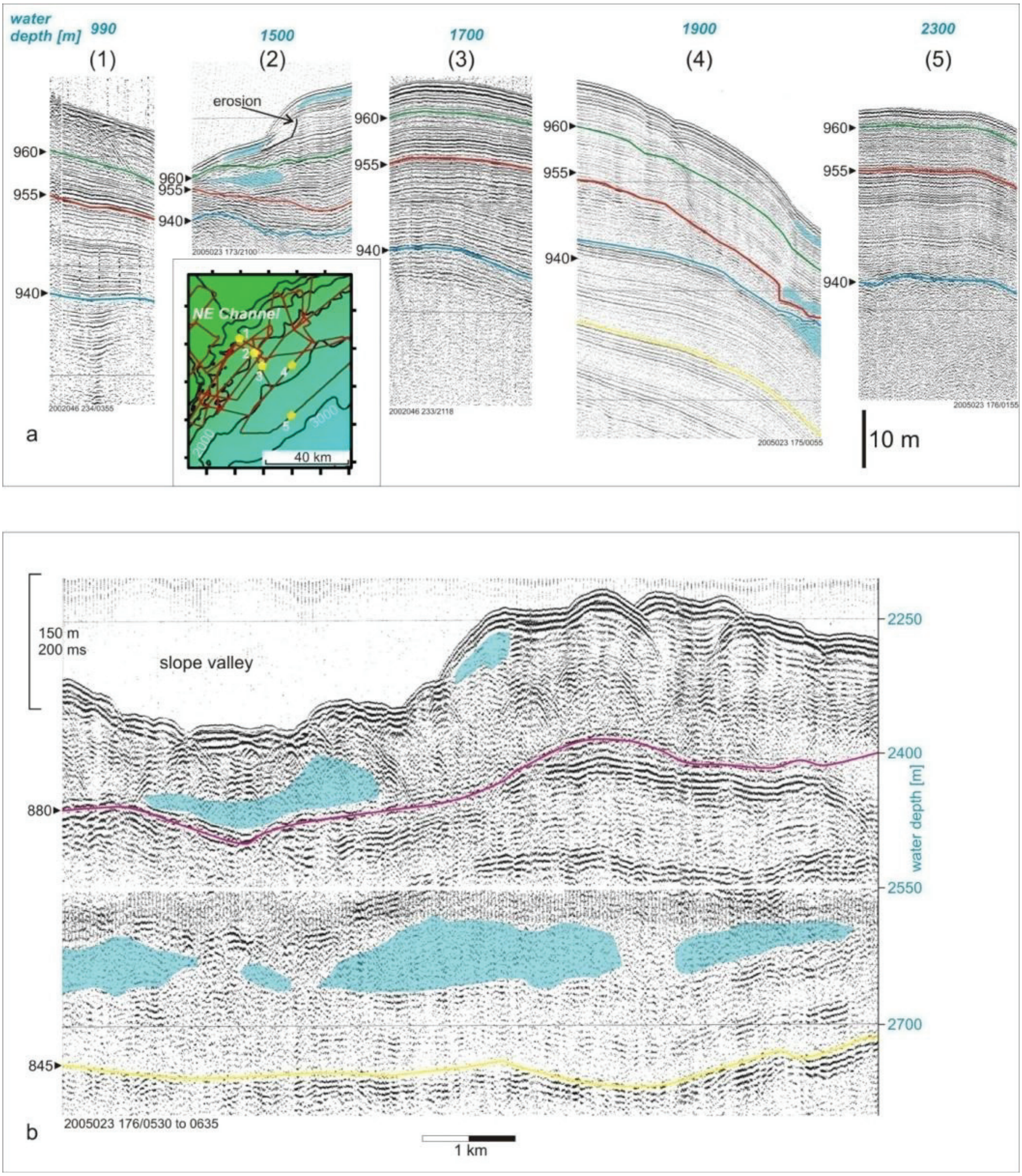

Figure 3.13: Seismic data from the slope off Northeast (NE) Channel (Fig. 3): (a) Huntec data showing the seismic reflections, major MTDs are highlighted in blue. Positions of seismic data are shown in index map: bathymetry in meters. (b) Airgun seismic data showing lower slope architecture: only thin stratified intervals are preserved and large MTDs (blue) are found throughout the sequence (position are also indicated in Fig. 3).

generally related to regional features such as local highs and canyons (**Fig. 4b**). This facies was interpreted as proglacial plume sedimentation based on its draping character and continuously deposition over larger areas. Such interpretation is supported by its character in piston cores (Piper et al., 2002; Hundert and Piper, 2008).The mounded continuous facies (AF 2) (**Figs 5, 6 and 13a**) is characterized by highly sinuous parallel reflections, which mimic underlying topography such as local highs (**Fig. 5b**) and small faults and escarpments (**Fig. 5d**). This facies reflects erosion by turbidity currents in areas of plume sedimentation (e.g. on the upper slope) (Piper and Sparkes, 1987).

The strong, continuous reflections facies (AF 3) (**Fig. 6c**) was not included in previously schemes. It consists of one or two high amplitude seismic cycles. In many cases, it either underlies failure deposits or can be traced laterally to a draped erosional scarp, implying that it marks an unconformity with a large acoustic impedance. This reflection facies represents major erosional surfaces and failure planes.

The highly disturbed and chaotic facies (AF 4) (**Fig. 6c**) is characterized by low amplitude incoherent reflections, which occur with lensoid geometry; basal erosional surfaces are frequently observed. It generally occurs within well stratified sequences throughout the slope. Within the incoherent reflections are local short coherent reflections. These characteristics are especially well recognized on airgun data (**Fig. 13b**). Numerous authors have interpreted this facies as mass-transport deposits (e.g. Mosher et al., 2004).

The sheet-like and poorly stratified facies (AF 5) (**Fig 6b**) consists of discontinuous reflections of variable amplitude, commonly in packets less than 5 ms thick. It is characteristically found within canyon settings and small narrow depressions perpendicular to the slope. Faint erosional features may be observed at the base (**Fig. 6b**). These observations are typical for sandy turbidite successions described principally from channel floors (Piper, 2005; Piper et al., 2011).

The highly reflective facies with no internal returns and very sharp bases and tops (AF 6) (**Fig 8**) is found only at the shelf break down to a maximum water depth of 600 m. This facies is continues onto the shelf and represents till tongues related to past ice sheet advances (Mosher et al., 1989; King, 1993; Piper and Brunt, 2006).

On the upper slope, the highly sinuous seabed facies (AF 7) is characterized by poorly stratified meter-scale waves. They are recognized in proximity to canyon heads (**Fig. 1**). These meter-scale features are observed on Huntec seismic data and multibeam images and have been interpreted as sediment waves (Pickerill et al., 2001).

3.4.3. Age model

The age model for the Huntec seismic stratigraphy (**Fig. 14**) is based on radiocarbon dates in several cores and is similar to previous age models (Campbell, 2000; Hundert and Piper, 2008), except that new radiocarbon dates have dated some of the shallower reflectors more precisely. As an example, the Last Glacial Maximum at 21 cal ka corresponds to the 990 reflection, bracketed by four dates of 20.3 to 21.5 ka (**Fig. 14**). The 955 reflection is older than 23.7 cal ka dated in core 38. The deepest directly dated reflection, at 46 cal ka, is the 940 reflection, dated directly by one date in core 30

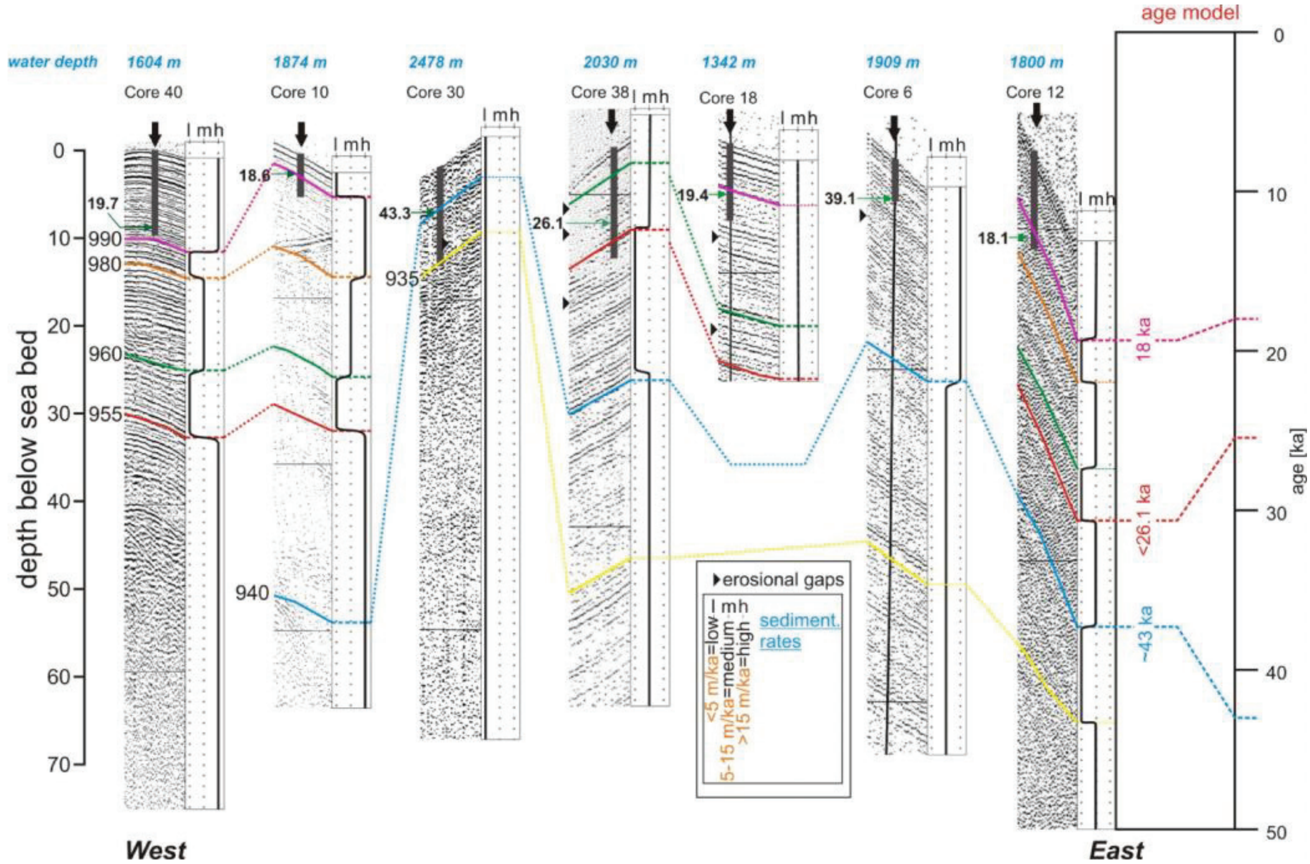

Figure 3.14: Radiocarbon dating control on the Huntec seismic stratigraphy from core data and resulting average sedimentation rates for the sequences to highlight variability alongslope: low values indicate rates lower than 5 m/ka, medium rates are between 5 and 15 m/ka and high rates are rates more than 15 m/ka.

and confirmed by the 41.2 ka date in core 6 (**Fig. 14**). Age control on the deeper airgun reflections (**Fig. 2**) is based on Mosher et al. (2004) and references cited therein.

3.4.4. Time slices

In a previous study on MTD distribution on the Scotian Slope (Huppertz et al., 2009) the slope was divided into several different MTD zones (**Fig. 1**) based on slope morphology and volume of MTDs. We adopted this zonal classification in this study, with minor modifications: Zone 4 has been separated into seawards of Northeast Channel (Zone 4) and seaward of the Laurentian Channel (Zone 8). The seismic facies other than MTDs are used to further characterize the different zones and their stratigraphic distribution to understand long-term slope evolution (**Fig. 1**). Five different time slices were defined (**Table 3**). The OIS 1 time slice represents the time since deglaciation represented by the upper few meters in cores and Huntec seismic data (Jenner et al., 2010). The OIS 2 time slice is defined by the reflections 955-990 (**Fig. 14**). The OIS 3 time slice is defined by reflections 955-940, the mid-Pleistocene time slice is defined by 940-880 (although it also includes OIS 4 and 5, generally regarded as Late Pleistocene) and the interval from 880-845 is termed the Early Pleistocene. The style of the lowest two time slices is dominated by glacial deposits, since interglacial sedimentation rates are likely low.

Table 3-3: Summary of the temporal distribution of the different facies in the different zones on the slope. This could be used to define the most dominant process occurring in the different zones.

	OIS 1	***OIS 2***	***OIS 3***	***Mid-Pleistocene***	***Early Pleistocene***	***dominant sedimentary process***
1	well stratified	well stratified, few MTDs with local extent	well stratified	well stratified	well stratified, few MTDs with local extent	hemipelagic and plume sedimentation
	AF 1	AF 1,4	AF 1	AF 1	AF 2,4	
2	well stratified	well stratified, turbidites	well stratified	upper slope stratified, lower slope large MTDs	upper slope poorly stratified, lower slope MTDs	plume sedimentation, turbidity currents
	AF 1	AF 1,5	AF 1	AF 1,2,3,4	AF 2,4	
3	well stratified	local highs stratified, few MTDs, canyon floors chaotic	local highs stratified, few MTDs, canyon floors chaotic	little stratification, large MTDs	poorly stratified	plume sedimentation, mass wasting, erosion
	AF 1	AF 1, 2,4,5	AF 1,2,4	AF 2,4	AF 2	
4	well stratified, thin MTDs	well stratified, few MTDs	well stratified, MTDs frequent	massive MTDs	massive MTDs	mass wasting, erosion
	AF 2,4	AF 1,2,4	AF 1,2,4	AF 3,4	AF 3,4	
5	well stratified, few MTDs	poorly stratified, few MTDs	poorly stratified, MTDs frequent	chaotic, stacked MTDs	chaotic, stacked MTDs	plume sedimentation, mass wasting, erosion
	AF 1,4	AF 2,4	AF 2,4	AF 3,4	AF 3,4	
6	well stratified, few MTDs	frequent small MTDs, cut and fill morphology	frequent MTDs, highly erosive, cut and fill morphology	chaotic, stacked MTDs	chaotic, stacked MTDs	plume sedimentation, mass wasting, erosion
	AF 2,4	AF 2,4	AF 2,3,4	AF 3,4	AF 3,4	
7	erosive, little deposition	erosive, frequent massive MTDs	erosive, some stratified sediments	chaotic, erosive, canyon cutting, MTDs frequent	chaotic, erosive, canyon cutting, MTDs frequent	mass wasting, erosion
	AF 3	AF 3,4	AF 2,3,4	AF 3,4	AF 3,4	
8	well laminated turbidites, few MTDs	well laminated turbidites, few MTDs	well laminated turbidites, few MTDs	well laminated turbidites, few MTDs	well laminated turbidites, few MTDs	bypassing of MTDs, turbidite sands widespread
	AF 2,4	AF 2,4	AF 2,4	AF 2,4	AF 2,4	

Zone 1 is characterized by thick, well-stratified continuous sequences (Huppertz et al., 2009), which have been deposited at least since OIS 6 (e.g. **Figs. 2 and 4a, Table 3**). Several significant erosional events are recognized within this zone. The youngest event occurred during the last termination at around 16 ka (Mosher et al., 2004, their Figure 13) and is marked by a major slope-wide headscarp (**Fig. 4a**), loss of the stratigraphic section downslope, and local thin MTDs (**Fig. 4b**). At ~3000 m, the complete Late Quaternary sequence has been removed and was draped only by thin younger deposits (**Figs. 10 and 11b**). This interpretation is supported by core data from the area (Fig. 14 and Jenner et al., 2010).

The slope in Zone 2 is highly dissected by canyons (**Figs. 15a and 16**) (Mosher et al., 2004; Jenner et al., 2007; Huppertz et al., 2009). The inter-canyon areas are dominated similarly as in Zone 1 by plume sediments. Canyon floors remains show either non-deposition or erosion of the stratified sequence: highly disturbed areas are typical (**Fig. 15b**). Below 3000 m, the canyons run out into channels and regional sedimentation rates reduce greatly (**Figs. 12 and 13b**).

Zone 3 is characterized by the widespread occurrence of small MTDs (**Fig. 15**) (Huppertz et al., 2009). Well-stratified sequences are found back to OIS 6. Large failures are present at the OIS 6 horizon and poorly stratified sequences make up older deposits (**Table 3**).

Zone 4, off Northeast Channel, is characterized by several small MTDs throughout the sequence; intercanyon highs show laminated intervals and few erosional surfaces (**Fig. 15**). Within the canyons, turbidite sands predominate: thin MTDs indicate bypassing of flows as the large MTD deposits are found in deeper water on the lower slope and rise (Hundert and Piper, 2008; Piper et al., 2011).

Zones 5 is characterized by thick-bedded MTDs covering large areas, some of which outcrop at seabed (Shor and Piper, 1989; Huppertz et al., 2009). Plume sedimentation is only found in the youngest sequences, interrupted by turbidite flow deposits (**Fig. 17**), but is likely present as thin units between deeper MTDs.

Zone 6, seaward of the Scotian Gulf (**Fig. 1**), is characterized by thick-bedded and extensive MTDs and cut-and-fill morphology (Piper, 2000; Huppertz et al., 2009). Smaller MTDs dominate the sequence from OIS 6 to the surface, interbedded with stratified plume sediments, whereas the older sequence, imaged in low resolution data, appears to be completely disturbed by MTDs (Huppertz and Piper, 2009). Piper and Normark (2009) identified some of the MTDs as glacigenic debris flows.

Zone 7 off Banquereau is characterized by deeply incised canyons, with widespread MTDs on the rise (Piper and Ingram, 2003; Huppertz et al., 2009). Intercanyon ridges are narrow, erosional and preserve stratified sediments younger than OIS 6 only locally (**Fig. 12**).

Zone 8, the slope above Laurentian Fan is generally erosional to 2000 m water depth. Large MTDs are only found on the lower slope (**Figs 12 c and d**) and may be locally derived from channel levees. During the 1929 Grand Banks earthquake, the resulting turbidity current eroded the floors of the three mayor canyons on the slope (Piper et al., 2007). Between the channels, well laminated plume sediments are found (Skene and Piper, 2006). The lower slope and rise has large sand lobes (Normark et al., 1983).

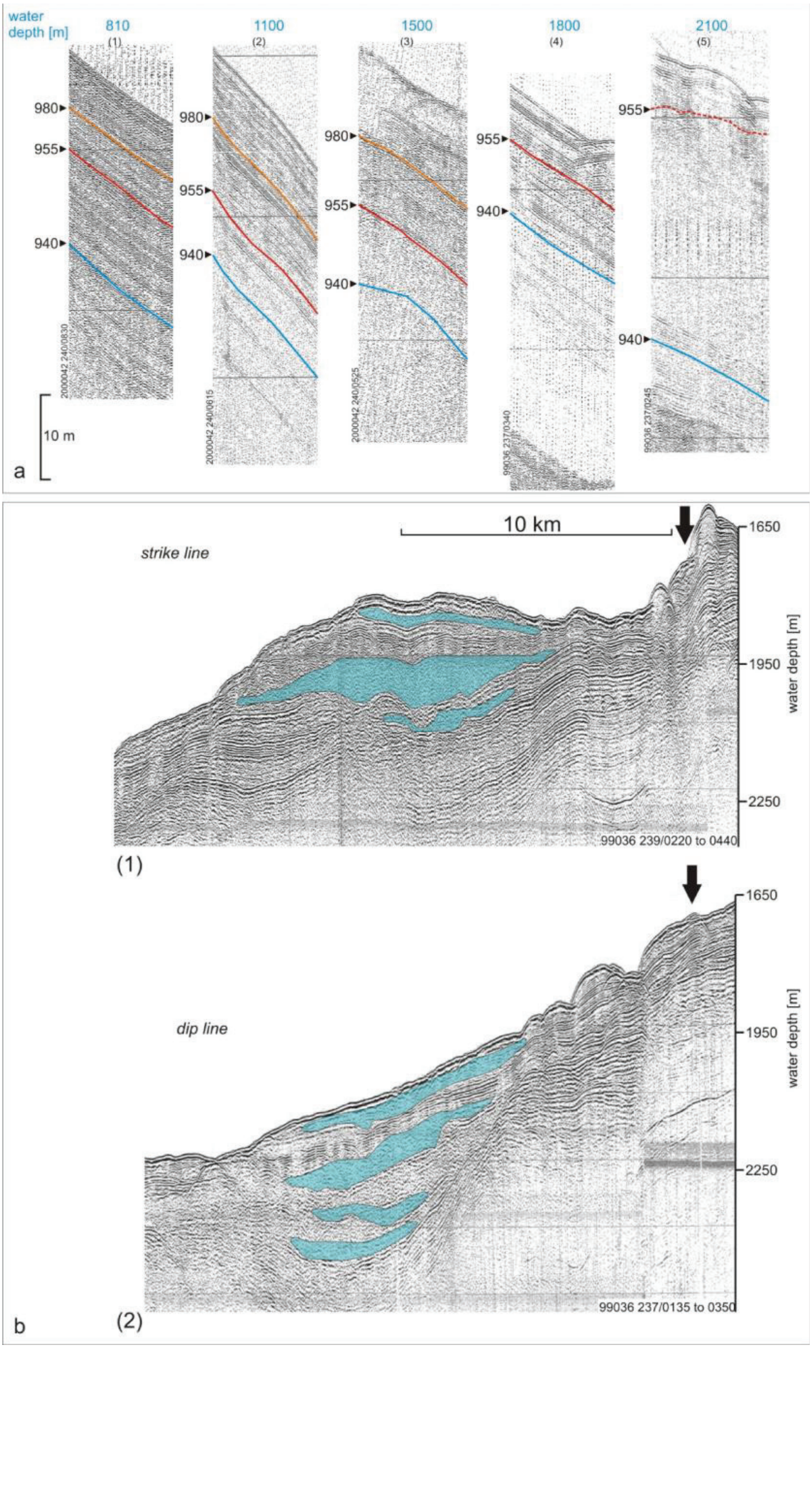
water depth [m]
810
(1)
1100
(2)
1500
(3)
1800
(4)
2100
(5)
980
955
940
10 m
a
10 km
strike line
1650
1950
2250
water depth [m]
99036 239/0220 to 0440
(1)
dip line
99036 237/0135 to 0350
b
(2)

Figure 3.15 on previous page: (a) Downslope Huntec jump correlation in zone 3 east of the Balvenie well (Fig. 3): most of the section is lost downslope due to erosion. Nevertheless, this study could achieve some stratigraphic control in this area. (b) airgun seismic data showing dip and stike lines to display the architecture in zone 3 east of the Balvenie well (black arrows indicate crossover), with thick MTDs; the airgun seismic stratigraphy could not be extended to this part of the slope due to large MTDs (see text for details).

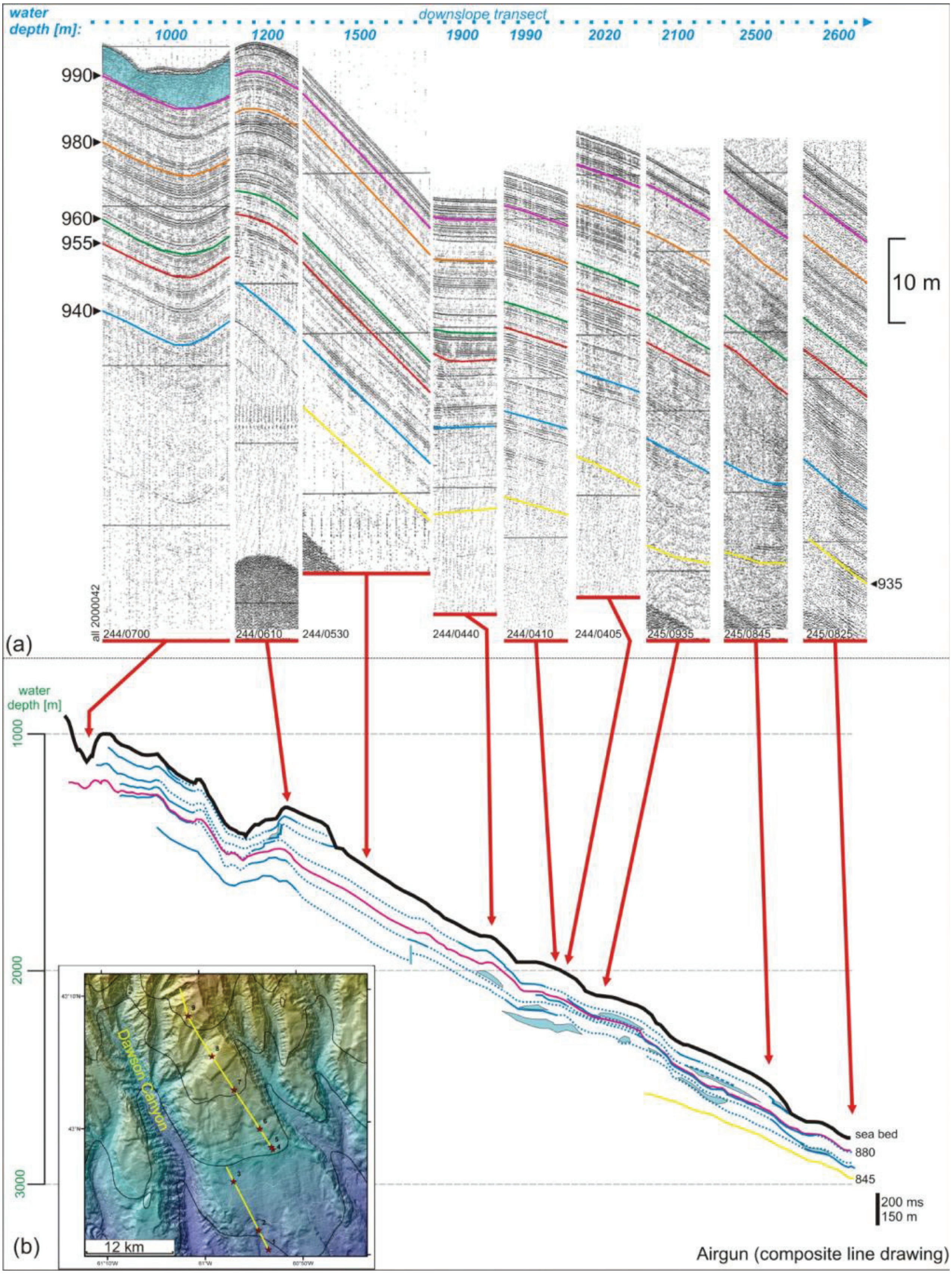

water depth [m]:
downslope transect
1000
1200
1500
1900
1990
2020
2100
2500
2600
990
980
960
955
940
935
10 m
all 2000042
244/0700
244/0610
244/0530
244/0440
244/0410
244/0405
245/0935
245/0845
245/0825
(a)
water depth [m]
1000
2000
3000
sea bed
880
845
200 ms
150 m
Dawson Canyon
12 km
(b)
Airgun (composite line drawing)

Figure 3.16 on previous page: Dip line on an intercanyon ridge east of Dawson Canyon (see index map) showing downdip variations in (a) Huntec seismic data and (b) airgun seismic data. Note the lack of major MTDs in the uppermost sequence of OIS 2 age.

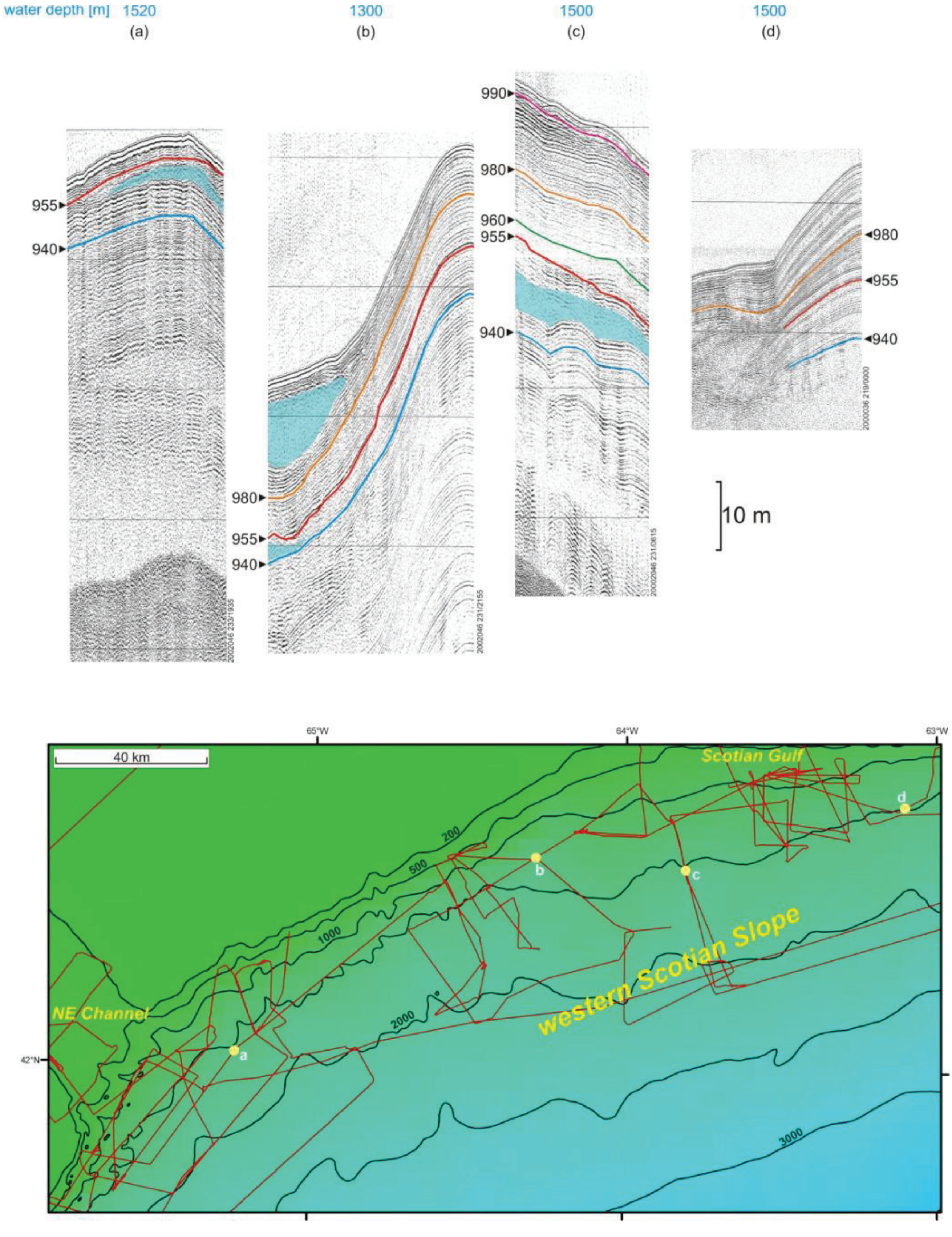

water depth [m]
1520
1300
1500
1500
(a)
(b)
(c)
(d)
955
940
980
955
940
990
980
960
955
940
980
955
940
10 m
65°W
64°W
63°W
42°N
40 km
Scotian Gulf
NE Channel
western Scotian Slope
200
500
1000
2000
3000
a
b
c
d

Figure 3.17 on previous page: Huntec seismic data from the western Scotian Slope showing few positions of the jump-correlation from Northeast Channel to the area west of Western Bank. This area is highly disturbed by young failures and very few stratified areas remain (see Fig. 13).

3.4.5. Distal sediment sink: the Sohm Abyssal Plain

Seawards of ~4500 m water depth, on the lower rise and abyssal plain, the zoning of the slope (**Fig. 1**) does not apply. Here on the Scotian Rise and Sohm Abyssal Plain (SAP), long-term sediment storage spanning several glacial cycles occurs. Thick turbidite successions cover large areas on the plain. This observation is based on core 50 (**Fig. 18**), where at 10 m core depth only 15.1 cal ka (13 ^{14}C ka) have been reached (Benetti, 2006): extrapolation indicates that the LGM is at ~22 m depth indicating very high sedimentation rates since the LGM compared to slope values. A similar rate can be estimated on the SAP, using CIELab color data to correlate with dated cores on the Bermuda Rise and Scotian Rise e.g. ODP site 1064A (Shipboard Scientific Party, 2001), using the assumption that the supply of red turbidites to the SAP is also reflected in more red mud in hemipelagic or pelagic sediments. The result is that here on the SAP the LGM occurs at ~20 m depth (**Fig. 19**).

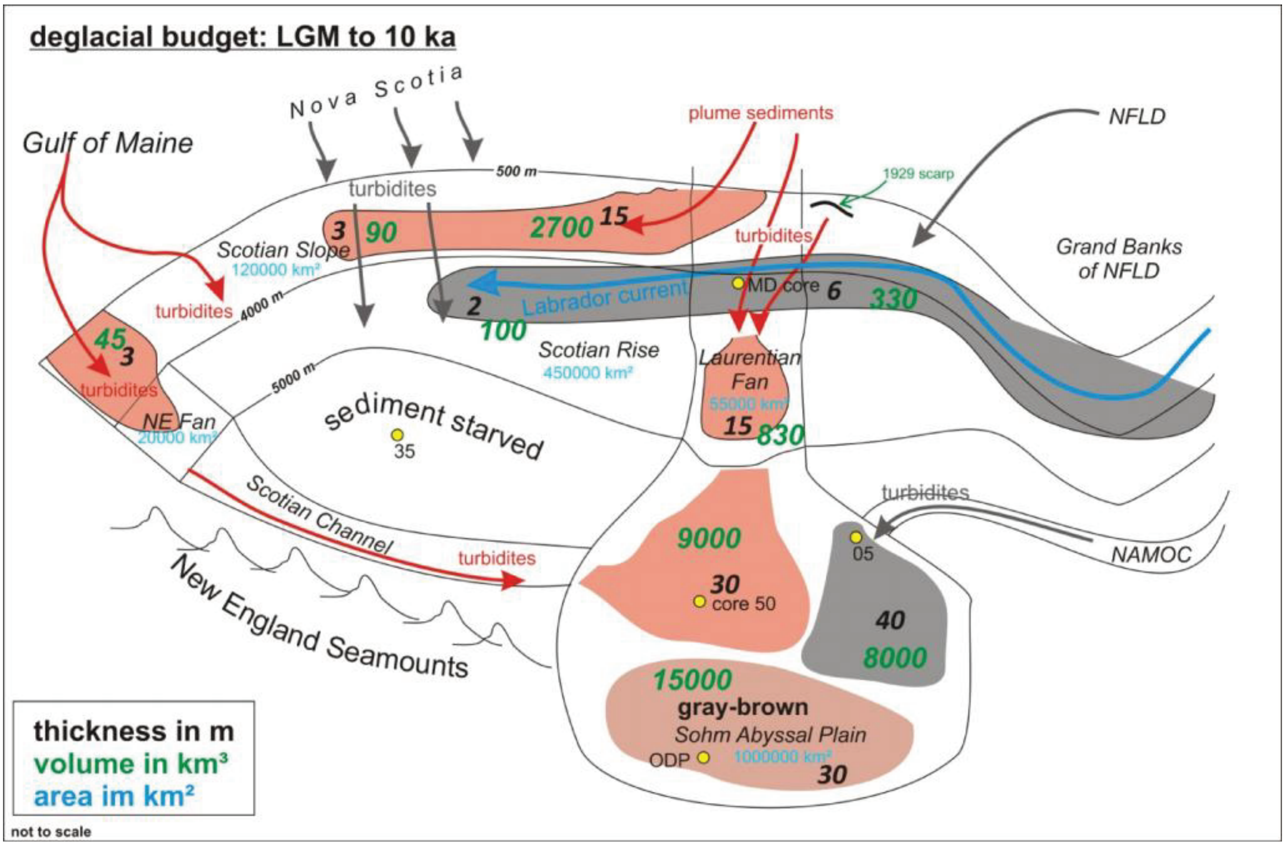

Figure 3.18: An attempt of a sediment budget of the Scotian Slope between the LGM and 10 ka; not to scale (see text for details)

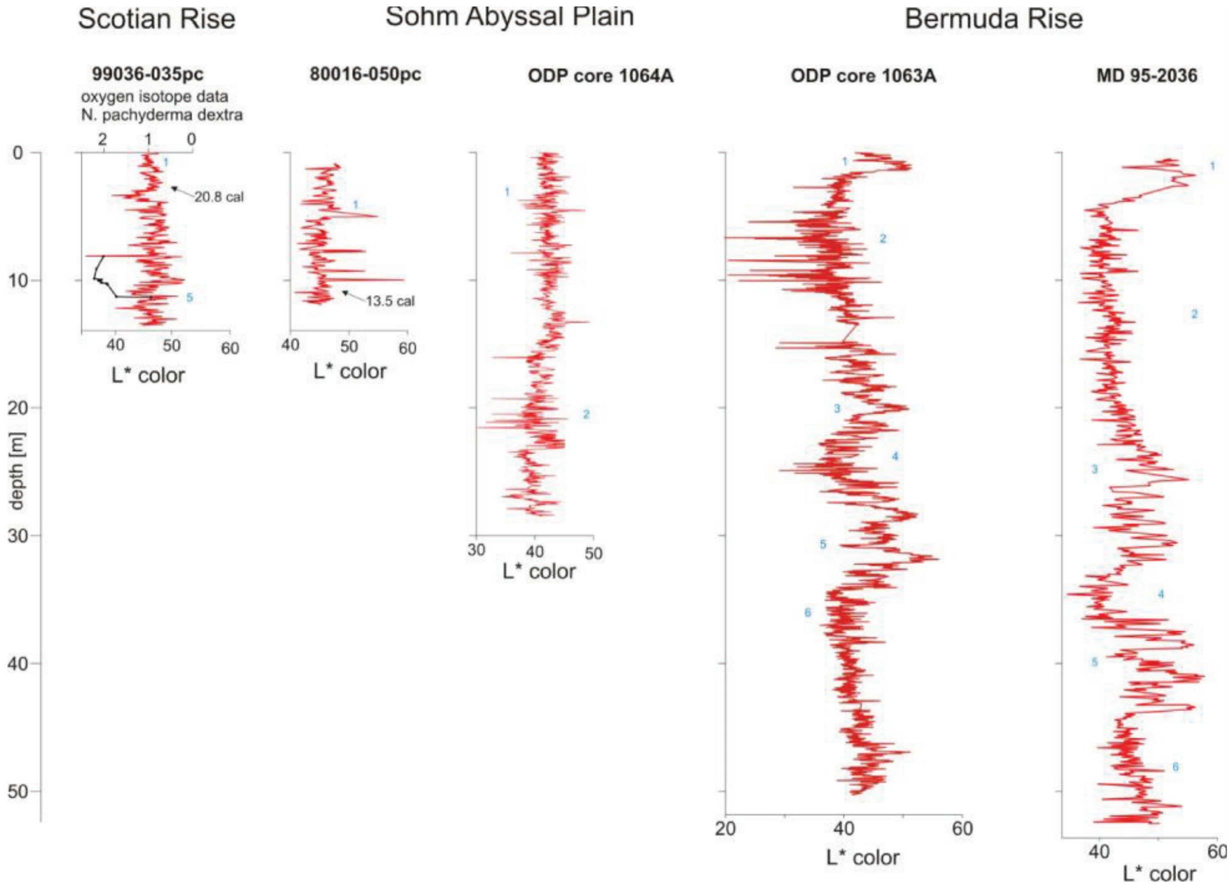

Figure 3.19: Core control and age model on the Sohm Abyssal Plain and the correlation to the Bermuda Rise based on CIELab color data. ODP data from LEG 172 (Keigwin et al., 1997; Keigwin, 2001), MD 95-2036 from Boyle (1997).

3.5. Discussion

Slope deposition along the Scotian Slope is dominated by sediment supply driven by the ice sheet fluctuations of the Nova Scotian ice sheet related to the Laurentide ice sheet (Piper, 2005; Shaw et al., 2006). The ice sheet behavior had a direct impact on slope sedimentation, resulting in highly variable sedimentation rates along-strike (**Figs. 14 and 20**). During the youngest time slice (OIS 1), very little sedimentation occurred and deposited thin hemipelagic drapes influenced by alongslope currents (Piper and Campbell, 2002). Very few erosional features have been observed (**Table 3**).

3.5.1. The Last Glacial Maximum on the Scotian Slope

During the LGM, the ice sheet terminated on the Scotian Margin along the shelf break (Shaw et al., 2006), where till tongues indicative of shelf-break ice sheets are present off several banks (**Fig. 1**) (Piper and Brunt, 2006).

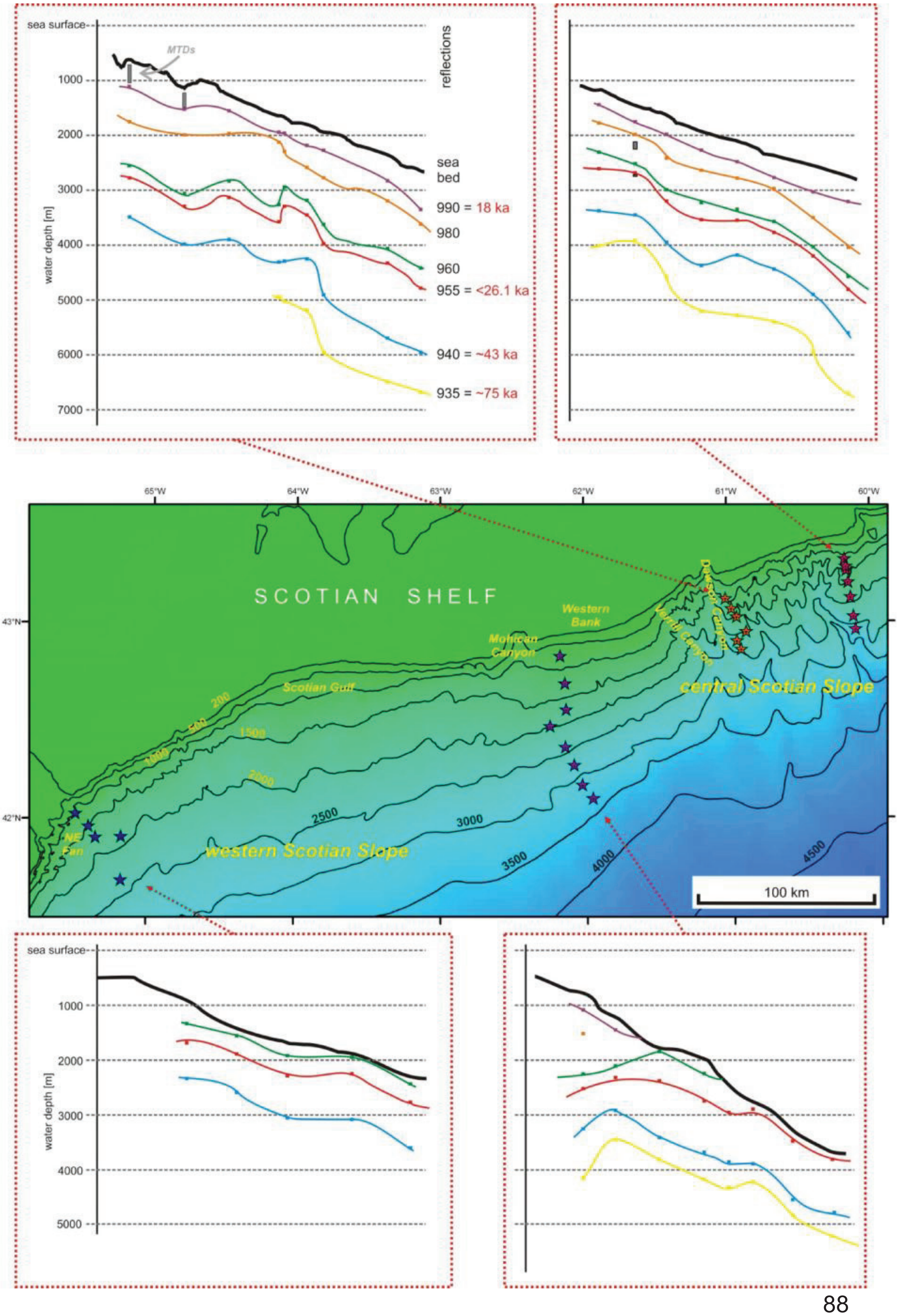

sea surface
MTDs
reflections
sea bed
990 = 18 ka
980
960
955 = <26.1 ka
940 = ~43 ka
935 = ~75 ka
water depth [m]
1000
2000
3000
4000
5000
6000
7000
65°W
64°W
63°W
62°W
61°W
60°W
43°N
42°N
SCOTIAN SHELF
Western Bank
Mohican Canyon
Dawson Canyon
Verrill Canyon
Scotian Gulf
central Scotian Slope
western Scotian Slope
NE Fan
200
500
1000
1500
2000
2500
3000
3500
4000
4500
100 km

Figure 3.20 on previous page: Summary diagram showing the alongslope variability in age of seabed and continuity of sequence downslope (from Huntec seismic data). The overall architecture and sedimentation rates are similar along the slope with few MTDs in the uppermost sequence. See details on ages of reflections in Fig. 14; bathymetry in meters.

Seaward of the major ice outlets (Laurentian Fan (Piper et al., 2007) and Northeast Channel (Schnitker et al., 2001; Hundert and Piper, 2008)) the sedimentary sequence is completely disturbed either by major MTDs and/or erosion by glacial meltwater (**Table 1**) (Piper et al., 2011).

Plume sedimentation prevailed on the open central Scotian Slope (Zone 1) with little erosion (**Fig. 5, Table 3**), except for a major scarp at 2900 m removing the LGM sequence completely (**Fig. 10**). The presence of plume sedimentation in this area is mostly driven by iceberg discharge from the Laurentian Channel (Piper and DeWolfe, 2003). Till tongues (**Figs. 1 and 8**) indicate less mobile ice on Western Bank for longer time spans (**Fig. 21**). Turbidity current deposits and wall failures dominate canyon systems, best documented in Zone 2 (**Fig. 21**). The western Scotian Slope (mainly Zones 5 and 6 (**Fig. 21**)) has been completely disturbed by MTDs. In Zone 6, these MTDs are glacigenic debris flows related to an ice stream in the Scotian Gulf (Huppertz et al., 2009), whereas in Zone 5 larger blocky MTDs resulting from slope failure are found. Very little deposition occurred in the eastern part of the slope, where the OIS 2 section is only present in rare canyon ridges: cores have recovered 1-2 m of reddish muds, which represent plume deposition during OIS 2 (Piper and DeWolfe, 2003).

3.5.2. The earlier evolution of the slope

The style of sedimentation during earlier time slices was greatly different from the OIS 2 system and the following Holocene. The volumetric importance of MTDs was higher and more widely spread (**Fig. 21 and Table 1**). The difficulty of reconstructing the paleo-slope morphology during earlier time slices is also that parts of the sequence have been removed by erosion, reflected in the major erosional events observed on the lower slope (**Figs. 12 and 16**). Nevertheless, during the older time slices, the slope morphology was not strongly different from the present sea floor as most smaller canyon systems were established near the base Quaternary (Piper et al., 1978) and the major canyons were established as early as the Paleogene (Campbell et al., 2004).

3.5.2.1. Oxygen isotope stage 3

During OIS 3, the ice sheet did not reach the shelf break on the Scotian Slope, but much of the adjacent continent remained glaciated (Stea et al., 1998; Stea et al., 2001). The central area of the Scotian Slope (**Fig. 1**: Zone 1 and 2) was dominated by plume sedimentation presumably related to proximal supply of glacial meltwater: most other areas along the slope show infrequent small-scale MTDs and related erosional features (**Figs. 11, and 12**). The lack of MTDs and till tonges at this time (**Fig. 8**) is consistent with the absence of glacial ice at the shelf break. The small-scale MTDs and the cut-and-fill morphology observed on the eastern Scotian Slope (**Fig. 11 and Table 3**) are likely related to infrequent passive margin earthquakes (Piper, 2005).

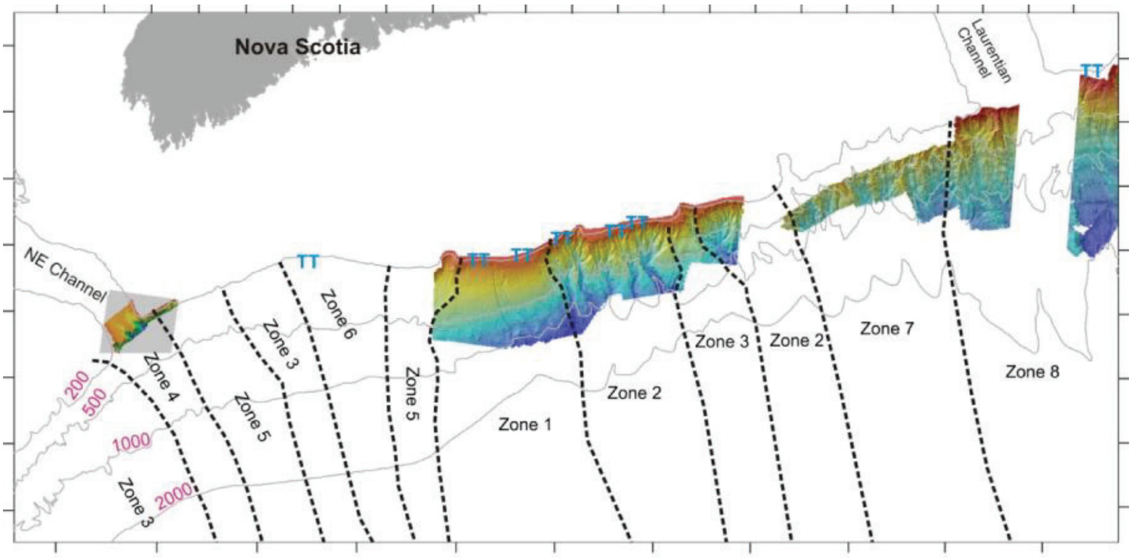

	Zone 1	Zone 2	Zone 3	Zone 4	Zone 5	Zone 6	Zone 7	Zone 8
OIS 2 -ice sheet at shelf break, -till tongue formation, -failures off ice streams -plume sedimentation on open slope	slope: well stratified with thin MTDs thoughout, turbidite sands common rise: sand waves and distal turbidites	slope: well stratified with few MTDs showing little erosion, turbidite sands throughout rise: distal turbidites	slope: well stratified with thin MTDs thoughout, turbidite sands common rise: turbidite sands in valleys seawards of canyons, scattered MTDs	slope: well stratified with thin MTDs thoughout, turbidite sands common rise: sand waves and distal turbidites, large MTDs common	slope: poorly statified sequence with frequent MTDs and turbidites throughout rise: some erosion, few small MTDs	slope: well stratified with few MTDs showing little erosion, turbidite sands throughout rise: distal turbidites and few MTDs	slope: well stratified with few MTDs thoughout, turbidite sands common rise: distal turbidites, few MTDs	slope: well stratified with few MTDs thoughout, turbidite sands common, bypassing frequent rise: distal turbidites, few MTDs
OIS 3 -ice sheet terminates onshore: slope marine -plume sedimentation in central area -infrequent small MTDs common	slope: well stratified few turbidite sands rise: few distal turbidites	slope: well stratified few turbidite sands rise: few distal turbidites	slope: well stratified with thin MTDs thoughout, turbidite sands common rise: sand waves and distal turbidites	slope: well stratified with few MTDs showing little erosion, turbidite sands throughout rise: distal turbidites and few MTDs	slope: poorly statified sequence with frequent MTDs and turbidites throughout rise: some erosion, few small MTDs	slope: well stratified with few MTDs thoughout, turbidite sands common rise: distal turbidites, few MTDs	slope: well stratified with few MTDs thoughout, turbidite sands common rise: distal turbidites, few MTDs	slope: well stratified with few MTDs showing little erosion, turbidite sands throughout rise: distal turbidites and few MTDs
Mid-Pleistocene -ice sheet terminates at the shelf break -till tongue formation -major MTDs on slope	slope: stratified, turbidite sands common rise: few distal turbidites, major erosion at 2500 m	slope: major wall failures, MTDs and turbidites on thalwegs rise: turbidite sands, few small MTDs	slope: widespread erosion, differently sized stacked MTDs rise: MTDs and turbidites common	slope: local erosion, few MTDs, turbidites common rise: small MTDs and turbidites common	slope: local erosion, small MTDs common rise: few MTDs	slope: widespread erosion, major MTDs, glacigenic debris flows rise: few MTDs, turbidite sands frequent	slope: widespread erosion, major MTDs, frequent wall failures rise: few MTDs, turbidite sands widespread	slope: well stratified with few MTDs showing little erosion, turbidite sands throughout rise: distal turbidites and few MTDs
Early Pleistocene -long-term slope evolution -by-passing and erosion frequent	slope: stratified, turbidite sands common rise: distal turbidites, major erosional surfaces, few MTDs	slope: major wall failures, MTDs and turbidites on thalwegs rise: turbidite sands, small MTDs	slope: widespread erosion, differently sized stacked MTDs rise: MTDs and turbidites common	slope: stratified, turbidite sands common rise: distal turbidites, major erosional surfaces, few MTDs	slope: widespread erosion, differently sized stacked MTDs rise: MTDs and turbidites common	slope: widespread erosion, differently sized stacked MTDs, few glacigenic debris flows rise: MTDs and turbidites common	slope: widespread erosion, differently sized stacked MTDs rise: MTDs and turbidites common	slope: well stratified with few MTDs showing little erosion, turbidite sands throughout rise: distal turbidites and few MTDs

Figure 3.21 on previous page: Summary of the temporal and spatial variability in styles of sedimentation on the Scotian Slope since OIS 2; the sedimentation patterns during the youngest OIS 1 time slice (younger than reflection 990) are not vary variable (Table 3) as plume and hemipelagic sedimentation influenced by ocean currents dominated in this time slice. The OIS 2 time is defined by the 990-955 reflections, the OIS 3 slice is bound by the 955-940 reflections. Both are described from Huntec seismic data. The airgun data defines the Mid-Pleistocene (940-880) and Early Pleistocene (880-845) time slices.

3.5.2.2. Mid-Pleistocene

During the OIS 4-12, the dynamics of the slope appear greatly different from younger stages, and voluminous MTDs covered vast areas along the slope (**Fig. 21**, **Table 3**). Stratified plume-sedimentation was only present in Zone 1 (**Fig. 21 and Table 3**) (Huppertz et al., 2009). The lower slope below 2500 m water depth failed almost completely (**Fig. 16b**) down to below the OIS 6 reflector 920 (**Fig. 10**).

The slope system differs greatly from the OIS 2 time slice (**Fig. 21**). More slope failures and deeper erosional cuts indicate higher energy in the slope system likely due to the presence of more ice volume at the shelf break over longer time spans. The presence of ice at the margin initiates more slope failures. Similar findings could be done along other parts of the SE Canadian Margin (Piper, 2005; Huppertz and Piper, 2009), indicating a direct link of slope failure to ice volume on the outer shelf areas.

5.2.3. Early Pleistocene

For understanding long-term sediment budgets on the slope, the OIS 12 to base of Quaternary section was analyzed (**Fig. 21**). This time span covers ~1.3 million years and thus reflects a different resolution than the other slices studied. The value of this time slice is to understand long-term slope evolution and may be used for estimating preservation potential of sedimentary units over longer time series. This unit is in general ~150 m thick (**Figs. 11 and 16**). This implies that either (a) due to the lack of major glaciations before oxygen isotope stage 12 (Piper et al., 1994) sedimentation rates were lower, or (b) most of the sequences deposited during this time slice has been eroded and deposited on the Sohm Abyssal Plain.

If case (b) were true, major erosion would be observed in the seismic data: nevertheless, fewer erosional surfaces and fewer MTDs are described from this time slice (**Figs. 10 and 11c**). This may suggest a more likeliness for case (a) in that the absence of widespread continental ice sheets changed sedimentation rates greatly. The few described MTDs may have been initiated by similar processes affecting today’s non-glaciated continental margins (e.g. Piper and Normark, 2001). This would explain the very different appearance in character of this slice depositing in more proximal basin settings (**Fig. 12**) rather than bypassing the lowermost slope and upper rise and depositing only on the Sohm Abyssal Plain (**Fig. 18**).

5.3. An attempt at a LGM-10 ka sediment budget

The Sohm Abyssal Plain is an important sediment sink on the SE Canadian continental margin, where not only the erosional products from the Scotian Slope are deposited, but the Northwest Atlantic Mid-Ocean Channel (NAMOC) also supplies turbidite sands from Labrador (**Fig. 18**) (Piper and Hundert, 2002). The overall sediment color can be used to estimate origin of the sediments in the area (Piper and Hundert, 2002; Piper and DeWolfe, 2003). Gray colors originate either from the north [Grand Banks of Newfoundland or transport within the Labrador current or through the NAMOC from Labrador] (**Fig. 18**) (Piper, 2005; Piper et al., 2007) or from mainland Nova Scotia (**Fig. 18**) (Stea et al., 1998), whereas reddish colored sediments come out of the Laurentian Channel or NE Fan (**Fig. 18**) (Piper and DeWolfe, 2003; Hundert and Piper, 2008).

The distribution of these different colored sediments on the margin can be used to infer sources and estimate volumes of sediment supplied from the different sources to the area (**Fig. 18**). Turbidite beds are commonly found on the slope indicative of by-passing on the slope resulting in greatly smaller sedimentation rates compared to the abyssal plain (e.g. core 35 in **Fig. 18**). A similar observation of bypassing was also observed during the 1929 earthquake on the Laurentian Fan (Piper and Aksu, 1987).

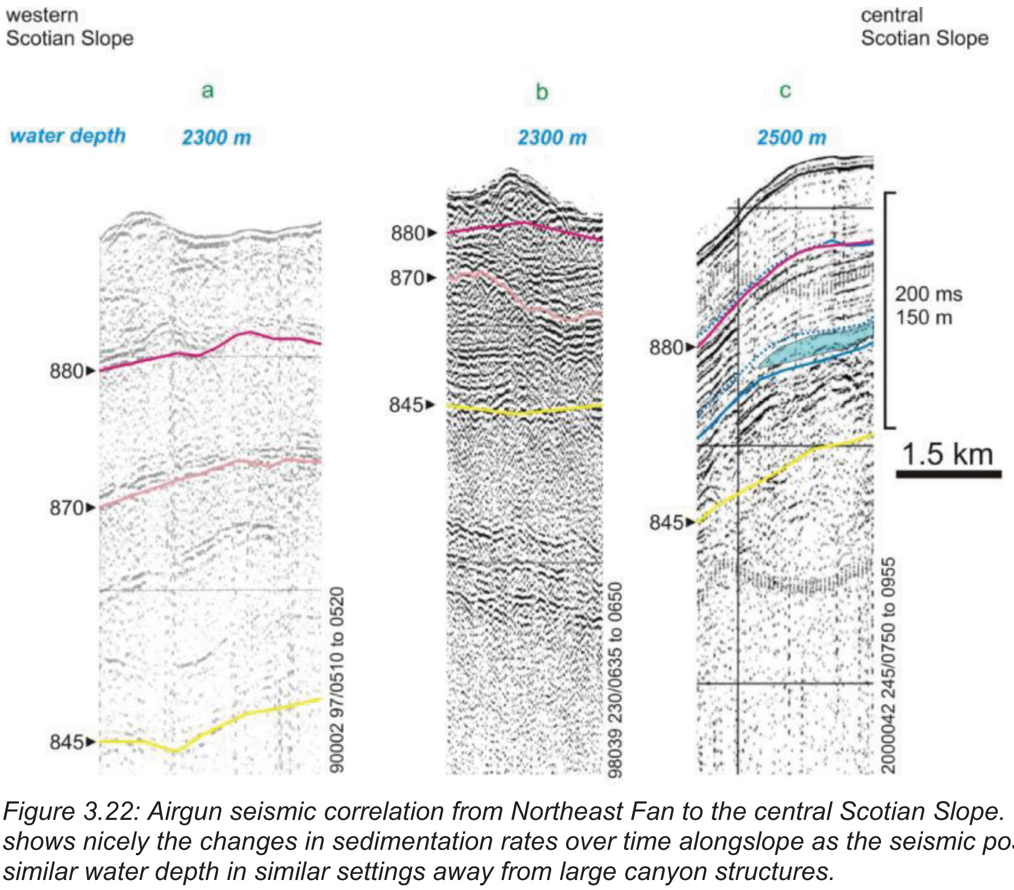

Figure 3.22: Airgun seismic correlation from Northeast Fan to the central Scotian Slope. This transect shows nicely the changes in sedimentation rates over time alongslope as the seismic positions are at similar water depth in similar settings away from large canyon structures.

5.4 Slope sedimentation rates

Huntec and lower resolution airgun data are used to define sedimentation rates throughout the slope (**Figs. 12. 20 and 22**). Huntec data shows the record of the last

~75 ka. Over this time span, sedimentation rates did not vary greatly along- or downslope (**Fig. 20**). Nevertheless, ages from the lower part of piston cores are generally older on the western Scotian Slope compared to the central Scotian Slope (**Fig. 20**). Similarly, the overall sedimentary sequence thins seawards.

This observation differs from previous studies on Northeast Fan (Hundert and Piper, 2008) where similar sedimentation rates were found as in the central Scotian Slope. The main reason for this finding is the variability of sedimentation in intercanyon highs and adjacent canyons (**Fig. 13a(2)**) due to erosion and/or non-deposition. Thus, sedimentation rates are highly depending on the setting as most canyons show activity throughout the glacial sequences.

When looking at the sedimentation rates on lower resolution airgun data, a very different picture must be drawn: in mid-slope positions (**Fig. 22**) rates are generally high, but vary greatly between the western and central Scotian Slope, whereas deep-water rates are significantly lower (**Fig. 12**).

This variability of sedimentation rates over long time scales may relate to the Mid-Pleistocene and Early Pleistocene time slices. Since OIS 12 (~ reflection 880, **Fig. 12**), very little sediment has been deposited on the rise, likely due to bypassing: deposition only occurred seawards on the SAP (**Figs. 19 and 21**). These much lower sedimentation rates at the toe of slope compared to mid-slope positions (**Figs. 12 and 22**) may suggest that during glacial times (since OIS 12), MTDs have (i) greater volumes (Fig. 21 and Huppertz et al., 2009), (ii) higher flow speeds, bypassing the toe of slope, (iii) occur more frequently (**Fig. 21**) and (iv) deposition is highly dependent on slope angles, enabling mid-slope deposition (**Fig. 22**) and remobilization during preceding flows.

5.5. Glaciated margin evolution

When comparing the Scotian Slope to other glaciated continental margins, e.g. the Norwegian Margin, three main differences are observed: (1) the frequency and spatial occurrence of glacigenic debris flows, (2) the abundance of large canyons and (3) the volumes and sizes of individual failures.

On the Scotian Slope, glacigenic debris flows are restricted to the Scotian Gulf (**Figs. 1 and 21**) (Piper and Normark, 2009), whereas they are widespread on the Norwegian Slope (King et al., 1998; Laberg and Vorren, 2000; Nygard et al., 2002). Glacigenic debris flows are direct evidence of ice streams (King et al., 1996) and low slope angles. When higher slope angles are encountered, as on the Laurentian Fan (Huppertz et al., 2009), these flows likely transform into turbidity currents and deposit only on the rise and abyssal plain (Piper and Normark, 2009). Lower slope angles were observed off the Scotian Gulf enabling their preservation. Thus, the overall slope angles seawards of ice streams on the Scotian Slope (**Fig. 1**) are much higher compared to the Norwegian Margin (Laberg and Vorren, 1995; Laberg and Vorren, 2000).

The Scotian Slope is characterized by large canyons (**Fig. 1**) seawards of meltwater gullies (Piper et al., 2007). The steep upper slope (**Fig. 1**) enables these flows to accelerate quickly and erode thereby canyons. On the less steep Norwegian Slope, either (i) the inertia of the flows is not large enough to accelerate and they start to deposit below the shelf break (Vorren and Laberg, 1997) or (ii) there may be less meltwater or fewer meltwater channels reaching the shelf break as this water was channelized within the trough mouths (Vorren et al., 1989). The lack of trough mouths on the Scotian Slope inhibits rapid drainage of the shelf and results in more frequently spaced but smaller scale meltwater channels at the shelf break (Piper et al., 2007), which feed and possibly incise canyons on the slope.

Only a few, but much larger MTDs were described from the Norwegian Slope (Taylor et al., 2002) compared to the Scotian Slope, where few large and frequently small MTDs have been found (**Fig. 21**). Massive failures are only found within Zone 1 on the Scotian Slope (**Fig. 12**). Possible explanations may be (a) the presence of canyons, or (b) the slope angle.

The (a) presence of canyons (**Fig. 21**) may (i) prevent failure from pore water pressure by draining the sediment easily, (ii) inhibit gas build-up, (iii) prevent long-term sediment buildup by frequent canyon wall failures and (iv) prevent erosion from mass wasting close to the shelf break as upslope failures are deflected into canyons. Therefore only places, where sediment can accumulate over large areas (e.g. Zone 1 on the Scotian slope, **Fig. 12**) or large parts of the Norwegian Slope (Taylor et al., 2002) are prone to large-scale failure events, whereas areas with several canyons show fewer MTDs in their succession (e.g. Zone 2 on the Scotian Slope, **Fig. 21**).

The (b) ice sheet behavior is closely related to canyon formation (Piper et al., 2011) and thus slope morphology. Seawards of shelf troughs, large ice streams supply vast amounts of sediment initiating frequent failures. High slope angles result in flow acceleration (e.g. Laurentian Fan, Northeast Fan, **Fig. 21**) and transformation to turbidity currents whereas lower slope angles result in upper slope deposition (e.g. offshore the Scotian Gulf or large parts of the Norwegian Slope (Taylor et al., 2002)). Small MTDs may be the result of uneven seabed microtopography filling in lows. This was observed on the western Scotian Slope (**Figs. 6 and 13**).

From the comparison of the Scotian Slope to the Norwegian Slope, our understanding of driving processes on the Scotian slope has improved. The main governing factors for slope sedimentation are (a) the slope angle, (b) the distribution of shelf troughs, (c) the distribution of canyons and (d) the availability and drainage passages of meltwater. The variability of these factors alongslope (**Figs. 1 and 19**) can be used to explain the changes in slope deposition (**Figs. 12, 20 and 22**). Few areas are more similar to the Norwegian Margin (Taylor et al., 2002), e.g. the Scotian Gulf characterized by glacigenic debris flows deposited on low slope angles below the shelf break. Other areas, as the Laurentian and Northeast Fan, are distinctly different in having much steeper slope angles where transformation to turbidity currents occurs rapidly on the upper slope (Piper and Normark, 2009; Piper et al., 2011).

5.6. Slope sedimentation model

Having established main factors of slope deposition in context of slope morphology on glaciated continental margins, a generic slope-sedimentation model can be developed. This model is valid for the Scotian Slope; nevertheless, it is likely also applicable to other glaciated continental slopes as similar features are also observed on other glaciated margins.

Five different depositional styles can be defined (Fig. 23). The styles are found (1) in areas with low slope angles and upper slope MTDs; (2) in areas with high slope angles, where net deposition is very low as debris flows are frequently transformed into turbidity currents and are deposited only on the lower slope or beyond; (3) in areas characterized by canyons with intercanyon areas that are stable showing long stratigraphic records whereas canyon floors are characterized by turbidites initiated by meltwater, (4) in areas that have till tongues at the shelf break, lack shelf troughs and show a thick continuous section; and (5) where large trough mouths fans were constructed from glacigenic debris flows (Fig. 23).

Each style is characterized by specific depositional processes. Style 1 has typical cut and fill structures and small MTDs throughout the section. The MTDs have generally low erosional potential but disturb the overall sedimentation greatly. Plume sedimentation may be present at times. Such a setting is found on parts of the western Scotian Slope (**Fig. 1**) or in the Riiser Larsen Sea on the Antarctic slope (Kuvaas et al., 2004).

Style 2 is characterized by high slope angles and very little slope deposition. These areas are usually seaward of large shelf troughs and are within canyon systems predating frequently the glacial stages (Skene and Piper, 2006). On these steep slopes, transformation of flows into turbidity currents is inferred to be common. Deposition only occurs on the lower slope and beyond building large abyssal plain turbidite lobes (**Fig. 18**). This has been observed on the Scotian Slope (Laurentian Fan and to some extent on Northeast Fan), and on parts of the Antarctic slope (Dowdeswell et al., 2006). Such high slope angles are not encountered on the Norwegian Slope (Taylor et al., 2002).

Style 3 is characterized by several slope canyons and plume sedimentation in intercanyon highs (**Figs. 9 and 16**). The canyons are mostly fed by meltwater. This is different from the Norwegian Margin where shelf troughs and related trough mouth fans are observed (Vorren et al., 1989; Vorren and Laberg, 1997). Thalwegs are characterized by turbidites and rare wall failures. Similar observations have also been made on the Greenland (Johnson et al., 1975; Vorren et al., 1998) and Antarctic margin (Wright and Anderson, 1982) which also show frequent deeply incised canyons on the slope likely cut by meltwater.

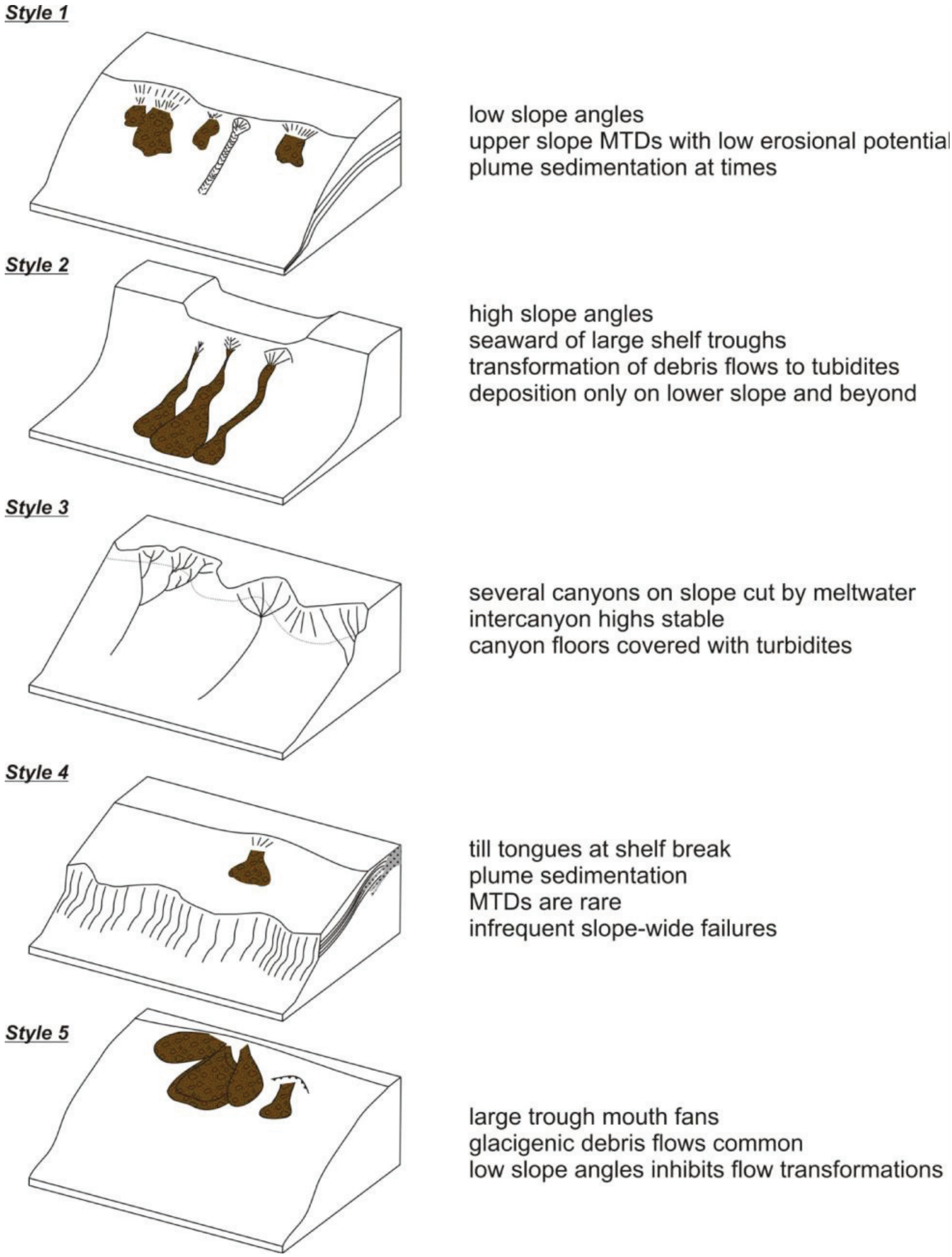

Figure 3.23: Block diagrams showing the schematic character of the different styles of slope deposition defined from the study of the Scotian Slope in comparison to other glaciated slope systems.

Style 4 is characterized by till tongues at the shelf break (**Fig. 8**), and thick sections of mostly undisturbed plume sedimentation characterizes the upper and mid-slope (**Fig. 4**), MTDs are rare within the section(**Fig. 21**), nevertheless infrequent slope-wide failures may affect at times this slopes (**Fig. 12**). Slope angles are low (Huppertz et al., 2009). Similar features are present on the Norwegian Margin were large slope failures occur within areas dominated by plume-sedimentation (Sejrup et al., 2003; Hjelstuen et al., 2004; Sejrup et al., 2005).

Style 5 is characterized by large MTDs, some of which are glacigenic debris flows showing the direct evidence of ice sheets at the shelf edge (King et al., 1998). This was observed seawards of the Scotian Gulf on the Scotian Slope and has also been observed much more frequently along the Norwegian Slope (Vorren and Laberg, 1997; King et al., 1998) and the Greenland margin (Wilken and Mienert, 2006). These types of flows are only preserved on comparably low slope angles where the failed sediment does not accelerate after entering the upper slope forming turbidity currents as observed in style 2.

When classifying glaciated continental margins (**Fig. 21** and Huppertz et al. (2009)), most of these described styles are likely present, nevertheless their spatial extent may vary greatly between slopes, as was shown on the Norwegian Slope in comparison to the Scotian Slope. Nevertheless, this classification scheme appears to be a very valuable tool applicable to very different margins for understanding not only more detailed slope processes including (a) the timing and extent of failures but also to define (b) variations in ice sheet dynamics including positions and size of former ice streams, the (c) flow paths of meltwater or the (d) improved understanding of slope stability governed by canyon frequency along the slope.

5.7. Changes of slope sedimentation in the Mid-Pleistocene: a slope-wide consideration

Five different slope styles were defined for establishing a slope depositional model (Fig. 23). These styles are only observed within the section when ice sheets were present at the margin (above refection 880 with an age of ~450 ka, e.g. Fig. 2) (Piper et al., 1994). The older section below reflection 880 is characterized by fewer MTDs, less erosion (Figs. 10 and 11c) and has a character more similar to non-glaciated slope systems (Piper and Normark, 2001). This observation highlights the impact of glaciations on a slope system, as the supply of sediment to the shelf break is significantly higher at those times compared to the setting when ice sheets do not cross the shelf, even if they are still present in the hinterland (Piper et al., 1994). Therefore, dynamics of slope systems are highly driven by the dynamics of ice sheets and thus ultimately climate changes on global scales.

6. Conclusions

A new slope-wide low- and high-resolution seismic stratigraphy has been established for the Scotian Slope based on previous seismic stratigraphic approaches.

The new seismic stratigraphy is used to understand the spatial and temporal variation in plume sedimentation, mass wasting and sediment bypassing on the entire Scotian Slope and parts of the Scotian Rise. At different times, different types of MTDs characterize the slope, depending directly on the ice sheet behavior at the shelf break: stagnant ice results in only small MTDs and mostly sandy turbidites, whereas seawards of ice streams (trough mouth fans) glacigenic and other debris flows characterize large parts of the sedimentary sequence. Additionally, styles of deposition are highly dependent on local slope angle, frequency and size of canyons and types of sediment available. Seawards of shelf troughs, bypassing and widespread erosion characterize the Scotian Slope: the most complete stratigraphic record is found seawards of stagnant ice: on the Scotian Slope, this is the case seawards of Western Bank. This information is used to understand not only long-term slope development, but also to establish a generic slope sedimentation model, which may be applied to various glaciated slope systems.

Acknoledgements

This study was supported by an NSERC Discovery Grant to DJWP and by the Canadian Program for Energy R&D through the Geological Survey of Canada. This is Geological Survey of Canada Contribution no. 2011XXXX.

References:

Armishaw, J.E., Holmes, R.W. and Stow, D.A.V., 1998. Morphology and sedimentation on the Hebrides Slope and Barra Fan, NW UK continental margin. In: M.S. Stoker, D. Evans and A. Cramp (Editors), Geological processes on continetal margins: mass-wasting and stability. Geological Society, Special Publication 129, London, pp. 81-104.

Baltzer, A., Cochonat, P. and Piper, D.J.W., 1994. In situ geotechnical characterization of sediments on the Nova Scotian Slope, eastern Canadian continental margin. Marine Geology, 120(3-4): 291-308.

Baltzer, A., Holmes, R. and Evans, D., 1998. Debris flows on the Sula Sgeir Fan, NW of Scotland. In: M.S. Stoker, D. Evans and A. Cramp (Editors), Geological processes on continental margins: sedimentation, mass-wasting and stability. Geological Society, 129, London, pp. 105-115.

Benetti, S., 2006. Late Quaternary sedimentary processes along the western North Atlantic margin. Ph. D. Thesis, University of Southampton, Southampton, 188 pp.

Berry, J.A. and Piper, D.J.W., 1993. Seismic stratigraphy of the central Scotian rise: a record of continental margin glaciation. Geo-Marine Letters, 13(4): 197-206.

Bondevik, S., Mangerud, J., Birks, H.H., Gulliksen, S. and Reimer, P., 2006. Changes in North Atlantic radiocarbon reservoir ages during the Allerød and Younger Dryas. Science, 312(5779): 1514-1517.

Boyle, E.A., 1997. Characteristics of the deep ocean carbon system during the past 150,000 years: ΣCO_2 distributions, deep water flow patterns, and abrupt climate

change. Proceedings of the National Academy of Sciences of the United States of America, 94(16): 8300-8307.
Campbell, D.C., 2000. Relationship of sediment properties to failure horizons for a small area of the Scotian Slope. Current research 2000-D8, Geological Survey of Canada, Dartmouth.
Campbell, D.C., Shimeld, J.W., Mosher, D.C. and Piper, D.J.W., 2004. Relationships between sediment mass-failure modes and magnitudes in the evolution of the Scotian Slope, offshore Nova Scotia, Offshore Technology Conference, Houston, Texas, pp. OTC 16743.
Cao, L., Fairbanks, R.G., Mortlock, R.A. and Risk, M.J., 2007. Radiocarbon reservoir age of high latitude North Atlantic surface water during the last deglacial. Quaternary Science Reviews, 26(5-6): 732-742.
Chubbs, J.F., 2003. Geohazards at the proposed Weymouth wellsite, Central Scotian Slope, offshore eastern Canada. B.Sc. Thesis, Saint Mary's University, Halifax, 75 pp.
Clausen, L., 1998. 1. Late Neogene and Quaternary sedimentation on the continental slope and upper rise offshore southeast Greenland: interplay of contour and turbidity processes. In: A.D. Saunders, H.C. Larsen and S.W. Wise (Editors), Proceedings of the Ocean Drilling Program, Scientific Results, 152, College Station, TX, pp. 3-18.
Dowdeswell, J.A., Evans, J., Ó Cofaigh, C. and Anderson, J.B., 2006. Morphology and sedimentary processes on the continental slope off Pine Island Bay, Amundsen Sea, West Antarctica. Geological Society of America Bulletin, 118(5-6): 606-619.
Gauley, B.-J.L., 2001. Lithostratigraphy and sediment failure on the central Scotian slope. M. Sc. Thesis, Dalhousie University, Halifax, 214 pp.
Gipp, M.R. and Piper, D.J.W., 1989. Chronology of Late Wisconsin glaciation, Emerald Basin, Scotian Shelf. Canadian Journal of Earth Sciences, 26: 333-335.
Gipp, M.R., 1994. Late Wisconsinan deglaciation of Emerald Basin, Scotian Shelf. Canadian Journal of Earth Sciences, 31(3): 554-566.
Han, G., 2004. Scotian Slope circulation and eddy variability from TOPEX//Poseidon and frontal analysis data. Journal of Geophysical Research, 109: C03028.
Hesse, R., Klauck, I., Khodabakhsh, S. and Piper, D.J.W., 1999. Continental slope sedimentation adjacent to an ice margin. III. The upper Labrador Slope. Marine Geology, 155(3-4): 249-276.
Hjelstuen, B.O., Sejrup, H.P., Haflidason, H., Nygård, A., Berstad, I.M. and Knorr, G., 2004. Late Quaternary seismic stratigraphy and geological development of the south Vøring margin, Norwegian Sea. Quaternary Science Reviews, 23(16-17): 1847-1865.
Hogg, N.G., 1983. A note on the deep circulation of the western North Atlantic: its nature and causes. Deep Sea Research Part A. Oceanographic Research Papers, 30(9): 945-961.
Hundert, T. and Piper, D.J.W., 2008. Late Quaternary sedimentation on the southwestern Scotian Slope, eastern Canada: relationship to glaciation. Canadian Journal of Earth Sciences, 45(3): 267-285.
Huppertz, T.J. and Piper, D.J.W., 2009. The influence of shelf-crossing glaciation on continental slope sedimentation, Flemish Pass, eastern Canadian continental margin. Marine Geology, 265(1-2): 67-85.

Huppertz, T.J., Piper, D.J.W., Mosher, D.C. and Jenner, K.A., 2009. The significance of mass transport deposits for the evolution of a proglacial continental slope. In: D.C. Mosher, C.R. Shipp, L. Moscardelli, J.D. Chaytor, C.D.P. Baxter, H.J. Lee and R. Urgeles (Editors), Submarine mass movements and their consequences IV. Springer Verlag, Dordrect, Heidelberg, London, New York, pp. 631-641.
Jenner, K.A., Piper, D.J.W., Campbell, D.C. and Mosher, D.C., 2007. Lithofacies and origin of Late Quaternary mass transport deposits in submarine canyons, central Scotian Slope, Canada. Sedimentology, 54(1): 19-38.
Jenner, K.A., Piper, D.J.W., Campbell, C.D. and Mosher, D.C., 2010. Piston cores and supporting high-resolution seismic data, Scotian Slope, Eastern Canada: data and interpretations. Open File 6558, Geological Survey of Canada, Ottawa.
Johnson, G.L., Sommerhoff, G. and Egloff, J., 1975. Structure and morphology of the West Reykjanes Basin and the southeast Greenland continental margin. Marine Geology, 18(4): 175-196.
Keigwin, L.D., Rio, D. and Acton, G.D., 1997. LEG 172 Preliminary Report. Preliminary Report No. 72, Ocean Drilling Program, College Station TX.
Keigwin, L.D., 2001. 9. Data report: Late Pleistocene stable isotope studies of ODP sites 1054, 1055 and 1063. In: L.D. Keigwin, D. Rio, G.D. Acton and E. Arnold (Editors), Proceedings of the Ocean Drilling Program, Scientific Results. Ocean Drilling Program, Volume 172, College Station, TX, pp. 1-14.
King, E.L., Sejrup, H.P., Haflidason, H., Elverhøi, A. and Aarseth, I., 1996. Quaternary seismic stratigraphy of the North Sea Fan: glacially-fed gravity flow aprons, hemipelagic sediments, and large submarine slides. Marine Geology, 130(3-4): 293-315.
King, E.L., Haflidason, H., Sejrup, H.P. and Løvlie, R., 1998. Glacigenic debris flows on the North Sea Trough Mouth Fan during ice stream maxima. Marine Geology, 152(1-3): 217-246.
King, L.H. and Fader, G.B.J., 1986. Wisconsin glaciation of the Atlantic continental shelf of southeast Canada. Bulletin 363, Geological Survey of Canada, Ottawa.
King, L.H., 1993. Till in the marine environment. Journal of Quaternary Science, 8(4): 347-358.
King, L.H., 1996. Late Wisconsinan ice retreat from the Scotian Shelf. Geological Society of America Bulletin, 108(8): 1056-1067.
Kuvaas, B., Kristoffersen, Y., Guseva, J., Leitchenkov, G., Gandjukhin, V. and Kudryavtsev, G., 2004. Input of glaciomarine sediments along the east Antarctic continental margin; depositional processes on the Cosmonaut Sea continental slope and rise and a regional acoustic stratigraphic correlation from 40° W to 80° E. Marine Geophysical Researches, 25(3-4): 247-263.
Laberg, J.S. and Vorren, T.O., 1995. Late Weichselian submarine debris flow deposits on the Bear Island Trough Mouth Fan. Marine Geology, 127(1-4): 45-72.
Laberg, J.S. and Vorren, T.O., 2000. Flow behaviour of the submarine glacigenic debris flows on the Bear Island Trough Mouth Fan, western Barents Sea. Sedimentology, 47(6): 1105-1117.
McCave, I.N., 1985. Sedimentology and stratigraphy of box cores from the HEBBLE site on the Nova Scotian continental rise. Marine Geology, 66(1-4): 59-89.

Mosher, D.C., Piper, D.J.W., Vilks, G.V., Aksu, A.E. and Fader, G.B.J., 1989. Evidence for Wisconsinan glaciation in the Verill canyon area, Scotian slope. Quaternary Research, 31(1): 27-40.
Mosher, D.C., Moran, K. and Hiscott, R.N., 1994. Late Quaternary sediment, sediment mass flow processes and slope stability on the Scotian slope, Canada. Sedimentology, 41(5): 1039-1061.
Mosher, D.C. and Simpkin, P.G., 1999. Environmental marine geosciences 1: status and trends of marine high-resolution seismic reflection profiling: data acquisition. Geoscience Canada, 26(4): 174-188.
Mosher, D.C., Piper, D.J.W., Campbell, D.C. and Jenner, K.A., 2004. Near-surface geology and sediment-failure geohazards of the central Scotian Slope. AAPG Bulletin, 88(6): 703-723.
Mosher, D.C. and Piper, D.J.W., 2007. Multibeam seafloor imagery of the Laurentian Fan and the 1929 Grand Banks landslide area. Open File 5638, Geological Survey of Canada, Ottawa.
Mosher, D.C., Xu, Z. and Shimeld, J., 2009. The Pliocene Shelburne mass-movement and consequent tsunami, western Scotian slope. In: D.C. Mosher, C.R. Shipp, L. Moscardelli, J.D. Chaytor, C.D.P. Baxter, H.J. Lee and R. Urgeles (Editors), Submarine mass movements and their consequences IV. Springer Verlag, Dordrect, Heidelberg, London, New York, pp. 765-775.
Mulder, T. and Moran, K., 1995. Relationship among submarine instabilities, sea level variations, and the presence of an ice sheet on the continental shelf: An example from the Verrill Canyon Area, Scotian Shelf. Paleoceanography, 10(1): 137-154.
Normark, W.R., Piper, D.J.W. and Stow, D.A.V., 1983. Quaternary development of channels, levees, and lobes on middle Laurentian Fan. AAPG Bulletin, 67(9): 1400-1409.
Nygard, A., Sejrup, H.P., Haflidason, H. and King, E.L., 2002. Geometry and genesis of glacigenic debris fows on the North Sea Fan: TOBI imagery and deep-tow boomer evidence. Marine Geology, 188(1-2): 15-33.
Pickerill, R.K., Piper, D.J.W., Collins, J., Kleiner, A. and Gee, L., 2001. Scotian slope mapping project: The benefits of an integrated regional high-resolution multibeam survey, Offshore Technology Conference, Houston, Texas, pp. OTC 12995.
Piper, D.J.W., Mudie, P.J., Aksu, A.E. and Hill, P.R., 1978. Late Quatenary sedimentation, 50°N, north-east Newfoundland shelf. Géographie physique et Quaternaire, 32(4): 321-332.
Piper, D.J.W. and Sparkes, R., 1987. Proglacial sediment instability features on the Scotian Slope at 63°W. Marine Geology, 76: 15-31.
Piper, D.J.W. and Aksu, A.E., 1987. The source and origin of the 1929 Grand Banks turbidity current inferred from sediment budgets. Geo-Marine Letters, 7: 177-182.
Piper, D.J.W. and Sparkes, R., 1990. Pliocene - Quaternary geology of the central Scotian Slope. Open File 2233, Geological Survey of Canada, Ottawa.
Piper, D.J.W. and Fehr, S.D., 1991. Radiocarbon chronology of late Quaternary sections on the inner and middle Scotian Shelf, south of Nova Scotia. Current Research Paper 91-1E, Geological Survey of Canada, Ottawa.
Piper, D.J.W., Mudie, P.J., Aksu, A.E. and Skene, K.I., 1994. A 1 Ma record of sediment flux south of the Grand Banks used to infer the development of glaciation in southeastern Canada. Quaternary Science Reviews, 13(1): 23-37.

Piper, D.J.W. and Skene, K.I., 1998. Latest Pleistocene ice-rafting events on the Scotian Margin (eastern Canada) and their relationship to Heinrich events. Paleoceanography, 13(2): 205-214.
Piper, D.J.W., 2000. Pleistocene ice outlets on the central Scotian Slope, offshore Nova Scotia. Current research 2000-D7, Geological Survey of Canada, Dartmouth.
Piper, D.J.W., 2001. The geological framework of sediment instability on the Scotian Slope: studies to 1999. Open File 3920, Geological Survey of Canada, Ottawa.
Piper, D.J.W. and Normark, W.R., 2001. Sandy fans—from Amazon to Hueneme and beyond. AAPG Bulletin, 85(8): 1407-1438.
Piper, D.J.W. and MacDonald, A., 2001. Timing and position of late Wisconsinan ice margins on the upper slope seaward of Laurentian channel. Géographie physique et Quaternaire, 55(2): 131-140.
Piper, D.J.W., Mosher, D.C. and Newton, S., 2002. Ice-margin seismic stratigraphy of the central Scotian Slope, eastern Canada. Current Research 2002-E16, Geological Survey of Canada, Dartmouth.
Piper, D.J.W. and Hundert, T., 2002. Provenance of distal Sohm Abyssal Plain sediments: history of supply from the Wisconsinan glaciation in eastern Canada. Geo-Marine Letters, 22(2): 75-85.
Piper, D.J.W. and Campbell, D.C., 2002. Surficial geology of the Scotian Slope, eastern Canada. Current Research 2002-E15, Geological Survey of Canada, Dartmouth.
Piper, D.J.W., Mosher, D.C., Gauley, B.-J., Jenner, K.A. and Campbell, D.C., 2003. The chronology and recurrence of submarine mass movements on the continental slope off southeastern Canada. In: J. Locat and J. Mienert (Editors), Submarine mass movements and their consequences: First international symposium. Kluwer Academic Publishers, pp. 299-306.
Piper, D.J.W. and Ingram, S., 2003. Major Quaternary sediment failures on the east Scotian Rise, eastern Canada. Current Research 2003-D1, Geological Survey of Canada (Atlantic), Dartmouth.
Piper, D.J.W. and DeWolfe, M., 2003. Petrographic evidence from the eastern Canadian margin of shelf-crossing glaciations. Quaternary International, 99-100: 99-113.
Piper, D.J.W. and McCall, C., 2003. A synthesis of the distribution of submarine mass movements on the eastern Canadian margin. In: J. Locat and J. Mienert (Editors), Submarine mass movements and their consequences: First international symposium. Kluwer Academic Publishers, pp. 291-298.
Piper, D.J.W., Adam, W.A.M., Stephen, I., Williams, G.L. and McCall, C., 2005. Late Cenozoic architecture of the St. Pierre Slope. Canadian Journal of Earth Sciences, 42(11): 1967-1985.
Piper, D.J.W., 2005. Late Cenozoic evolution of the continental margin of eastern Canada. Norwegian Journal of Geology (Norsk Tidsskrift), 85: 305-318.
Piper, D.J.W. and Brunt, R.A., 2006. High-resolution seismic transects of the upper continental slope off southeastern Canada. Open File 5310, Geological Survey of Canada (Atlantic), Dartmouth.
Piper, D.J.W., Shaw, J. and Skene, K.I., 2007. Stratigraphic and sedimentological evidence for late Wisconsinan sub-glacial outburst floods to Laurentian Fan. Paleogeography, Paleoclimatology, Paleoecology, 246(1): 101-119.

Piper, D.J.W. and Normark, W.R., 2009. Processes that initiate turbidity currents and their influence on turbidites: a marine geology perspective. Journal of Sedimentary Research, 79(6): 347-362.
Piper, D.J.W., Deptuck, M., Mosher, D.C., Hughes Clarke, J.E. and Migeon, S., 2011. Erosional and depositional features of glacial meltwater discharges on the eastern Canadian continental margin, SEPM Special Publication
Robichaud, M., 2006. Late Quaternary evolution of the Northeast Fan, offshore Nova Scotia. B.Sc. Thesis, Dalhousie University, Halifax, 98 pp.
Schnitker, D., Belknap, D.F., Bacchus, T.S., Friez, J.K., Lusardi, B.A. and Popek, D.M., 2001. Deglaciation of the Gulf of Maine. In: T.K. Weddle and M.J. Retelle (Editors), Deglacial history and relative sea level changes, northern New England and adjacent Canada. Geological Society of America, Special Paper 351, Boulder, pp. 9-34.
Sejrup, H.P., Larsen, E., Haflidason, H., Berstad, I.M., Hjelstuen, B.O., Jonsdottir, H.E., King, E.L., Landvik, J., Longva, O., Nygård, A., Ottesen, D., Raunholm, S., Rise, L. and Knut, S., 2003. Configuration, history and impact of the Norwegian Channel Ice Stream. Boreas, 32(1): 18-36.
Sejrup, H.P., Hjelstuen, B.O., Dahlgren, K.I.T., Haflidason, H., Kuijpers, A.H., Nygård, A., Praeg, D., Stoker, M.S. and Vorren, T.O., 2005. Pleistocene glacial history of the NW European continental margin. Marine and Petroleum Geology, 22(9-10): 1111-1129.
Shaw, J., Piper, D.J.W., Fader, G.B.J., King, E.L., Todd, B.J., Bell, T., Batterson, M.J. and Liverman, D.G.E., 2006. A conceptual model of the deglaciation of Atlantic Canada. Quaternary Science Reviews, 25(17-18): 2059-2081.
Shipboard Scientific Party, 2001. 6. Bermuda Rise and Sohm Abyssal Plain, sites 1063 and 1064. In: L.D. Keigwin, D. Rio, G.D. Acton, G.G. Bianchi, W. Borowski, N. Cagatay, W.P. Chaisson, B.M. Clement, E. Cortijo, G.B. Dunbar, R.D. Flood, S.-O. Franz, L. Giosan, J. Gruetzner, S. Hagen, B. Haskell, M.J. Horowitz, E.P. Laine, S.P. Lund, M. Okada, M.-S. Poli, I. Raffi, M.K. Reuer, Y.G. Ternois, T. Williams, D.M. Winter, M.E. Yokokawa and S.E. Swanson (Editors), Proceedings of the Ocean Drilling Program, Part A: Initial Reports 172. Ocean Drilling Program, 172, College Station, TX, pp. 251-308.
Shor, A.N. and Piper, D.J.W., 1989. A large Late Pleistocene blocky debris flow on the central Scotian slope. Geo-Marine Letters, 9: 153-160.
Skene, K.I. and Piper, D.J.W., 2003. Late Quaternary stratigraphy of Laurentian Fan: a record of events off the eastern Canadian continental margin during the last deglacial period. Quaternary International, 99-100: 135-152.
Skene, K.I. and Piper, D.J.W., 2006. Late Cenozoic evolution of Laurentian Fan: development of a glacially-fed submarine fan. Marine Geology, 227(1-2): 67-92.
Stea, R.R., Piper, D.J.W., Fader, G.B.J. and Boyd, R., 1998. Wisconsinan glacial and sea-level history of Maritime Canada and the adjacent continental shelf: A correlation of land and sea events. Geological Society of America Bulletin, 110(7): 821-845.
Stea, R.R., Fader, G.B.J., Scott, D.B. and Wu, P., 2001. Glaciation and relative sea level change in Maritime Canada. In: T.K. Weddle and M.J. Retelle (Editors), Deglacial history and relative sea level changes. Geological Society of America, Special Paper 351, Boulder, pp. 35-49.

Taylor, J., Dowdeswell, J.A. and Siegert, M.J., 2002. Late Weichselian depositional processes, fuxes, and sediment volumes on the margins of the Norwegian Sea (62-75°N). Marine Geology, 188(1-2): 61-77.
Tripsanas, E.K. and Piper, D.J.W., 2008. Late Quaternary stratigraphy and sedimentology of Orphan Basin: implications for meltwater dispersal in the southern Labrador Sea. Paleogeography, Paleoclimatology, Paleoecology, 260(3-4): 521-539.
Tucholke, B.E., Hollister, C.D., Biscaye, P.E. and Gardner, W.D., 1985. Abyssal current character determined from sediment bedforms on the Nova Scotian continental rise. Marine Geology, 66(1-4): 43-57.
Vorren, T.O., Lebesbye, E., Andreassen, K. and Larsen, K.B., 1989. Glacigenic sediments on a passive continental margin as exemplified by the Barents Sea. Marine Geology, 85(2-4): 251-272.
Vorren, T.O. and Laberg, J.S., 1997. Trough mouth fans — palaeoclimate and ice-sheet monitors. Quaternary Science Reviews, 16(8): 865-881.
Vorren, T.O., Laberg, J.S., Blaume, F., Dowdeswell, J.A., Kenyon, N.H., Mienert, J., Rumohr, J. and Werner, F., 1998. The Norwegian-Greenland Sea continental margins: morphology and late Quaternary sedimentary processes and environment. Quaternary Science Reviews, 17(1-3): 273-302.
Wade, J.A. and MacLean, B.C., 1990. The geology of the southeastern margin of Canada, Part 2: Aspects of the geology of the Scotian Basin from recent seismic and well data. In: M.J. Keen and G.L. Williams (Editors), Geology of the continental margin of eastern Canada. Geological Survey of Canada, Ottawa, pp. 190-238.
Wilken, M. and Mienert, J., 2006. Submarine glacigenic debris flows, deep-sea channels and past ice-stream behaviour of the East Greenland continental margin. Quaternary Science Reviews, 25(7-8): 784-810.
Wright, R. and Anderson, J.B., 1982. The importance of sediment gravity flow to sediment transport and sorting in a glacial marine environment: Eastern Weddell Sea, Antarctica. Geological Society of America Bulletin, 93(10): 951-963.

4. Shelf to slope sedimentary regimes on the northern Argentine and Uruguay continental margin: a critical review

Citation: Huppertz, T.J., Henrich, R. and Chiessi, C.M., draft. Shelf to slope sedimentary regimes on the northern Argentine and Uruguay continental margin: a critical review.

4.0. Abstract

Sedimentation processes on the northern Argentine and Uruguay continental margin are highly influenced by the fluvial discharge of the Paraná and Uruguay rivers, which drain the second largest basin in South America, and the Brazil Malvinas Confluence where Antarctic and tropical water masses confluence, detach from the margin and flow southeastwards into the Argentine Basin.

Shelf sedimentation is mainly governed by the fluvial La Plata plume, which supplies large amounts of clay and silt to the shelf. Due to relict Pleistocene and early Holocene sand and gravel bars across the estuary, fluvial sediment is deflected northwards along the Uruguayan Shelf. These Pleistocene sand and gravel bars were likely the reason why also during lower sea level sediment only reached the shelf break to the north of the estuary, whereas the southern part of the shelf seaward of the estuary has few pronounced channels. This deflection of fluvial sediment is also seen in slope sedimentation as the area to the north of the estuary is characterized by mass wasting whereas south of it along- and downslope driven processes are acting.

Therefore, slope morphology and thus sedimentation changes greatly seaward of the estuary. The southern part of the study area is characterized by the Ewing terrace on which contourite deposition occurs, whereas within canyons contourite sands fail and initiate turbidites. To the north, mass wasting, especially during the Pleistocene with lowered sea level, characterizes slope sedimentation patterns.

4.1. Introduction

Since the first description by Darwin (1846) almost 200 years ago, the northern Argentine and Uruguay margin has been subject of many studies including oceanographic, sedimentological and seismic studies with very different scopes and approaches. However, the interaction of many of the described processes is still poorly investigated.

The morphology of the northern Argentine and Uruguay continental margin is highly dominated by the funnel-shaped Rio de la Plata estuary, where the Paraná and Uruguay rivers enter the marine realm (Clapperton, 1993). This fluvial system, also referred to as the La Plata river system (Framinan and Brown, 1996), transports annually between 80 and 130x10^6 tons of coarse and fine-grained sediments to the southwest Atlantic Ocean (Depetris and Griffin, 1968; Gilberto et al., 2004).

4.1.1. Oceanographic setting

Apart from the impact of the La Plata Rivers, the regional oceanographic setting in the southwest Atlantic is characterized by the Brazil Malvinas confluence zone (BMC), in which Antarctic and equatorial-derived surficial water masses collide (Fig. 1). During collision, water masses detach from the slope and flow into the Argentine Basin. Within the collision zone, the northward flowing Falkland/Malvinas current collides with the southward directed Brazil current (Piola and Matano, 2001). Both currents are formed by two water masses: the Falkland/Malvinas current includes the Subantarctic Surface Waters and the Antarctic Intermediate Waters; the Brazil Current is formed by Tropical Waters and re-circulated Antarctic Intermediate Water termed South Atlantic Central Water: this setting results in the confluence of Antarctic Intermediate water with re-circulated Antarctic Intermediate Water (Stramma and England, 1999; Schmid et al., 2000; Piola and Matano, 2001; Sijp and England, 2008). Below this surficial confluence, the southward directed North Atlantic Deep Water results in vertical splitting of the Circumpolar Deep Water (Fig. 1) (Stramma and England, 1999; Mémery et al., 2000; Schmid et al., 2000; Piola and Matano, 2001). Below these intermediate water masses at a water depth of more than 4000 m, circulates the Antarctic Bottom Water clockwise through the Argentine Basin. At ~37°S it splits and parts of this water mass escape seawards, whereas other parts continue along the margin (Fig. 1) (Coles et al., 1996; Stramma and England, 1999).

The continental shelf circulation on the northern Argentine and Uruguay Shelf is highly governed by the slope circulation to the south of the BMC as the Subantarctic Shelf Waters are coupled with the Falkland/Malvinas current (Fig. 1) (Blanc et al., 1983; Rivas and Langer, 1996; Rivas, 1997). The shelf circulation does not change to the north of the estuary as parts of it continue as the Brazil Counter Current northwards (Stevenson et al., 1998; Zavialov et al., 2003). This circulation patterns forms to the north of the BMC the Subtropical Shelf Front along the contact of the Antarctic shelf waters and the tropical derived Brazil Current flowing southwards on the slope (Fig. 1) (Piola et al., 2000). Additionally, during the southern hemisphere winter, strong wind forcing drives the water masses to the NE following the prevalent wind directions (Guerrero and Piola, 1997; Piola and Rivas, 1997; Palma et al., 2004b).

Fluvial runoff from the La Plata rivers is generally deflected northwards due to the Coriolis force and the shelf circulation (Fig. 1) (Piola et al., 2005; Piola et al., 2008a). In today's setting, the coarse fluvial bedload is trapped within the estuary (Violante and Parker, 2004) and only mud is transported seawards along the northern coast line of the estuary within the plume, which slowly mixes with the shelf waters (Piola et al., 2005; Möller et al., 2008).

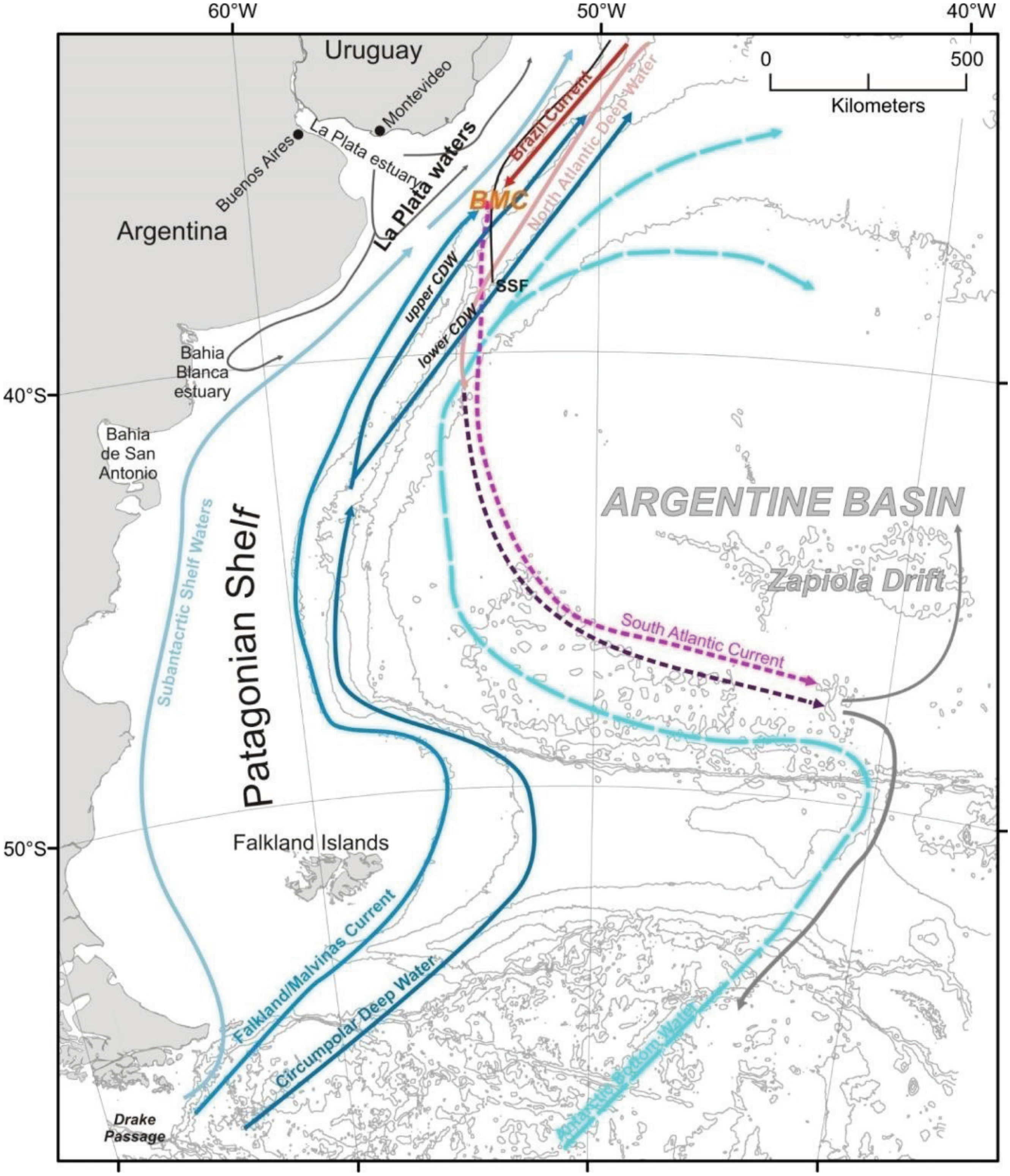

Figure 4.1: Simplified oceanographic setting in the southwest Atlantic Ocean where Antarctic and tropical water masses collide forming the Brazil Malvinas Confluence (BMC). SSF: Subtropical Shelf Front, CDW: Circumpolar Deep Water (after work of Blanc et al., 1983; Stramma and England, 1999; Piola and Matano, 2001; Palma et al., 2004a; Piola et al., 2008a).

4.1.2. Approach and goals

So far, most studies, covering the region have concentrated on specific aspects, e.g. (paleo-) oceanographic setting, the climate setting or the general sedimentation patterns. What is lacking up to now is an integrated approach covering oceanography, climate and sediment dynamics and their main drivers.

Here we present the current state of knowledge on this margin. The main aims are to (a) identify the main sedimentary processes acting along this margin, (b) to understand changes of shelf and slope deposition over time and with changing ocean circulation and sea level and (c) to define driving processes of shelf and slope sedimentary regimes and their dynamic interaction.

After briefly reviewing the general geological, hydrodynamic and climatic setting of the shelf and slope region, processes and resulting products are synthesized, sedimentary provinces identified and viewed in context of ocean circulation, long-term climate change and resulting sea level changes. This enables us to improve the understanding of this very complex sedimentary system on the northern Argentine and Uruguay continental margin.

4.2. Sediment dynamics along the northern Argentine and Uruguay continental margin

4.2.1. Morphology and geological setting of the Rio de la Plata estuary and inner shelf

At the Rio de la Plata estuary, the La Plata River, draining the second largest basin in South America, enters the South Atlantic Ocean (Depetris and Griffin, 1968; Depetris and Pasquini, 2007). The two rivers forming the La Plata River system, are the small Uruguay river and the much larger Paraná river (Depetris and Griffin, 1968). The annual sediment discharge from this river system ranges between 80 (Gilberto et al., 2004) and 130 (Depetris and Griffin, 1968) million tons. This variability of sediment discharge is highly driven by hinterland climate (Fig. 2) due to ENSO effects, as e.g. El Nino years are much wetter and thus reflect years of highest discharge (Depetris et al., 1996; Berbery and Barros, 2002). Additionally, runoff also shows seasonality as during austral summer (December to February) precipitation occurs in the northern part of the La Plata basin in tropical regions, whereas during austral winter (June-Spetember) precipitation is shifted southwards to the Argentine Plains (Garcia and Vargas, 1996; Zhou and Lau, 1998; Grimm, 2003; Cruz et al., 2009).

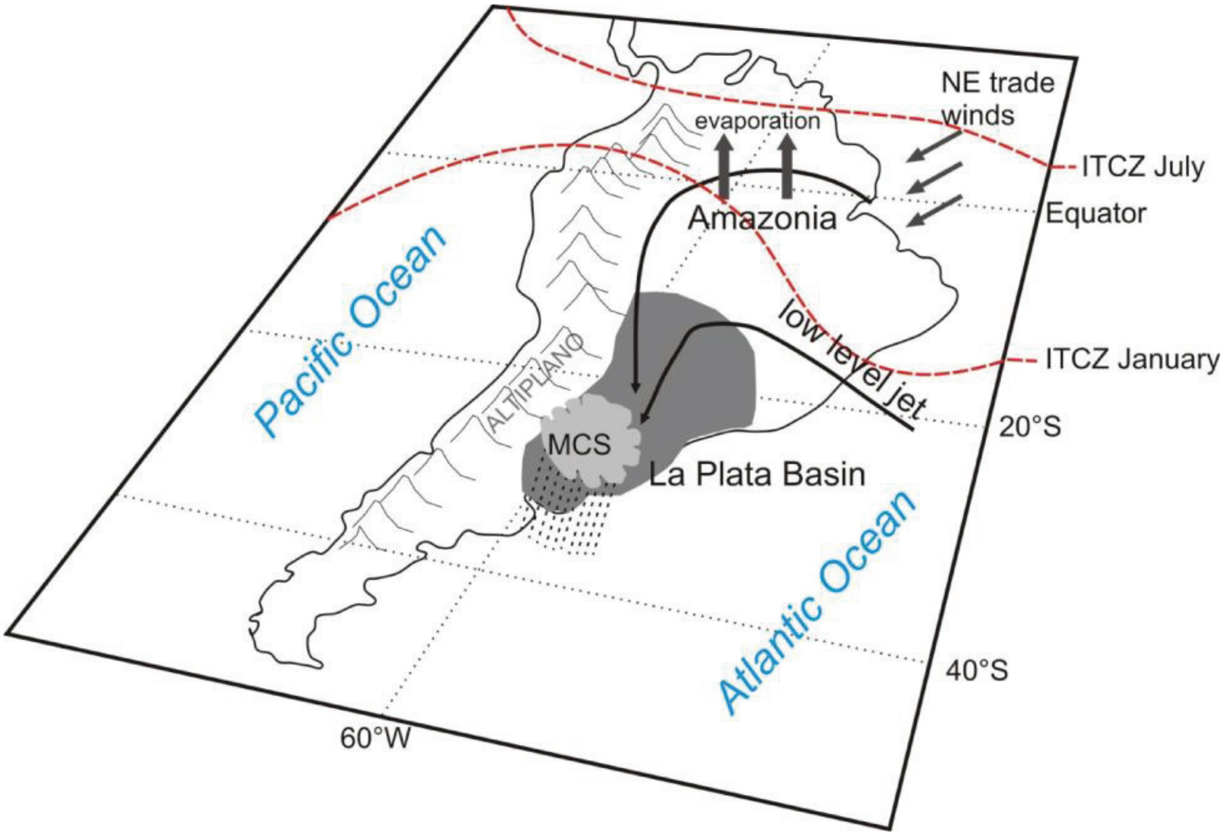

Figure 4.2: Simplified climatic setting in South America showing the major atmospheric circulation features that control today's climate in the Rio de la Plata basin (indicated in dark gray); the dry NE trade winds take up moisture over the Amazon Basin and supply moisture to the study area mainly through a low level jet system (MCS: mesoscale convective system); the seasonal position of the Intertropical Convergence Zone (ITCZ) is also indicated (modified after Vera et al., 2006).

The morphology of the estuary and the area of the delta from the La Plata Rivers has been mapped extensively between 1964 and 1969 (Wells and Daborn, 1997). During this mapping, 11 different "morphological units" (Wells and Daborn, 1997 and references therein) have been observed in the estuary (Fig. 3) and been linked to different hydrodynamic processes including variability in plume sedimentation, tides and storm reworking (Framinan and Brown, 1996; Wells and Daborn, 1997).

Playa Honda (Fig. 3, no. 1) is the seaward extension of the Parana River delta. This shallow area (max. 6 m water depth) is mainly being constructed by fluvial material. Delta-front advancement occurs by migrating sediment bars. The average yearly progradation is ~19 m (Wells and Daborn, 1997). The northern coastline of the estuary is characterized by a large channel system, the *Northern Channel* (Fig. 3, no. 2), which is currently being used as the main freshwater outflow from the La Plata Rivers and here the seabed is characterized by large furrow structures. Short-term morphological changes are frequently observed. Seawards, this canal system deepens gradually and changes its name to *Mudwells area* (Fig. 3, no. 11) seaward of Punta del Este (Wells and Daborn, 1997). South of this channel system is the large, and shallow *Bank Ortiz* (Fig. 3). Maximum water depths are 6 m. To the south of this bank is the *Intermedio*

Channel (Fig. 3) (Framinan and Brown, 1996; Wells and Daborn, 1997), which is a large tidal channel in the center of the estuary. Seawards of these banks and tidal channels are several consecutive banks perpendicular to the direction of fluvial discharge [*Barra del Indio, Bank Rouen, English Bank, Bank Arquímedes*] (Fig. 3) (Framinan and Brown, 1996).

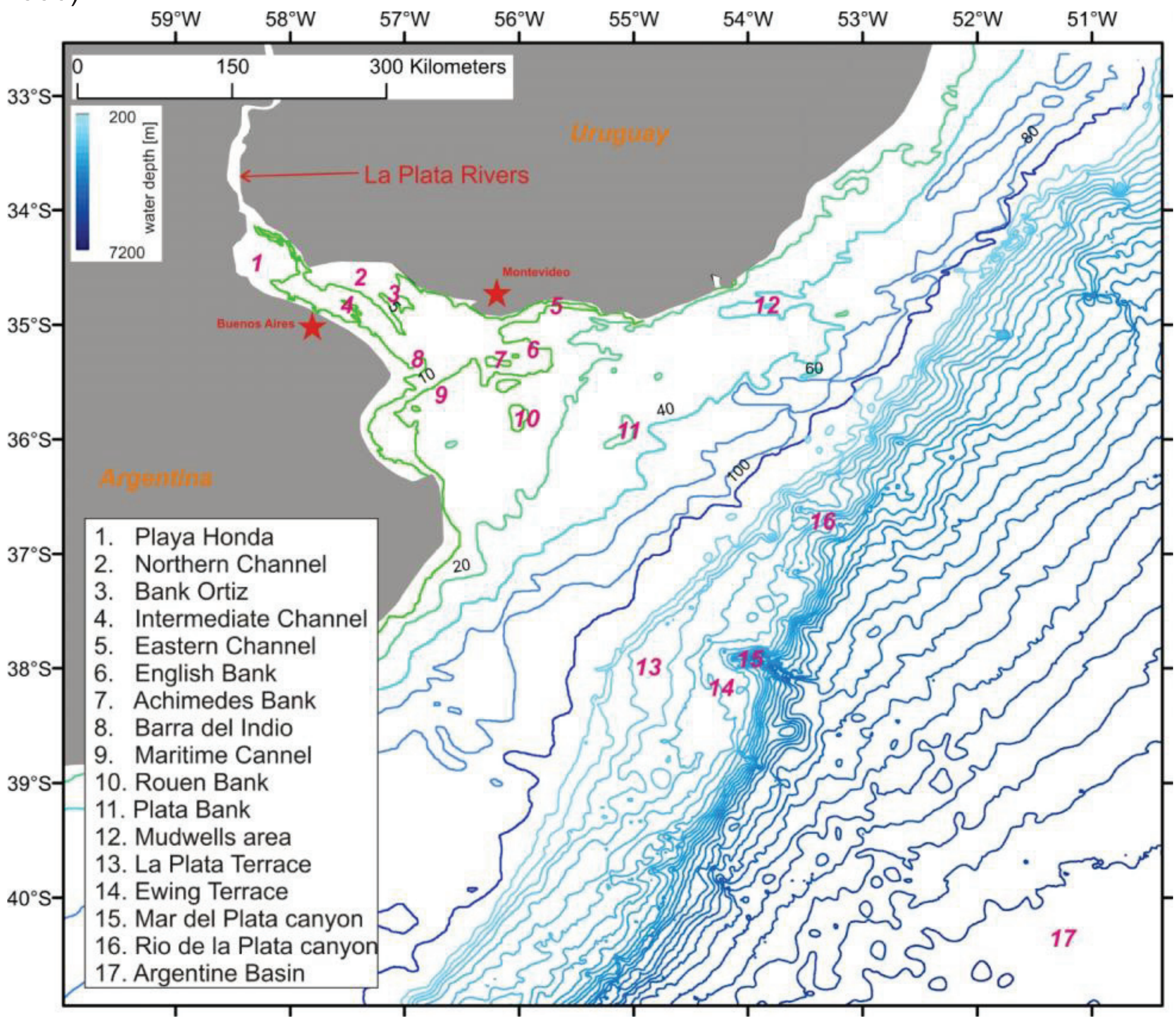

Figure 4.3: Bathymetry of the northern Argentine and Uruguay continental margin showing morphological features of this margin (after work of Framinan and Brown, 1996; Wells and Daborn, 1997), shelf bathymetry after Martins and Correa (1996), slope bathymetry from Gebco 2008 (www.gebco.net).

The arrangement of these shallow areas and deeper channels either of tidal or fluvial origin result in complex seabed morphology. This has a direct impact on surficial sediments (Fig. 4): the fluvial discharge channel along the northern coastline is silt-dominated (Martins and Correa, 1996). Seawards and away from the sand source, which are the La Plata Rivers (Iriondo, 2004; Pereyra et al., 2004), sand content decreases (Wells and Daborn, 1997). Banks are being constructed by sediment from

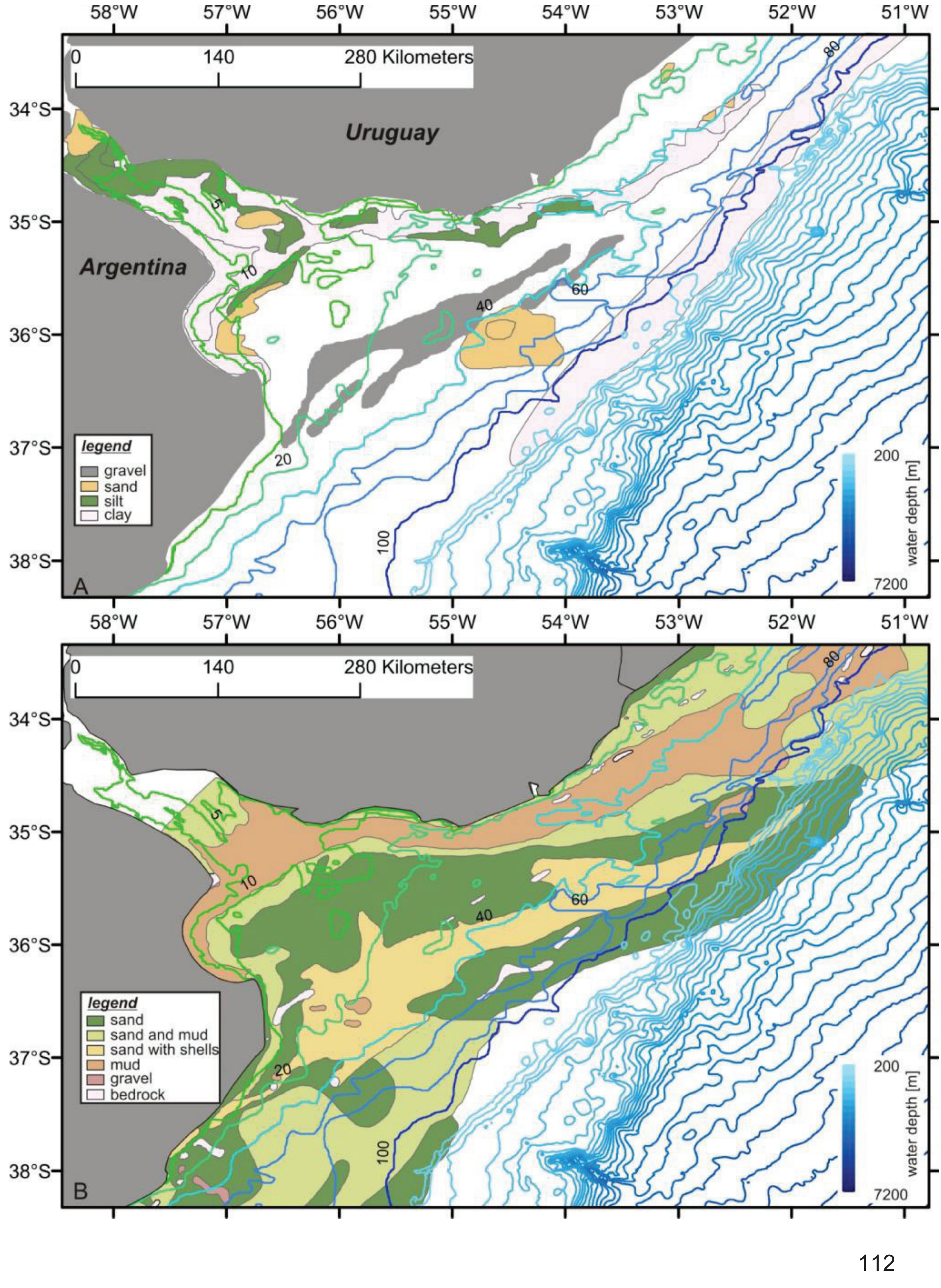
58°W
57°W
56°W
55°W
54°W
53°W
52°W
51°W
34°S
35°S
36°S
37°S
38°S
0
140
280 Kilometers
Uruguay
Argentina
5
10
20
40
60
80
100
legend
gravel
sand
silt
clay
200
water depth [m]
7200
A
legend
sand
sand and mud
sand with shells
mud
gravel
bedrock
B

Figure 4.4 on previous page: Different mapping approaches along the northern Argentine and Uruguay continental shelf and uppermost slope. These two maps show the difficulty of mapping regionally seabed as differences exist: nevertheless, the overall trends are similar in both maps. Map A after work of Martins and Correa (1996) with additions from Martins et al. (2005c); Map B from database www.freplata.org.

river discharge. These banks are sediment traps and prevent export of coarse-grained material to the shelf areas (Violante and Parker, 2004).

During the LGM, regional sea level was lowered by as much as 120 meters, which displaced the shoreline several tens of km seawards (Fig. 5) (Guilderson et al., 2000; Rostamini et al., 2000; Kaiser and Lamy, 2010). The post LGM sea level rise started at 17-15 ka (Violante and Parker, 2004) and at ~6.0 ka sea level was up to 7 m above current sea level (Farinati, 1985; Cavallotto et al., 2004). This observation of higher sea level in the mid Holocene (Fig. 6a) is supported by inland beach ridges (Fig. 6b) along most of the northern Argentine and Uruguay coastline (Delaney, 1966; Perillo et al., 2005), even though the elevation of highstands varies along the coastline. In Patagonia, the sea level during the Holocene was only 1-2 meters above present sea level, whereas in northern Argentina and Uruguay it may have been as much as 7 m above modern level (Fig. 6) (Guilderson et al., 2000; Rostamini et al., 2000; Schnack, 2009). This along-coast variability is also dependent on the local isostatic rebound observed especially along the southern coastlines (Rostamini et al., 2000; Peltier and Drummond, 2002).

4.2.2. Morphology and geology of the mid and outer shelf

At the mid shelf offshore the Rio de la Plata estuary, medium to fine grained sand shoals (Fig. 4) are interpreted as relict Pleistocene deposits and linked to a former barrier islands of the La Plata Rivers (Urien and Ewing, 1974; Martins et al., 2005c). Seawards of the shoals, the shelf is sand-dominated (Fig. 4) (Parker et al., 1997; Martins et al., 2005c), except for a small stretch along the shelf break, where mud-dominated sediments cover seabed (Urien and Ewing, 1974). At 85-90 m and 110-120 m water depth, pronounced morphological steps occur at the modern seafloor (Parker et al., 1997; Perillo et al., 2005), which may either be the product of erosion caused by sea level variations (Parker et al., 1997), or are related to deeper structural elements on this continental margin (Perillo et al., 2005). Sediment cores from the shelf area are mostly composed of quartz sands (typically 120 to 300 µm in mean grain size) with high abundance of shell fragments (Fray and Ewing, 1963).

The distribution of the muddy and silty sediments on the shelf is governed by the Rio de la Plata plume, which drifts northwards along the Uruguayan coastline (Fig. 4) (Wells and Daborn, 1997; Piola et al., 2005). Along the Uruguay shelf and in front of the La Plata estuary, relict Pleistocene coarse sand and gravel ridges and mud deposits are currently being reworked. Paleo-channels are gradually being in-filled by fluvial sediments from the La Plata Rivers and other small drainages feeding the lagoons along the Uruguay coastline (Martins et al., 2003; Martins and Urien, 2004; Martins et al., 2005c).

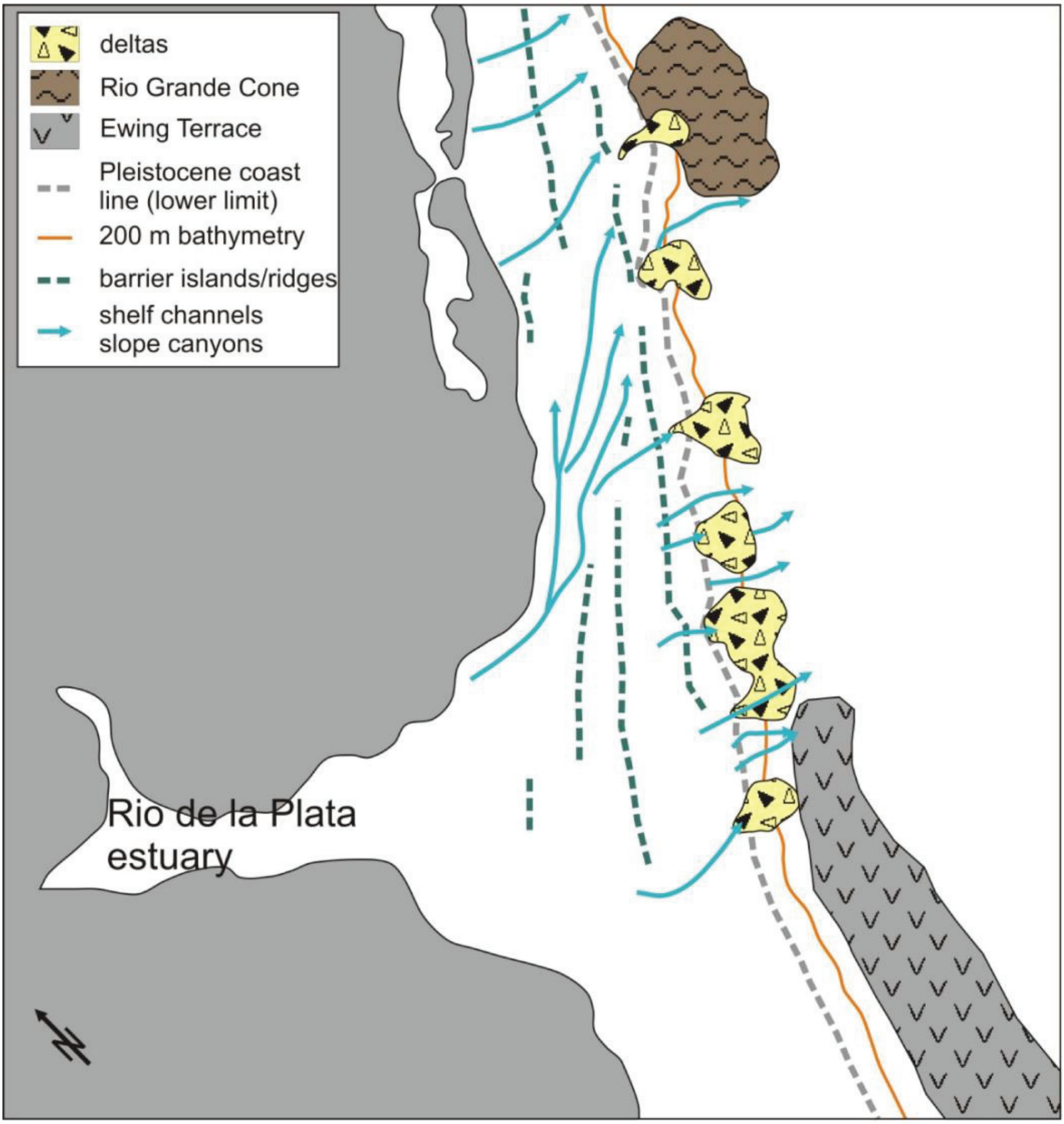

Figure 4.5: Setting of the northern Argentine and Uruguay Continental Margin during the Pleistocene with a lowered sea level; see text for details (after Martins and Willwock, 1987).

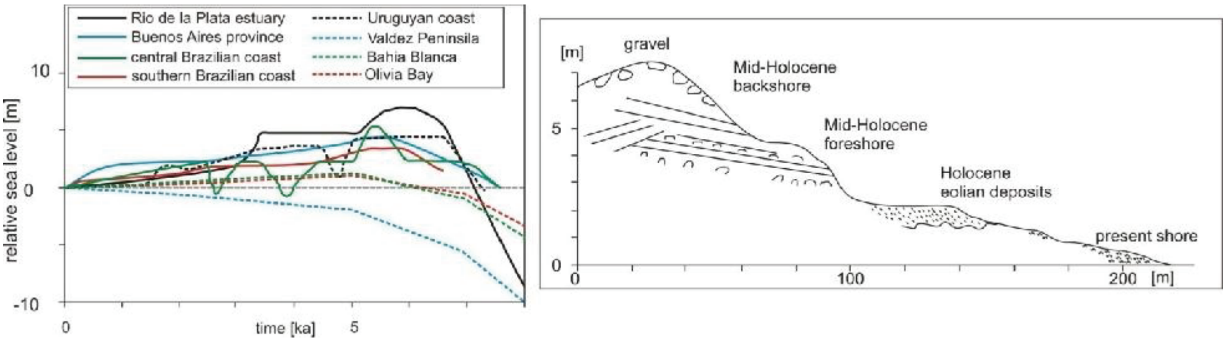

Figure 4.6: Holocene sea level curves from the Argentine, Uruguay and southern Brazil margin showing the variability of sea level in the area in the last 10 ka; Rio de la Plata estuary (Cavallotto et al., 2004), Buenos Aires Province (Isla, 1998), central Brazilian coast (Martin and Suguio, 1992), southeastern Brazil coast (Angulo et al., 2006), Uruguay (Baracco et al., 2008), Valdez Peninsula (Rostamini et al., 2000), Bahia Blanca (Rostamini et al., 2000) and Olivia Bay (Rostamini et al., 2000). b. generalized beach cross-section: raised beaches covered by late Holocene eolian deposits are frequently observed (not to scale) (after Isla et al., 1996).

4.2.3. Synthesis: sediment dispersal on the continental shelf: source to sink approach

The sedimentary regime on the northern Argentine and Uruguay continental margin is generally influenced by two main sources: (1) terrestrial sediment discharged from the La Plata Rivers and (2) sediment from southern sources, mainly runoff of Patagonia and Antarctica transported with the shelf currents to the area (Fig. 1) (Mahiques et al., 2008). Both sources can be differentiated using neodymium isotope data (Mahiques et al., 2008). Patagonian sediments can additionally be transported to the study area by wind-transport (Gaiero et al., 2003). This wind system also drives to some extent on a seasonal basis (mainly July-September) the shelf currents northwards (Palma et al., 2004b). On the Uruguayan coast, lagoonal runoff may be observed during intense hinterland precipitation and flooding events of small rivers along this coastline. This water is usually entrained into the La Plata plume (Jackson, 1985; Martins and Willwock, 1987).

Additionally, sediment may be transported to the area offshore the Rio de la Plata estuary from the Bahia Blanca estuary (Fig. 1), which is currently being eroded as it was shown that sediment wave fields offshore and to the north are fed by sediment from this estuary (So et al., 1974). Similarly, recent satellite images show this sediment export from the coastlines to at least mid-shelf areas (Fig. 7). In the following discussion, we will shed light on the possible sources and try to quantify discharge and discuss their possible variability through time.

The annual discharge of sediment from the La Plata Rivers is between 80 and $130x10^{-6}$ t (Depetris and Griffin, 1968; Gilberto et al., 2004). This number is likely changing depending highly on hinterland climate variability. These variations include changes in the El Niño/Southern Oscillation intensity and the variability of the Inner-tropical convergence zone (Zhou and Lau, 1998; Gan et al., 2004). During El Nino years, higher precipitation is observed within the La Plata Basin, resulting in higher runoff rates (Berbery and Barros, 2002). Similarly, the impact of monsoon climate may change annually (Zhou and Lau, 1998) and thus increased precipitation may result.

Furthermore, the area where the Paraná and Paraguay Rivers merge, is a large continental floodplain where sediment from the upper catchment areas is currently stored (Drago and Amsler, 1998; Wilkinson et al., 2006; Iriondo and Paira, 2007). At the moment, no data exists to whether this continental flood plain is currently active or how its storage capacity may have varied over longer time spans, especially during the glacial stages, when more intense weathering was active within parts of the catchment of the Paraná tributaries (Cruz et al., 2007). It is generally assumed that the discharge during the Last Glacial Maximum was significantly increased, even though the southernmost part of the Paraná basin (Argentine Plains) was likely drier and cooler compared to today's situation due to a northward migration of the circum-Antarctic fronts (Iriondo and Garcia, 1993; Panario and Gutiérrez, 1999; Tonni et al., 1999). As of now, a more detailed quantification of increase in sediment discharge is not possible due to lack of reliable data.

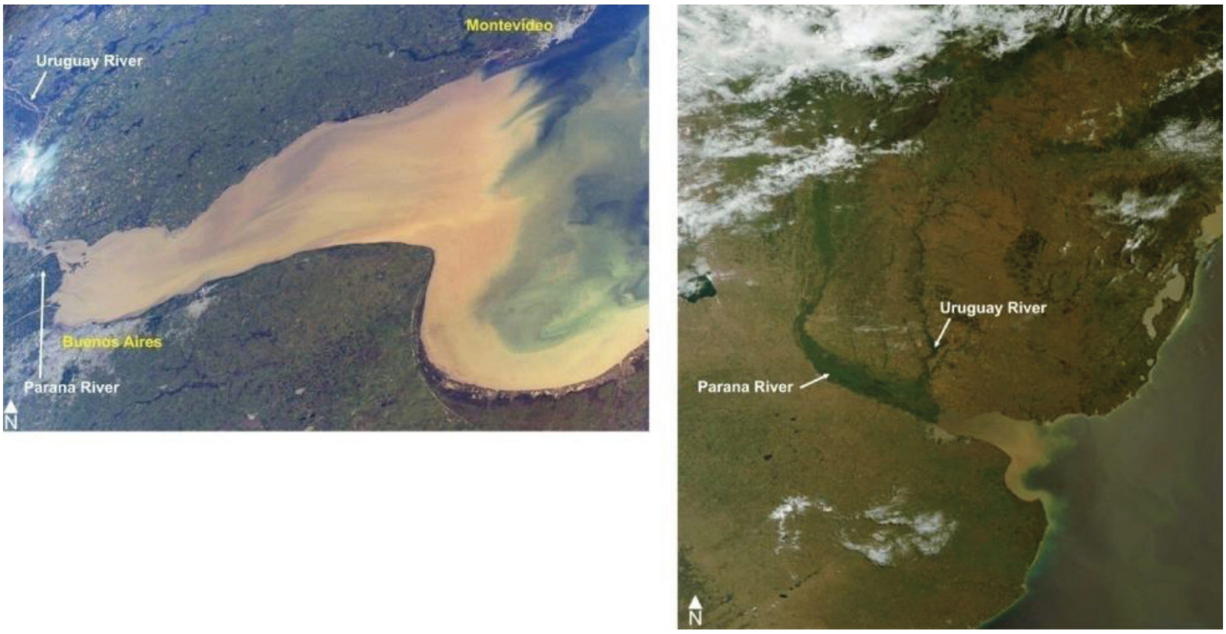

Figure 4.7: Satellite images of the Rio de la Plata estuary showing the distribution of the fluvial plume in the estuary. Sources: Photo 1: Astronaut photograph ISS008-E-5983 taken November 14, 2003, with a Kodak DCS760 digital camera equipped with an 80 mm lens and provided by the Earth Observations Laboratory, Johnson Space Center, http://earthobservatory.nasa.gov/IOTD/view.php?id=4028, Photo 2: from http://www.eosnap.com/image-of-the-day/confluence-of-the-uruguay-and-parana-rivers-argentina-december-10th-2010/ taken on December 10th 2010.

The fluvial sediment bedload enters at the head of the Rio de la Plata estuary. Today, the sedimentary bedload forms a plume extending along the northern coastline northwards. During exceptional flood events, this plume may be detected as far north as offshore southernmost Brazil (Piola and Romero, 2004; Piola et al., 2005; Piola et al., 2008a). Due to insufficient availability of coarse fluvial discharged material, Mulder and

Syvitski (1995) classified this river system of having a low possibility to form hyperpycnal flows, which may create seabed erosion (Mulder et al., 2003). Recent satellite imagery shows sediment-laden water extending from the river mouth seawards, along both the northern and southern coastline (Fig. 7).

The main channels within the Rio de la Plata estuary are considered being tidal channels (Fig. 3), which flush therefore very frequently (daily) and prevent any major fine-grained deposition (Framinan and Brown, 1996). Thus, a model described for deposition of fluvial material within the estuary predicting the trapping of such fines within the estuary (Wells and Daborn, 1997; Violante and Parker, 2004), does not agree with the dynamics of tidal channels in general, which would transport this fine material as bedload seawards. Due to the surge by the tides, this sediment described from banks within the estuary would not remain over longer time spans within the innermost estuary. Additionally, this type of erosion has recently been observed in the Bahia Blanca estuary just south of the Rio de la Plata estuary, where fine and even coarser (silty-fine sand) sediment is being exported seawards (Perillo and Sequeira, 1989). Thus the statement that all of the coarse sediment is trapped within the estuary (Violante and Parker, 2004) cannot be completely supported as it would not agree with the described hydrodynamic processes within such an estuary (O'Connor, 1991; Guerrero et al., 1997), which shows generally very variable sediment distribution patters over short-term monitoring.

When now looking at the setting during the last glacial cycle with a lowering of sea level by 110 m along this margin (Guilderson et al., 2000), more intense storm systems in the area (Clark and Wilson, 1992; Delmonte et al., 2002), likely even more intense reworking affected the shelf area, particular at its outer parts. Additionally, the seaward migration of the coastline (Fig. 5) (Guilderson et al., 2000) exported large amounts of medium to coarse sediment either by wind (Gaiero et al., 2003; Gaiero et al., 2007) from the much drier northern Argentine plains (Tonni et al., 1999) or by fluvial discharge to the shelf (Urien et al., 2003).

The sand ridges described from the outer shelf (Fig. 4) (Urien and Ewing, 1974) are considered relictic deposits constructed during lowered sea level by aeolian and fluvial processes (Martins et al., 2005c; Martins et al., 2005a; Parker et al., 2008), deposited during the last glacial sea level lowstand and being currently inactive. Similar sand ridges have also been observed offshore the Bahia Blanca estuary, which appear to be at times active, and are being built from sand exported from the coastline (So et al., 1974; Gómez and Perillo, 1991; Perillo et al., 2005). Thus, as there is no data shown to support the claim that similar sand ridges offshore the La Plata estuary are relic features (Martins et al., 2005c; Parker et al., 2008), they likely show similarly to the ones described seaward of the Bahia Blanca estuary, at least temporal activity. Further support is given by studies using suspended sediment concentrations at the sea bed, which could show a late Holocene net shelf export of up to 117 million MT/yr on this margin (Pierce and Siegel, 1979). Therefore, these large sand bodies offshore the Rio de la Plata estuary should be considered at least temporarily active. This activity does not necessarily need to involve deposition of new material but the winnowing of fine-grained muddy sediment within the area. This interpretation would agree with similar observation offshore southern Brazil. There, such coarse grained sand bars (Martins and Willwock, 1987; Martins et al., 2005b) have been interpreted as Holocene storm deposits (Figueiredo, 1980; Figueiredo et al., 1982).

Besides observing coarse-grained sediment at the shelf edge, several studies have mapped a large silty mud deposit at the shelf break just to the north of the estuary (Fig. 4) (Urien and Ewing, 1974; Martins et al., 2005c). It has even been recognized in core data (Urien and Ewing, 1974). Nevertheless, it was never commented about its origins. No apparent connection exists between the mud deposit and the possible sources for this mud along the coastline: fluvial discharge from the La Plata Rivers and Uruguayan coastal lagoons (Jackson, 1985; Piola et al., 2008a). This part of the slope is characterized by several shelf steps at 20-30, 85-100 and 110-120 m water depth (Perillo et al., 2005). These have been interpreted to represent marine terraces cut by the post-glacial sea level rise (Urien and Ewing, 1974; Urien et al., 2003; Perillo et al., 2005). A sea level rise would have reworked such a fine-grained mud deposit, thus it must have been deposited after the sea level rise was at these current water depths. Additionally, fluvial sources are unlikely as currently the mud from the La Plata Rivers was cored and imaged in seismic data in a channel on the central part of the Uruguayan shelf in the Mudwells area (Urien and Ewing, 1974; Urien et al., 2003; Martins and Urien, 2004; Martins et al., 2005c).

There are two possibilities to solve this enigma: the first is the simplest: its extent was mapped incorrectly and the deposit is not as extensive. The cores were taken by chance in a muddy depression and represents mud transported to the area by random wave processes. Similar observations have been made on the sandy Brazilian Shelf in the area of the Amazon delta, where small pockets of mud surrounded by sandy substrate have been observed (Trowbridge and Kinecke, 1994). The second possibility is that this mud deposit on the shelf break has been mapped correctly. This case is more difficult to explain. Its timing must be younger than the sea level rise starting around 18 ka (Fig. 5) (Guilderson et al., 2000). Nevertheless, deposition may have occurred close to the coastline as this part of the shelf is still comparably steep (Fig. 4) (Urien and Ewing, 1974), which would change the relative position of wave base during sea level rise rapidly enabling mud deposition relatively close to the former coastline. Then the source of this mud may in fact most likely be linked to fluvial runoff either from the La Plata Rivers (Urien and Ewing, 1974), or from the Uruguayan coastline, characterized even today by coastal erosion (Esteves et al., 2002; Isla and Schnack, 2009). The most challenging task with the depositional center is to explain why deposition occurred in this area rather than transporting the fine grained material offshore onto the slope, being steep in this area (Fig. 4) (Perillo et al., 2005). One possible explanation may be the oceanographic setting in this area: it is in the area of the Subtropical Shelf Front, in which the northward directed Antarctic shelf waters encounter the seaward lying equatorial-derived slope waters (Brazil Current) flowing southwards (Fig. 1). This creates eddies along the contact zone between the two water masses (Piola et al., 2000; Piola et al., 2008b). Within this eddy system, in which waters of both currents may be re-circulated (Piola et al., 2008b), lies the mud depositional area. Clay deposition may occur in such a setting either through (a) flocculation when the two water masses with different temperatures meet or (b) flow speeds are very low within such water mass contact zones and result in fine grained sediment deposition. Thereby, the observed mud depositional center may be formed. This depositional model may explain the observed distribution of the mud depositional center along the shelf break just to the north of the Rio de la Plata estuary.

Overall, the described shelf sedimentation patterns are highly driven by the oceanic circulation and perturbation from fluvial discharge from either the La Plata Rivers of local coastal discharge. Short- and long-term temporal variability may have a great influence on depositional patterns and change thereby seabed morphology greatly. Nevertheless, open questions remain to be solved on this continental shelf, including: (1) the glacial geomorphology of the shelf by mapping glacial La Plata fluvial channels and (2) the true nature of the shelf break mud belt by mapping its extent and coring it to define source areas using adequate methods, e.g. neodymium isotopes and tracer minerals, as it was shown to work on the slope (Krinsley et al., 1973; Mahiques et al., 2008).

4.2.4. Morphology and geology of the continental slope and abyssal plain

The continental slope offshore Northern Argentina and Uruguay is characterized by a marine terrace in ~1200 water depths, termed the Ewing terrace. This terrace is on average 65 km wide and mostly flat in the northernmost part, whereas it is tilted basinwards on the central and southern Argentine Slope (Urien and Ewing, 1974; Urien et al., 2003). It deepens gradually southwards (Hernández-Molina et al., 2009). Seawards of the Rio de la Plata estuary is another smaller terrace termed the La Plata terrace (Urien and Zambrano, 1973). The La Plata terrace, 200 km long and up to 50 km wide, is found at a water depth of 500-600 m. It is only present just south of the Rio de la Plata estuary. On the slope in the axis of the Rio de la Plata estuary, the Ewing Terrace terminates and to the north, no terraces are found on the Uruguayan Slope (Urien and Zambrano, 1973; Perillo et al., 2005; Hernández-Molina et al., 2009).

The terraced slope of northern Argentina is characterized by very few canyons, of which most start only on the Ewing Terrace (Hernández-Molina et al., 2009). Thick sand deposits cores and imaged within the canyons suggests that these canyons are important conduits for turbidity currents (Ewing et al., 1971; Ewing and Lonardi, 1971).

Regional studies have characterized the surficial sediments on the northern Argentine and Uruguayan Slope using sedimentological and geochemical methods. Most of the surficial sediments on the northern Argentine slope have southern sources, as the outflow from the La Plata River does not influence sedimentation on this part of the slope greatly (Krinsley et al., 1973; Frenz et al., 2003; Mahiques et al., 2008). Regional grain size data indicates sandy sediments south of the Rio de la Plata estuary (Urien and Ewing, 1974; Frenz et al., 2003). In the northern part of the study area, mainly the northernmost Argentine and Uruguay Slope, seismic data was used to define areas of mass wasting (Ewing et al., 1964; Antobreh, 2005). Several canyons characterize the seabed (Ewing and Lonardi, 1971; Lonardi and Ewing, 1971). Preliminary core descriptions from this part of the slope indicate highly muddy sediments with few sand beds interpreted as turbidite sands (Segl and Shipboard Scientific Party, 1994). Such interpretation is supported by more recent seismic data collected within the area (Spieß and Shipboard Scientific Party, 2002).

Very few detailed core studies have focused on the northern Argentine and Uruguayan Slope. Most of the studies were aiming at reconstructing ocean currents or other oceanographic parameters as ocean temperatures using proxies as biogenic particles (Romero and Hensen, 2002), surficial sediments (Frenz et al., 2003) or alkenone data (Benthien and Müller, 2000).

Age models were based on either pollen defining stratigraphic markers as glacial interglacial boundaries (Groot and Groot, 1966; Groot et al., 1967) or used chemical elements and their downcore variations to estimate ages (Stevenson and Cheng, 1969; Hensen et al., 2003; Riedinger et al., 2005). These studies mostly agree that the Holocene is thin with thicknesses of up to 50 cm maximum. This is underlain by stacked glacial deposits of the Wisconsin and earlier glaciations (Groot and Groot, 1966; Groot et al., 1967) depending on the core location: slope cores reach back to the LGM whereas basin cores show much longer stratigraphic records.

A wide range of studies exists in the Argentine Basin, the abyssal plain offshore Argentina and Uruguay. The basin is characterized by a large mud waves fields (Manley and Flood, 1993b) and the large sandy Zapiola sediment drift (von Lom-Keil et al., 2002). The sources of sediments for these sedimentary features are the continental slope and sediment transported within bottom water to the area (Ledbetter and Klaus, 1987; Hernández-Molina et al., 2009).

The Zapiola Drift, constructed by the Antarctic Bottom Water (von Lom-Keil et al., 2002) from reworked turbidite sands, has constructed a 2-3 km thick sandy drift deposit (Ewing and Lonardi, 1971). Variations of construction of the sediment drift are directly related to temporal and spatial bottom water fluctuations (Ledbetter and Klaus, 1987; von Lom-Keil et al., 2002). Similarly, the much finer grained mud waves study area was used to monitor Late Pleistocene and Holocene ocean current variability by using core data (Ellwood, 1993) and/or seismic data (Manley and Flood, 1993a; 1993b).

4.2.5. Synthesis: sediment dispersal on the continental slope: source to sink approach

Very little detailed information is currently available from the northern Argentine and Uruguay slope. Deposition has been linked to either driven by (1) alongslope processes shown by contourite deposits (Hernández-Molina et al., 2009), or from (2) downslope driven processes as turbidites and MTDs (Ewing et al., 1964; Antobreh, 2005). Nevertheless, no studies have looked in detail at the interaction of these two processes along this slope yet.

Slope sedimentation is thus driven either by ocean circulation or from gravity driven processes. A major change in slope morphology occurs seawards of the Rio de la Plata estuary, where the terraces, characteristic for the Argentine margin (Hernández-Molina et al., 2009), terminate and no terraces are observed offshore Uruguay (Zambrano and Urien, 1970; Parker et al., 1997; Perillo et al., 2005). This observation was always only made from bathymetry data yet, even though such a change in slope sedimentation is obvious from contourite deposition on the Argentine slope (Hernández-Molina et al., 2009) to mass wasting on the Uruguayan slope (Ewing and Lonardi, 1971; Antobreh, 2005). The change in slope sedimentation was likely much more pronounced during glacial stages with lowered sea level and a much higher fluvial discharge from the La Plata Rivers (Wells and Daborn, 1997) and the presence of a delta system to the north of the estuary (Fig. 5) due north of the termination of the Ewing terrace (Urien et al., 2003). Therefore, it is surprising that no studies have recognized this change in slope sedimentation yet. Therefore, we discuss known slope sedimentation processes in the light of this morphological change, where to the north mass wasting dominates whereas south of it alongslope driven processes are mostly described.

4.2.5.1. Terraced slope section offshore Argentina

On the terraced part of the slope, none of the slope canyons start at the shelf break but on the Ewing terrace (Parker et al., 1997). The formation of this terrace is directly linked to the Antarctic Intermediate Water (Hernández-Molina et al., 2009). Most of the smaller terrace-cutting canyon systems are cut from sandy turbidites and are not directly related to deeper-rooted transform faults (Ewing and Lonardi, 1971; Lonardi and Ewing, 1971). The larger canyon systems, e.g. the deeply incising Mar del Plata canyon (Spieß and Shipboard Scientific Party, 2002), may well be related to such transform faults, as this canyon is for example close to one of these transform zones (Franke et al., 2007).

A recent study on the southern Argentine margin (Lastras et al., 2011) could show that initiation of the smaller canyons starts below the terraces and progresses upslope (retrogressive) reaching at some point the terrace. Initiating process are amalgamations of scours created from contour current processes (Lastras et al., 2011). Thus, most of the smaller sized canyons are retrogressive failure structures. Another likely process for initiating canyons in such a contour current influenced slope system is current-induced undercutting as it was observed in other continental slope systems, where the contour current destabilized slope sediments by undercutting (Dingle, 1980). Therefore the turbidites described from the canyons (Ewing and Lonardi, 1971; Spieß and Shipboard Scientific Party, 2002; Lastras et al., 2011) have failed from the contourite deposits described from the Ewing terrace (Hernández-Molina et al., 2009).

Nevertheless, downslope driven processes are also active in this part of the slope as preliminary core descriptions have observed shells and foraminifers on the slope, which have clearly shelf sources (Segl and Shipboard Scientific Party, 1994; Spieß and Shipboard Scientific Party, 2002). Such small shells would have been corroded within the Antarctic Bottom Water (Volbers and Henrich, 2004). Additionally, shelf sediment export has been estimated as high as 17 Mt/yr along this part of the slope (Pierce and Siegel, 1979). Therefore, the uppermost slope between the shelf break and the Ewing terrace is not only characterized by contour current activity (Hernández-Molina et al., 2009), but likely also by downslope driven processes. Furthermore, during lowered sea level (Guilderson et al., 2000; Rostamini et al., 2000) and resulting enhanced storminess (Clark and Wilson, 1992) even higher shelf export is likely. Therefore it is suggested that the terraced part of the slope is influenced not only by contour current activity but also by downslope driven processes affecting not only canyon systems below the terrace (Ewing and Lonardi, 1971) but also parts of the upper slope where no canyons are gullies are observed (Parker et al., 1997).

4.2.5.2. Un-terraced slope section offshore Uruguay

The un-terraced slope to the north of the Rio de la Plata estuary is highly influenced and shaped by mass wasting processes (Urien and Ewing, 1974; Antobreh, 2005). During the Holocene, little sediment is transported to the shelf break as the La Plata river plume remains on the central part of the shelf in the Mudwells area (Figs. 3 and 4) (Framinan and Brown, 1996; Piola and Romero, 2004). During glacial sea level lowstands (Fig. 5) a very different picture can been drawn: shelf sedimentation indicates fluvial sourced sediment (Urien and Ewing, 1974) supplied to the shelf break, and initiating turbidites and mass transport deposits (Spieß and Shipboard Scientific Party, 2002; Antobreh, 2005) which characterize subsurface slope deposition. The sources of the failing material are likely amongst others the La Plata Rivers, which supplied at times high rates of sediment to the slope just to the north of the estuary (Martins and Willwock, 1987). Nevertheless, no true delta complex has been imaged in this part of the slope. The reason for this is that the fluvial sediments were mostly channelized in large canyon structures present along this part of the margin (Urien and Ewing, 1974; Wells and Daborn, 1997; Urien et al., 2003; Martins et al., 2005a).

Slope failure initiation along this part of the slope may have occurred by (1) slope oversteepening, (2) due to passive margin seismicity, (3) porewater pressures, (4) gas hydrate dissociation or (5) from retrogressive failures. All five possibilities are evaluated and their likeliness to occur on this part of the slope evaluated.

(1) During glacial stages, the La Plata Rivers supplied at times large volumes of sediment to this part of the slope. The high sediment supply imaged on seismic data could be used to define oversteepening as the likely triggering process of some of the observed mass transport deposits (Antobreh, 2005).

(2) Passive margin seismicity is reported from the Uruguayan margin (Benavídez Sosa, 1998) and linked to random passive margin seismicity. As the few existing slope studies could not show the timing of failures along the slope it remains unclear if failures occurred simultaneously on the margin, which would support the idea of earthquakes triggering the failures.

The sediments found in this part of the slope are dominated by muds and intercalated sands (Urien and Ewing, 1974; Spieß and Shipboard Scientific Party, 2002). (3) Porewater pressure and its rapid changes during e.g. Pleistocene storm events may trigger failures in such sediments, as the imposed shear stresses cannot drain easily due to the muddy layers. This imposed stress may have initiated some of the observed failures along the northernmost Argentine and Uruguayan slope, as it has been suggested in previous studies (Antobreh, 2005).

Furthermore, the presence of (4) gas hydrates along this margin (de Santa Ana et al., 2008) suggests that during sea level changes, slope failures were likely also initiated by gas hydrate destabilization, which was identified as an important triggering process on several continental slopes during times of deglaciation (Maslin et al., 2004). This initiating process may be supported by the oceanographic setting. During the last glacial stage, the BMC, currently due south of the estuary, was likely much further to the north (Hemming et al., 2007) and due to a strengthening of the Antarctic currents (Marchitto and Broecker, 2006; Toggweiler and Russell, 2008) resulting in cold water masses along the Uruguayan slope as it is the case currently south of the BMC (Piola and Matano, 2001). During deglaciation and the establishment of the Holocene ocean circulation pattern (Chiessi et al., 2008), much warmer ocean currents (Brazil Current (Piola and Matano, 2001)) were present on the slope. This rapid change in temperature and reorganization of ocean circulation presumably may have caused dissociation of gas hydrates and initiation of slope failures as it was shown in other slope systems (Maslin et al., 2004).

However, it is important to conclude, that currently very little detailed information is available from the northern Argentine and Uruguay Continental Slope and thus all the above outlines explanations of potential triggers are highly speculative. More detailed studies will be needed to understand the impact of the La Plata River and the oceanographic circulation on the described change in slope deposition seaward of the Rio de la Plata estuary.

4.3. Conclusions

The northern Argentine and Uruguay continental margin is highly influenced by the fluvial discharge from the La Plata Rivers and the very complex oceanographic setting of the Brazil Malvinas Confluence. Reviewing critically previous work along this margin, mostly detailed information is known on shelf sediment distribution patters and only few deposits remain challenging to interpret. Remaining open questions include (a) the presence of mud at the shelf break and its formation just north of the estuary, (b) the today's fate of sediment within the estuary and (c) the detailed geometry and sedimentary architecture of the shelf and its connection to the slope during glacial stages with lowered sea level.

This is in contrast to the slope system, which is only poorly understood as few studies have looked at sedimentary processes that affect this part of the margin. Seawards of the estuary, slope deposition changes from alongslope dominated to downslope dominated slope processes: this observation had not been previously described from data other than bathymetric analyses. South of this change in slope deposition, processes include contourite and turbidite deposition whereas to the north, mostly debris flow and turbidite processes are observed in the slope system. Thus much more detailed data will be needed to understand the change in slope deposition seaward of the estuary and to evaluate the main factor responsible for this change in slope deposition.

4.4. References

Angulo, R.J., Lessa, G.C. and de Souza, M.C., 2006. A critical review of mid- to late-Holocene sea-level fluctuations on the eastern Brazilian coastline. Quaternary Science Reviews, 25(5-6): 486-506.

Antobreh, A.A., 2005. Channelised and open-slope processes of mass sediment transport: their morphological and seismic characterisation from selected Atlantic high productivity regions. Ph. D. Thesis, University of Bremen, Bremen, 130 pp.

Baracco, R., Garcia-Rodriguez, F., del Puerto, L., Inda, H. and Castineira, C., 2008. Holocene relative sea-level variation inferred from records in the basin of Castillos, Shallow Lakes Conference 2008: Structure and function of world shallow lakes, Punta del Este, Uruguay, pp. 75.

Benavídez Sosa, A., 1998. Sismicidad y sismotectónica en Uruguay. Fisica de la Tierra, 10: 167-186.

Benthien, A. and Müller, P.J., 2000. Anomalously low alkenone temperatures caused by lateral particle and sediment transport in the Malvinas Current region, western Argentine Basin. Deep Sea Research Part I: Oceanographic Research Papers, 47(12): 2369-2393.

Berbery, E.H. and Barros, V.R., 2002. The hydrologic cycle of the La Plata Basin in South America. Journal of Hydrometeorology, 3(6): 630-645.

Blanc, S., Goni, G. and Novarini, J., 1983. Surface mixed layer temperature and layer depth in water off the Argentinian coast. Journal of Geophysical Research, 88(C10): 5987–5996.

Cavallotto, J.L., Violante, R.A. and Parker, G., 2004. Sea-level fluctuations during the last 8600 years in the de la Plata river (Argentina). Quaternary International, 114(1): 155-165.
Chiessi, C.M., Mulitza, S., Paul, A., Pätzold, J., Groeneveld, J. and Wefer, G., 2008. South Atlantic interocean exchange as the trigger for the Bølling warm event. Geology, 36(12): 919-922.
Clapperton, C.M., 1993. Quaternary geology and geomorphology of South America. Elsevier, Amsterdam, 780 pp.
Clark, R. and Wilson, P., 1992. Occurrence and significance of ventifacts in the Falkland Islands, South Atlantic. Geografiska Annaler. Series A, Physical Geography, 74(1): 35-46.
Coles, V.J., McCartney, M.S., Olson, D.B. and Smethie, W.M., 1996. Changes in Antarctic Bottom Water properties in the western South Atlantic in the late 1980s. Journal of Geophysical Research, 101(C4): 8957-8970.
Cruz, F.W., Burnsa, S.J., Jercinovic, M., Karmann, I., Sharp, W.D. and Vuille, M., 2007. Evidence of rainfall variations in Southern Brazil from trace element ratios (Mg/Ca and Sr/Ca) in a Late Pleistocene stalagmite. Geochimica et Cosmochimica Acta, 71(9): 2250-2263.
Cruz, F.W., Vuille, M., Burns, S.J., Wang, X., Cheng, H., Edwards, R.L., Karmann, I., Auler, A.S. and Nguyen, H., 2009. Orbitally driven east–west antiphasing of South American precipitation. Nature Geosciences, 2(3): 210-214.
Darwin, C., 1846. Geological observations on South America. Smith, Elder and Co., London, 279 pp.
de Santa Ana, H., Latrónica, L., Tomasini, J., Morales, E., Ferro, S., Gristo, P., Machado, L., Veroslavsky, G. and Ucha, N., 2008. Economic and exploratory review of gas hydrates and other gas manifestations of the Uruguayan continental shelf, 6th International Conference on Gas Hydrates (ICGH 2008), Vancouver, BC , Canada.
Delaney, P.J.V. (Editor), 1966. Geology and geomorpholohy of the coastal plain of Rio Grande do Sul, Brazil and northern Uruguay. Coastal Studies Series, Coastal Studies Series 15. Lusiana State University Press, Baton Rouge, 58 pp.
Delmonte, B., Petit, J.R. and Maggi, V., 2002. Glacial to Holocene implications of the new 27000-year dust record from the EPICA Dome C (East Antarctica) ice core. Climate Dynamics, 18(8): 647-660.
Depetris, P.J. and Griffin, J.J., 1968. Suspended load in the Rio de la Plata drainage basin. Sedimentology, 11(1-2): 53-60.
Depetris, P.J., Kempe, S., Latif, M. and Mook, W.G., 1996. ENSO-controlled flooding in the Paraná River (1904–1991) Naturwissenschaften, 83(3): 127-129.
Depetris, P.J. and Pasquini, A.I., 2007. The geochemistry of the Paraná River: an overview. In: M.H. Iriondo, J.C. Paggi and A.R. Paira (Editors), The Middle Paraná River: Limnology of a Subtropical Wetland. Springer Verlag, Berlin, Heidelberg, pp. 143-174.
Dingle, R.V., 1980. Large allochthonous sediment masses and their role in the construction of the continental slope and rise off southwestern Africa. Marine Geology, 37(3-4): 333-354.
Drago, E.C. and Amsler, M.L., 1998. Suspended sediment at a cross section of the Middle Parana River: concentration, granulometry and influence of the main

tributaries. In: M.P. Bordas and D.E. Walling (Editors), Sediment budgets. IAHS Publication, 174, Wallingford, pp. 381-396.
Ellwood, B.B., 1993. Magnetic properties of Argentine Basin Project MUDWAVE samples. Deep Sea Research Part II, 40(4/5): 921-937.
Esteves, L.S., Toldo, E.E., Dillenburg, S.R. and Tomazelli, L.J., 2002. Long- and short-term coastal erosion in southern Brazil. Journal of Coastal Research, Special Issue 36(ICS 2002 Proceedings): 273-282.
Ewing, M., Ludwig, W.J. and Ewing, J.I., 1964. Sediment distribution in the oceans: the Argentine Basin. Journal of Geophysical Research, 69(10): 2003-2032.
Ewing, M., Eittreim, S.L., Ewing, J.I. and Le Pichon, X., 1971. Sediment transport and distribution in the Argentine Basin. 3. Nepheloid layer and processes of sedimentation. Physics and Chemistry of the Earth, 8: 49-77.
Ewing, M. and Lonardi, A.G., 1971. Sediment transport and distribution in the Argentine Basin. 5. Sedimentary structure of the Argentine margin, basin, and related provinces. Physics and Chemistry of the Earth, 8: 123-251.
Farinati, E.A., 1985. Radiocarbon dating of Holocene marine deposits, Bahía Blanca area, Buenos Aires province, Argentina. In: J. Rabassa (Editor), Quaternary of South America and Antarctic peninsula. A. A. Balkema, 3, Rotterdam, Boston, pp. 197-206.
Figueiredo, A.G., 1980. Response of water column to strong wind forcing, southern Brazilian inner shelf: Implications for sand ridge formation. Marine Geology, 35(4): 367-376.
Figueiredo, A.G., Sanders, J.E. and Swift, D.J.P., 1982. Storm-graded layers on inner continental shelves: Examples from southern Brazil and the Atlantic coast of the Central United States. Sedimentary Geology, 31(3-4): 171-190.
Framinan, M.B. and Brown, O.B., 1996. Study of the Río de la Plata turbidity front, Part 1: spatial and temporal distribution. Continental Shelf Research, 16(10): 1259-1282.
Franke, D., Neben, S., Ladage, S., Schreckenberger, B. and Hinz, K., 2007. Margin segmentation and volcano-tectonic architecture along the volcanic margin off Argentina/Uruguay, South Atlantic. Marine Geology, 244(1-4): 46-67.
Fray, C. and Ewing, M., 1963. Pleistocene sedimentation and fauna of the Argentine shelf: I. Wisconsin sea level as indicated in Argentine continental shelf sediments. Proceedings of the Academy of Natural Sciences of Philadelphia, 115: 113-126.
Frenz, M., Höppner, R., Stuut, J.-B.W., Wagner, T. and Henrich, R., 2003. Surface sediment bulk geochemistry and grain size composition related to the oceanic circulation along the South American continental margin in the southwest Atlantic. In: G. Wefer, S. Mulitza and V. Ratmeyer (Editors), The South Atlantic in the Late Quaternary: reconstruction of material budgets and current systems. Springer Verlag, Berlin, Heidelberg, pp. 347-373.
Gaiero, D.M., Probst, J.-L., Depetris, P.J., Bidart, S.M. and Leleyter, L., 2003. Iron and other transition metals in Patagonian riverborne and windborne materials: geochemical control and transport to the southern South Atlantic Ocean. Geochimica et Cosmochimica Acta, 67(19): 3603-3623.
Gaiero, D.M., Brunet, F., Probst, J.-L. and Depetris, P.J., 2007. A uniform isotopic and chemical signature of dust exported from Patagonia: Rock sources and occurrence in southern environments. Chemical Geology, 238(1-2): 107-120.

Gan, M.A., Kousky, V.E. and Ropelewaki, C.F., 2004. The South America monsoon circulation and its relationship to rainfall over west-central Brazil. Journal of Climate, 17(1): 47-66.
Garcia, N.O. and Vargas, W.M., 1996. The spatial variability of runoff and precipitation in the Rio de la Plata basin. Hydrological Sciences Journal, 41(3): 279-299.
Gilberto, D.A., Bremec, C.S., Acha, E.M. and Mianzán, H.W., 2004. Large-scale spatial patterns of benthic assemblages in the SW Atlantic: the Río de la Plata estuary and adjacent shelf waters. Estuarine, Coastal and Shelf Science, 61(1): 1-13.
Gómez, E.A. and Perillo, G.M.E., 1991. Submarine outcrops underneath shoreface-connected sand ridges, outer Bahía Blanca estuary, Argentina. In: J. Rabassa (Editor), Quaternary of South America and Antarctic Peninsula. A. A. Balkema, 9, Rotterdam, Boston, pp. 23-37.
Grimm, A.M., 2003. The El Niño impact on the summer monsoon in Brazil: regional processes versus remote influences. Journal of Climate, 16(2): 263-280.
Groot, J.J. and Groot, C.R., 1966. Pollen spectra from deep-sea sediments as indicators of climatic changes in southern South America. Marine Geology, 4(6): 525-537.
Groot, J.J., Groot, C.R., Ewing, M., Burckle, L. and Conolly, J.R., 1967. Spores, pollen, diatoms and provenance of the Argentine Basin sediments. In: M. Sears (Editor), Progress in Oceanography, Volume 4. Pergamon Press, pp. 179-217.
Guerrero, R.A. and Piola, A.R., 1997. Masas de agua en la plataforma continental. In: E.E. Boschi (Editor), Antecedentes históricos de las exploraciones en el mar y las características ambientales. Instituto Nacional de Investigación y Desarrollo Pesquero (INIDEP), Mar del Plata, pp. 107-118.
Guerrero, R.A., Acha, E.M., Framinan, M.B. and Lasta, C.A., 1997. Physical oceanography of the Río de la Plata Estuary, Argentina Continental Shelf Research, 17(7): 727-742.
Guilderson, T.P., Burckle, L., Hemming, S.R. and Peltier, W.R., 2000. Late Pleistocene sea level variations derived from the Argentine Shelf. Geochemistry, Geophysics, Geosystems, 1(12): 1055.
Hemming, S.R., Van de Flierdt, T., Goldstein, S.L., Franzese, A.M., Roy, M., Gastineau, G. and Landrot, G., 2007. Strontium isotope tracing of terrigenous sediment dispersal in the Antarctic Circumpolar Current: Implications for constraining frontal positions. Geochemistry, Geophysics, Geosystems, 8: Q06N13.
Hensen, C., Zabel, M., Pfeifer, K., Schwenk, T., Kasten, S., Riedinger, N., Schulz, H.D. and Boetius, A., 2003. Control of sulfate pore-water profiles by sedimentary events and the significance of anaerobic oxidation of methane for the burial of sulfur in marine sediments. Geochimica et Cosmochimica Acta, 67(14): 2631-2647.
Hernández-Molina, F.J., Paterlini, M., Violante, R.A., Marshall, P., de Isasi, M., Somoza, L. and Rebesco, M., 2009. Contourite depositional system on the Argentine slope: an exceptional record of the influence of Antarctic water masses. Geology, 37(6): 507-510.
Iriondo, M.H. and Garcia, N.O., 1993. Climatic variations in the Argentine plains during the last 18,000 years. Palaeogeography, Palaeoclimatology, Palaeoecology, 101: 209-220.
Iriondo, M.H., 2004. The littoral complex at the Paraná mouth. Quaternary International, 114(1): 143-154.

Iriondo, M.H. and Paira, A.R., 2007. Physical geography of the basin. In: M.H. Iriondo, J.C. Paggi and A.R. Paira (Editors), The Middle Paraná River: Limnology of a Subtropical Wetland. Springer Verlag, Berlin, Heidelberg, pp. 7-31.
Isla, F.I., Cortizo, L.C. and Schnack, E.J., 1996. Pleistocene and Holocene beaches and estuaries along the southern barrier of Buenos Aires, Argentina. Quaternary Science Reviews, 15(8-9): 833-841.
Isla, F.I., 1998. Holocene coastal evolution of Buenos Aires. In: J. Rabassa (Editor), Quaternary of South America and Antarctic Peninsula. A. A. Balkema, 11, Rotterdam, Boston, pp. 297-321.
Isla, F.I. and Schnack, E.J., 2009. The changing coastlines of South America. In: E.M. Latrubesse (Editor), Natural Hazards and Human-Exacerbated Disasters in Latin America. Elsevier, 13, Amsterdam, pp. 49-73.
Jackson, J.M., 1985. Uruguay. In: M.L. Schwartz and E.C.F. Bird (Editors), The world's coastline. van Nostrand Reinhold, New York, pp. 79-84.
Kaiser, J. and Lamy, F., 2010. Links between Patagonian Ice Sheet fluctuations and Antarctic dust variability during the last glacial period (MIS 4-2). Quaternary Science Reviews, 29(11-12): 1464-1471.
Krinsley, D., Biscaye, P.E. and Turekian, K.K., 1973. Argentine Basin sediment sources as indicated by quartz surface textures. Journal of Sedimentary Petrology, 43(1): 251-257.
Lastras, G., Acosta, J., Munoz, A. and Canals, M., 2011. Submarine canyon formation and evolution in the Argentine Continental Margin between 44°30'S and 48°S. Geomorphology, 128(3-4): 116-139.
Ledbetter, M.T. and Klaus, A., 1987. Influence of bottom currents on sediment texture and sea-floor morphology in the Argentine Basin. In: P.P.E. Weaver and J. Thomson (Editors), Geology and Geochemistry of Abyssal Plains. Geological Society, Special Publication 31, London, pp. 23-31.
Lonardi, A.G. and Ewing, M., 1971. Sediment transport and distribution in the Argentine Basin. 4. Bathymetry of the continental margin, Argentine Basin and other related provinces. Canyons and sources of sediments. Physics and Chemistry of the Earth, 8: 79-121.
Mahiques, M.M., Tassinardi, C.C.G., Marcolini, S., Violante, R.A., Figueira, R.C.L., da Silveira, I.C.A., Burone, L. and de Mello e Sousa, S.H., 2008. Nd and Pb isotope signatures on the southeastern South American upper margin: Implications for sediment transport and source rocks. Marine Geology, 250(1-2): 51-63.
Manley, P.L. and Flood, R.D., 1993a. Paleoflow history determined from mudwave migration: Argentine Basin. Deep-Sea Research II, 40(4/5): 1033-1055.
Manley, P.L. and Flood, R.D., 1993b. Project mudwaves. Deep-Sea Research II, 20(4/5): 851-857.
Marchitto, T.M. and Broecker, W.S., 2006. Deep water mass geometry in the glacial Atlantic Ocean: A review of constraints from the paleonutrient proxy Cd/Ca. Geochemistry, Geophysics, Geosystems, 7: Q12003.
Martin, L. and Suguio, K., 1992. Variation of coastal dynamics during the last 7000 years recorded in beach-ridge plains associated with river mouths: example from the central Brazilian coast. Palaeogeography, Palaeoclimatology, Palaeoecology, 99(1-2): 119-140.

Martins, L.R. and Willwock, J.A., 1987. Eastern South America Quaternary coastal and marine geology: a synthesis, Quaternary coastal geology of Western Africa and South America. Unesco Reports in Marine Sciences, 43, Dakar, pp. 28-96.
Martins, L.R. and Correa, I.C.S., 1996. Atlas morphology and sedimentology of the southwest Atlantic coastal zone and continental shelf from Cabo Frio (Brazil) and Peninsula Valdés (Argentina), Universidade Federal do Rio Grande do Sul, Rio Grande do Sul.
Martins, L.R., Martins, I.R. and Urien, C.M., 2003. Aspectos sedimentares da plataforma continental na área de influência do Rio de la Plata. Gravel, 1: 68-80.
Martins, L.R. and Urien, C.M., 2004. Areias da plataforma e a erosão costeira. Gravel, 2: 4-24.
Martins, L.R., Urien, C.M. and Martins, I.R., 2005a. Gênese dos sedimentos da plataforma continental Atlântica entre o Rio Grande do Sul (Brasil) e Tierra del Fuego (Argentina). Gravel, 3: 85-102.
Martins, L.R., Martins, I.R. and Urien, C.M., 2005b. Sand bodies of the Santa Catarina inner continental shelf, Brazil. Gravel, 3: 103-108.
Martins, L.R., Martins, I.R. and Martins, R.R., 2005c. Utilização de testemunhador livre na região dos Poços de Lama. Gravel, 3: 1-8.
Maslin, M.A., Owen, M., Day, S. and Long, D., 2004. Linking continental-slope failures and climate change: Testing the clathrate gun hypothesis. Geology, 32(1): 53-56.
Mémery, L., Arhan, M., Alvarez-Salgado, X.A., Mercier, H., Castro, C.G. and Rios, A.F., 2000. The water masses along the western boundary of the south and equatorial Atlantic. Progress In Oceanography, 47(1): 69-98.
Möller, O.O., Piola, A.R., Freitas, A.C. and Campos, E.J.D., 2008. The effects of river discharge and seasonal winds on the shelf off southeastern South America. Continental Shelf Research, 28(13): 1607-1624.
Mulder, T. and Syvitski, J.P.M., 1995. Turbidity currents generated at river mouths during exceptional discharges to the world oceans. Journal of Geology, 103(3): 285-299.
Mulder, T., Syvitski, J.P.M., Migeon, S., Faugères, J.-C. and Savoye, B., 2003. Marine hyperpycnal flows: initiation, behavior and related deposits. A review. Marine and Petroleum Geology, 20(6-8): 861-882.
O'Connor, W.P., 1991. A numerical model of tides and storm surges in the Rio de la Plata Estuary. Continental Shelf Research, 11(12): 1491-1508.
Palma, E.D., Matano, R.P., Piola, A.R. and Sitz, L.E., 2004a. A comparison of the circulation patterns over the southwestern Atlantic shelf driven by different wind stress climatologies. Geophysical Research Letters, 31: L24303.
Palma, E.D., Matano, R.P. and Piola, A.R., 2004b. A numerical study of the southwestern Atlantic shelf circulation: barotropic response to tidal and wind forcing. Journal of Geophysical Research, 109: C08014.
Panario, D. and Gutiérrez, O., 1999. The continental Uruguayan Cenozoic: an overview. Quaternary International, 62(1): 75-84.
Parker, G., Paterlini, C.M. and Violante, R.A., 1997. El fondo marino. In: E. Boschi (Editor), El Mar Argentino y sus recursos pesqueros, Tomo 1: Antecedentes historicos de las exploraciones en el mar y las caracteristicas ambientaies. Instituto Nacional de Investigación y Desarrollo Pesquero Secretaría de

Agricultura, Ganadería, Pesca y Allmentación, Mar del Plata, Argentina, pp. 65-87.
Parker, G., Violante, R.A., Paterlini, C.M., Costa, I.P., Marcolini, S. and Cavallotto, J.L., 2008. Las secuencias depositacionales del plioceno-cuaternario en la plataforma submarina adyacente al litoral del este Bonaerense. Latin American Journal of Sedimentology and Basin Analysis, 15(2): 105-124.
Peltier, W.R. and Drummond, R., 2002. A “broad-shelf effect” upon postglacial relative sea level history. Geophysical Research Letters, 29: 1169.
Pereyra, F.X., Baumann, V., Altinier, V., Ferrer, J. and Tchilinguirian, P., 2004. Génesis de suelos y evolución del paisaje en el delta del río Paraná. Revista de la Asociación Geológica Argentina, 59(2): 229-242.
Perillo, G.M.E. and Sequeira, M.E., 1989. Geomorphologic and sediment transport characteristics of the middle reach of the Bahia Blanca estuary (Argentina). Journal of Geophysical Research, 94(C10): 14351-14362.
Perillo, G.M.E., Piccolo, M.C. and Marcovecchio, J., 2005. Coastal oceanography of the western South Atlantic continental shelf (33 to 55°S). In: A.R. Robinson and K.H. Brink (Editors), The sea. Havard Collage, 14, Boston, pp. 295-327.
Pierce, J.W. and Siegel, F.R., 1979. Supended particulate matter on the southern Argentine shelf. Marine Geology, 29(1-4): 73-91.
Piola, A.R. and Rivas, A.L., 1997. Corrientes en la plataforma continental. In: E. Boschi (Editor), El mar Argentino y sus recursos pesqueros, Volume 1, pp. 119-132.
Piola, A.R., Campos, E.J.D., Möller, O.O., Charo, M. and Martinez, C., 2000. Subtropical shelf front off eastern South America. Journal of Geophysical Research, 105(C3): 6565-6578.
Piola, A.R. and Matano, R.P., 2001. Brazil and Falklands (Malvinas) currents. In: J.H. Steele and S.A. Thorpe (Editors), Encyclopedia of Ocean Sciences. Academic Press, San Diego, pp. 340-349.
Piola, A.R. and Romero, S.I., 2004. Analysis of space-time variability of the Plata river plume. Gayana (Concepción), 68(2): 482-486.
Piola, A.R., Matano, R.P., Palma, E.D., Möller, O.O. and Campos, E.J.D., 2005. The influence of the Plata River discharge on the western South Atlantic shelf. Geophysical Research Letters, 32: L01603.
Piola, A.R., Romero, S.I. and Zyjaczkovski, U., 2008a. Space- time variability of the Plata plume inferred from ocean color. Continental Shelf Research, 28(13): 1556-1567.
Piola, A.R., Möller, O.O., Guerrero, R.A. and Campos, E.J.D., 2008b. Variability of the subtropical shelf front off eastern South America: Winter 2003 and summer 2004. Continental Shelf Research, 28(13): 1639-1648.
Riedinger, N., Pfeifer, K., Kasten, S., Garming, J.F.L., Vogt, C. and Hensen, C., 2005. Diagenetic alteration of magnetic signals by anaerobic oxidation of methane related to a change in sedimentation rate. Geochimica et Cosmochimica Acta, 69(16): 4117-4126.
Rivas, A.L. and Langer, A.F., 1996. Mass and heat transport in the Argentine continental shelf. Continental Shelf Research, 16(10): 1283-1295.
Rivas, A.L., 1997. Current-meter observations in the Argentine continental shelf. Continental Shelf Research, 17(4): 391-406.

Romero, O.E. and Hensen, C., 2002. Oceanographic control of biogenic opal and diatoms in surface sediments of the Southwestern Atlantic. Marine Geology, 186(3-4): 263-280.
Rostamini, K., Peltier, W.R. and Mangini, A., 2000. Quaternary marine terraces, sea-level changes and uplift history of Patagonia, Argentina: comparisons with predictions of the ICE-4G (VM2) model of the global process of glacial isostatic adjustment Quaternary Science Reviews, 19(14-15): 1495-1525.
Schmid, C., Siedler, G. and Zenk, W., 2000. Dynamics of Intermediate Water Circulation in the subtropical South Atlantic. Journal of Physical Oceanography, 30(12): 3191-3211.
Schnack, E.J., 2009. The vulnerability of the east coast of South America to sea level rise and possible adjustment strategies. In: R.A. Warrick, E.M. Barrow and T.M.L. Wigley (Editors), Climate and sea level change: observations, projections and implications. Cambridge University Press, Cambridge, pp. 336-348.
Segl, M. and Shipboard Scientific Party, 1994. Meteor Berichte Geo Bremen South Atlantic 1994, Cruise No. 29/1, 17 June - 5 September 1994. 95-2, Leitstelle Meteor, Institut für Meereskunde der Universität Hamburg.
Sijp, W.P. and England, M.H., 2008. The effect of a northward shift in the southern hemisphere westerlies on the global ocean. Progress In Oceanography, 79(1): 1-19.
So, L.C., Pierce, J.W. and Siegel, F.R., 1974. Sand waves in the Gulf of San Matias, Argentina. Geografiska Annaler. Series A, Physical Geography, 56(3-4): 227-235.
Spieß, V. and Shipboard Scientific Party, 2002. ODP Südatlantik 2001, Cruise No. 49, Leg 2, 13 February – 7 March 2001, Montevideo – Montevideo. 02-1, Leitstelle Meteor, Institut für Meereskunde der Universität Hamburg.
Stevenson, F.J. and Cheng, C.-N., 1969. Amino acid levels in the Argentine Basin sediments; correlation with Quaternary climatic changes. Journal of Sedimentary Research, 39(1): 345-349.
Stevenson, M.R., Dias-Brito, D., Stech, J.L. and Kampel, M., 1998. How do cold water biota arrive in a tropical bay near Rio de Janeiro, Brazil? Continental Shelf Research, 18(13): 1595-1612.
Stramma, L. and England, M.H., 1999. On the water masses and mean circulation of the South Atlantic Ocean. Journal of Geophysical Research, 104(C9): 20863-20883.
Toggweiler, J.R. and Russell, J., 2008. Ocean circulation in a warming climate. Nature, 451: 286-288.
Tonni, E.P., Cione, A.L. and Figini, A.J., 1999. Predominance of arid climates indicated by mammals in the pampas of Argentina during the Late Pleistocene and Holocene. Palaeogeography, Palaeoclimatology, Palaeoecology, 147(3-4): 257-281.
Trowbridge, J.H. and Kinecke, G.C., 1994. Structure and dynamics of fluid muds on the Amazon continental shelf. Journal of Geophysical Research, 99(C1): 865-874.
Urien, C.M. and Zambrano, J.J., 1973. The geology of the basins of the Argentine continental margin and Malvinas Plateau. In: A.E.M. Nairn and F.G. Stehli (Editors), The ocean basins and margins. Plenum Press, 1, New York, pp. 135-170.
Urien, C.M. and Ewing, M., 1974. Recent sediments and environments of southern Brazil, Uruguay, Buenos Aires and Rio Negro continental shelf. In: C.A. Burke

and C.L. Drake (Editors), The geology of continental margins. Springer Verlag, Berlin, pp. 157-177.
Urien, C.M., Martins, L.R. and Martins, I.R., 2003. Paleoplataformas e progradação deltaica do neógeno na margem continental do Uruguai e norte da Argentina. Gravel, 1: 40-46.
Vera, C.S., Baez, J., Douglas, M., Emmanuel, C.B., Marengo, J., Meitin, J., Nicolini, M., Nogues-Paegle, J., Paegle, J., Penalba, O., Salio, P., Saulo, C., Silva Dias, M.A., Silva Dias, P. and Zipser, E., 2006. The South American low-level jet experiment. Bulletin of the American Meteorological Society, 87(1): 63-77.
Violante, R.A. and Parker, G., 2004. The post-last glacial maximum transgression in the de la Plata River and adjacent inner continental shelf, Argentina. Quaternary International, 114(1): 167-181.
Volbers, A.N.A. and Henrich, R., 2004. Calcium carbonate corrosiveness in the South Atlantic during the Last Glacial Maximum as inferred from changes in the preservation of Globigerina bulloides: A proxy to determine deep-water circulation patterns? Marine Geology, 204(1-2): 43-57.
von Lom-Keil, H., Spieß, V. and Hopfauf, V., 2002. Fine-grained sediment waves on the western flank of the Zapiola Drift, Argentine Basin: evidence for variations in Late Quaternary bottom flow activity. Marine Geology, 192(1-3): 239-258.
Wells, P.G. and Daborn, G.R., 1997. The Rio de la Plata - an environmental overview. Dalhousie University, Halifax, 248 pp.
Wilkinson, M.J., Marshall, L.G. and Lungberg, J.G., 2006. River behavior on megafans and potential influences on diversification and distribution of aquatic organisms. Journal of South American Earth Sciences, 21(1-2): 151-172.
Zambrano, J.J. and Urien, C.M., 1970. Geological outline of the basins in southern Argentina and their continuation off the Atlantic shore. Journal of Geophysical Research, 75(8): 1363-1396.
Zavialov, P.O., Kostianoy, A.G. and Möller, O.O., 2003. SAFARI cruise: Mapping river discharge effects on Southern Brazilian shelf. Geophysical Research Letters, 30(21): 2126.
Zhou, J. and Lau, K.-M., 1998. Does a monsoon climate exist over South America? Journal of Climate, 11(5): 1020-1040.

5. A morpho-sedimentary approach to the northern Argentine and Uruguay continental slope

Citation: Huppertz, T.J., Chiessi, C.M., Henrich, R., Piper, D.J.W., and Preu, B.M., draft. A morpho-sedimentary approach to the northern Argentine and Uruguay continental slope. Aimed for submission to the Journal of South American Earth Sciences.

5.0 Abstract

Two main processes influence sedimentation on the northern Argentine and Uruguay continental slope: the fluvial discharge of the La Plata Rivers and the Brazil-Malvinas Confluence in which tropical and Sub-antarctic Ocean currents collide. Few core studies have characterized the seabed and shallow subsurface in the area. Sedimentation patterns on northern Argentine and Uruguay continental slope are driven by the interaction of alongslope and downslope driven processes. Using the Gebco 08 bathymetry, downslope trending core transects, and sea bed photos, the dominating processes of sedimentation can be identified. The continental slope was classified in five different zones characterized each by distinct different sedimentary processes. A significant change in slope sedimentation occurs at ~37°S where slope terraces, typical for most of the Argentine slope, terminate abruptly. The terraced slope to the south of 37°S is characterized by the interaction of contourite processes, dominating mostly sedimentation patters, and to a lesser extent turbidity currents, which supply at times especially during glacial stages sediment to the terrace. Such sediment may be subject to ocean current reworking. To the north of 37°S, mass wasting and turbidites characterize seabed and the subsurface. This change in slope dynamics can also be seen in on the rise and abyssal plain, the Argentine Basin, imaged in core data, seabed roughness and bottom photography. It is suggested that to the north of 37°S the main driving process for slope deposition is the high terrigenous input of the La Plata Rivers whereas to the south of 37°S, the ocean circulation, and to a lesser extent mass wasting, drives slope deposition.

5.1 Introduction

Continental margin sedimentation is highly influenced by the interaction of alongslope and downslope driven processes modifying margin morphology and changing sediment stability of continental margins (Piper and Normark, 2001; Hernández-Molina et al., 2008b; Mulder et al., 2008). Additionally, ocean circulation may further influence deposition by winnowing seabed and changing the sedimentological and seismic appearance of the deposit (Shanmugam, 2008), complicating the recognition of the initial processes that controlled deposition of the sedimentary sequence (Stow et al., 2008). Within clastic sedimentary slope systems, the main challenge is frequently the distinction between contourite and turbidite processes, as the resultant deposit may look very similar (Carter, 2007; Mulder et al., 2008). Different types of mass wasting in form of debris flows or other mass transport deposits, on the other hand, are relatively easy to identify and distinguish from each other in core and seismic data. Such mass transport deposits are in cores generally highly disturbed and show either complex folded layers or a chaotic fabric of variable sized clasts and sediment blocks (Tripsanas et al., 2009). On seismic data, grainy character is typical for such deposits (Mienert et al., 2002; Tripsanas et al., 2003; Jenner et al., 2007).

The northern Argentine (N of 44°S) and Uruguay continental margin is a very dynamic sedimentary system highly influenced by the Brazil Malvinas Confluence (Piola and Matano, 2001). Within the confluence, subantarctic and tropical water masses collide and create a highly complex current system (Stramma and England, 1999; Piola and Matano, 2001). Such current systems are frequently characterized by eddies and water mass contact zones (Piola and Matano, 2001) possibly initiating internal waves which may cause erosion on the slope (Boczar-Karakiewicz et al., 1991; Syvitski et al., 1996a; Cacchione et al., 2002)

The purpose of this paper is to (a) use the Late Quaternary slope deposits to characterize general seabed and subsurface sediment distributions and (b) link the sediment distribution patterns to the morphology and the oceanographic setting along the margin. This enabled us to estimate the impact of the La Plata Rivers on slope sedimentation. The slope could be classified into five different morpho-sedimentary zones that contributed to the determination of the dominant sedimentary process in the study area.

5.2 Regional setting

5.2.1 Physiography

The northern Argentine and Uruguay continental margin is a passive continental margin formed during initial rifting of the South Atlantic since Cretaceous times (Uliana et al., 1989). The main geo-morphological feature in this area is the Rio de la Plata estuary, where the Paraná and Uruguay (La Plata) rivers drain into the South Atlantic Ocean (Iriondo, 2007).

The shelf break occurs at 160-200 m water depth and is located between 300 and 500 km seaward of the coastline (Fig. 1) (Parker et al., 1997). The continental slope of northern Argentina is characterized by a series of marine terraces, of which the Ewing Terrace with an average width of 65 km (Fig. 1) is the most dominant feature at ~1200 m water depth spanning most of the Argentine Slope. Just south of the Rio de la Plata estuary, at a water depth of 400 to 500 m, the much smaller and slightly shallower La

Plata Terrace with a maximum width of 45 km and a length of ~200 km is found (Fig. 1). Slope canyons generally do not reach the shelf break but start on the Ewing Terrace (Urien and Ewing, 1974; Parker et al., 1997; Perillo et al., 2005; Hernández-Molina et al., 2009). No marine terraces have been described from the Uruguay continental slope. Here, some of the slope canyons reach the shelf break (Fig. 1) (Parker et al., 1996; Parker et al., 1997).

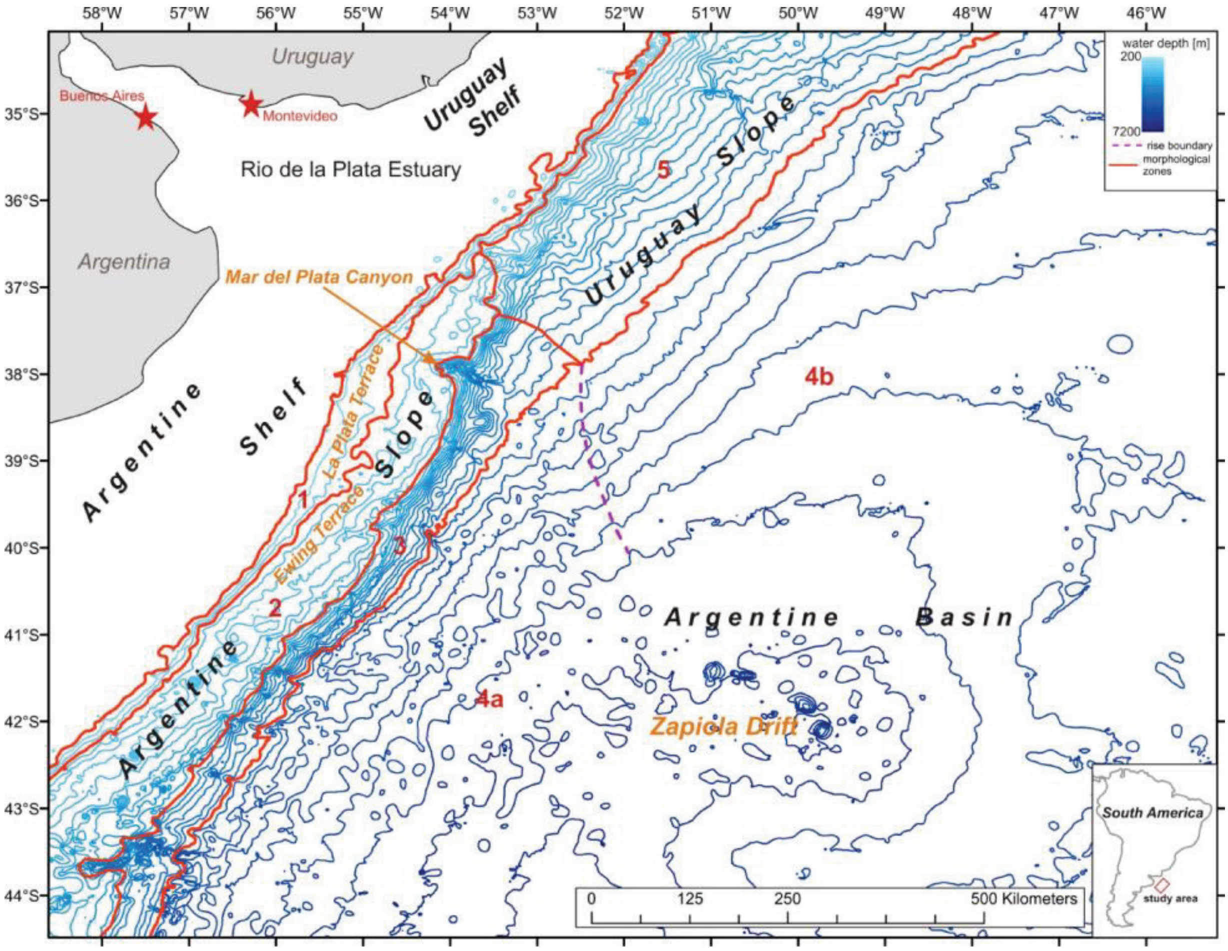

Figure 5.1: Map showing the Gebco 08 bathymetry on the northern Argentine and Uruguay continental margin (see index map for location). The bathymetry line spacing is at 200 m with 200 m being the shallowest line. Important morphological features are labeled in orange and the morphological zones are indicated in red (see text for details).

The toe of the slope is in 4500 m water depth, where the rise and abyssal plain, termed Argentine Basin, continues (Ewing, 1965; Ewing and Lonardi, 1971). The main canyon incising on the northern Argentine margin into the Ewing Terrace is the Mar del Plata Canyon (Fig. 1) (Urien and Ewing, 1974; Perillo et al., 2005; Hernández-Molina et al., 2009). This canyon system has very steep flanks (up to 10°, Fig. 2), and is characterized by significantly higher sedimentation rates compared to other parts of the slope. It acts as a sediment trap (Voigt et al., 2011).

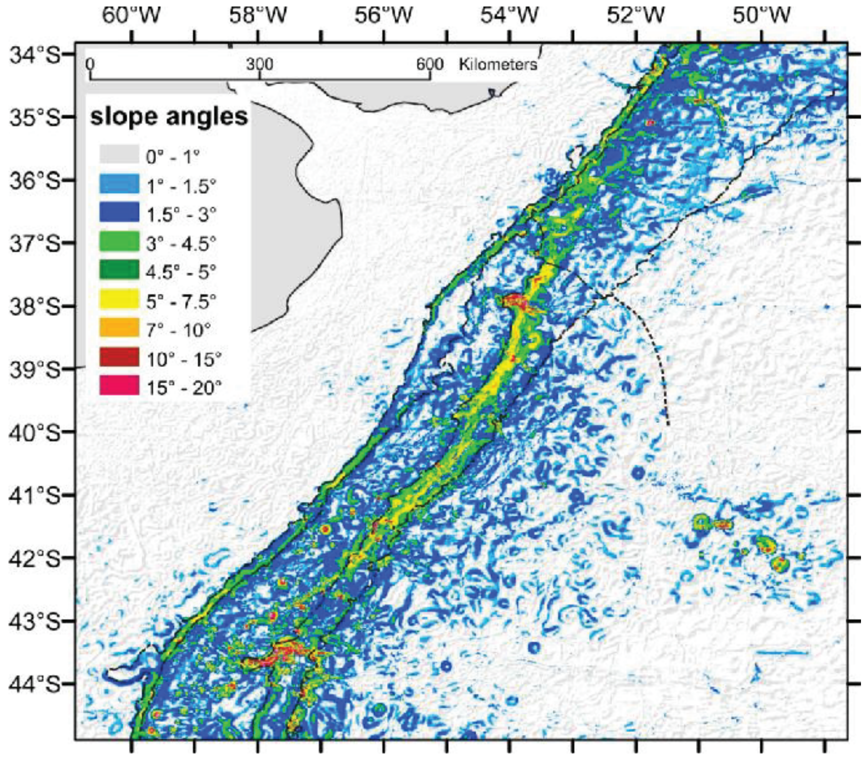

Figure 5.2: Slope angles in ° on the northern Argentine and Uruguay Slope

5.2.2 Geological setting

Few detailed studies have focused on the northern Argentine and Uruguay continental slope. Regional seabed mapping for ocean current tracers resulted in a general surficial seabed characterization of the southwest Atlantic Ocean (Romero and Hensen, 2002; Frenz et al., 2003; Chiessi et al., 2007). On the central Argentine Slope, core studies have focused on developing an age model based on either pollen data (Groot and Groot, 1966; Groot et al., 1967) or using variations of element ratios within pore water chemistry to define sedimentation processes and their general rates and timing (Stevenson and Cheng, 1969; Hensen et al., 2000; Riedinger et al., 2005).

Seismic studies have mapped large contourite drifts on the southern and central Argentine slope (Hernández-Molina et al., 2009), whereas numerous mass transport deposits (MTDs) were recognized on the Uruguayan Slope (Antobreh, 2005). The lower slope and rise sedimentation processes are poorly understood: turbidite lobes and contourite sheets are likely present (Hernández-Molina et al., 2009).

The abyssal plain is dominated by the large Zapiola contourite drift, which is being built by the Antarctic Bottom Water (von Lom-Keil et al., 2002; von Lom-Keil et al., 2003). To the northeast of this large drift deposit continues a mudwave field which has been studied extensively (e.g. Flood et al., 1993; Manley and Flood, 1993b). Using size and shape of the mudwaves, this area could also be used to estimate bottom water flow in the basin over time: highest flow speeds were detected during the time of 20 to 40 ka and in the early Holocene (Ledbetter, 1993).

5.2.3 Oceanography of the area

The Brazil Malvinas Confluence (BMC) is the dominant oceanographic feature in the area (Fig. 3, inset a). This zone is mainly defined based on surface circulation patterns, where the northward flowing Falkland/Malvinas current and the southward flowing Brazil Current interact (Stramma and England, 1999; Piola and Matano, 2001). At their confluence, these surficial water masses detach from the continental slope and flow southeastwards into the South Atlantic. The Brazil current can be further divided into tropical waters and re-circulated Antarctic intermediate Waters (Piola and Matano, 2001).

The surface currents affect the upper ~400-600 m of the water column. Below these currents is the Antarctic Intermediate water found, which encounters its re-circulated part flowing southwards and detaches partly from the margin (Piola and Matano, 2001; Frenz et al., 2003). Below this water mass at ~1600 m water depth, the Circumpolar Deep Water, which continues northwards, collides with the southward-directed North Atlantic Deep Water, which results in vertical splitting of the Circumpolar Deep Water. Below these water masses, the northward flowing Antarctic Bottom Water circulates clockwise through the Argentine Basin (e.g. Gordon and Greengrove, 1986; Stramma, 1989; Stramma and England, 1999; Piola and Matano, 2001; Piola, 2006).

5.2.4 Mixed turbidite and contourite systems

Alongslope and downslope driven processes affect and modify slope sedimentation patterns greatly (Mulder et al., 2008). (1) Alongslope processes are driven by ocean currents. Such currents can either result in short-term perturbation forming benthic storms and seabed winnowing or over longer time scales and continuous bedload within such a contour current can initiate contourite deposition constructing large km-scale drift bodies (Hernández-Molina et al., 2008b; Stow and Faugères, 2008; Stow et al., 2008). (2) Gravity driven processes are directly linked to slope angles and influence sedimentation patterns in most slope systems (Pratson et al., 2007), and include turbidity currents or other mass transport processes (Takahashi, 1981; Middleton, 1993; Piper and Normark, 2001).

Frequently, it is challenging to establish whether a sedimentary deposit has a contouritic or a turbiditic origin (Mulder et al., 2006; Mulder et al., 2008) as both processes can lead to very similar deposits (Stow, 1979; Hernández-Molina et al., 2006; Mulder et al., 2008; Huppertz and Piper, 2010).

Additionally, when alongslope processes interact with downslope conduits, e.g. canyons and gullies, very complex flow patterns may change the bed load of the contour current enhancing deposition. This results in either canyon filling or in significant changes in contourite deposition (Marchès et al., 2006; Marchès et al., 2007; Marchès et al., 2010). Furthermore, contour currents may rework turbidites and MTDs, forming contourites down current, resulting in winnowed lag deposits (Mulder et al., 2008). Nevertheless, such lag deposits can also be formed by current intensity variations (Stow et al., 2002).

Thus, the differentiation between contourite and turbidite deposits remains enigmatic (Mulder et al., 2008). Nevertheless, various indicative sedimentary properties and structures, and seismic characteristics have been suggested to help the identification of the original depositional process. Using sediment cores, the following properties and structures may be useful: the degree of sorting, trends in grading, bed thickness or the shape and sources of the sediments (Gonthier et al., 1984; Yokokawa, 2001; Stow et al., 2002; Stow and Faugères, 2008; Huppertz and Piper, 2010). On seismic data, contourites are frequently semi-transparent and show ripples and sand waves of various sizes (Stow et al., 2002; Rasmussen et al., 2003; Stow et al., 2008; Stow et al., 2009), whereas well laminated sequences with few thicker, grainy appearing layers with basal erosion may indicate thin sandy turbidite beds in seismic data (Piper, 2005; Jenner et al., 2007).

5.3 Materials and methods

The slope morphology of the northern Argentine and Uruguay continental slope was analyzed from the latest Gebco dataset (Gebco_08, www.gebco.net). Additionally, ArcGIS™ was used to create downslope trending bathymetric profiles at even spacing on the slope and thus define the main morphological zones. Core top lithologies from the University of Bremen (GeoB) and from the Lamont Doherty Earth Observatory (LDEO) core data (http://www.ngdc.noaa.gov/ngdc.html) could be used to define surficial and shallow subsurface sediment architecture (cores are up to 10 m long) in context of the bathymetry. Additionally, LDEO seabed photography imaged seabed morphology and supports determined seabed lithologies defined from core top data. These datasets allowed defining main surficial sedimentary units. Furthermore, downcore core lithological descriptions of selected cores resulted in downslope core profiles defining the overall distribution of subsurface features on the slope. These are either newly described cores (GeoB cores) or older LDEO cores, which do not have at this point any biostratigraphy or other age control available.

5.4 Results

5.4.1 Margin morphology

Newly released Gebco 08 bathymetry has improved greatly on the northern Argentine and Uruguay Slope by imaging the study area at a significantly better spatial resolution of 0.5 degrees compared to previous Gebco versions, making it possible to detect several new bathymetric features (Fig. 1). This enabled us to define five morphological zones in the study area (Figs. 1 and 2, Table 1): Zone 1 includes the upper slope with slope angles varying between 1-3°. The uppermost slope just below the shelf break at 160-200 m water depth is steepest (up to 5°, Figs. 1 and 2). Due south of the La Plata estuary, the small La Plata terrace is found (400 to 500 m water depth, Fig. 1). Zone 2 is formed by the Ewing Terrace defined between 800 and 1200 m water depth. The slope below the Ewing terrace is significantly steeper with values up to 7.5° (Fig. 2) compared to the upper slope above the Ewing Terrace. Zone 3 is the slope area below the Ewing Terrace between 1200 and 4500 m water depth. Beyond 4500 m water depth is Zone 4 comprising the Argentine Rise and the Argentine Basin. This zone can be subdivided into an area characterized by (a) complex morphology characterized by ridges and basins throughout, and an area with (b) smooth seabed morphology (Zones 4 a and 4b on Fig. 2). The last morphological zone, Zone 5 was defined seaward of Uruguay where there is no terrace present forming an un-terraced slope area with canyons and gullies, some of which are reaching up to the shelf break (Figs. 1 and 2). On the continental rise, very few channels are observed. Either this observation may be due to their lack or at this water depth the data resolution of 0.5 degrees is too poor to image such subtle features (Fig. 1).

5.4.2 Bathymetric transects

Evenly spaced slope bathymetric transects (spacing of ~80-100 km) between 35° and 43°S are used to visualize the changes of the slope morphology from the northern un-terraced slope (Zone 5) to the terraced slope in the south (Zones 1-3) (Figs. 2 and 3). The un-terraced slope is generally less steep (1-3°) and shows few lower slope morphological features compared to the terraced slope where especially the lower slope below the Ewing Terrace is significantly steeper (3-7°) compared to the upper slope above the terrace (1-3°) (Fig. 2). Above the Ewing Terrace, the slope angle is generally highest just below the shelf break (up to 5°, Fig. 2). Towards the south, the La Plata Terrace terminates and the Ewing Terrace shallows and is morphologically less well developed (Figs. 2, 3 and 4).

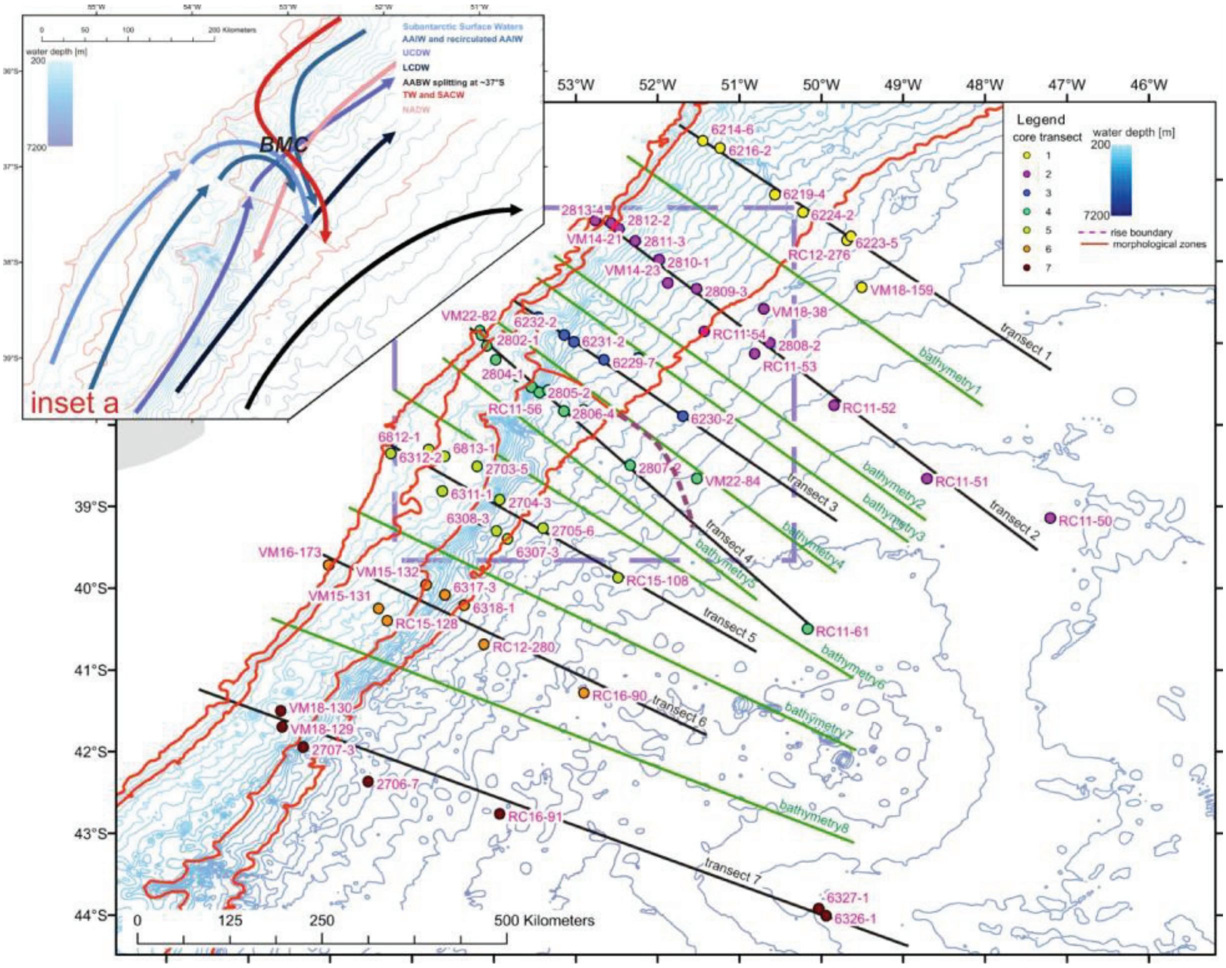

Figure 5.3: Bathymetry and core transects used to define the sedimentary and morphological characteristics of this margin. The bathymetric transects can be found in Figure 4. The morphological areas are shown in red. Inset a shows the ocean currents on the margin, for more detail see Stramma and England (1999).

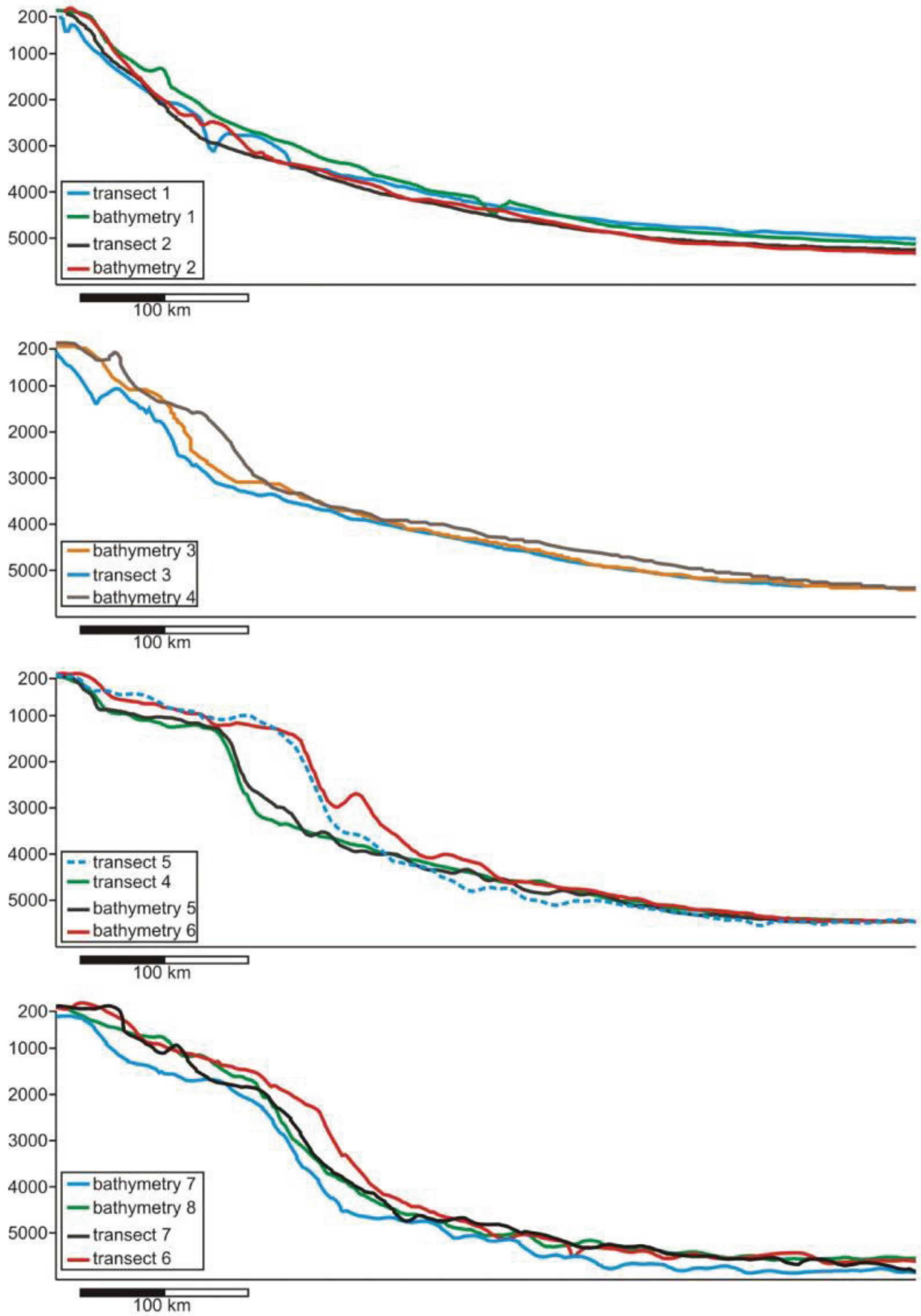

Figure 5.4: Bathymetry of the bathymetry and core transects shown in Figure 3. The terraced transects are significantly different from the ones where there is no slope terrace.

5.4.3 Seabed surficial sediments

Surficial sediment distribution patterns were established from all available core top data in the study area (Fig. 5, Table 1). This dataset was used to define the main surficial sediment distribution patterns. The shelf break, upper slope and terraced area (Zones 1 and 2) are generally sandy with only few exceptions. The lower slope below the Ewing Terrace is muddy again with some sand present in canyon settings (Zone 3). The surficial sediment type changes significantly towards Zone 5, where there is no terrace present. Here, the shelf break is also sandy, but the slope is mud-dominated except for few exceptions in canyons (Figs. 1 and 5). The lowermost slope and rise in Zone 4b is mostly mud-dominated except for areas seawards of canyons, whereas the lower slope in Zone 4a is generally sandy (Fig. 5, Table 1). Surficial sediment distribution on the rise (Fig. 5) may be linked to the rise morphology, which is in Zone 4a wavy with typical mini-basins throughout, whereas in Zone 4b the rise is smooth and shows few morphological features (Figs. 1, 2 and 5). The boundary between the two rise zones is at the seaward position of the termination of the Ewing Terrace (Figs. 1, 2 and 5).

Table 5-1: Main sedimentary characters and their interpretation of the different zones defined on the northern Argentine and Uruguay continental slope.

	observations			***interpretations***		
zone	slope angle [°]	dominating surficial sediment	dominating subsurface sediment	type of deposit	main processes	main driver
1	1-3	sand	sand	shelf sands hemipelagic muds	shelf export: storm sedimentation	downslope
2	0-3	sand	sand	intercalated contourite and turbidite sands	contourites and shelf export	along and downslope
3	up to 7.5	sand and mud	sand and mud	hemipelagic mud and turbidite sands	turbidity currents	downslope
4a	0-3	sand and gravel	sand	intercalated contourite and turbidite sands	contourite deposition and turbidity current deposition	along and downslope
4b	0-3	mud and sand	mud	hemipelagic mud and turbidite sands	turbidity currents and winnowing	downslope
5	up to 5	mud	mud	hemipelagic mud and turbidite sands	turbidiity currents and hemipelagic sedimentation	downslope

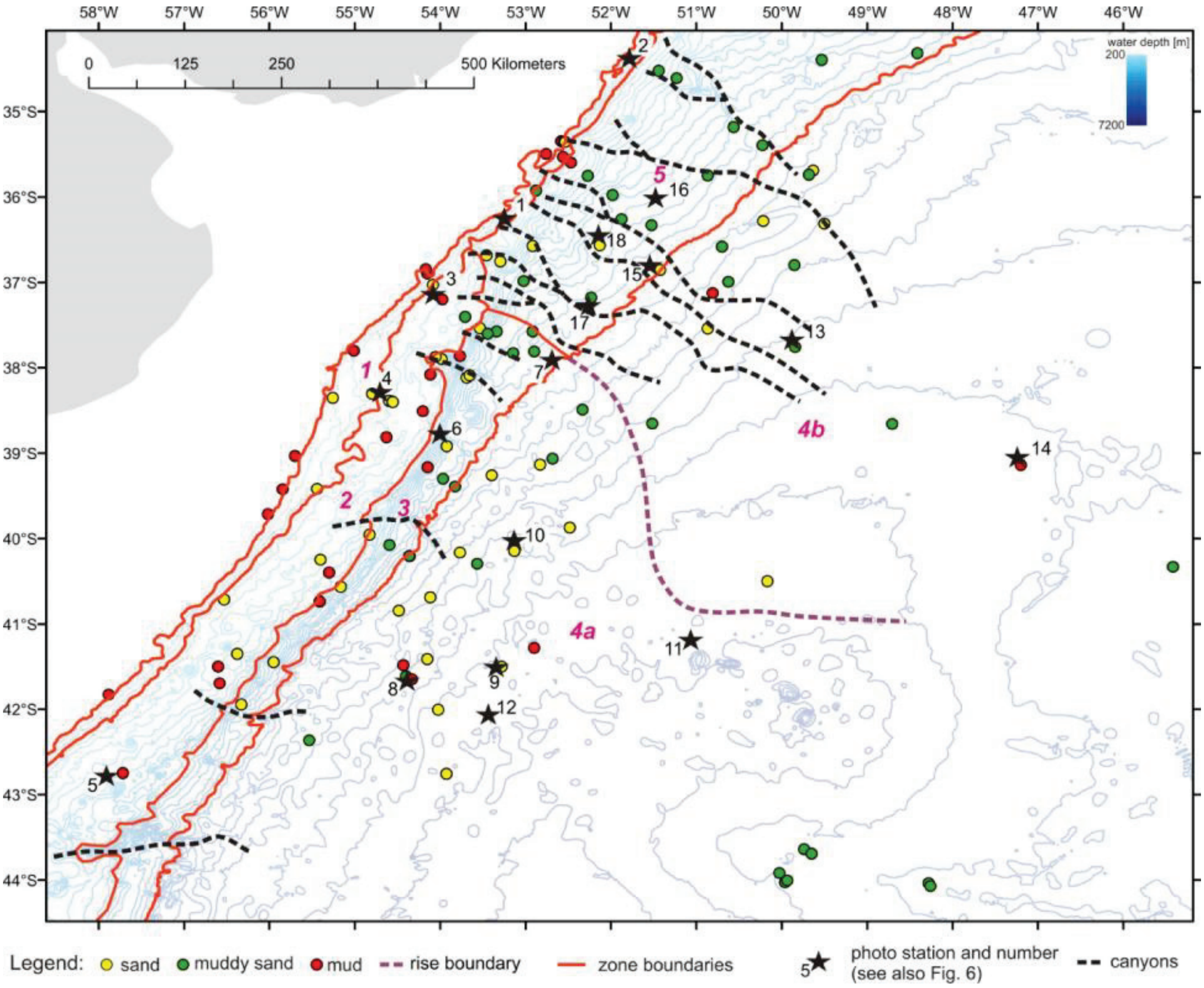

Figure 5.5: Surficial seabed sediments from GeoB and LDEO cores (from http://www.ngdc.noaa.gov/ngdc.html) on the margin. Additionally, positions of seabed photos, shown in Figure 6, are indicated. The morphological areas are shown again in red.

Seabed photos are used to characterize seabed morphology (Figs. 5 and 6). Observations from the photos support the findings of the core top data. The photos also show the change in seabed character on the continental rise between the northern and southern subzones 4 a and b respectively. The southern subzone (Fig. 6: Zone 4a) is characterized by rough seabed microtopography with the presence of sand and locally even gravel (Fig. 6, photo 12), whereas the northern lower slope and rise (Zone 4b) shows smooth seabed microtopography (Fig. 6: Zone 4b). The Ewing Terrace does show in places a thin mud drape, but is nevertheless on seabed photos generally characterized by surficial sand deposits; in places ripples with small wavelength can be observed (Fig. 6, photo 4).

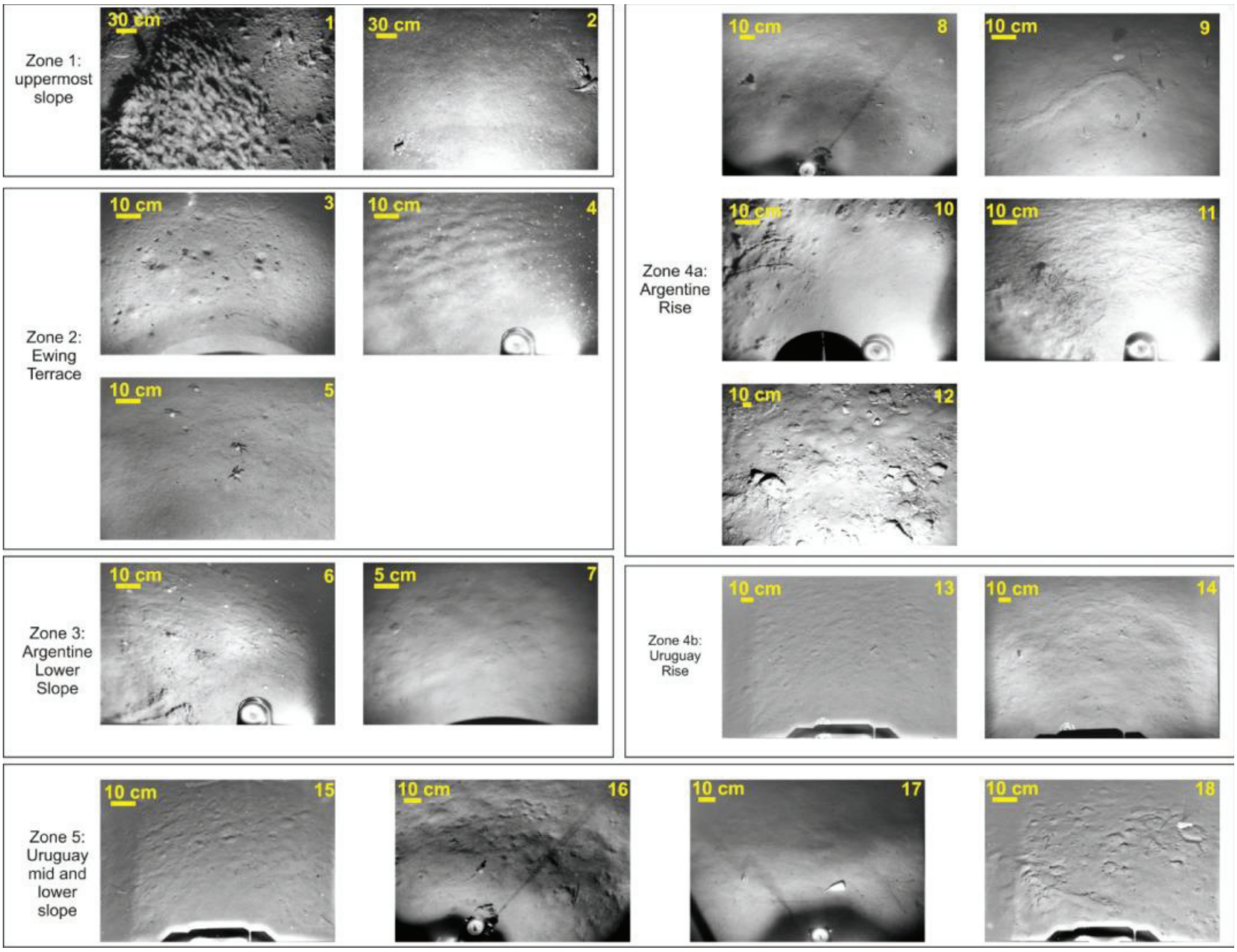

Figure 5.6: Surficial seabed photos on the slope and rise (from the National Geophysical Data Center, http://www.ngdc.noaa.gov/ngdc.html). The morphological classification of seabed can support the core data observations, see text for details.

5.4.4 Downslope core transects

Downslope-oriented sediment core transects (Fig. 3) establish the shallow (upper ~10 m) subsurface sediment architecture on the northern Argentine and Uruguay continental slope. Seven downslope transects at ~160 km spacing were used to characterize slope sedimentation.

Core transect 1 (Fig. 7) has cores ranging in depth between 1500 and 4600 m. The slope morphology is characterized by a steep upper slope (angles up to 7.5°, Fig. 2); the central slope has several mounds and may show a small terrace at ~2000 m water depth. The lower slope is smooth. At 4700 m is a small channel-like feature. The upper 4 cores of this transect are mud-dominated with few sand beds, which are commonly graded, and have sharp erosional bases. Between the sand beds, olive gray muds with sand blebs and mud clasts with erosional surfaces throughout are found. The lower three cores are sand-dominated with few sharp erosional surfaces. The silt to fine sandy beds are muddy, thick bedded (meter-scale) and have olive gray colors.

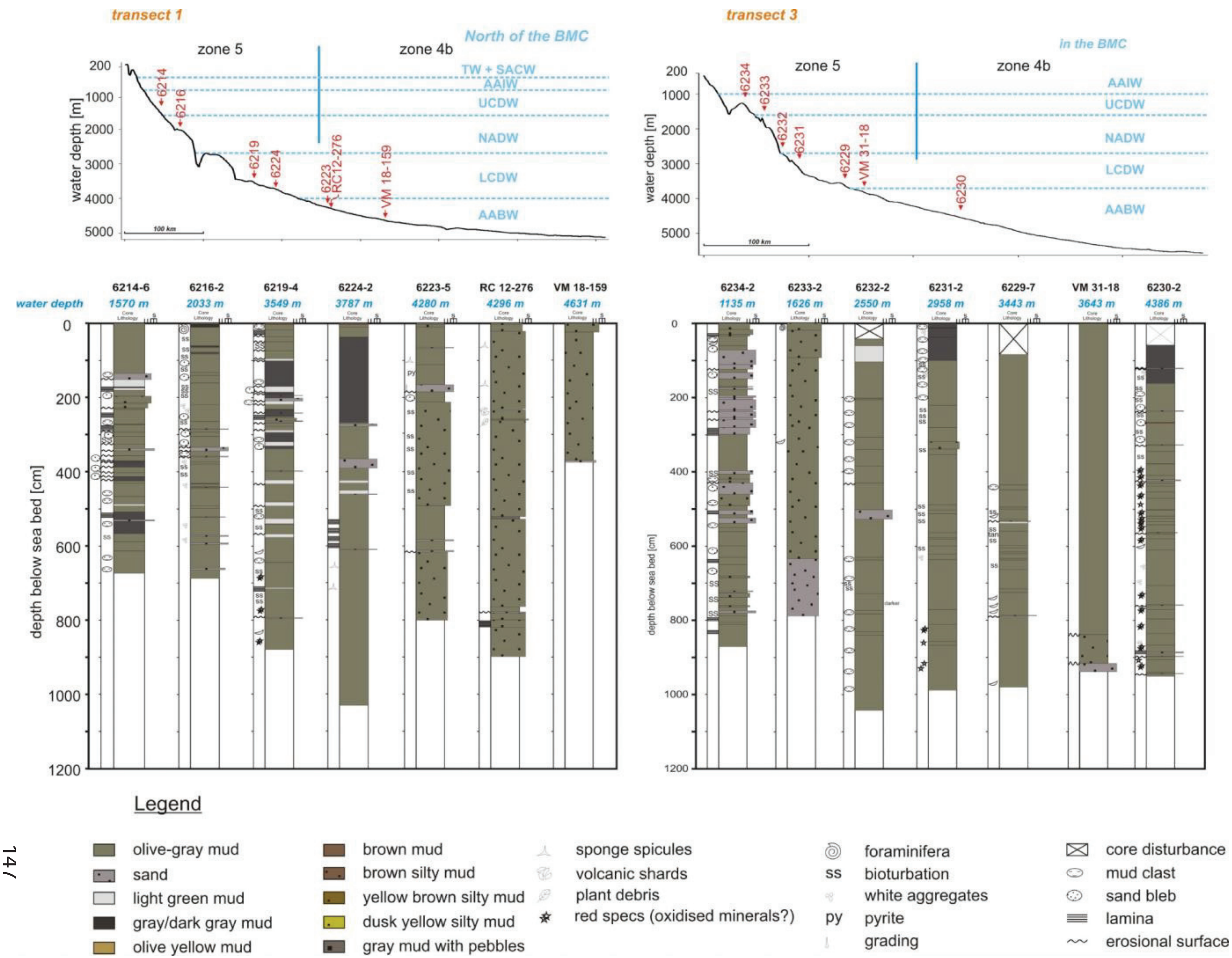
transect 1
zone 5
zone 4b
North of the BMC
TW + SACW
AAIW
UCDW
NADW
LCDW
AABW
water depth [m]
100 km
6214
6216
6219
6224
6223
RC12-276
VM 18-159
transect 3
zone 5
zone 4b
in the BMC
6234
6233
6232
6231
6229
VM 31-18
6230
water depth
6214-6 1570 m
6216-2 2033 m
6219-4 3549 m
6224-2 3787 m
6223-5 4280 m
RC 12-276 4296 m
VM 18-159 4631 m
6234-2 1135 m
6233-2 1626 m
6232-2 2550 m
6231-2 2958 m
6229-7 3443 m
VM 31-18 3643 m
6230-2 4386 m
Core Lithology
depth below sea bed [cm]
Legend
olive-gray mud
sand
light green mud
gray/dark gray mud
olive yellow mud
brown mud
brown silty mud
yellow brown silty mud
dusk yellow silty mud
gray mud with pebbles
sponge spicules
volcanic shards
plant debris
red specs (oxidised minerals?)
foraminifera
ss bioturbation
white aggregates
py pyrite
grading
core disturbance
mud clast
sand bleb
lamina
erosional surface

Figure 5.7 on previous page: Core transect 1 and 3 showing muddy cores throughout with few sand beds interpreted as turbidite sands. Bathymetry transects after Gebco 08, water masses from Piola and Matano (2001) and Hernández-Molina (2009). The blue dotted lines indicate approximate position of water mass boundaries. Also indicated are the position and number of different slope zones separated by vertical dark blue solid lines. BMC=Brazil-Malvinas Confluence, TW+SACW=Tropical Waters and South Atlantic Central Water, AAIW=Antarctic Intermediate Water, UCDW=Upper Circumpolar Deep Water, NADW= North Atlantic Deep Water, LCDW=Lower Circumpolar Deep Water, AABW=Antarctic Bottom Water.

Core transect 2 (Fig. 8) has cores ranging between 200 and 5300 m water depth. No terrace is present in this transect. The slope is steep and has no major morphological features (Figs. 2 and 8). At 3000 m, a significant change in slope angle occurs and the lower slope and rise are much gentler (Figs. 2 and 8). Very few erosional surfaces are observed in the transect. At the shelf break, the cores are dominated by medium to coarse sand. Below the shelf break, sand beds are generally thin (max. 10 cm) and if present, its grain size is fine to medium sand. Megascopic grading can be seen in few beds. Exceptions are two cores, RC11-54 and RC11-51, which have thick muddy sand beds throughout.

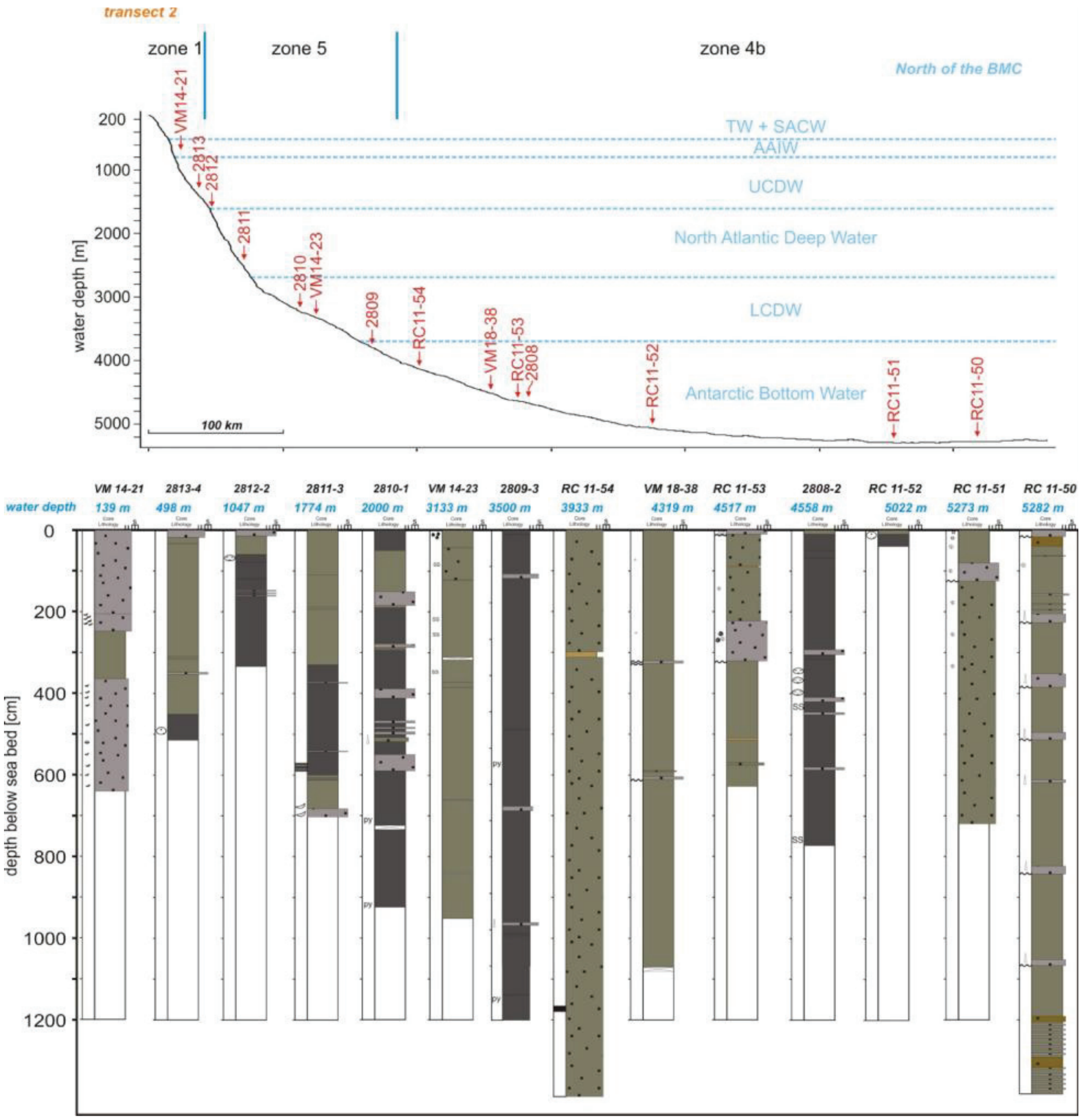

Figure 5.8 on previous page: Core transect 2 showing muddy cores throughout with few sand beds interpreted as turbidite sands; the legend and detailed figure information can be found in Fig. 7.

Core transect 3 (Fig. 7) has cores ranging from 1000 to 4500 m water depth. In this area, the Ewing terrace, being broader to the south, terminates and is very narrow (Figs. 1, 3 and 7). To the northeast, the terrace ends in canyon systems, which can be traced to the rise using the bathymetric map (Fig. 5). The upper two cores, which are on the edge of the terrace, are sand dominated with medium sand present throughout (Fig. 7). Shell fragments indicate shelf sources for at least some of the sand. The lower slope below 1800 m water depth is muddy with very few sandy beds and few erosional surfaces. Mud clasts are common.

Core transect 4 (Fig. 9) has cores ranging from the shelf break to 5500 m water depth. In this transect (Fig. 9), the Ewing terrace is pronounced and its top is almost flat (Figs. 1 and 4). The seaward side of the terrace is very steep (Figs. 2, 4 and 9). The lower slope and rise angle is again similar to the other transects. Cores on the upper slope and the Ewing Terrace are dominated by medium-sized sand (Fig. 9). Shell fragments and sponge spicules are common. No erosional surfaces are present. Towards both sides of the terrace, cores get slightly muddier (Fig. 9, e.g. cores VM22-82 and 2803-2). Beyond 2000 m water depth, cores have no sand beds and show no sedimentary structures. The continental rise cores below 4500 m water depth are again sand-dominated and show normal graded sequences.

Core transect 5 has cores ranging between 400 and 5000 m water depth (Fig. 10). Morphologically, the Ewing terrace is well developed. Additionally, above the Ewing terrace is the relatively narrow La Plata terrace at 400 to 500 m water depth situated (Fig. 1). Sand and muddy sand is present throughout the transect (Fig. 10), except for cores 6308-3 and 6307-3 which are at the toe of the slope and show no sand beds. Sand is generally fine to medium grained. Cores closest to the shelf break have shell and coral fragments present. The lowermost slope and rise (below 3600 m water depth, Fig. 10) shows several steps and mounds.

Core transect 6 (Fig. 11) has cores ranging between 100 and 5500 m water depth. The Ewing Terrace is poorly developed but still present, and is now dipping significantly seawards (Figs. 3 and 4). The lower slope beyond the terrace is steep and has little morphology except for a little dent at 3350 m water depth. Cores are sandy throughout except for core 6317-3, which is on the steepest part of the slope. Cores on the terrace have granules throughout and show no sedimentary structures (Fig. 11).

Core transect 7 (Fig. 11) has cores ranging between 1400 and 5600 m water depth. This transect terminates on the Zapiola Drift in the central Argentine Basin (Fig. 1). The upper slope is steep and the Ewing terrace is even less well developed compared to the transects farther to the north. The slope cores are sandy; the rise is muddy and the abyssal plain shows sand beds again (Fig. 11). The Zapiola drift has mud throughout. Erosional surfaces are only present on cores from the Ewing terrace.

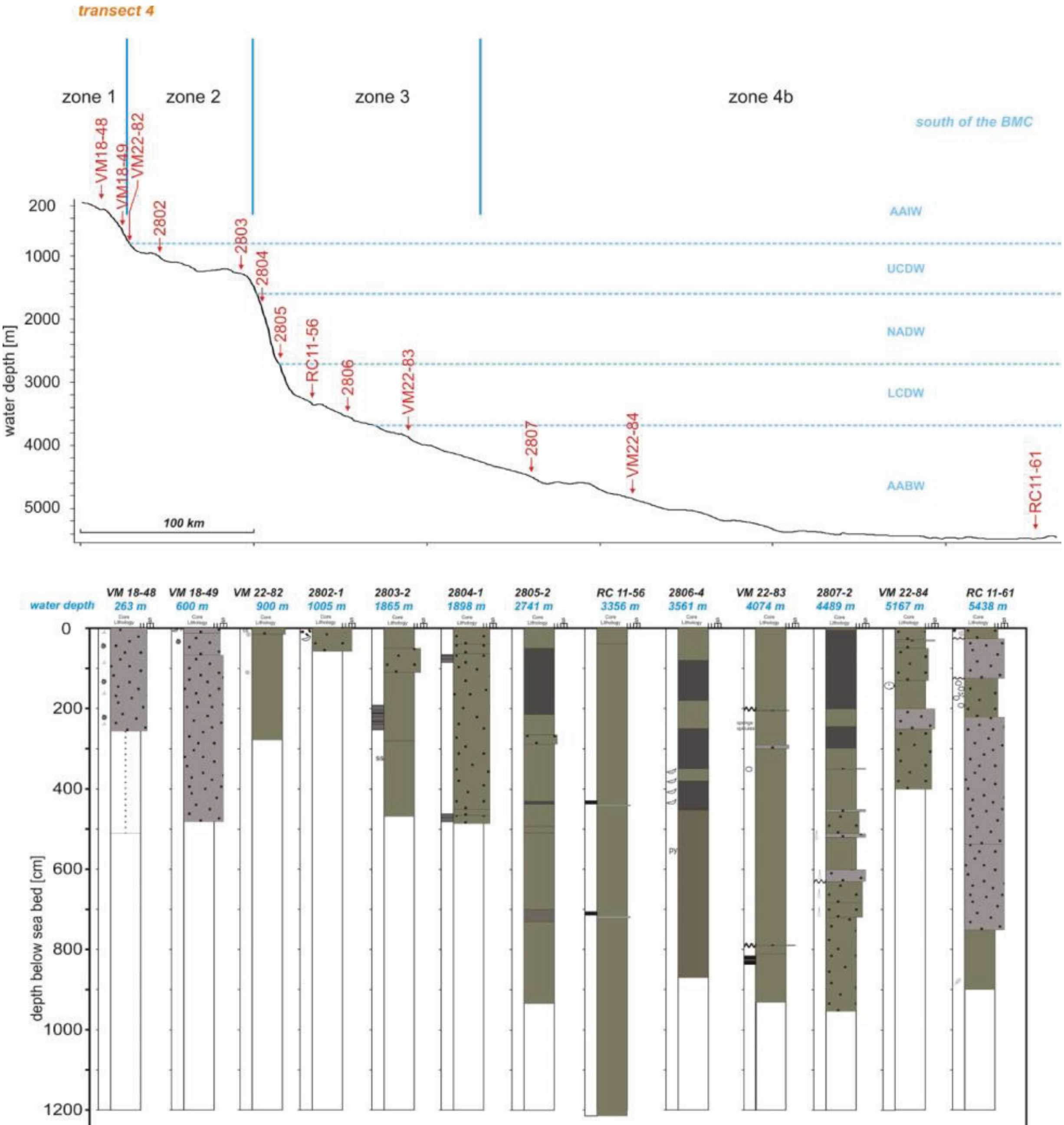

Figure 5.9: Core transect 4. The Ewing terrace is morphologically well developed and characterized by thick-bedded sand. Distal cores have thick sand beds and very little mud; the legend and detailed figure information can be found in Fig. 7.

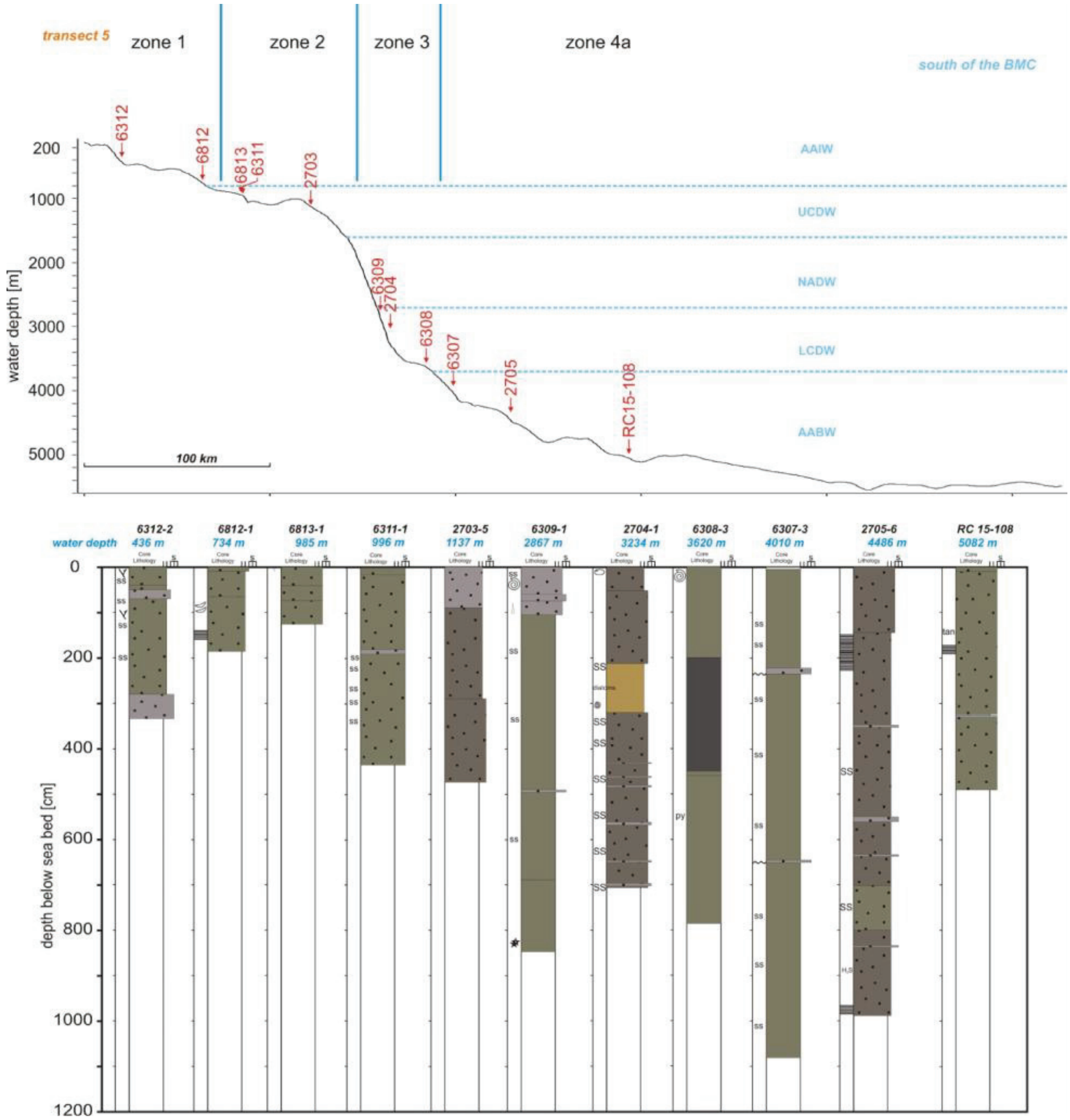

Figure 5.10: Core transect 5. The Ewing terrace is morphologically well developed, but dips basinwards. Cores on the terrace are characterized by thick-bedded sand. Distal cores have thick sand beds and very little mud. Depositional processes are along- and downslope driven; the legend and detailed figure information can be found in Fig. 7.

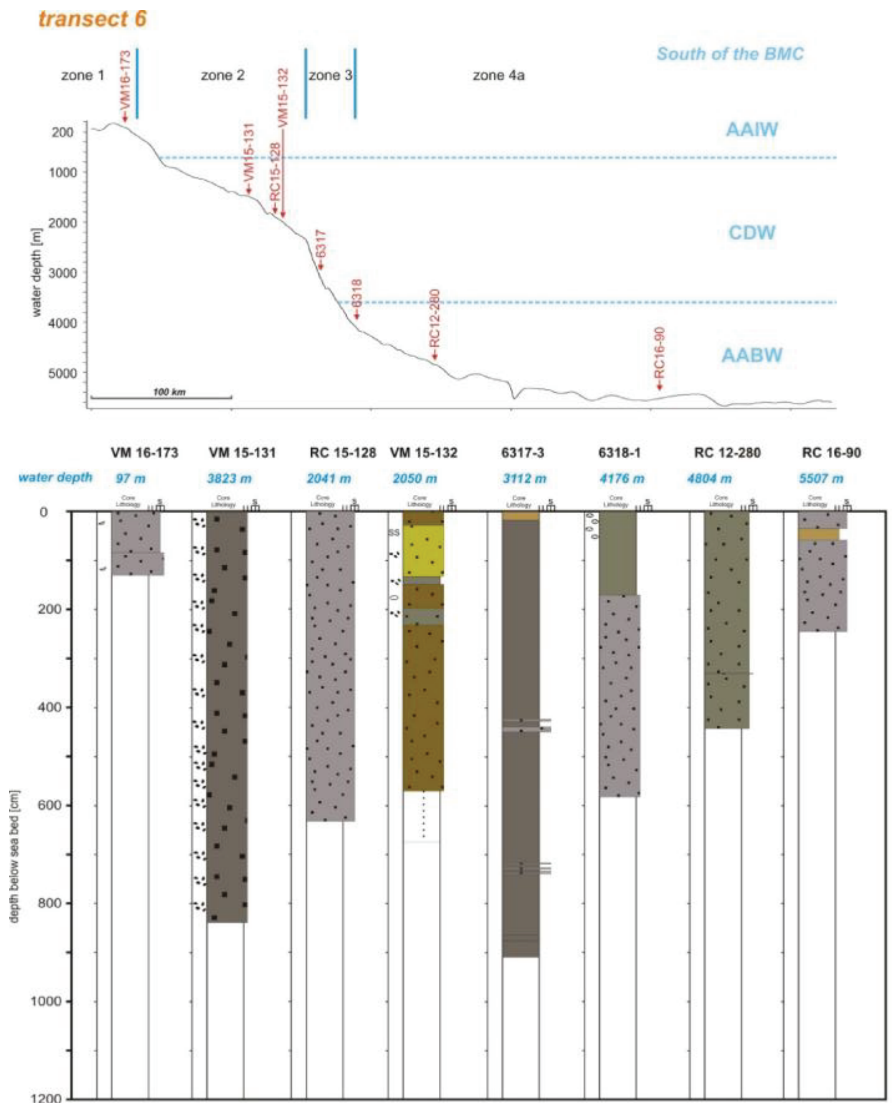
transect 6
South of the BMC
zone 1
zone 2
zone 3
zone 4a
AAIW
CDW
AABW
VM16-173
VM15-131
RC15-128
VM15-132
6317
6318
RC12-280
RC16-90
water depth [m]
100 km
VM 16-173
VM 15-131
RC 15-128
VM 15-132
6317-3
6318-1
RC 12-280
RC 16-90
water depth
97 m
3823 m
2041 m
2050 m
3112 m
4176 m
4804 m
5507 m
depth below sea bed [cm]

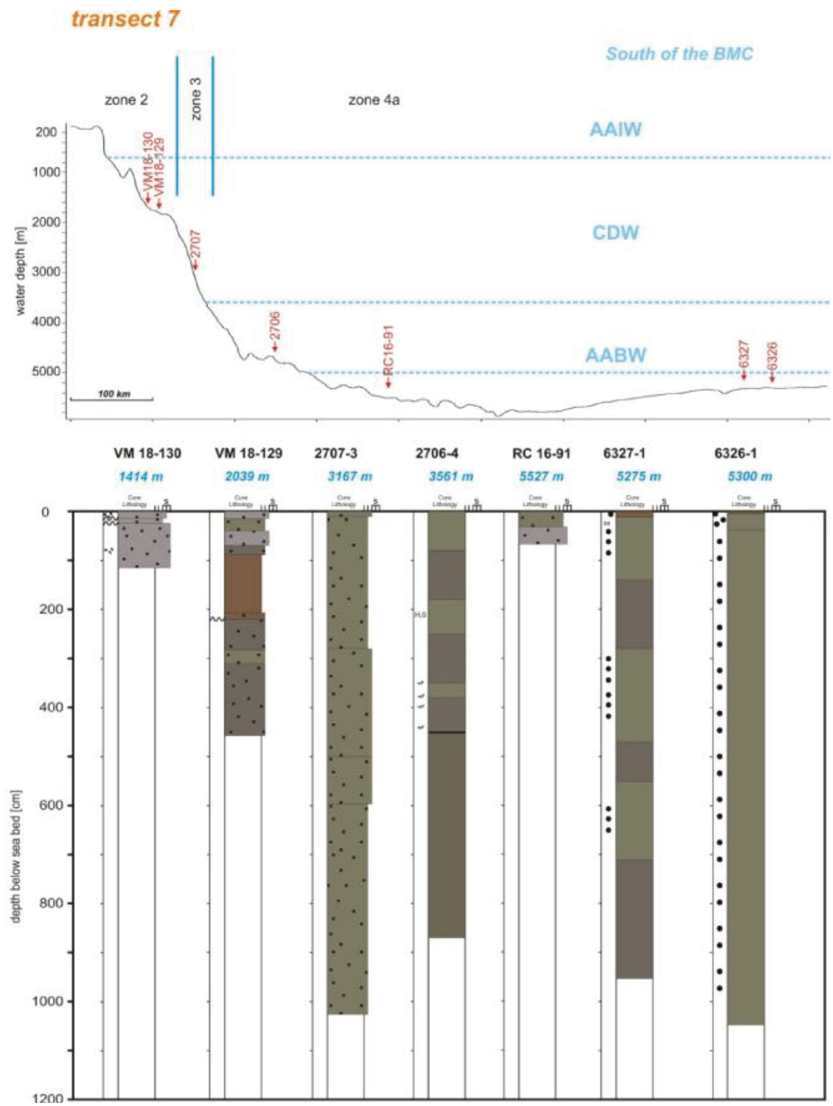
transect 7
South of the BMC
zone 2
zone 3
zone 4a
AAIW
CDW
AABW
VM18-130
VM18-129
2707
2706
RC16-91
6327
6326
water depth [m]
100 km
VM 18-130
VM 18-129
2707-3
2706-4
RC 16-91
6327-1
6326-1
1414 m
2039 m
3167 m
3561 m
5527 m
5275 m
5300 m
depth below sea bed [cm]

Figure 5.11 on previous page: Core transect 6 and 7. In core transect 6, the Ewing terrace is morphologically still recognizable, but less well developed compared to previous transects. It dips basinwards and is characterized by sand and rare granules. Distal cores have thick sand beds and very little mud. Depositional processes are along- and downslope driven. In core transect 7, the Ewing terrace is morphologically still recognizable, but less well developed compared to previous transects. It dips basinwards and is characterized by sand. Distal cores have thick sand beds and very little mud. Depositional processes are along- and downslope driven; the legend and detailed figure information can be found in Fig. 7.

5.5 Discussion

5.5.1 Continental slope and rise architecture

Utilizing the slope morphology and the most dominant core lithology, the continental slope offshore northern Argentina and Uruguay can be divided into two main depositional areas: an area in the south, where (1) the Ewing terrace is present forming a morphological step in the slope and (2) an area to the north where the slope does not show the presence of a terrace (Figs. 1 and 2). This change between the terraced slope and un-terraced slope occurs at ~37°S (Figs. 1 and 2). This change in slope morphology is not only expressed in slope zoning (Zones 1, 2, 3 and 5) but also affects sedimentation patterns on the lowermost slope and rise area (Zones 4a and b).

This change of seabed morphology and linked surface sediment distribution can also be seen in the core transects (Fig. 3) where the trends observed from surficial data can also be traced downcore. Core transects 1-3 (Figs 7 and 8) show on the slope below the shelf break thin sand beds. Thick sand is only present on the rise and abyssal plain. In core transect 3 (Fig. 7), first signs of the Ewing Terrace are seen, reflected in sandy cores on the poorly developed termination of the terrace. This is in contrast to the sand-dominated core transects 4-7 (Figs. 9-11). In these transects, the sand content increases southwards. This implies that due to the great variability in sand content, the first three core transects 1-3 are dominated by different sedimentary processes compared to the core transects 4 through 7 (Fig. 3).

5.5.1.1 Core transects 1-3: turbidite sands and debris flow deposits

The northernmost three core transects (transects 1-3) are characterized by thin bedded sand beds with a maximum thickness of 10 cm. These beds are commonly normally graded (Figs. 7 and 8). Such normal-graded sequences are typical characteristics of sandy turbidite beds (Middleton and Hampton, 1973), whereas contourite sand deposits are usually not bound this sharply to surrounding muds and do not usually show such well-developed graded sequences (Stow et al., 2002; Rebesco et al., 2007; Stow and Faugères, 2008).

Additionally, a turbidite origin of these sand beds in this Zone 5 (Fig. 1) is supported by the (1) presence of very local basal erosion (Figs. 7 and 8) typical of turbidity current flows in slope conduits (Middleton, 1993). Furthermore, the (2) bed thicknesses of less than 10 cm, which can be directly linked to slope angle (Fig. 2) and/or sorting of the failing material (Sadler, 1982; Middleton and Neal, 1989; Talling et al., 2007), are typical indicators of turbidity current processes (Talling et al., 2007). (3) The lack of mud within these sand beds is more typical for turbidity currents (Lowe and Guy, 2000) rather than contourite deposits which have, due to bioturbation, frequently muds throughout (Stow and Faugères, 2008). Additionally, the slope and rise morphology (Fig. 1) points also towards downslope driven processes rather than alongslope driven processes, as the slope shows frequent canyons (Fig. 5) characterized by sand and sandy muds (Figs. 5, 7 and 8).

Between these sand beds, structureless mud from hemipelagic sedimentation with few bioturbation straructures is present (Figs. 7 and 8). In few instances, differently colored mud clasts and sand blebs are observed (Figs. 7 and 8). These mud clast conglomerates are also linked to frequent erosional surfaces in the cores (Fig. 7). Such sedimentary sequences are highly indicative of mud clasts conglomerates typical of mass transport deposits created by disintegrating of source material after failure during flow establishment (Tripsanas et al., 2009). Few of the thin sand beds (cm-scale, Fig. 7) and some of the elongated sand blebs may suggest bypassing of turbidity currents (Postma and Roep, 1985; Piper et al., 1987). Slope angles and the comparison of thicknesses of slope and upper rise sand beds support the interpretation of the presence of turbidity current bypassing lower slope core positions. Some of the observed mass transport deposits are also likely related to turbidity current activity generated from retrogressive failures.

Therefore, using the lithology and megascopic sedimentary structures of transect 1-3, it is suggested that this part of the slope is characterized by downslope driven processes (Figs. 7 and 8, Table 1): sands are interpreted as turbidite sands and debris flows are responsible for the mud clasts and sand blebs found in the cores. This general mode of deposition has also been described from previous studies at this part of the slope looking at either the distribution and thicknesses of debris flows in seismic sections (Antobreh, 2005) or using core data, which indicates terrestrial sourced sand in this part of the basin from turbidity currents (Ewing et al., 1964; Ledbetter and Klaus, 1987).

The likeliness of coarser material to be present in the cores is highly dependent on local morphological features as small valleys or canyons (Figs. 1, 2 and 5). Generally, sand beds cannot be correlated easily downslope as observed sand bed thickness variations (Fig. 7) are linked to variations in slope angle (Fig. 2), resulting frequently in bypassing and thus inhibiting simple downslope bed correlations. Additionally, the simple sand bed correlations are also not possible as most canyons are sinuous (Fig. 5), whereas the core transects were taken on straight, slope-dipping transects (Fig. 3).

As the slope angle changes on the lower slope (Fig. 4), thick-bedded sands are deposited on the lowermost slope and upper rise (Figs. 7 and 8). These thick bedded sands are either (1) the result of amalgamated turbidite beds (Kuenen and Menard, 1952; Walker, 1967), which cannot be distinguished from each other anymore solely by detailed core descriptions or (2) are the result of contourite sheets built by the Antarctic Bottom Water (Fig. 7). Such thick-bedded sands are only found in one of the core transects (Figs. 5, 7 and 8). Hence, these thick sand beds have a very limited spatial extent and may thus these represent more likely amalgamated turbidite beds rather than contourite sheets, which would reveal at such water depth a much greater spatial extent (Hernández-Molina et al., 2008a). Nevertheless, more detailed sedimentological data will be needed to exclude either suggested process of deposition.

The Argentine Abyssal Plain is locally sandy (transect 2 (Fig. 8), beyond 5000 m water depth). As these thin sand beds show basal erosion and distinct grading (Fig. 8), these beds are interpreted as typical turbidite beds deposited due to change in seabed angle, which are thinning basinwards (Fig. 8, core RC 11-50). Between the turbidite events, hemipelagic sedimentation or seabed winnowing prevailed and resulted in smooth seabed topography, as it was also shown on seabed photography (Fig. 6, photos 13 and 14).

Furthermore, this part of the slope (Zone 5 and 4b) is cut by several canyons (Fig. 5). Some of them reach the shelf break. Few canyons start at the northward termination of the Ewing terrace at ~1300 m water depth, suggesting that they are fed at least partially by sand from the terrace (Fig. 5).

5.5.1.2 Core transects 4-7: interaction of along- and downslope processes

Core transects 4-7 (Figs. 9-11) are very different from the previous three transects 1-3. The sediment cores found in transects 4-7 are dominated by thick-bedded (several 10s cm thickness), frequently muddy sand beds. Seabed morphology is generally smooth with few small ripples present (Figs. 6). No major internal erosional surfaces are observed in the cores (Figs. 9-11). The Ewing Terrace broadens southwards and is always sand-dominated (Figs. 3, 4, 5 and 6). Very few cores show muddy beds: only transect 4 (Fig. 9) has cores with mud on the terrace. This coincides with the widest and flattest part of the Ewing Terrace and the presence of the slightly shallower La Plata Terrace (Fig. 1). The large amounts of sand and little mud over long stretches on the Ewing Terrace can generally be explained by 2 different types of processes: (1) contourite deposition in a sandy contourite system with the introduction of mud after deposition by winnowing and bioturbation processes or (2) by upper slope sands and muds failing by various processes and being trapped on the terrace.

On the Ewing Terrace, evidence can be found for both suggested sedimentary processes, along- and downslope driven processes, forming thick-bedded sand packets with little mud present (Table 1). Shelf sediment export is present in some cores, shown by frequent shell fragments throughout sand beds (Figs. 9, 10 and 11). Nevertheless, seabed photography (Fig. 6) also shows rippled sandy seafloor on the Ewing Terrace indicating alongslope bottom current activity. These observations suggest an interaction of alongslope and downslope driven processes affecting terrace deposition.

In general, triggering processes for the downslope driven deposits within this setting may include (a) prodelta slumping, (b) passive margin seismicity, (c) high sedimentation rates, leading to oversteepening, or (d) may be related to rapid changes in porewater pressures by cyclic wave loading. Prodelta slumping is unlikely along this margin, as the La Plata fluvial outflow seems to be deflected northwards not only during times of high sea level (Mahiques et al., 2008), but also during sea level lowstands (Martins and Willwock, 1987; Urien et al., 2003). Thus oversteepening is also unlikely, as this process requires rapid deposition of large sediment volumes at the shelf break, which is not the case as the shelf break is terraced at this slope section, and fluvial sourced material does not reach this part of the shelf break (Urien, 1967; Urien and Ewing, 1974; Mahiques et al., 2008). Therefore case (b) or (d) are the most likely triggering processes affecting this part of the slope, as recent passive margin seismicity has been observed just to the north offshore Uruguay (Benavídez Sosa, 1998) and storms frequently track in this area (Swift et al., 1978).

Cores in Zone 3 (Fig. 3), just below the Ewing terrace on the steepest part of the slope (Fig. 2), show no sand beds at all (Figs. 9-11). This observation may be due to the fact that (i) no sand export occurs from the Ewing Terrace downslope, or (ii) the exported sand bypasses the lower steep slope (Fig. 2) and is deposited only on the sandy rise due to rapid change in slope angle. Nevertheless, large amounts of coarse sand and even granules are observed on the lowermost slope and rise (Zone 4a, Fig. 6). If little sediment is exported from the Ewing terrace, as proposed by (i), the alongslope current system on the terrace must be sufficient strong to prevent deposition on the seaward side of the terrace. If (ii) seaward export is present, these flows must be able to develop enough inertia to bypass the lower slope completely and only deposit in the less steep outermost slope and rise area.

5.5.1.3 Continental rise depositional processes: mixed turbidite-contourite system winnowed by ocean currents

The cores on the lowermost continental slope and rise are sand-dominated again. There may be again two possible sources for the sand: (a) sand coming from upslope being export from the Ewing terrace, as discussed above, or (b) sand transported to the area by contour-current activity. Downslope driven transport as proposed in (a) would be either in the form of debris flows or by turbidity currents. The high sand content and the lack of observed deformational structures (Figs. 9-11) more likely points to turbidity current or grain flows (Lowe, 1976; Middleton, 1993) rather than typical debris flows, which are generally characterized by high mud content (Takahashi, 1981). Few beds

(Fig. 10) do show lamina, grading and sharp basal erosional surfaces. Such structures suggest turbidity current or grain processes depositing such sand beds (Lowe, 1976; Middleton, 1993). Additionally, abundant shell fragments (Fig. 11, core 2706-4) suggests some direct downslope shelf-sourced material rather than long distance along-slope transported, as such small shell fragments would have been corroded quickly within the Antarctic Bottom Water during transport (Volbers and Henrich, 2004).

Nevertheless, the more massive sand beds (several 10s of cm to meter scale, e.g. Fig. 10) suggest a different process of deposition. The presence of diatoms may indicate southern sources (Krinsley et al., 1973). Seabed photography (Fig. 6) imaged coarse sand and gravel in some places indicative of gravel lags, a typical indicator of alongslope sediment transport (Stow et al., 2002). Additionally, rippled seabed highlights the presence of bottom currents (Fig. 6). Thus, there are also alongslope current processes active, winnowing seabed sediments as suggested in (b).

The sources of the sand may either be (α) from upslope and represents reworked turbidite sands and/or grain flows or (β) are transported to the area by an alongslope current. The sediments transported to the areas within the alongslope current are either from distant sources, which are ultimately the surroundings of Antarctica, or transported to the basin by canyons situated further to the south (Hernández-Molina et al., 2009; Lastras et al., 2011). This is shown by the presence of frequent siliceous organisms (Fig. 11), and is supported by previous studies from the area (Krinsley et al., 1973; Romero and Hensen, 2002).

In conclusion, the sand beds in this part of the lowermost slope and rise (Zone 4a) are therefore the result of the interaction of downslope and alongslope processes as shelf-sourced, as well as local and distal-sourced components have been described from cores in the area (Figs. 9-11).

5.5.2 Driving processes of slope architecture

The main challenge in this process-oriented classification of the northern Argentine and Uruguay continental slope is the explanation of the morphological and lithological change on the slope and rise between the southern sector where terraces are present and where the slope is sandy and hummocky and the northern sector, where no terrace is present and the slope is muddy and shows smooth topography (Fig. 1, Table 1). Core data and seabed morphology (Figs. 3 and 5) shows these differences also and suggest that the southern, terraced slope is characterized by the interaction of alongslope and downslope driven processes, whereas the northern study area shows on the slope mostly elements of downslope driven processes (Figs. 3 and 5).

Two main changes occur at the position of the observed change in slope sedimentation at ~37°S. The (i) ocean circulation changes due to the presence of the Brazil-Malvinas Confluence and its implications for deeper circulation patterns (Piola and

Matano, 2001), just where the terraced slope terminates, and during sea level lowstands the (ii) discharge of the La Plata Rivers was probably deflected northwards (Martins and Willwock, 1987), supplying sediment to the outer shelf and slope to the north of the observed change in slope dynamics (Figs. 12 and 13). Therefore, both processes, the (i) change in the oceanographic setting and the (ii) input of terrestrial runoff can be used to explain the significant change in slope sedimentation. A conceptual model (Figs. 12 and 13) discussing both influences was used to estimate the impact of each process on slope deposition and the ability of explaining the observed features (Figs. 1, 5 and 7-11).

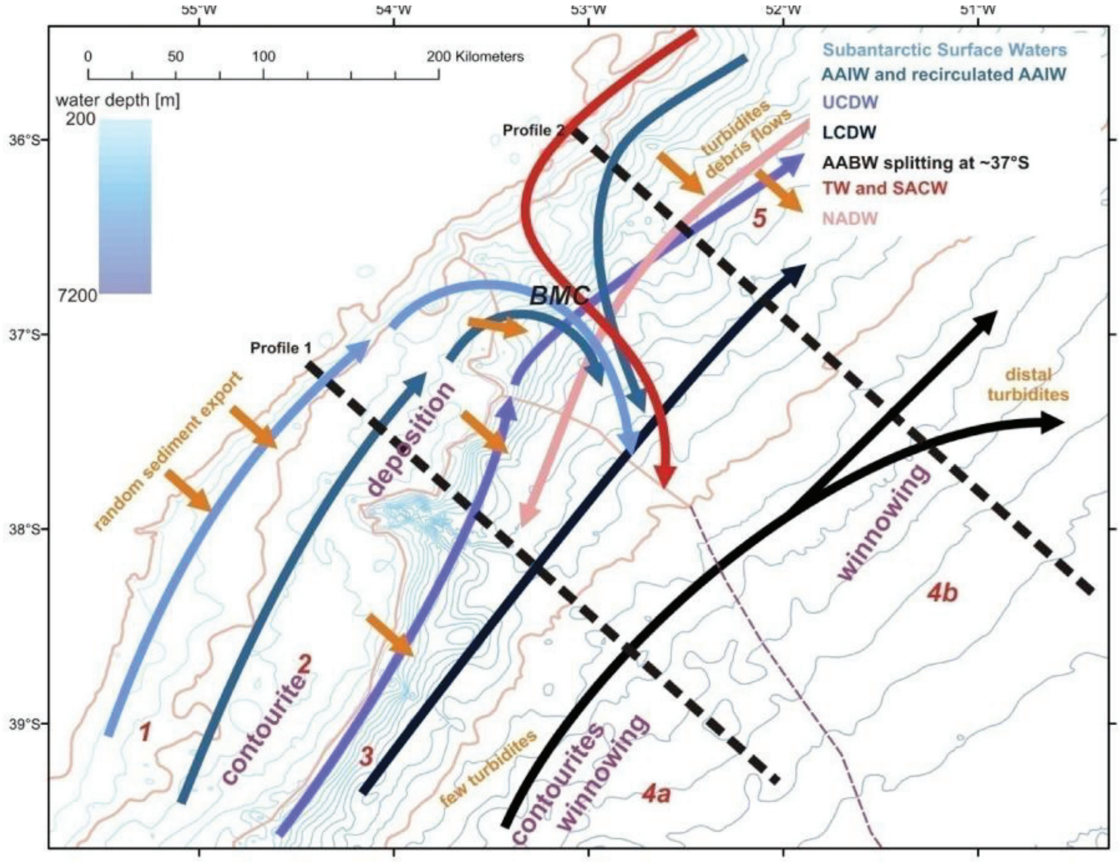

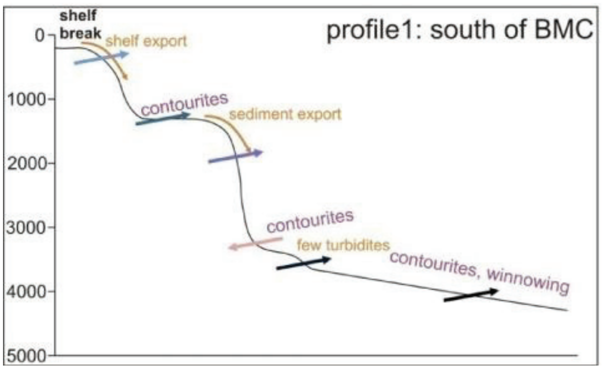

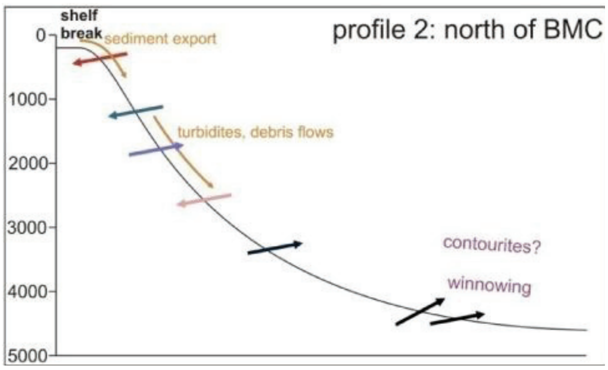

Figure 5.12: Summary sketch (bathymetry from Gebco 08) showing interaction of the main depositional processes with the oceanographic setting. Orange colors depict downslope driven processes, whereas lilac colors show alongslope processes. Profile 1 and 2 are schematic transects depicting the sedimentation processes with the interaction of ocean circulation. BMC: Brazil-Malvinas Confluence.

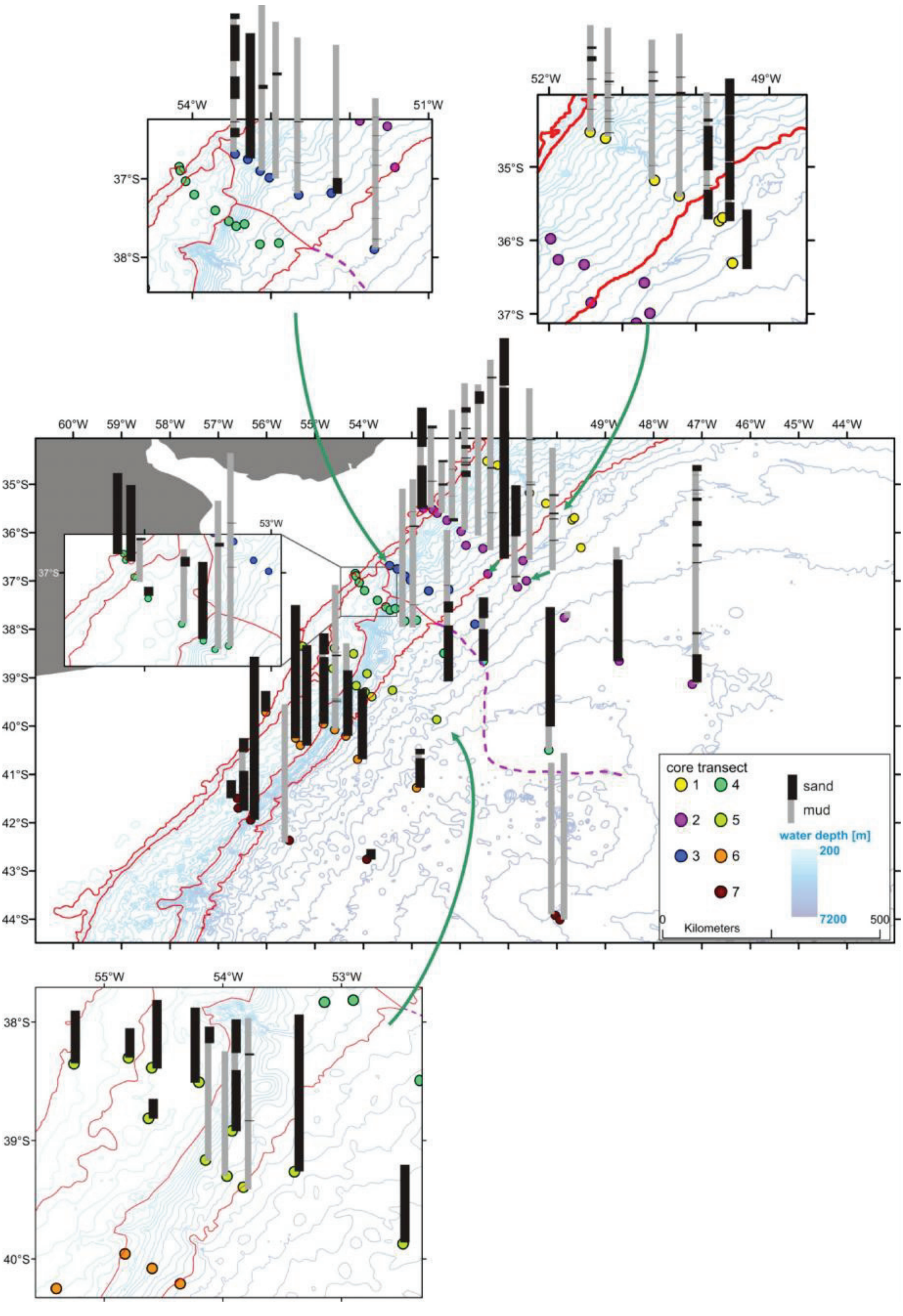

core transect
1
2
3
4
5
6
7
sand
mud
water depth [m]
200
7200
Kilometers
0
500
60°W
59°W
58°W
57°W
56°W
55°W
54°W
49°W
48°W
47°W
46°W
45°W
44°W
35°S
36°S
37°S
38°S
39°S
40°S
41°S
42°S
43°S
44°S
53°W
52°W
51°W

Figure 5.13 on previous page: The variability of sand and mud downcore along the slope and rise (bathymetry from Gebco 08). This images nicely the significant change in sand content between the northern and southern slope area. This change is due to changes in ocean circulation and/or fluvial discharge affecting greatly slope deposition.

5.5.2.1 Impact of ocean circulation

The termination of the Ewing Terrace coincides with the position of the Brazil-Malvinas Confluence zone, where stacks of water masses flowing either north- or southwards (Fig. 12), confluence (Stramma and England, 1999; Piola and Matano, 2001). This results in the detachment of several water masses from the slope, initiating seaward flow into the Argentine Basin (Fig. 12) (Stramma and England, 1999; Piola and Matano, 2001; Sijp and England, 2008), and ultimately flow into the subtropical gyre, which causes basin-wide recirculation patterns (Stramma and England, 1999; Schmid et al., 2000). Recently it was shown that to the south of the BMC each change in slope angle coincides with a specific water mass boundary, forming terraces and other smaller slope indents (Hernández-Molina et al., 2009). Additionally, such water mass contact zones are known to initiate randomly eddies of various sizes, resulting in non-linear flow behavior of the water mass, which may result in specific cases even in slope erosion (Puig et al., 2004a).

This significant change in flow direction away from the continental slope terminates the terraces on the slope (Figs. 1, 5 and 12). Sediment within these water masses seems to be channelized in few slope canyons and transported downslope (Fig. 5). To the north of 37°S, the slope shows besides canyons reaching the shelf break no major morphological features anymore (Figs. 1, 5, 6 and 13). Core data (Figs. 7-11 and 13) indicates at least on the slope processes as turbidites, grain flows and debris flows deposited within hemipelagic sedimentation; ocean currents play a minor role in sedimentation and may winnow seabed locally (Fig. 6). Nevertheless, basin sedimentation below ~4500 m water depth (Fig. 13) may not change greatly across the BMC as massive sands have been also observed in Zone 4b (Figs. 5, 7 and 8), which cannot be surely linked to either turbidite or contourite processes.

To the south of the BMC, contourites are constructed by the AAIW and AABW, which transport southern sourced sediments (Krinsley et al., 1973; Mahiques et al., 2008; Hernández-Molina et al., 2009). Thus, on the northern Argentine and Uruguay continental slope, contourite deposition may be driven by two main processes: (1) slope morphology or (2) sediment availability. (1) Slope morphology likely plays an important role, as it interacts with water mass geometry, as it is the case to the south of 37°S where terraces and smaller slope indents can be linked to specific water masses (Hernández-Molina et al., 2009). Such slope terraces trap downslope driven sediments early on, before such flows develop high inertia resulting in major erosional potential. Thus, downslope driven sediment is trapped early on and reworked by the contour current flow on the terrace (Figs. 12 and 13).

To the north of 37°S with the more complex oceanographic setting with re-circulated and/or counter-flowing water masses (Fig. 12) (Stramma and England, 1999; Mémery et al., 2000), such slope terraces are not formed. This fact may be related to (2) sediment availability. Water masses to the north of the BMC seem to be sediment starved, as these water masses are either re-circulated Antarctic-sourced waters (Fig. 12) (Stramma and England, 1999) and lose their bed load either during detachment from the slope or when flowing across the abyssal contourite lobes (e.g. the Zapiola Drift (von Lom-Keil et al., 2002)). Additionally, the equatorial derived water masses (mainly the NADW) seem to also not construct large –scale contourite deposits on the Brazilian Slope, as contourites are there generally linked to the Brazil Current (Viana, 2002), which is at a shallower water depth close to the shelf break (Viana et al., 1998b). Additionally, slope angles to the north of 37°S are too high (Fig. 2) to initiate any major contourite deposition on the slope. Sediment is channelized in canyons and deposition only occurs beyond the lower slope (Fig. 5).

The rise zoning (Fig. 1) can be explained in a similar way. To the south of 37°S in Zone 4a, ocean currents are not sufficient strong to rework all of the downslope supplied sediment. This creates hummocky seabed with several small depressions. When the Antarctic Bottom Water enters Zone 4b (Fig. 5), it splits (Fig. 12) (Coles et al., 1996) and is also shifted eastward due to morphology and modified Coriolis force. This forced shift may result in increased flow speed resulting in smooth seabed along this part of the margin (Fig. 6). Additionally, distal turbidites are the feeding processes to this area (Zone 4b), which also are generally characterized by smooth seabed morphology.

5.5.2.2 The impact of the La Plata Rivers

The other possible explanation for the abrupt change in slope morphology (Fig. 1) and dominating sedimentary processes around 37°S (Fig. 13) is the impact of the discharged sediments from the La Plata River to the slope. The discharged fluvial sediment is mostly being deflected northwards (Martins and Willwock, 1987; Urien et al., 2003; Mahiques et al., 2008), reaching the slope just to the north of 37°S (Fig. 1) (Martins and Willwock, 1987). The discharged sediment reaching this position is mostly fine-grained. Additionally, a mud depositional area has been mapped to the north of 37°S at the shelf break (Urien and Ewing, 1974; Martins et al., 2005c) supporting the idea of fluvial sediment reaching at times this part of the shelf break.

To the south of 37° S, sediment from downslope driven processes is mostly sandy (Figs. 9-11 and 13). Failure is linked to random events such as storms or passive margin seismicity, thus sediment supply is not constant (Figs. 12 and 13). Therefore, in this area (south of 37°S, Fig. 5) the failing sediment does not influence the alongslope sediment transport at all times, and the alongslope current is sufficiently strong to rework the downslope driven sediments and incorporate it into the contourite deposits found on the terraces (Figs. 9-11 and 13).

To the north of 37°S, outer shelf (Urien and Ewing, 1974) and slope sediments (Figs. 7, 8 and 13) are muddy and few coarser turbidite beds characterize the slope system. Some of the turbidite beds seem to occur at an even spacing (Figs. 7 and 8). Failing may thus be linked to either (1) cyclic flooding events triggered by hinterland climate processes, or (2) driven by upper slope sediment storage capacity. In both cases, fluvial supply of sediment destabilizes the slope by oversteepening and results in mass wasting, e.g. turbidites and debris flows. This inhibits or destroys possible initiated contourite deposition, as these contourite deposits would be eroded together with the turbidite beds and the material incorporated into the turbidity currents (Fig. 12).

Both processes, the (i) oceanographic regime and (ii) the discharge of fluvial sediment to the shelf break to the north of 37°S can be used to interpret the observed changes in slope sedimentation from the south to the north (Fig. 12). Thus, it is most likely a combination of both processes responsible for the observed changes of styles of slope sedimentation.

5.5.2.3 Driving processes of slope sedimentation

It is very challenging to estimate the relative importance of the two factors, the oceanic circulation or the fluvial discharge, on slope sedimentation, but the discharge of fine-grained sediment is likely the more important processes driving the change in slope sedimentation. The reason for this assumption is as follows: the change in slope dynamics does not seem to change over time (see core transects, Figs. 7-11 and 13). Nevertheless, during sea level lowstands, oceanic circulation probably changed in the area due to a strengthening of the northward flowing currents (Ledbetter and Johnson, 1976; Hemming et al., 2007; Sijp and England, 2008; Laprida et al., accepted) likely resulting in a northward migration of the Brazil-Malvinas Confluence. Even though the studied cores do not have age control, ages on other cores on this slope (Turekian and Stuvier, 1964; Groot and Groot, 1966; Groot et al., 1967; Riedinger et al., 2005; Laprida et al., accepted) suggest that the cores from this study also reach into at least marine isotope stage 2.

This preliminary timing suggests that the observed change in slope sedimentation are more pronounced during lower sea levels in glacial stages when the slope south of 37°S is characterized by shelf sediment export. Similarly, at this time, high bed loads reached the shelf break to the north of 37°S, initiating mass wasting and triggering turbidity currents. During sea level highstands, as observed during e.g. the Holocene, less energetic storm systems track this area, and less fluvial bed load reaches the shelf break. During such times, the oceanic circulation may have a greater impact on slope sedimentation compared to the La Plata river discharge, which results in fewer slope failures at this time (Fig. 13).

These observations may lead to the conclusion that the recorded changes in the dominant sedimentary process was also present during the last glacial when the Brazil-

Malvinas Confluence was shifted northwards. Therefore, the changes in styles of sedimentation are more likely linked to the influence of the La Plata River, which had higher bedload during glacial stages (Martins et al., 2003). Nevertheless, especially on the northern Argentine Slope, ocean currents do have a great impact on slope sedimentation in the area (Figs. 5 and 12) by winnowing and/or building of contourite deposits on the slope and rise (Hernández-Molina et al., 2009).

5.6 Conclusions

Sedimentation on the northern Argentine and Uruguay continental slope is highly influenced by the ocean circulation and the fluvial discharge of the La Plata Rivers transporting currently mainly fine-grained sediments. Detailed bathymetric analysis and the description of 67 sediment cores were used to define five different zones on the continental margin characterized by changing slope angles and sedimentary characters. This zoning is also supported by seabed photography. At ~37°S, a major change in morphology and sedimentation patterns occurs. To the south of 37°S, the slope is terraced, whereas to the north no terraces are found on the slope. The mean annual position of the Brazil-Malvinas Confluence, in which northward and southward flowing water masses collide, coincides with the change in morphology and sediment distribution. Roughly 37°S also marks the southernmost reach of the fluvial sedimentary load from the La Plata River. The effect of both elements on continental margin morphology and sediment distribution were evaluated and we show that the fluvial discharged sediments likely play a more significant role if compared to the oceanographic feature, particularly during sea level lowstands. Nevertheless, contourite deposition does occur on the margin and thus especially during sea level highstands the oceanic circulation does play a significant role in slope sedimentation processes.

5.7 References

Adams, E.A. and Schlager, W., 2000. Basic types of submarine slope curvature. Journal of Sedimentary Geology, 70(4): 814-828.

Aksu, A.E. and Hiscott, R.N., 1989. Slides and debris flows on the high-latitude continental slopes of Baffin Bay. Geology, 17(10): 885-888.

Anderson, J.B., Kurtz, D.D., Domack, E.W. and Balshaw, K.M., 1980. Glacial and glacial marine sediments of the Antarctic continental shelf. Journal of Geology, 88(4): 399-414.

Angulo, R.J., Lessa, G.C. and de Souza, M.C., 2006. A critical review of mid- to late-Holocene sea-level fluctuations on the eastern Brazilian coastline. Quaternary Science Reviews, 25(5-6): 486-506.

Antobreh, A.A., 2005. Channelised and open-slope processes of mass sediment transport: their morphological and seismic characterisation from selected Atlantic high productivity regions. Ph. D. Thesis, University of Bremen, Bremen, 130 pp.
Antonioli, F., Bard, E., Potter, E.-K., Silenzi, S. and Improta, S., 2004. 215-ka History of sea-level oscillations from marine and continental layers in Argentarola Cave speleothems (Italy). Global and Planetary Change, 43(1-2): 57-78.
Arhan, M., Naveira Garabato, A.C., Heywood, K.J. and Stevens, D.P., 2002. The Antarctic Circumpolar Current between the Falkland Islands and South Georgia. Journal of physical Oceanography, 32(6): 1914–1931.
Armishaw, J.E., Holmes, R.W. and Stow, D.A.V., 1998. Morphology and sedimentation on the Hebrides Slope and Barra Fan, NW UK continental margin. In: M.S. Stoker, D. Evans and A. Cramp (Editors), Geological processes on continetal margins: mass-wasting and stability. Geological Society, Special Publication 129, London, pp. 81-104.
Assumpcao, M., 1998. Seismicity and stresses in the Brazilian passive margin. Bulletin of the Seismological Society of America, 88(1): 160-169.
Baltzer, A., Cochonat, P. and Piper, D.J.W., 1994. In situ geotechnical characterization of sediments on the Nova Scotian Slope, eastern Canadian continental margin. Marine Geology, 120(3-4): 291-308.
Baltzer, A., Holmes, R. and Evans, D., 1998. Debris flows on the Sula Sgeir Fan, NW of Scotland. In: M.S. Stoker, D. Evans and A. Cramp (Editors), Geological processes on continental margins: sedimentation, mass-wasting and stability. Geological Society, 129, London, pp. 105-115.
Baracco, R., Garcia-Rodriguez, F., del Puerto, L., Inda, H. and Castineira, C., 2008. Holocene relative sea-level variation inferred from records in the basin of Castillos, Shallow Lakes Conference 2008: Structure and function of world shallow lakes, Punta del Este, Uruguay, pp. 75.
Beaubouef, R.T. and Friedmann, S.J., 2000. High resolution seismic/sequence stratigraphic framework for the evolution of Pleistocene intra slope basins, western Gulf of Mexico: depositional models and reservoir analogs, GCSSEPM Foundation 20th Annual Research Conference: Deep Water reservoirs of the World, Houstan, TX, pp. 40-60.
Benavídez Sosa, A., 1998. Sismicidad y sismotectónica en Uruguay. Fisica de la Tierra, 10: 167-186.
Benetti, S., 2006. Late Quaternary sedimentary processes along the western North Atlantic margin. Ph. D. Thesis, University of Southampton, Southampton, 188 pp.
Benthien, A. and Müller, P.J., 2000. Anomalously low alkenone temperatures caused by lateral particle and sediment transport in the Malvinas Current region, western Argentine Basin. Deep Sea Research Part I: Oceanographic Research Papers, 47(12): 2369-2393.
Berbery, E.H. and Barros, V.R., 2002. The hydrologic cycle of the La Plata Basin in South America. Journal of Hydrometeorology, 3(6): 630-645.
Berry, J.A. and Piper, D.J.W., 1993. Seismic stratigraphy of the central Scotian rise: a record of continental margin glaciation. Geo-Marine Letters, 13(4): 197-206.
Blanc, S., Goni, G. and Novarini, J., 1983. Surface mixed layer temperature and layer depth in water off the Argentinian coast. Journal of Geophysical Research, 88(C10): 5987–5996.

Blatt, H., Middleton, G. and Murry, R., 1980. Origin of sedimentary rocks. Prentice-Hall, Inc., Englewood Cliffs, New Jersey, 782 pp.
Blum, M.D. and Törnqvist, T.E., 2000. Fluvial responses to climate and sea-level change: a review and look forward. Sedimentology, 47: 2-48.
Boczar-Karakiewicz, B., Bona, J.L. and Pelchat, B., 1991. Interaction of internal waves with the seabed on continental shelves. Continental Shelf Research, 11(8-10): 1181-1197.
Bondevik, S., Mangerud, J., Birks, H.H., Gulliksen, S. and Reimer, P., 2006. Changes in North Atlantic radiocarbon reservoir ages during the Allerød and Younger Dryas. Science, 312(5779): 1514-1517.
Bouma, A.H., 1962. Sedimentology of some flysch deposits. Elsevier Publishing Company, Amsterdam, 168 pp.
Boyle, E.A., 1997. Characteristics of the deep ocean carbon system during the past 150,000 years: ΣCO_2 distributions, deep water flow patterns, and abrupt climate change. Proceedings of the National Academy of Sciences of the United States of America, 94(16): 8300-8307.
Brink, K.H., Bane, J.M., Church, T.M., Fairall, C.W., Geernaert, G.L., Hammond, D.E., Henrichs, S.M., Martens, C.S., Nittrouer, C.A., Rogers, D.P., Roman, M.R., Roughgarde, J.D., Smith, R.L., Wright, L.D. and Yoder, J.A., 1992. Coastal ocean processes: a science prospectus. Technical Report WHOI-92-18, Wood Hole Oceanographic Institute.
Bryn, P., Berg, K., Stoker, M.S., Haflidason, H. and Solheim, A., 2005a. Contourites and their relevance for mass wasting along the mid-Norwegian margin. Marine and Petroleum Geology, 22(1-2): 85-96.
Bryn, P., Berg, K., Forsberg, C.F., Solheim, A. and Kvalstad, T.J., 2005b. Explaining the Storegga Slide. Marine and Petroleum Geology, 22(1-2): 11-19.
Cacchione, D.A., Pratson, L.F. and Ogston, A.S., 2002. The shaping of continental slopes by internal tides. Science, 296: 724-727.
Campbell, D.C., 2000. Relationship of sediment properties to failure horizons for a small area of the Scotian Slope. Current research 2000-D8, Geological Survey of Canada, Dartmouth.
Campbell, D.C., Shimeld, J.W., Mosher, D.C. and Piper, D.J.W., 2004. Relationships between sediment mass-failure modes and magnitudes in the evolution of the Scotian Slope, offshore Nova Scotia, Offshore Technology Conference, Houston, Texas, pp. OTC 16743.
Campbell, D.C. and MacDonald, A.W.A., 2006. Geohazard assessment of five deepwater pipeline scenarios on the Scotian Slope. Open File 5079, Geological Survey of Canada, Ottawa.
Canals, M., Urgeles, R. and Calafat, A.M., 2000. Deep sea-floor evidence of past ice streams off the Antarctic Peninsula. Geology, 28(1): 31-34.
Canals, M., Puig, P. and Durrieu de Madron, X., 2006. Flushing submarine canyons. Nature, 444: 354-357.
Cao, L., Fairbanks, R.G., Mortlock, R.A. and Risk, M.J., 2007. Radiocarbon reservoir age of high latitude North Atlantic surface water during the last deglacial. Quaternary Science Reviews, 26(5-6): 732-742.
Carter, L., 2007. The role of intermediate-depth currents in continental shelf-slope accretion: Canterbury Drifts, SW Pacific Ocean. In: A.R. Viana and M. Rebesco

(Editors), Economic and palaeoceanographic significance of contourite deposits. Geological Society, Special Publication 276, London, pp. 129-154.
Cavallotto, J.L., Violante, R.A. and Parker, G., 2004. Sea-level fluctuations during the last 8600 years in the de la Plata river (Argentina). Quaternary International, 114(1): 155-165.
Chiessi, C.M., Ulrich, S., Mulitza, S., Pätzold, J. and Wefer, G., 2007. Signature of the Brazil-Malvinas Confluence (Argentine Basin) in the isotopic composition of planktonic foraminifera from surface sediments. Marine Micropaleontology, 64(1-2): 52-66.
Chiessi, C.M., Mulitza, S., Paul, A., Pätzold, J., Groeneveld, J. and Wefer, G., 2008. South Atlantic interocean exchange as the trigger for the Bølling warm event. Geology, 36(12): 919-922.
Chiessi, C.M., Mulitza, S., Pätzold, J. and Wefer, G., 2010. How different proxies record precipitation variability over southeastern South America. IOP Conference Series: Earth and Environmental Science, 9: 012007.
Chubbs, J.F., 2003. Geohazards at the proposed Weymouth wellsite, Central Scotian Slope, offshore eastern Canada. B.Sc. Thesis, Saint Mary's University, Halifax, 75 pp.
Clapperton, C.M., 1993. Quaternary geology and geomorphology of South America. Elsevier, Amsterdam, 780 pp.
Clark, P.U. and Mix, A.C., 2002. Ice sheets and sea level of the Last Glacial Maximum. Quaternary Science Reviews, 21(1-3): 1-7.
Clark, R. and Wilson, P., 1992. Occurrence and significance of ventifacts in the Falkland Islands, South Atlantic. Geografiska Annaler. Series A, Physical Geography, 74(1): 35-46.
Clausen, L., 1998. 1. Late Neogene and Quaternary sedimentation on the continental slope and upper rise offshore southeast Greenland: interplay of contour and turbidity processes. In: A.D. Saunders, H.C. Larsen and S.W. Wise (Editors), Proceedings of the Ocean Drilling Program, Scientific Results, 152, College Station, TX, pp. 3-18.
Coles, V.J., McCartney, M.S., Olson, D.B. and Smethie, W.M., 1996. Changes in Antarctic Bottom Water properties in the western South Atlantic in the late 1980s. Journal of Geophysical Research, 101(C4): 8957-8970.
Coward, M.P., Purdy, E.G., Ries, A.C. and Smith, D.G., 1999. The distribution of petroleum reserves in basins of the South Atlantic margins. In: N.R. Cameron, R.H. Bate and V.S. Clure (Editors), The oil and gas habitats of the South Atlantic. Geological Society, Special Publication 153, London, pp. 101-131.
Cruz, F.W., Burnsa, S.J., Jercinovic, M., Karmann, I., Sharp, W.D. and Vuille, M., 2007. Evidence of rainfall variations in Southern Brazil from trace element ratios (Mg/Ca and Sr/Ca) in a Late Pleistocene stalagmite. Geochimica et Cosmochimica Acta, 71(9): 2250-2263.
Cruz, F.W., Vuille, M., Burns, S.J., Wang, X., Cheng, H., Edwards, R.L., Karmann, I., Auler, A.S. and Nguyen, H., 2009. Orbitally driven east–west antiphasing of South American precipitation. Nature Geosciences, 2(3): 210-214.
Darwin, C., 1846. Geological observations on South America. Smith, Elder and Co., London, 279 pp.

de Santa Ana, H., Latrónica, L., Tomasini, J., Morales, E., Ferro, S., Gristo, P., Machado, L., Veroslavsky, G. and Ucha, N., 2008. Economic and exploratory review of gas hydrates and other gas manifestations of the Uruguayan continental shelf, 6th International Conference on Gas Hydrates (ICGH 2008), Vancouver, BC , Canada.
Delaney, P.J.V. (Editor), 1966. Geology and geomorpholohy of the coastal plain of Rio Grande do Sul, Brazil and northern Uruguay. Coastal Studies Series, Coastal Studies Series 15. Lusiana State University Press, Baton Rouge, 58 pp.
Delmonte, B., Petit, J.R. and Maggi, V., 2002. Glacial to Holocene implications of the new 27000-year dust record from the EPICA Dome C (East Antarctica) ice core. Climate Dynamics, 18(8): 647-660.
Depetris, P.J. and Griffin, J.J., 1968. Suspended load in the Rio de la Plata drainage basin. Sedimentology, 11(1-2): 53-60.
Depetris, P.J., Kempe, S., Latif, M. and Mook, W.G., 1996. ENSO-controlled flooding in the Paraná River (1904–1991) Naturwissenschaften, 83(3): 127-129.
Depetris, P.J. and Pasquini, A.I., 2007. The geochemistry of the Paraná River: an overview. In: M.H. Iriondo, J.C. Paggi and A.R. Paira (Editors), The Middle Paraná River: Limnology of a Subtropical Wetland. Springer Verlag, Berlin, Heidelberg, pp. 143-174.
Dingle, R.V., 1980. Large allochthonous sediment masses and their role in the construction of the continental slope and rise off southwestern Africa. Marine Geology, 37(3-4): 333-354.
Dingle, R.V. and Robson, S., 1985. Slumps, canyons and related features on the continental margin off East London, SE Africa (SW Indian Ocean). Marine Geology, 67(1-2): 37-54.
Domack, E.W., Jacobson, E.A., Shipp, S. and Anderson, J.B., 1999. Late Pleistocene–Holocene retreat of the West Antarctic Ice-Sheet system in the Ross Sea: Part 2—Sedimentologic and stratigraphic signature. Geological Society of America Bulletin, 111(10): 1517-1536.
Dowdeswell, J.A. and Murray, T., 1990. Modelling rates of sedimentation from icebergs. In: J.A. Dowdeswell and J.D. Scourse (Editors), Glacimarine Environments: Processes and Sediments. Geological Society, Special Publication 53, London, pp. 121-137.
Dowdeswell, J.A., Ó Cofaigh, C. and Pudsey, C.J., 2004. Continental slope morphology and sedimentary processes at the mouth of an Antarctic palaeo-ice stream. Marine Geology, 204(1-2): 203-214.
Dowdeswell, J.A., Evans, J., Ó Cofaigh, C. and Anderson, J.B., 2006. Morphology and sedimentary processes on the continental slope off Pine Island Bay, Amundsen Sea, West Antarctica. Geological Society of America Bulletin, 118(5-6): 606-619.
Drago, E.C. and Amsler, M.L., 1998. Suspended sediment at a cross section of the Middle Parana River: concentration, granulometry and influence of the main tributaries. In: M.P. Bordas and D.E. Walling (Editors), Sediment budgets. IAHS Publication, 174, Wallingford, pp. 381-396.
Ducassou, E., Mulder, T., Migeon, S., Gonthier, E., Murat, A., Revel, M., Capotondi, L., Bernasconi, S.M., Mascle, J. and Zaragosi, S., 2008. Nile floods recorded in deep Mediterranean sediments. Quaternary Research, 70(3): 382-391.

Einsele, G. and Seilacher, A., 1991. Distinction of tempestites and turbidites. In: G. Einsele, W. Ricken and A. Seilacher (Editors), Cycles and events in stratigraphy. Springer Verlag, Berlin, Heidelberg, New York, pp. 377-382.
Einsele, G., 1996. Event deposits: the role of sediment supply and relative sea-level changes - overview. Sedimentary Geology, 104(1-4): 11-37.
Ellwood, B.B., 1993. Magnetic properties of Argentine Basin Project MUDWAVE samples. Deep Sea Research Part II, 40(4/5): 921-937.
Esteves, L.S., Toldo, E.E., Dillenburg, S.R. and Tomazelli, L.J., 2002. Long- and short-term coastal erosion in southern Brazil. Journal of Coastal Research, Special Issue 36(ICS 2002 Proceedings): 273-282.
Ewing, M., Ludwig, W.J. and Ewing, J.I., 1964. Sediment distribution in the oceans: the Argentine Basin. Journal of Geophysical Research, 69(10): 2003-2032.
Ewing, M., 1965. The sediments of the Argentine Basin (Harold Jeffreys Lecture). Quarterly Journal of the Royal Astronomical Society, 6: 10-27.
Ewing, M., Eittreim, S.L., Ewing, J.I. and Le Pichon, X., 1971. Sediment transport and distribution in the Argentine Basin. 3. Nepheloid layer and processes of sedimentation. Physics and Chemistry of the Earth, 8: 49-77.
Ewing, M. and Lonardi, A.G., 1971. Sediment transport and distribution in the Argentine Basin. 5. Sedimentary structure of the Argentine margin, basin, and related provinces. Physics and Chemistry of the Earth, 8: 123-251.
Farinati, E.A., 1985. Radiocarbon dating of Holocene marine deposits, Bahía Blanca area, Buenos Aires province, Argentina. In: J. Rabassa (Editor), Quaternary of South America and Antarctic peninsula. A. A. Balkema, 3, Rotterdam, Boston, pp. 197-206.
Faugères, J.-C., Gonthier, E. and Stow, D.A.V., 1984. Contourite drift molded by deep Mediterranian outflow. Geology, 12(5): 296-300.
Faugères, J.-C. and Stow, D.A.V., 1993. Bottom-current-controlled sedimentation: a synthesis of the contourite problem. Sedimentary Geology, 82(1-4): 287-297.
Faugères, J.-C., Mézerais, M.L. and Stow, D.A.V., 1993. Contourite drift types and their distribution in the North and South Atlantic Ocean basins. Sedimentary Geology, 82(1-4): 189-203.
Figueiredo, A.G., 1980. Response of water column to strong wind forcing, southern Brazilian inner shelf: Implications for sand ridge formation. Marine Geology, 35(4): 367-376.
Figueiredo, A.G., Sanders, J.E. and Swift, D.J.P., 1982. Storm-graded layers on inner continental shelves: Examples from southern Brazil and the Atlantic coast of the Central United States. Sedimentary Geology, 31(3-4): 171-190.
Flood, R.D., Shor, A. and Manley, P.L., 1993. Morphology of abyssal mudwaves at Project MUDWAVES sites in the Argentine Basin. Deep Sea Research Part II: Topical Studies in Oceanography, 40(4/5): 859-888.
Framinan, M.B. and Brown, O.B., 1996. Study of the Río de la Plata turbidity front, Part 1: spatial and temporal distribution. Continental Shelf Research, 16(10): 1259-1282.
Franke, D., Neben, S., Ladage, S., Schreckenberger, B. and Hinz, K., 2007. Margin segmentation and volcano-tectonic architecture along the volcanic margin off Argentina/Uruguay, South Atlantic. Marine Geology, 244(1-4): 46-67.

Fray, C. and Ewing, M., 1963. Pleistocene sedimentation and fauna of the Argentine shelf: I. Wisconsin sea level as indicated in Argentine continental shelf sediments. Proceedings of the Academy of Natural Sciences of Philadelphia, 115: 113-126.

Frenz, M., Höppner, R., Stuut, J.-B.W., Wagner, T. and Henrich, R., 2003. Surface sediment bulk geochemistry and grain size composition related to the oceanic circulation along the South American continental margin in the southwest Atlantic. In: G. Wefer, S. Mulitza and V. Ratmeyer (Editors), The South Atlantic in the Late Quaternary: reconstruction of material budgets and current systems. Springer Verlag, Berlin, Heidelberg, pp. 347-373.

Friedrichs, C.T., 2004. Gravity-driven sediment transport on the continental shelf: implications for equilibrium profiles near river mouths. Coastal Engineering, 51(8-9): 795-811.

Gaiero, D.M., Probst, J.-L., Depetris, P.J., Bidart, S.M. and Leleyter, L., 2003. Iron and other transition metals in Patagonian riverborne and windborne materials: geochemical control and transport to the southern South Atlantic Ocean. Geochimica et Cosmochimica Acta, 67(19): 3603-3623.

Gaiero, D.M., Brunet, F., Probst, J.-L. and Depetris, P.J., 2007. A uniform isotopic and chemical signature of dust exported from Patagonia: Rock sources and occurrence in southern environments. Chemical Geology, 238(1-2): 107-120.

Gan, M.A., Kousky, V.E. and Ropelewaki, C.F., 2004. The South America monsoon circulation and its relationship to rainfall over west-central Brazil. Journal of Climate, 17(1): 47-66.

Garcia, N.O. and Vargas, W.M., 1996. The spatial variability of runoff and precipitation in the Rio de la Plata basin. Hydrological Sciences Journal, 41(3): 279-299.

Gauley, B.-J.L., 2001. Lithostratigraphy and sediment failure on the central Scotian slope. M. Sc. Thesis, Dalhousie University, Halifax, 214 pp.

Gilberto, D.A., Bremec, C.S., Acha, E.M. and Mianzán, H.W., 2004. Large-scale spatial patterns of benthic assemblages in the SW Atlantic: the Río de la Plata estuary and adjacent shelf waters. Estuarine, Coastal and Shelf Science, 61(1): 1-13.

Gipp, M.R. and Piper, D.J.W., 1989. Chronology of Late Wisconsin glaciation, Emerald Basin, Scotian Shelf. Canadian Journal of Earth Sciences, 26: 333-335.

Gipp, M.R., 1994. Late Wisconsinan deglaciation of Emerald Basin, Scotian Shelf. Canadian Journal of Earth Sciences, 31(3): 554-566.

Gómez, E.A. and Perillo, G.M.E., 1991. Submarine outcrops underneath shoreface-connected sand ridges, outer Bahía Blanca estuary, Argentina. In: J. Rabassa (Editor), Quaternary of South America and Antarctic Peninsula. A. A. Balkema, 9, Rotterdam, Boston, pp. 23-37.

Gonthier, E., Faugères, J.-C. and Stow, D.A.V., 1984. Contourite facies of the Faro Drift, Gulf of Cadiz. In: D.A.V. Stow and D.J.W. Piper (Editors), Fine grained sediments: deep water processes and facies. Geological Society, Special Publication 15, London, pp. 275-292.

Gordon, A.L. and Greengrove, C.L., 1986. Geostrophic circulation of the Brazil-Falkland confluence. Deep Sea Research Part I: Oceanographic Research Papers, 33(5): 573-585.

Grimm, A.M., 2003. The El Niño impact on the summer monsoon in Brazil: regional processes versus remote influences. Journal of Climate, 16(2): 263-280.

Groot, J.J. and Groot, C.R., 1966. Pollen spectra from deep-sea sediments as indicators of climatic changes in southern South America. Marine Geology, 4(6): 525-537.
Groot, J.J., Groot, C.R., Ewing, M., Burckle, L. and Conolly, J.R., 1967. Spores, pollen, diatoms and provenance of the Argentine Basin sediments. In: M. Sears (Editor), Progress in Oceanography, Volume 4. Pergamon Press, pp. 179-217.
Gross, G.M., 1972. Oceanography: A View of the Earth. Prentice-Hall, Inc., Englewood Cliffs.
Guerrero, R.A. and Piola, A.R., 1997. Masas de agua en la plataforma continental. In: E.E. Boschi (Editor), Antecedentes históricos de las exploraciones en el mar y las características ambientales. Instituto Nacional de Investigación y Desarrollo Pesquero (INIDEP), Mar del Plata, pp. 107-118.
Guerrero, R.A., Acha, E.M., Framinan, M.B. and Lasta, C.A., 1997. Physical oceanography of the Río de la Plata Estuary, Argentina Continental Shelf Research, 17(7): 727-742.
Guilderson, T.P., Burckle, L., Hemming, S.R. and Peltier, W.R., 2000. Late Pleistocene sea level variations derived from the Argentine Shelf. Geochemistry, Geophysics, Geosystems, 1(12): 1055.
Hampton, M.A., Lee, H.J. and Locat, J., 1996. Submarine landslides. Reviews of Geophysics, 34(1): 33-59.
Han, G., 2004. Scotian Slope circulation and eddy variability from TOPEX//Poseidon and frontal analysis data. Journal of Geophysical Research, 109: C03028.
Hart, B.S., Prior, D.B., Barrie, J.V., Curry, R.G. and Luternauer, J.L., 1992. A river mouth submarine channel and failure complex, Fraser Delta, Canada. Sedimentary Geology, 81(1-2): 73-87.
Haughton, P.D.W., Davis, C., McCaffrey, W.D. and Barker, S., 2009. Hybrid sediment gravity flow deposits – Classification, origin and significance. Marine and Petroleum Geology, 26(10): 1900-1918.
Hemming, S.R., Van de Flierdt, T., Goldstein, S.L., Franzese, A.M., Roy, M., Gastineau, G. and Landrot, G., 2007. Strontium isotope tracing of terrigenous sediment dispersal in the Antarctic Circumpolar Current: Implications for constraining frontal positions. Geochemistry, Geophysics, Geosystems, 8: Q06N13.
Henrich, R., Hanebuth, T.J.J., Krastel, S., Neubert, N. and Wynn, R.B., 2008. Architecture and sediment dynamics of the Mauritania Slide Complex. Marine and Petroleum Geology, 25(1): 17-33.
Henrich, R., Cherubini, Y. and Meggers, H., 2010. Climate and sea level induced turbidite activity in a canyon system offshore the hyperarid Western Sahara (Mauritania): the Timiris Canyon. Marine Geology, 275(1-4): 178-198.
Hensen, C., Zabel, M. and Schulz, H.D., 2000. A comparison of benthic nutrient fluxes from deep-sea sediments off Namibia and Argentina. Deep Sea Research Part II, 47(9-11): 2029-2050.
Hensen, C., Zabel, M., Pfeifer, K., Schwenk, T., Kasten, S., Riedinger, N., Schulz, H.D. and Boetius, A., 2003. Control of sulfate pore-water profiles by sedimentary events and the significance of anaerobic oxidation of methane for the burial of sulfur in marine sediments. Geochimica et Cosmochimica Acta, 67(14): 2631-2647.

Héquette, A. and Hill, P.R., 1995. Response of the seabed to storm-generated combined flows on a sandy Arctic shoreface, Canadian Beaufort Sea. Journal of Sedimentary Research, 65(3a): 461-471.
Héquette, A., Desrosiers, M., Hill, P.R. and Forbes, D.L., 2001. The influence of coastal morphology on shoreface sediment transport under storm-combined flows, Canadian Beaufort Sea. Journal of Coastal Research, 17(3): 507-516.
Hernández-Molina, F.J., Llave, E., Stow, D.A.V., García, M., Somoza, L., Vázquez, J.T., Lobo, F.J., Maestro, A., Dias-del-Rio, V., León, R., Medialdea, T. and Gardner, J., 2006. The contourite depositional system of the Gulf of Cádiz: A sedimentary model related to the bottom current activity of the Mediterranean outflow water and its interaction with the continental margin. Deep Sea Research Part II: Topical Studies in Oceanography, 53(11-13): 1420-1463.
Hernández-Molina, F.J., Malodonado, A. and Stow, D.A.V., 2008a. Abyssal plain contourites. In: M. Rebesco and A. Camerlenghi (Editors), Developments in Sedimentology 60. Elsevier, pp. 347-378.
Hernández-Molina, F.J., Llave, E. and Stow, D.A.V., 2008b. Continental slope contourites. In: M. Rebesco and A. Camerlenghi (Editors), Developments in Sedimentology 60. Elsevier, pp. 379-408.
Hernández-Molina, F.J., Paterlini, M., Violante, R.A., Marshall, P., de Isasi, M., Somoza, L. and Rebesco, M., 2009. Contourite depositional system on the Argentine slope: an exceptional record of the influence of Antarctic water masses. Geology, 37(6): 507-510.
Hernández-Molina, F.J., Paterlini, C.M., Somoza, L., Violante, R.A., Arecco, M.A., de Isasi, M., Rebesco, M., Uenzelmann-Neben, G. and Mashall, P., 2010. Giant mounded drifts in the Argentine Continental Margin: Origins, and global implications for the history of thermohaline circulation. Marine and Petroleum Geology, 27(7): 1508-1530.
Hesse, R., Klauck, I., Khodabakhsh, S. and Piper, D.J.W., 1999. Continental slope sedimentation adjacent to an ice margin. III. The upper Labrador Slope. Marine Geology, 155(3-4): 249-276.
Hesse, R. and Khodabakhsh, S., 2006. Significance of fine-grained sediment lofting from melt-water generated turbidity currents for the timing of glaciomarine sediment transport into the deep sea. Sedimentary Geology, 186(1-2): 1-11.
Hieke, W., 2000. Transparent layers in seismic reflection records from the central Ionian Sea (Mediterranean)—evidence for repeated catastrophic turbidite sedimentation during the Quaternary. Sedimentary Geology, 135(1-4): 89-98.
Hill, P.R., 1983. Detailed morphology of a small area on the Nova Scotian continental slope. Marine Geology, 53(1-2): 55-76.
Hill, P.R., 1984a. Facies and sequence analysis of Nova Scotian slope muds: turbidites vs 'hemipelagic' deposition. In: D.A.V. Stow and D.J.W. Piper (Editors), Fine grained sediments: deep water processes and facies. Geological Society, Special Publication 15, London, pp. 311-318.
Hill, P.R., 1984b. Sedimentary facies of the Nova Scotian upper and middle continental slope, offshore eastern Canada. Sedimentology, 31(3): 293-309.
Hjelstuen, B.O., Sejrup, H.P., Haflidason, H., Nygård, A., Berstad, I.M. and Knorr, G., 2004. Late Quaternary seismic stratigraphy and geological development of the

south Vøring margin, Norwegian Sea. Quaternary Science Reviews, 23(16-17): 1847-1865.
Hogg, N.G., 1983. A note on the deep circulation of the western North Atlantic: its nature and causes. Deep Sea Research Part A. Oceanographic Research Papers, 30(9): 945-961.
Horn, D.R., Ewing, M., Horn, B.M. and Delach, M.N., 1971. Turbidites of the Hatteras and Sohm Abyssal Plains, western North Atlantic. Marine Geology, 11(5): 287-323.
Howe, J.A., 1995. Sedimentary processes and variations in slope-current activity during the last Glacial-Interglacial episode on the Hebrides Slope, northern Rockall Trough, North Atlantic Ocean. Sedimentary Geology, 96(3-4): 201-230.
Hughes Clarke, J.E., O'Leary, D.W. and Piper, D.J.W., 1992. The relative importance of mass wasting and deep boundary current activity on the continental rise off western Nova Scotia. In: C.W. Poag and P.C. de Graciansky (Editors), Geologic evolution of Atlantic continental rises. van Nostrand Reinhold, New York, pp. 266-281.
Hundert, T. and Piper, D.J.W., 2008. Late Quaternary sedimentation on the southwestern Scotian Slope, eastern Canada: relationship to glaciation. Canadian Journal of Earth Sciences, 45(3): 267-285.
Huppertz, T.J., 2007. Late Quaternary history of Flemish Pass, southeast Canadian continental margin. M.Sc. Thesis, Dalhousie University, Halifax, 124 pp.
Huppertz, T.J. and Piper, D.J.W., 2009. The influence of shelf-crossing glaciation on continental slope sedimentation, Flemish Pass, eastern Canadian continental margin. Marine Geology, 265(1-2): 67-85.
Huppertz, T.J., Piper, D.J.W., Mosher, D.C. and Jenner, K.A., 2009. The significance of mass transport deposits for the evolution of a proglacial continental slope. In: D.C. Mosher, C.R. Shipp, L. Moscardelli, J.D. Chaytor, C.D.P. Baxter, H.J. Lee and R. Urgeles (Editors), Submarine mass movements and their consequences IV. Springer Verlag, Dordrect, Heidelberg, London, New York, pp. 631-641.
Huppertz, T.J. and Piper, D.J.W., 2010. Interbedded Late Quaternary turbidites and contourites in Flemish Pass, off southeast Canada: their recognition, origin and temporal variation. Sedimentary Geology, 228(1-2): 46-60.
Huppertz, T.J. and Piper, D.J.W., in preparation. Scotian slope seismic stratigraphy and failure history. Marine and Petroleum Geology.
Huppertz, T.J. and Piper, D.J.W., submitted. Scotian slope seismic stratigraphy and failure history. Marine and Petroleum Geology.
Husebyea, E.S. and Mäntyniemib, P., 2005. The Kaliningrad, West Russia earthquakes on the 21st of September 2004 - Surprise events in a very low-seismicity area. Physics of the Earth and Planetary Interiors, 153(4): 227-236.
Iriondo, M.H. and Garcia, N.O., 1993. Climatic variations in the Argentine plains during the last 18,000 years. Palaeogeography, Palaeoclimatology, Palaeoecology, 101: 209-220.
Iriondo, M.H., 2004. The littoral complex at the Paraná mouth. Quaternary International, 114(1): 143-154.
Iriondo, M.H., 2007. Geomorphology. In: M.H. Iriondo, J.C. Paggi and A.R. Paira (Editors), The Middle Paraná River: Limnology of a Subtropical Wetland. Springer Verlag, Berlin, Heidelberg, pp. 33-52.

Iriondo, M.H. and Paira, A.R., 2007. Physical geography of the basin. In: M.H. Iriondo, J.C. Paggi and A.R. Paira (Editors), The Middle Paraná River: Limnology of a Subtropical Wetland. Springer Verlag, Berlin, Heidelberg, pp. 7-31.
Isla, F.I., Cortizo, L.C. and Schnack, E.J., 1996. Pleistocene and Holocene beaches and estuaries along the southern barrier of Buenos Aires, Argentina. Quaternary Science Reviews, 15(8-9): 833-841.
Isla, F.I., 1998. Holocene coastal evolution of Buenos Aires. In: J. Rabassa (Editor), Quaternary of South America and Antarctic Peninsula. A. A. Balkema, 11, Rotterdam, Boston, pp. 297-321.
Isla, F.I. and Schnack, E.J., 2009. The changing coastlines of South America. In: E.M. Latrubesse (Editor), Natural Hazards and Human-Exacerbated Disasters in Latin America. Elsevier, 13, Amsterdam, pp. 49-73.
Jackson, J.M., 1985. Uruguay. In: M.L. Schwartz and E.C.F. Bird (Editors), The world's coastline. van Nostrand Reinhold, New York, pp. 79-84.
Jenner, K.A., Piper, D.J.W., Campbell, D.C. and Mosher, D.C., 2007. Lithofacies and origin of Late Quaternary mass transport deposits in submarine canyons, central Scotian Slope, Canada. Sedimentology, 54(1): 19-38.
Jenner, K.A., Piper, D.J.W., Campbell, C.D. and Mosher, D.C., 2010. Piston cores and supporting high-resolution seismic data, Scotian Slope, Eastern Canada: data and interpretations. Open File 6558, Geological Survey of Canada, Ottawa.
Johnson, G.L., Sommerhoff, G. and Egloff, J., 1975. Structure and morphology of the West Reykjanes Basin and the southeast Greenland continental margin. Marine Geology, 18(4): 175-196.
Kaiser, J. and Lamy, F., 2010. Links between Patagonian Ice Sheet fluctuations and Antarctic dust variability during the last glacial period (MIS 4-2). Quaternary Science Reviews, 29(11-12): 1464-1471.
Keigwin, L.D., Rio, D. and Acton, G.D., 1997. LEG 172 Preliminary Report. Preliminary Report No. 72, Ocean Drilling Program, College Station TX.
Keigwin, L.D., 2001. 9. Data report: Late Pleistocene stable isotope studies of ODP sites 1054, 1055 and 1063. In: L.D. Keigwin, D. Rio, G.D. Acton and E. Arnold (Editors), Proceedings of the Ocean Drilling Program, Scientific Results. Ocean Drilling Program, Volume 172, College Station, TX, pp. 1-14.
King, E.L., Sejrup, H.P., Haflidason, H., Elverhøi, A. and Aarseth, I., 1996. Quaternary seismic stratigraphy of the North Sea Fan: glacially-fed gravity flow aprons, hemipelagic sediments, and large submarine slides. Marine Geology, 130(3-4): 293-315.
King, E.L., Haflidason, H., Sejrup, H.P. and Løvlie, R., 1998. Glacigenic debris flows on the North Sea Trough Mouth Fan during ice stream maxima. Marine Geology, 152(1-3): 217-246.
King, E.L., 2001. A glacial origin for Sable Island: ice and sea-level fluctuations from seismic stratigraphy on Sable Island Bank, Scotian Shelf, offshore Nova Scotia. Current research 2001-D19, Geological Survey of Canada, Ottawa.
King, L.H. and Fader, G.B.J., 1986. Wisconsin glaciation of the Atlantic continental shelf of southeast Canada. Bulletin 363, Geological Survey of Canada, Ottawa.
King, L.H., Rokoengen, K., Fader, G.B.J. and Gunleiksrud, T., 1991. Till-tongue stratigraphy. Geological Society of America Bulletin, 103(5): 637-659.

King, L.H., 1993. Till in the marine environment. Journal of Quaternary Science, 8(4): 347-358.
King, L.H., 1996. Late Wisconsinan ice retreat from the Scotian Shelf. Geological Society of America Bulletin, 108(8): 1056-1067.
Krinsley, D., Biscaye, P.E. and Turekian, K.K., 1973. Argentine Basin sediment sources as indicated by quartz surface textures. Journal of Sedimentary Petrology, 43(1): 251-257.
Kuenen, P.H. and Menard, H.W., 1952. Turbidity currents, graded and non-graded deposits. Journal of Sedimentary Petrology, 22(2): 83-96.
Kuvaas, B., Kristoffersen, Y., Guseva, J., Leitchenkov, G., Gandjukhin, V. and Kudryavtsev, G., 2004. Input of glaciomarine sediments along the east Antarctic continental margin; depositional processes on the Cosmonaut Sea continental slope and rise and a regional acoustic stratigraphic correlation from 40° W to 80° E. Marine Geophysical Researches, 25(3-4): 247-263.
Laberg, J.S. and Vorren, T.O., 1995. Late Weichselian submarine debris flow deposits on the Bear Island Trough Mouth Fan. Marine Geology, 127(1-4): 45-72.
Laberg, J.S. and Vorren, T.O., 2000. Flow behaviour of the submarine glacigenic debris flows on the Bear Island Trough Mouth Fan, western Barents Sea. Sedimentology, 47(6): 1105-1117.
Laberg, J.S. and Andreassen, K., 2007. Submarine paleo-failure morphology on a glaciated continental margin from 3D seismic data. In: V. Lykousis, D. Sakellariou and J. Locat (Editors), Submarine mass movements and their consequences. Springer Verlag, 3rd International Symposium, Dordrecht, pp. 11-18.
Lambeck, K. and Chappell, J., 2001. Sea level change through the last glacial cycle. Science, 292: 679-686.
Laprida, C., Chapori, N.G., Chiessi, C.M., Violante, R.A., Watanabe, S. and Totah, V., accepted. Middle Pleistocene sea surface temperature in the Brazil-Malvinas Confluence Zone: Paleoceanographic implications based on planktonic foraminifera. Micropaleontology.
Lastras, G., Acosta, J., Munoz, A. and Canals, M., 2011. Submarine canyon formation and evolution in the Argentine Continental Margin between 44°30'S and 48°S. Geomorphology, 128(3-4): 116-139.
Ledbetter, M.T. and Johnson, D.A., 1976. Increased transport of Antarctic Bottom Water in the Vema Channel during the last ice age. Science, 194(4267): 837-839.
Ledbetter, M.T. and Klaus, A., 1987. Influence of bottom currents on sediment texture and sea-floor morphology in the Argentine Basin. In: P.P.E. Weaver and J. Thomson (Editors), Geology and Geochemistry of Abyssal Plains. Geological Society, Special Publication 31, London, pp. 23-31.
Ledbetter, M.T., 1993. Late Pleistocene to Holocene fluctuations in bottom-current speed in the Argentine Basin mudwave field Deep Sea Research Part II, 40(4/5): 911-920.
Lemmen, D.S., 1990. Glaciomarine sedimentation in Disraeli Fiord, high Arctic Canada. Marine Geology, 94(1-2): 9-22.
Lonardi, A.G. and Ewing, M., 1971. Sediment transport and distribution in the Argentine Basin. 4. Bathymetry of the continental margin, Argentine Basin and other related provinces. Canyons and sources of sediments. Physics and Chemistry of the Earth, 8: 79-121.

Loncke, L., Gaullier, V., Droz, L., Ducassou, E., Migeon, S. and Mascle, J., 2009. Multi-scale slope instabilities along the Nile deep-sea fan, Egyptian margin: A general overview. Marine and Petroleum Geology, 26(5): 633-646.
Lowe, D.R., 1976. Grain flow and grain flow deposits. Journal of Sedimentary Petrology, 46(1): 188-199.
Lowe, D.R., 1982. Sediment gravity flows: II. Depositional models with special reference to the deposits of high density turbidity currents. Journal of Sedimentary Petrology, 52(1): 279-297.
Lowe, D.R. and Guy, M., 2000. Slurry-flow deposits in the Britannia Formation (Lower Cretaceous), North Sea: a new perspective on the turbidity current and debris flow problem. Sedimentology, 47(1): 31-70.
Mahiques, M.M., Tassinardi, C.C.G., Marcolini, S., Violante, R.A., Figueira, R.C.L., da Silveira, I.C.A., Burone, L. and de Mello e Sousa, S.H., 2008. Nd and Pb isotope signatures on the southeastern South American upper margin: Implications for sediment transport and source rocks. Marine Geology, 250(1-2): 51-63.
Manley, P.L. and Flood, R.D., 1993a. Paleoflow history determined from mudwave migration: Argentine Basin. Deep-Sea Research II, 40(4/5): 1033-1055.
Manley, P.L. and Flood, R.D., 1993b. Project mudwaves. Deep-Sea Research II, 20(4/5): 851-857.
Marchès, E., Mulder, T., Cremer, M., Bonnel, C., Hanquiez, V., Gonthier, E. and Lecroart, P., 2006. Capture of a deep sea current by a canyon in the Gulf of Cadiz (Algarve margin, south Portugal), 5th symposium on the Iberian Atlantic Margin, Aveiro.
Marchès, E., Mulder, T., Cremer, M., Bonnel, C., Hanquiez, V., Gonthier, E. and Lecroart, P., 2007. Contourite drift construction influenced by capture of Mediterranean Outflow Water deep-sea current by the Portimão submarine canyon (Gulf of Cadiz, South Portugal). Marine Geology, 242(4): 247-260.
Marchès, E., Mulder, T., Gonthier, E., Cremer, M., Hanquiez, V., Garlan, T. and Lecroart, P., 2010. Perched lobe formation in the Gulf of Cadiz: Interactions between gravity processes and contour currents (Algarve Margin, Southern Portugal). Sedimentary Geology, 229(3): 81-94.
Marchitto, T.M. and Broecker, W.S., 2006. Deep water mass geometry in the glacial Atlantic Ocean: A review of constraints from the paleonutrient proxy Cd/Ca. Geochemistry, Geophysics, Geosystems, 7: Q12003.
Martín-Chivelet, J., Fregenal-Martínez, M.A. and Chacón, B., 2008. Traction structures in contourites. In: M. Rebesco and A. Camerlenghi (Editors), Developments in Sedimentology 60. Elsevier, pp. 159-182.
Martin, L. and Suguio, K., 1992. Variation of coastal dynamics during the last 7000 years recorded in beach-ridge plains associated with river mouths: example from the central Brazilian coast. Palaeogeography, Palaeoclimatology, Palaeoecology, 99(1-2): 119-140.
Martins, L.R. and Willwock, J.A., 1987. Eastern South America Quaternary coastal and marine geology: a synthesis, Quaternary coastal geology of Western Africa and South America. Unesco Reports in Marine Sciences, 43, Dakar, pp. 28-96.
Martins, L.R. and Correa, I.C.S., 1996. Atlas morphology and sedimentology of the southwest Atlantic coastal zone and continental shelf from Cabo Frio (Brazil) and

Peninsula Valdés (Argentina), Universidade Federal do Rio Grande do Sul, Rio Grande do Sul.
Martins, L.R., Martins, I.R. and Urien, C.M., 2003. Aspectos sedimentares da plataforma continental na área de influência do Rio de la Plata. Gravel, 1: 68-80.
Martins, L.R. and Urien, C.M., 2004. Areias da plataforma e a erosão costeira. Gravel, 2: 4-24.
Martins, L.R., Urien, C.M. and Martins, I.R., 2005a. Gênese dos sedimentos da plataforma continental Atlântica entre o Rio Grande do Sul (Brasil) e Tierra del Fuego (Argentina). Gravel, 3: 85-102.
Martins, L.R., Martins, I.R. and Urien, C.M., 2005b. Sand bodies of the Santa Catarina inner continental shelf, Brazil. Gravel, 3: 103-108.
Martins, L.R., Martins, I.R. and Martins, R.R., 2005c. Utilização de testemunhador livre na região dos Poços de Lama. Gravel, 3: 1-8.
Maslin, M.A., Owen, M., Day, S. and Long, D., 2004. Linking continental-slope failures and climate change: Testing the clathrate gun hypothesis. Geology, 32(1): 53-56.
Maslin, M.A. and Ridgwell, A.J., 2005. Mid-Pleistocene revolution and the 'eccentricity myth'. In: M.J. Head and P.L. Gibbard (Editors), Early-Middle Pleistocene transitions: the land-ocean evidence. Geological Society, Special Publication 247, London, pp. 19-34.
Matsumoto, K., 1997. Modeled glacial North Atlantic ice-rafted debris pattern and its sensitivity to various boundary conditions. Paleoceanography, 12(2): 271-280.
McCave, I.N., 1985. Sedimentology and stratigraphy of box cores from the HEBBLE site on the Nova Scotian continental rise. Marine Geology, 66(1-4): 59-89.
McHugh, C.M.G., Damuth, J.E. and Mountain, G.S., 2002. Cenozoic mass-transport facies and their correlation with relative sea-level change, New Jersey continental margin. Marine Geology, 184(3-4): 295-334.
Mémery, L., Arhan, M., Alvarez-Salgado, X.A., Mercier, H., Castro, C.G. and Rios, A.F., 2000. The water masses along the western boundary of the south and equatorial Atlantic. Progress In Oceanography, 47(1): 69-98.
Middleton, G. and Hampton, M.A., 1973. Sediment gravity flows: mechanics of flow and deposition. In: G. Middleton and A.H. Bouma (Editors), Turbidites and deep water sedimentation. Pacific Section S. E. P. M., Short Course 1, Los Angeles, pp. 1-38.
Middleton, G.V. and Hampton, M.A., 1976. Subaqueous sediment transport and deposition by sediment gravity flows. In: D.J. Stanley and D.J.P. Swift (Editors), Marine sediment transport and environmental management. Wiley & sons, New York, London, Toronto, Sidney, pp. 197-218.
Middleton, G.V. and Neal, W.J., 1989. Experiments on the thickness of beds deposited by turbidity currents Journal of Sedimentary Research, 59(2): 297-307.
Middleton, G.V., 1993. Sediment deposition from turbidity currents. Annual Review of Earth and Planetary Sciences, 21: 89-114.
Mienert, J., Berndt, C., Laberg, J.S. and Vorren, T.O., 2002. Slope instability of continental margins. In: G. Wefer, D. Billett, D. Hebbeln, B.B. Jorgensen, M. Schlüter and T.C.E. van Weering (Editors), Ocean Margin Systems. Springer, Berlin, Heidelberg, pp. 179-193.
Migeon, S., Ducassou, E., Le Gonidec, Y., Rouillard, P., Mascle, J. and Revel-Rolland, M., 2010. Lobe construction and sand/mud segregation by turbidity currents and

debris flows on the western Nile deep-sea fan (Eastern Mediterranean). Sedimentary Geology, 229(3): 124-143.
Möller, O.O., Piola, A.R., Freitas, A.C. and Campos, E.J.D., 2008. The effects of river discharge and seasonal winds on the shelf off southeastern South America. Continental Shelf Research, 28(13): 1607-1624.
Mosher, D.C., Piper, D.J.W., Vilks, G.V., Aksu, A.E. and Fader, G.B.J., 1989. Evidence for Wisconsinan glaciation in the Verill canyon area, Scotian slope. Quaternary Research, 31(1): 27-40.
Mosher, D.C., Moran, K. and Hiscott, R.N., 1994. Late Quaternary sediment, sediment mass flow processes and slope stability on the Scotian slope, Canada. Sedimentology, 41(5): 1039-1061.
Mosher, D.C. and Simpkin, P.G., 1999. Environmental marine geosciences 1: status and trends of marine high-resolution seismic reflection profiling: data acquisition. Geoscience Canada, 26(4): 174-188.
Mosher, D.C., Piper, D.J.W., Campbell, D.C. and Jenner, K.A., 2004. Near-surface geology and sediment-failure geohazards of the central Scotian Slope. AAPG Bulletin, 88(6): 703-723.
Mosher, D.C. and Piper, D.J.W., 2007a. Analysis of multibeam seafloor imagery of the Laurentian Fan and the 1929 Grand Banks landslide area. In: V. Lykousis, D. Sakellariou and J. Locat (Editors), Submarine mass movements and their consequences. Springer Verlag, Dordrecht, pp. 77-88.
Mosher, D.C. and Piper, D.J.W., 2007b. Multibeam seafloor imagery of the Laurentian Fan and the 1929 Grand Banks landslide area. Open File 5638, Geological Survey of Canada, Ottawa.
Mosher, D.C., Xu, Z. and Shimeld, J., 2009. The Pliocene Shelburne mass-movement and consequent tsunami, western Scotian slope. In: D.C. Mosher, C.R. Shipp, L. Moscardelli, J.D. Chaytor, C.D.P. Baxter, H.J. Lee and R. Urgeles (Editors), Submarine mass movements and their consequences IV. Springer Verlag, Dordrect, Heidelberg, London, New York, pp. 765-775.
Mulder, T. and Moran, K., 1995. Relationship among submarine instabilities, sea level variations, and the presence of an ice sheet on the continental shelf: An example from the Verrill Canyon Area, Scotian Shelf. Paleoceanography, 10(1): 137-154.
Mulder, T. and Syvitski, J.P.M., 1995. Turbidity currents generated at river mouths during exceptional discharges to the world oceans. Journal of Geology, 103(3): 285-299.
Mulder, T., Migeon, S., Savoye, B. and Faugères, J.-C., 2001. Inversely graded turbidite sequences in the deep Mediterranean: a record of deposits from flood-generated turbidity currents? Geo-Marine Letters, 21(2): 86-93.
Mulder, T., Syvitski, J.P.M., Migeon, S., Faugères, J.-C. and Savoye, B., 2003. Marine hyperpycnal flows: initiation, behavior and related deposits. A review. Marine and Petroleum Geology, 20(6-8): 861-882.
Mulder, T., Lecroart, P., Hanquiez, V., Marches, E., Gonthier, E., Guedes, J.-C., Thiébot, E., Jaaidi, B., Kenyon, N.H., Voisset, M., Perez, C., Sayago, M., Fuchey, Y. and Bujan, S., 2006. The western part of the Gulf of Cadiz: contour currents and turbidity currents interactions. Geo-Marine Letters, 26(1): 31-41.

Mulder, T., Faugères, J.-C. and Gonthier, E., 2008. Mixed turbidite–contourite systems. In: M. Rebesco and A. Camerlenghi (Editors), Developments in Sedimentology 60. Elsevier, pp. 435-456.
Myrow, P.M. and Southard, J.B., 1996. Tempestite deposition. Journal of Sedimentary Research, 66(5): 875-887.
National Geographic Society; Cartographic Division, 1990. World ocean floors [cartographic material] / produced by the Cartographic Division, National Geographic Society ; John B. Garver Jr., chief cartographer ; painting by Tibor G. Toth ; design, Allen Caroll. In: A. Carroll, J.B. Garver and T.G. Toth (Editors). The Society, Washington, D.C. .
Niedoroda, A.W., Reed, C., Das, H., Hatchett, L. and Perlet, A.B., 2006. Controls of the behaviour of marine debris flows. Norwegian Journal of Geology (Norsk Tidsskrift), 86(3): 256-274.
Niedoroda, A.W., Reed, C.W., Das, H. and Hatchett, L., 2007. The general behavior of mass gravity flows in the marine environment. In: V. Lykousis, D. Sakellariou and J. Locat (Editors), Submarine mass movements and their consequences. Springer Verlag, 3rd International Symposium, Dordrecht, pp. 111-118.
Nittrouer, C.A., Austin, J.A., Field, M.E., Kravitz, J.H., Syvitski, J.P.M. and Wiberg, P.L., 2007. Writing a Rosetta stone: insights into continental-margin sedimentary processes and strata. In: C.A. Nittrouer, J.A. Austin, M.E. Field, J.H. Kravitz, J.P.M. Syvitski and P.L. Wiberg (Editors), Continental margin sedimentation: from sediment transport to sequence stratigraphy. Blackwell Publishing, Oxford, UK, pp. 1-48.
Normark, W.R., Piper, D.J.W. and Stow, D.A.V., 1983. Quaternary development of channels, levees, and lobes on middle Laurentian Fan. AAPG Bulletin, 67(9): 1400-1409.
Normark, W.R. and Piper, D.J.W., 1991. Initiation processes and flow evolution of turbidity currents: implications for the depositional record. SEPM Special Publication, 46: 207-230.
Nygard, A., Sejrup, H.P., Haflidason, H. and King, E.L., 2002. Geometry and genesis of glacigenic debris fows on the North Sea Fan: TOBI imagery and deep-tow boomer evidence. Marine Geology, 188(1-2): 15-33.
O'Connor, W.P., 1991. A numerical model of tides and storm surges in the Rio de la Plata Estuary. Continental Shelf Research, 11(12): 1491-1508.
Owen, M., Day, S. and Maslin, M., 2007. Late Pleistocene submarine mass movements: occurrence and causes. Quaternary Science Reviews, 26(7-8): 958-978.
Palma, E.D., Matano, R.P., Piola, A.R. and Sitz, L.E., 2004a. A comparison of the circulation patterns over the southwestern Atlantic shelf driven by different wind stress climatologies. Geophysical Research Letters, 31: L24303.
Palma, E.D., Matano, R.P. and Piola, A.R., 2004b. A numerical study of the southwestern Atlantic shelf circulation: barotropic response to tidal and wind forcing. Journal of Geophysical Research, 109: C08014.
Panario, D. and Gutiérrez, O., 1999. The continental Uruguayan Cenozoic: an overview. Quaternary International, 62(1): 75-84.
Parker, G., Paterlini, C.M. and Violante, R.A., 1994. Edad y génesis del Río de la Plata. Revista de la Asociación Geológica Argentina, 49(1-2): 11-18.

Parker, G., Violante, R.A. and Paterlini, M.C., 1996. Fisiografia de la plataforma continental. In: V.A. Ramos and M.A. Turic (Editors), Geologia y recursos naturales de la plataforma continental Argentina. Asociacion Geologica Argentina, Buenos Aires.

Parker, G., Paterlini, C.M. and Violante, R.A., 1997. El fondo marino. In: E. Boschi (Editor), El Mar Argentino y sus recursos pesqueros, Tomo 1: Antecedentes historicos de las exploraciones en el mar y las caracteristicas ambientaies. Instituto Nacional de Investigación y Desarrollo Pesquero Secretaría de Agricultura, Ganadería, Pesca y Allmentación, Mar del Plata, Argentina, pp. 65-87.

Parker, G., Violante, R.A., Paterlini, C.M., Costa, I.P., Marcolini, S. and Cavallotto, J.L., 2008. Las secuencias depositacionales del plioceno-cuaternario en la plataforma submarina adyacente al litoral del este Bonaerense. Latin American Journal of Sedimentology and Basin Analysis, 15(2): 105-124.

Peltier, W.R. and Drummond, R., 2002. A “broad-shelf effect” upon postglacial relative sea level history. Geophysical Research Letters, 29: 1169.

Pereyra, F.X., Baumann, V., Altinier, V., Ferrer, J. and Tchilinguirian, P., 2004. Génesis de suelos y evolución del paisaje en el delta del río Paraná. Revista de la Asociación Geológica Argentina, 59(2): 229-242.

Perillo, G.M.E. and Sequeira, M.E., 1989. Geomorphologic and sediment transport characteristics of the middle reach of the Bahia Blanca estuary (Argentina). Journal of Geophysical Research, 94(C10): 14351-14362.

Perillo, G.M.E., Piccolo, M.C. and Marcovecchio, J., 2005. Coastal oceanography of the western South Atlantic continental shelf (33 to 55°S). In: A.R. Robinson and K.H. Brink (Editors), The sea. Havard Collage, 14, Boston, pp. 295-327.

Pickerill, R.K., Piper, D.J.W., Collins, J., Kleiner, A. and Gee, L., 2001. Scotian slope mapping project: The benefits of an integrated regional high-resolution multibeam survey, Offshore Technology Conference, Houston, Texas, pp. OTC 12995.

Pierce, J.W. and Siegel, F.R., 1979. Supended particulate matter on the southern Argentine shelf. Marine Geology, 29(1-4): 73-91.

Pierson, T.C., 1981. Dominant particle support mechanisms in debris flows at Mt Thomas, New Zealand, and implications for flow mobility. Sedimentology, 28: 49-60.

Piola, A.R. and Rivas, A.L., 1997. Corrientes en la plataforma continental. In: E. Boschi (Editor), El mar Argentino y sus recursos pesqueros, Volume 1, pp. 119-132.

Piola, A.R., Campos, E.J.D., Möller, O.O., Charo, M. and Martinez, C., 2000. Subtropical shelf front off eastern South America. Journal of Geophysical Research, 105(C3): 6565-6578.

Piola, A.R. and Matano, R.P., 2001. Brazil and Falklands (Malvinas) currents. In: J.H. Steele and S.A. Thorpe (Editors), Encyclopedia of Ocean Sciences. Academic Press, San Diego, pp. 340-349.

Piola, A.R. and Romero, S.I., 2004. Analysis of space-time variability of the Plata river plume. Gayana (Concepción), 68(2): 482-486.

Piola, A.R., Matano, R.P., Palma, E.D., Möller, O.O. and Campos, E.J.D., 2005. The influence of the Plata River discharge on the western South Atlantic shelf. Geophysical Research Letters, 32: L01603.

Piola, A.R., 2006. Antarctic intermediate water. In: B. Riffenburgh (Editor), Encyclopedia of the Antarctic. Routledge, New York, pp. 62-65.
Piola, A.R., Romero, S.I. and Zyjaczkovski, U., 2008a. Space- time variability of the Plata plume inferred from ocean color. Continental Shelf Research, 28(13): 1556-1567.
Piola, A.R., Möller, O.O., Guerrero, R.A. and Campos, E.J.D., 2008b. Variability of the subtropical shelf front off eastern South America: Winter 2003 and summer 2004. Continental Shelf Research, 28(13): 1639-1648.
Piper, D.J.W., Mudie, P.J., Aksu, A.E. and Hill, P.R., 1978. Late Quatenary sedimentation, 50°N, north-east Newfoundland shelf. Géographie physique et Quaternaire, 32(4): 321-332.
Piper, D.J.W., 1978. Turbidite muds and silts on deep sea fans and abyssal plains. In: D.J. Stanley and G. Kelling (Editors), Sedimentation in submarine canyons, fans and trenches. Dowden, Hutchinson & Ross, Inc., Stroudsburg, pp. 163-176.
Piper, D.J.W., Farre, J.A. and Shor, A.N., 1985. Late Quaternary slumps and debris flows on the Scotian Slope. Geological Society of America Bulletin, 96(12): 1508–1517.
Piper, D.J.W., Normark, W.R. and Sparkes, R., 1987. Late Cenozoic stratigraphy of the central Scotian slope, eastern Canada. Bulletin of Canadian Petroleum Geology, 35(1): 1-11.
Piper, D.J.W. and Sparkes, R., 1987. Proglacial sediment instability features on the Scotian Slope at 63°W. Marine Geology, 76: 15-31.
Piper, D.J.W. and Aksu, A.E., 1987. The source and origin of the 1929 Grand Banks turbidity current inferred from sediment budgets. Geo-Marine Letters, 7: 177-182.
Piper, D.J.W. and Normark, W.R., 1989. Late Cenozoic sea-level changes and the onset of glaciation: impact on continental slope progradation off eastern Canada. Marine and Petroleum Geology, 6(4): 336-347.
Piper, D.J.W. and Sparkes, R., 1990. Pliocene - Quaternary geology of the central Scotian Slope. Open File 2233, Geological Survey of Canada, Ottawa.
Piper, D.J.W. and Fehr, S.D., 1991. Radiocarbon chronology of late Quaternary sections on the inner and middle Scotian Shelf, south of Nova Scotia. Current Research Paper 91-1E, Geological Survey of Canada, Ottawa.
Piper, D.J.W., Mudie, P.J., Aksu, A.E. and Skene, K.I., 1994. A 1 Ma record of sediment flux south of the Grand Banks used to infer the development of glaciation in southeastern Canada. Quaternary Science Reviews, 13(1): 23-37.
Piper, D.J.W. and Deptuck, M., 1997. 5. Fine-grained turbidites of the Amazon Fan: facies characterization and interpretation. In: R.D. Flood, D.J.W. Piper, A. Klaus and L.C. Peterson (Editors), Proceedings of the Ocean Drilling Program, Scientific Results, Volume 155. Ocean Drilling Program, College Station, TX, pp. 79-108.
Piper, D.J.W., Pirmez, C., Manley, P.L., Long, D., Flood, R.D., Normark, W.R. and Showers, W., 1997. 6. Mass transport deposits of the Amazon fan. In: R.D. Flood, D.J.W. Piper, A. Klaus and L.C. Peterson (Editors), Proceedings of the Ocean Drilling Program, Scientific Results, Volume 155, College Station, TX, pp. 109-146.

Piper, D.J.W. and Skene, K.I., 1998. Latest Pleistocene ice-rafting events on the Scotian Margin (eastern Canada) and their relationship to Heinrich events. Paleoceanography, 13(2): 205-214.
Piper, D.J.W., Skene, K.I. and Morash, N., 1999. History of major debris flows on the Scotian Rise, offshore Nova Scotia. Current research 1999-E, Geological Survey of Canada, Ottawa.
Piper, D.J.W., 2000. Pleistocene ice outlets on the central Scotian Slope, offshore Nova Scotia. Current research 2000-D7, Geological Survey of Canada, Dartmouth.
Piper, D.J.W., 2001. The geological framework of sediment instability on the Scotian Slope: studies to 1999. Open File 3920, Geological Survey of Canada, Ottawa.
Piper, D.J.W. and Normark, W.R., 2001. Sandy fans—from Amazon to Hueneme and beyond. AAPG Bulletin, 85(8): 1407-1438.
Piper, D.J.W. and MacDonald, A., 2001. Timing and position of late Wisconsinan ice margins on the upper slope seaward of Laurentian channel. Géographie physique et Quaternaire, 55(2): 131-140.
Piper, D.J.W., Mosher, D.C. and Newton, S., 2002. Ice-margin seismic stratigraphy of the central Scotian Slope, eastern Canada. Current Research 2002-E16, Geological Survey of Canada, Dartmouth.
Piper, D.J.W. and Hundert, T., 2002. Provenance of distal Sohm Abyssal Plain sediments: history of supply from the Wisconsinan glaciation in eastern Canada. Geo-Marine Letters, 22(2): 75-85.
Piper, D.J.W. and Campbell, D.C., 2002. Surficial geology of the Scotian Slope, eastern Canada. Current Research 2002-E15, Geological Survey of Canada, Dartmouth.
Piper, D.J.W., Mosher, D.C., Gauley, B.-J., Jenner, K.A. and Campbell, D.C., 2003. The chronology and recurrence of submarine mass movements on the continental slope off southeastern Canada. In: J. Locat and J. Mienert (Editors), Submarine mass movements and their consequences: First international symposium. Kluwer Academic Publishers, pp. 299-306.
Piper, D.J.W. and Ingram, S., 2003. Major Quaternary sediment failures on the east Scotian Rise, eastern Canada. Current Research 2003-D1, Geological Survey of Canada (Atlantic), Dartmouth.
Piper, D.J.W. and DeWolfe, M., 2003. Petrographic evidence from the eastern Canadian margin of shelf-crossing glaciations. Quaternary International, 99-100: 99-113.
Piper, D.J.W. and McCall, C., 2003. A synthesis of the distribution of submarine mass movements on the eastern Canadian margin. In: J. Locat and J. Mienert (Editors), Submarine mass movements and their consequences: First international symposium. Kluwer Academic Publishers, pp. 291-298.
Piper, D.J.W., Adam, W.A.M., Stephen, I., Williams, G.L. and McCall, C., 2005. Late Cenozoic architecture of the St. Pierre Slope. Canadian Journal of Earth Sciences, 42(11): 1967-1985.
Piper, D.J.W., 2005. Late Cenozoic evolution of the continental margin of eastern Canada. Norwegian Journal of Geology (Norsk Tidsskrift), 85: 305-318.
Piper, D.J.W. and Brunt, R.A., 2006. High-resolution seismic transects of the upper continental slope off southeastern Canada. Open File 5310, Geological Survey of Canada, Ottawa.

Piper, D.J.W., Shaw, J. and Skene, K.I., 2007. Stratigraphic and sedimentological evidence for late Wisconsinan sub-glacial outburst floods to Laurentian Fan. Paleogeography, Paleoclimatology, Paleoecology, 246(1): 101-119.

Piper, D.J.W. and Normark, W.R., 2009. Processes that initiate turbidity currents and their influence on turbidites: a marine geology perspective. Journal of Sedimentary Research, 79(6): 347-362.

Piper, D.J.W., Deptuck, M., Mosher, D.C., Hughes Clarke, J.E. and Migeon, S., 2011. Erosional and depositional features of glacial meltwater discharges on the eastern Canadian continental margin, SEPM Special Publication

Piper, D.J.W. and Normark, W.R., submitted. Journal of Sedimentary Research.

Popescu, I., Lericolais, G., Panin, N., Normand, A., Dinu, C. and Le Drezen, E., 2004. The Danube submarine canyon (Black Sea): morphology and sedimentary processes. Marine Geology, 206(1-4): 249-265

Porebski, S.J., Meischner, D. and Görlich, K., 1991. Quaternary mud turbidites from the South Shetland Trench (West Antarctica): recognition and implications for turbidite facies modelling. Sedimentology, 38(4): 691-715.

Postma, G. and Roep, T.B., 1985. Resedimented conglomerates in the bottomsets of Gilbert-type gravel deltas. Journal of Sedimentary Research, 55(6): 874-885.

Powell, R.D. and Molnia, B.F., 1989. Glacimarine sedimentary processes, facies and morphology of the south-southeast Alaska shelf and fjords. Marine Geology, 85(2-4): 359-390.

Pratson, L.F., Ryan, W.B.F., Mountain, G.S. and Twichell, D.C., 1994. Submarine canyon initiation by downslope-eroding sediment flows: Evidence in late Cenozoic strata on the New Jersey continental slope. Geological Society of America Bulletin, 106(3): 395-412.

Pratson, L.F. and Coakley, B.J., 1996. A model for the headward erosion of submarine canyons induced by downslope-eroding sediment flows. Geological Society of America Bulletin, 108(2): 225-234.

Pratson, L.F. and Haxby, W.F., 1996. What is the slope of the U.S. continental slope? Geology, 24(1): 3-6.

Pratson, L.F., Nittrouer, C.A., Wiberg, P.L., Steckler, M.S., Swenson, J.B., Cacchione, D.A., Karson, J.A., Murray, A.B., Wolinsky, M.A., Gerber, T.P., Mullenbach, B.L., Spinelli, G.A., Fulthorpe, C.S., O'Grady, D.B., Parker, G., Driscoll, N.W., Burger, R.L., Paola, C., Orange, D.L., Field, M.E., Friedrichs, C.T. and Fedele, J.J., 2007. Seascape evolution on clastic continental shelves and slopes. In: C.A. Nittrouer, J.A. Austin, M.E. Field, J.H. Kravitz, J.P.M. Syvitski and P.L. Wiberg (Editors), Continental margin sedimentation: from sediment transport to sequence stratigraphy. Blackwell Publishing, Oxford, UK, pp. 339-380.

Prior, D.B., Coleman, J.L. and Garrison, L.E., 1979. Digitally acquired undistorted side-scan sonar images of submarine landslides, Mississippi River delta. Geology, 7(9): 423-425.

Prior, D.B. and Doyle, E.H., 1985. Intra-slope canyon morphology and its modification by rockfall processes, U.S. Atlantic continental margin. Marine Geology, 67(1-2): 177-196.

Puig, P., Ogston, A.S., Mullenbach, B.L., Nittrouer, C.A. and Sternberg, R.W., 2003. Shelf-to-canyon sediment-transport processes on the Eel continental margin (northern California). Marine Geology, 193(1-2): 129-149.

Puig, P., Palanques, A., Guillen, J. and El Khatab, M., 2004. Role of internal waves in the generation of nepheloid layers on the northwestern Alboran slope: Implications for continental margin shaping. Journal of Geophysical Research, 109: C09011.
Rasmussen, T.L., Oppo, D.W., Thomsen, E. and Lehman, S.J., 2003. Deep sea records from the southeast Labrador Sea: Ocean circulation changes and ice-rafting events during the last 160,000 years. Paleoceanography, 18(1): 1018.
Rebesco, M., Camerlenghi, A., Volpi, V., Neagu, C., Accettella, D., Lindberg, B., Cova, A., Zgur, F. and Magico Party, 2007. Interaction of processes and importance of contourites: insights from the detailed morphology of sediment Drift 7, Antarctica. In: A.R. Viana and M. Rebesco (Editors), Economic and palaeoceanographic significance of contourite deposits. Geological Society, Special Publication 276, London, pp. 95-110.
Reynolds, T., 2000. Reservoir architecture in the Mars field, deepwater Gulf of Mexico, USA: the implications of production, seismic, core and well-log data, GCSSEPM Foundation 20th Annual Research Conference: Deep Water reservoirs of the World, Houston, TX, pp. 877-893.
Riedinger, N., Pfeifer, K., Kasten, S., Garming, J.F.L., Vogt, C. and Hensen, C., 2005. Diagenetic alteration of magnetic signals by anaerobic oxidation of methane related to a change in sedimentation rate. Geochimica et Cosmochimica Acta, 69(16): 4117-4126.
Rise, L., Ottensen, D., Berg, K. and Lundin, E., 2005. Large-scale development of the mid-Norwegian margin during the last 3 million years. Marine and Petroleum Geology, 22(1-2): 33-44.
Rivas, A.L. and Langer, A.F., 1996. Mass and heat transport in the Argentine continental shelf. Continental Shelf Research, 16(10): 1283-1295.
Rivas, A.L., 1997. Current-meter observations in the Argentine continental shelf. Continental Shelf Research, 17(4): 391-406.
Robichaud, M., 2006. Late Quaternary evolution of the Northeast Fan, offshore Nova Scotia. B.Sc. Thesis, Dalhousie University, Halifax, 98 pp.
Rodriguez, A.N. and Anderson, J.B., 2004. Contourite origin for shelf and upper slope sand sheet, offshore Antarctica. Sedimentology, 51(4): 699-711.
Romero, O.E. and Hensen, C., 2002. Oceanographic control of biogenic opal and diatoms in surface sediments of the Southwestern Atlantic. Marine Geology, 186(3-4): 263-280.
Rose, L.E. and Kuehl, S.A., 2010. Recent sedimentation patterns and facies distribution on the Poverty Shelf, New Zealand. Marine Geology, 270(1-4): 160-174.
Rostamini, K., Peltier, W.R. and Mangini, A., 2000. Quaternary marine terraces, sea-level changes and uplift history of Patagonia, Argentina: comparisons with predictions of the ICE-4G (VM2) model of the global process of glacial isostatic adjustment Quaternary Science Reviews, 19(14-15): 1495-1525.
Sadler, P.M., 1982. Bed-thickness and grain size of turbidites. Sedimentology, 29(1): 37-51.
Schaaf, A., 1996. Sea level changes, continental shelf morphology, and global paleoecological constraints in the shallow benthic realm: a theoretical approach. Palaeogeography, Palaeoclimatology, Palaeoecology, 121(3-4): 259-271.

Schlager, W. and Camber, O., 1986. Submarine slope angles, drowning unconformities, and self-erosion of limestone escarpments. Geology, 14(9): 762-765.
Schmid, C., Siedler, G. and Zenk, W., 2000. Dynamics of Intermediate Water Circulation in the subtropical South Atlantic. Journal of Physical Oceanography, 30(12): 3191-3211.
Schnack, E.J., 2009. The vulnerability of the east coast of South America to sea level rise and possible adjustment strategies. In: R.A. Warrick, E.M. Barrow and T.M.L. Wigley (Editors), Climate and sea level change: observations, projections and implications. Cambridge University Press, Cambridge, pp. 336-348.
Schnitker, D., Belknap, D.F., Bacchus, T.S., Friez, J.K., Lusardi, B.A. and Popek, D.M., 2001. Deglaciation of the Gulf of Maine. In: T.K. Weddle and M.J. Retelle (Editors), Deglacial history and relative sea level changes, northern New England and adjacent Canada. Geological Society of America, Special Paper 351, Boulder, pp. 9-34.
Segl, M. and Shipboard Scientific Party, 1994. Meteor Berichte Geo Bremen South Atlantic 1994, Cruise No. 29/1, 17 June - 5 September 1994. 95-2, Leitstelle Meteor, Institut für Meereskunde der Universität Hamburg.
Sejrup, H.P., Larsen, E., Haflidason, H., Berstad, I.M., Hjelstuen, B.O., Jonsdottir, H.E., King, E.L., Landvik, J., Longva, O., Nygård, A., Ottesen, D., Raunholm, S., Rise, L. and Knut, S., 2003. Configuration, history and impact of the Norwegian Channel Ice Stream. Boreas, 32(1): 18-36.
Sejrup, H.P., Hjelstuen, B.O., Dahlgren, K.I.T., Haflidason, H., Kuijpers, A.H., Nygård, A., Praeg, D., Stoker, M.S. and Vorren, T.O., 2005. Pleistocene glacial history of the NW European continental margin. Marine and Petroleum Geology, 22(9-10): 1111-1129.
Shanmugam, G. and Moiola, R.J., 1982. Eustatic control of turbidites and winnowed turbidites. Geology, 10(5): 231-235.
Shanmugam, G., 2008. Deep-water bottom currents and their deposits. In: M. Rebesco and A. Camerlenghi (Editors), Developments in Sedimentology 60. Elsevier, pp. 59-81.
Shaw, J., Piper, D.J.W., Fader, G.B.J., King, E.L., Todd, B.J., Bell, T., Batterson, M.J. and Liverman, D.G.E., 2006. A conceptual model of the deglaciation of Atlantic Canada. Quaternary Science Reviews, 25(17-18): 2059-2081.
Shepard, F.P., 1981. Submarine canyons: multiple causes and long-time persistence. AAPG Bulletin, 65(6): 1062-1077.
Shipboard Scientific Party, 2001. 6. Bermuda Rise and Sohm Abyssal Plain, sites 1063 and 1064. In: L.D. Keigwin, D. Rio, G.D. Acton, G.G. Bianchi, W. Borowski, N. Cagatay, W.P. Chaisson, B.M. Clement, E. Cortijo, G.B. Dunbar, R.D. Flood, S.-O. Franz, L. Giosan, J. Gruetzner, S. Hagen, B. Haskell, M.J. Horowitz, E.P. Laine, S.P. Lund, M. Okada, M.-S. Poli, I. Raffi, M.K. Reuer, Y.G. Ternois, T. Williams, D.M. Winter, M.E. Yokokawa and S.E. Swanson (Editors), Proceedings of the Ocean Drilling Program, Part A: Initial Reports 172. Ocean Drilling Program, 172, College Station, TX, pp. 251-308.
Shor, A.N. and Piper, D.J.W., 1989. A large Late Pleistocene blocky debris flow on the central Scotian slope. Geo-Marine Letters, 9: 153-160.

Sijp, W.P. and England, M.H., 2008. The effect of a northward shift in the southern hemisphere westerlies on the global ocean. Progress In Oceanography, 79(1): 1-19.
Sivkov, V., Gorbatskiy, V., Kuleshov, A. and Zhurov, Y., 2002. Muddy contourites in the Baltic Sea: an example of a shallow-water contourite system. In: D.A.V. Stow, C.J. Pudsey, J.-C. Faugères and A.R. Viana (Editors), Deep-water contourite systems: modern drifts and ancient series, seismic and sedimentary characteristics. Geological Society, Memoir 22, London, pp. 121-136.
Skene, K.I. and Piper, D.J.W., 2003. Late Quaternary stratigraphy of Laurentian Fan: a record of events off the eastern Canadian continental margin during the last deglacial period. Quaternary International, 99-100: 135-152.
Skene, K.I. and Piper, D.J.W., 2006. Late Cenozoic evolution of Laurentian Fan: development of a glacially-fed submarine fan. Marine Geology, 227(1-2): 67-92.
Smith, R.U., 2004. Silled sub-basins to connected tortuous corridors: sediment distribution systems on topographically complex sub-aqueous slopes. In: S.A. Lomas and P. Joseph (Editors), Confined turbidite systems. Geological Society, London, Special Publication 222, London, pp. 23-43.
So, L.C., Pierce, J.W. and Siegel, F.R., 1974. Sand waves in the Gulf of San Matias, Argentina. Geografiska Annaler. Series A, Physical Geography, 56(3-4): 227-235.
Solheim, A., Faleide, J.I., Andersen, E.S., Elverhøi, A., Forsberg, C.F., Vanneste, K., Uenzelmann-Neben, G. and Channell, J.E.T., 1998. Late Cenozoic seismic stratigraphy and glacial geological development of the East Greenland and Svalbard-Barents Sea continental margins. Quaternary Science Reviews, 17(1-3): 155-184.
Spieß, V. and Shipboard Scientific Party, 2002. ODP Südatlantik 2001, Cruise No. 49, Leg 2, 13 February – 7 March 2001, Montevideo – Montevideo. 02-1, Leitstelle Meteor, Institut für Meereskunde der Universität Hamburg.
Stanley, D.J., 1981. Unifites: structureless muds of gravity-flow origin in Mediterranean basins. Geo-Marine Letters, 1(2): 77-83.
Stea, R.R., Piper, D.J.W., Fader, G.B.J. and Boyd, R., 1998. Wisconsinan glacial and sea-level history of Maritime Canada and the adjacent continental shelf: A correlation of land and sea events. Geological Society of America Bulletin, 110(7): 821-845.
Stea, R.R., Fader, G.B.J., Scott, D.B. and Wu, P., 2001. Glaciation and relative sea level change in Maritime Canada. In: T.K. Weddle and M.J. Retelle (Editors), Deglacial history and relative sea level changes. Geological Society of America, Special Paper 351, Boulder, pp. 35-49.
Stevenson, F.J. and Cheng, C.-N., 1969. Amino acid levels in the Argentine Basin sediments; correlation with Quaternary climatic changes. Journal of Sedimentary Research, 39(1): 345-349.
Stevenson, M.R., Dias-Brito, D., Stech, J.L. and Kampel, M., 1998. How do cold water biota arrive in a tropical bay near Rio de Janeiro, Brazil? Continental Shelf Research, 18(13): 1595-1612.
Stow, D.A.V. and Lovell, J.P.B., 1979. Contourites: their recognition in modern and ancient sediments. Earth-Science Reviews, 14(3): 251-291.
Stow, D.A.V., 1979. Distinguishing between fine-grained turbidites and contourites on the Nova Scotian deep water margin. Sedimentology, 26(3): 371-387.

Stow, D.A.V., 1982. Bottom currents and contourites in the North Atlantic. Bulletin de l'Institut de Geologie du Bassin d'Aquitaine, 31: 151-166.
Stow, D.A.V. and Piper, D.J.W., 1984. Deep-water fine-grained sediments: facies models. In: D.A.V. Stow and D.J.W. Piper (Editors), Fine grained sediments: deep water processes and facies. Geological Society, Special Publication 15, London, pp. 611-646.
Stow, D.A.V. and Holbrook, J.A., 1984. North Atlantic contourites: an overview. In: D.A.V. Stow and D.J.W. Piper (Editors), Fine grained sediments: deep water processes and facies. Geological Society, Special Publication 15, London, pp. 245-256.
Stow, D.A.V., 1985. Fine-grained sediments in deep water: An overview of processes and facies models. Geo-Marine Letters, 5(1): 17-23.
Stow, D.A.V. and Wetzel, A., 1990. Hemiturbidite: a new type of deep water sediment. In: J.R. Cochran and D.A.V. Stow (Editors), Proceedings Ocean Drilling Program Scientific Results, 116, College Station, TX, pp. 25-34.
Stow, D.A.V., Faugères, J.-C., Howe, J.A., Pudsey, C.J. and Viana, A.R., 2002. Bottom currents, contourites and deep-sea sediment drifts: current state of the art. In: D.A.V. Stow, C.J. Pudsey, J.A. Howe, J.-C. Faugères and A.R. Viana (Editors), Deep-water contourite systems: modern drifts and ancient series, seismic and sedimentary characteristics. The Geological Society, Memoir 22, London, pp. 7-20.
Stow, D.A.V. and Faugères, J.-C., 2008. Contourite facies and the facies model. In: M. Rebesco and A. Camerlenghi (Editors), Developments in Sedimentology 60. Elsevier, pp. 223-256.
Stow, D.A.V., Hunter, S.E., Wilkinson, D. and Hernández-Molina, F.J., 2008. The nature of contourite deposition. In: M. Rebesco and A. Camerlenghi (Editors), Developments in Sedimentology 60. Elsevier, pp. 143-156.
Stow, D.A.V., Hernández-Molina, F.J., Llave, E., Sayago-Gil, M., Díaz del Río, V. and Branson, A., 2009. Bedform-velocity matrix: The estimation of bottom current velocity from bedform observations. Geology, 37(4): 327-330.
Stramma, L., 1989. The Brazil current transport south of 23°S. Deep Sea Research Part A. Oceanographic Research Papers, 36(4): 639-646.
Stramma, L. and England, M.H., 1999. On the water masses and mean circulation of the South Atlantic Ocean. Journal of Geophysical Research, 104(C9): 20863-20883.
Sultan, N., Cochonat, P., Canals, M., Cattaneo, A., Dennielou, B., Haflidason, H., Laberg, J.S., Long, D., Mienert, J., Trincardi, F., Urgeles, R., Vorren, T.O. and Wilson, C., 2004. Triggering mechanisms of slope instability processes and sediment failures on continental margins: a geotechnical approach. Marine Geology, 213(1-4): 291-321.
Sultan, N., Gaudin, M., Berne, S., Canals, M., Urgeles, R. and Lafuerza, S., 2007. Analysis of slope failures in submarine canyon heads: An example from the Gulf of Lions. Journal of Geophysical Research, 112: F01009.
Swift, D.J.P., Parker, G., Lanfredi, N.W., Perillo, G.M.E. and Figge, K., 1978. Shoreface-connected sand ridges on American and European shelves: A comparison. Estuarine and Coastal Marine Science, 7(3): 257-273.

Syvitski, J.P.M., Alexander, C.R., Field, M.E., Gardner, J.V., Orange, D.L. and Yun, J.W., 1996a. Continental-slope sedimentation: the view from northern California. Oceanography, 9(3): 163-167.
Syvitski, J.P.M., Andrews, J.T. and Dowdeswell, J.A., 1996b. Sediment deposition in an iceberg-dominated glacimarine environment, East Greenland: basin fill implications. Global and Planetary Change, 12(1-4): 251-270.
Takahashi, T., 1981. Debris flow. Annual Review of Fluid Mechanics, 13(1): 57-77.
Talling, P.J., Lawrence, A.A. and Wynn, R.B., 2007. New insights into the evolution of large-volume turbidity currents: comparison of turbidite shape and previous modelling results. Sedimentology, 54(4): 737-769.
Taylor, J., Dowdeswell, J.A., Kenyon, N.H., Whittington, R.J., van Weering, T.C.E. and Mienert, J., 2000. Morphology and Late Quaternary sedimentation on the North Faeroes slope and abyssal plain, North Atlantic. Marine Geology, 168(1-4): 1-24.
Taylor, J., Dowdeswell, J.A. and Siegert, M.J., 2002. Late Weichselian depositional processes, fuxes, and sediment volumes on the margins of the Norwegian Sea (62-75°N). Marine Geology, 188(1-2): 61-77.
Toggweiler, J.R. and Russell, J., 2008. Ocean circulation in a warming climate. Nature, 451: 286-288.
Tonni, E.P., Cione, A.L. and Figini, A.J., 1999. Predominance of arid climates indicated by mammals in the pampas of Argentina during the Late Pleistocene and Holocene. Palaeogeography, Palaeoclimatology, Palaeoecology, 147(3-4): 257-281.
Traykovski, P.A., Geyer, W.R., Irish, J.D. and Lynch, J.F., 2000. The role of wave-induced density-driven fluid mud flows for cross-shelf transport on the Eel River continental shelf. Continental Shelf Research, 20(16): 2113-2140.
Tripsanas, E.K., Bryant, W.R. and Prior, D.B., 2003. Structural characteristics of cohesive gravity-flow deposits, and a sedimentological approach on their flow mechanisms. In: J. Locat and J. Mienert (Editors), Submarine mass movements and their consequences. Springer Verlag, 1st International Symposium, Dordrecht, pp. 129-136.
Tripsanas, E.K., Piper, D.J.W. and Campbell, D.C., 2008. Evolution and depositional structure of earthquake-induced mass movements and gravity flows: southwest Orphan Basin, Labrador Sea. Marine and Petroleum Geology, 25(7): 645-662.
Tripsanas, E.K. and Piper, D.J.W., 2008. Late Quaternary stratigraphy and sedimentology of Orphan Basin: implications for meltwater dispersal in the southern Labrador Sea. Paleogeography, Paleoclimatology, Paleoecology, 260(3-4): 521-539.
Tripsanas, E.K., Piper, D.J.W., Jenner, K.A. and Bryant, W., 2009. Submarine mass-transport facies: new perspectives on flow processes from cores on the eastern North American margin. Sedimentology, 55(1): 97-136.
Trowbridge, J.H. and Kinecke, G.C., 1994. Structure and dynamics of fluid muds on the Amazon continental shelf. Journal of Geophysical Research, 99(C1): 865-874.
Tucholke, B.E., Hollister, C.D., Biscaye, P.E. and Gardner, W.D., 1985. Abyssal current character determined from sediment bedforms on the Nova Scotian continental rise. Marine Geology, 66(1-4): 43-57.
Turekian, K.K. and Stuvier, M., 1964. Clay- and carbonate-accumulation rates in three South Atlantic deep-sea cores. Science, 146: 55-56.

Uliana, M.A., Biddle, K.T. and Cerdan, J., 1989. Mesozoic extension and the formation of Argentine sedimentary basins. In: A.J. Tankard and H.R. Balkwill (Editors), Extensional tectonics and stratigraphy of the North Atlantic margins. American Association of Petroleum Geologists, AAPG Memoir 46, Tulsa, Oklahoma, pp. 599-614.
Urien, C.M., 1967. Los sedimentos modernos del Rio de la Plata exterior. Boletín del Servicio de Hidrografía Naval, 6(2): 113-213.
Urien, C.M. and Zambrano, J.J., 1973. The geology of the basins of the Argentine continental margin and Malvinas Plateau. In: A.E.M. Nairn and F.G. Stehli (Editors), The ocean basins and margins. Plenum Press, 1, New York, pp. 135-170.
Urien, C.M. and Ewing, M., 1974. Recent sediments and environments of southern Brazil, Uruguay, Buenos Aires and Rio Negro continental shelf. In: C.A. Burke and C.L. Drake (Editors), The geology of continental margins. Springer Verlag, Berlin, pp. 157-177.
Urien, C.M., Martins, L.R. and Martins, I.R., 2003. Paleoplataformas e progradação deltaica do neógeno na margem continental do Uruguai e norte da Argentina. Gravel, 1: 40-46.
van Weering, T.C.E. and van Iperen, J., 1984. Fine-grained sediments of the Zaire deep-sea fan, southern Atlantic Ocean. In: D.A.V. Stow and D.J.W. Piper (Editors), Fine grained sediments: deep water processes and facies. Geological Society, Special Publication 15, London, pp. 95-113.
Vanney, J.-R. and Stanley, D.J., 1983. Shelf break physiography: an overview. In: D.J. Stanley and G.T. Moore (Editors), The Shelfbreak : critical interface on continental margins. Society of Economic Paleontologists and Mineralogists, Special Publication 33, Tulsa, pp. 1-24.
Vera, C.S., Baez, J., Douglas, M., Emmanuel, C.B., Marengo, J., Meitin, J., Nicolini, M., Nogues-Paegle, J., Paegle, J., Penalba, O., Salio, P., Saulo, C., Silva Dias, M.A., Silva Dias, P. and Zipser, E., 2006. The South American low-level jet experiment. Bulletin of the American Meteorological Society, 87(1): 63-77.
Verdicchio, G. and Trincardi, F., 2008. Mediterranean shelf-edge muddy contourites: examples from the Gela and South Adriatic basins. Geo-Marine Letters, 28(3): 137-151.
Viana, A., 2002. Seismic expression of shallow- to deep-water contourites along the south-eastern Brazilian margin. Marine Geophysical Researches, 22(5-6): 509-521.
Viana, A.R., Faugères, J.-C. and Stow, D.A.V., 1998a. Bottom-current-controlled sand deposits — a review of modern shallow- to deep-water environments. Sedimentary Geology, 115(1-4): 53-80.
Viana, A.R., Faugères, J.-C., Kowsmann, R.O., Lima, J.A.M., Caddah, L.F.G. and Rizzo, J.G., 1998b. Hydrology, morphology and sedimentology of the Campos continental margin, offshore Brazil. Sedimentary Geology, 115(1-4): 133-157.
Viana, A.R. and Faugères, J.-C., 1998. Upper slope sand deposits: the example of Campos Basin, a latest Pleistocene-Holocene record of the interaction between alongslope and downslope currents. In: M.S. Stoker and D. Evans (Editors), Geological processes on continental margins: sedimentation, mass-wasting and

stability. Geological Society, London, Special Publication 129, London, pp. 287-316.
Violante, R.A. and Parker, G., 2004. The post-last glacial maximum transgression in the de la Plata River and adjacent inner continental shelf, Argentina. Quaternary International, 114(1): 167-181.
Vittori, J., Morash, A., Savoye, B., Marsset, T., Lopez, M., Droz, L. and Cremer, M., 2000. The Quaternary Congo deep-sea fan: preliminary results on reservoir complexity in turbiditic systems using 2D high resolution seismic and multibeam data, GCSSEPM Foundation 20th Annual Research Conference: Deep Water reservoirs of the World, Houstan, TX, pp. 1045-1058.
Voigt, I., Hanebuth, T.J.J., Preu, B.M., Schwenk, T., Krastel, S. and Henrich, R., 2011. A submarine canyon as sink in the interplay of down-slope and along-slope processes – The Mar del Plata Canyon offshore Argentina, AGU Chapman Source to Sink. American Geophysical Union, Oxnard, CA.
Volbers, A.N.A. and Henrich, R., 2004. Calcium carbonate corrosiveness in the South Atlantic during the Last Glacial Maximum as inferred from changes in the preservation of Globigerina bulloides: A proxy to determine deep-water circulation patterns? Marine Geology, 204(1-2): 43-57.
von Lom-Keil, H., Spieß, V. and Hopfauf, V., 2002. Fine-grained sediment waves on the western flank of the Zapiola Drift, Argentine Basin: evidence for variations in Late Quaternary bottom flow activity. Marine Geology, 192(1-3): 239-258.
von Lom-Keil, H., Schlacht, R. and Spieß, V., 2003. Bottom current influenced sedimentation in the Argentine Basin and on the Argentine continental margin reflected in high resolution seismic data, EGS-AGU-EUG Joint Assembly. European Geophysical Society, pp. 11459.
Vorren, T.O., Lebesbye, E., Andreassen, K. and Larsen, K.B., 1989. Glacigenic sediments on a passive continental margin as exemplified by the Barents Sea. Marine Geology, 85(2-4): 251-272.
Vorren, T.O. and Laberg, J.S., 1997. Trough mouth fans — palaeoclimate and ice-sheet monitors. Quaternary Science Reviews, 16(8): 865-881.
Vorren, T.O., Laberg, J.S., Blaume, F., Dowdeswell, J.A., Kenyon, N.H., Mienert, J., Rumohr, J. and Werner, F., 1998. The Norwegian-Greenland Sea continental margins: morphology and late Quaternary sedimentary processes and environment. Quaternary Science Reviews, 17(1-3): 273-302.
Wade, J.A. and MacLean, B.C., 1990. The geology of the southeastern margin of Canada, Part 2: Aspects of the geology of the Scotian Basin from recent seismic and well data. In: M.J. Keen and G.L. Williams (Editors), Geology of the continental margin of eastern Canada. Geological Survey of Canada, Ottawa, pp. 190-238.
Waelbroeck, C., Labeyrie, L., Michel, E., Duplessy, J.-C., McManus, J.F., Lambeck, K., Balbon, E. and Labracherie, M., 2002. Sea level and deep water temperature changes derived from benthic foraminifera isotopic records. Quaternary Science Reviews, 21(1-3): 295-305.
Walker, R.G., 1967. Turbidite sedimentary structures and their relationship to proximal and distal depositional environments. Journal of Sedimentary Research, 37(1): 25-43.

Wells, P.G. and Daborn, G.R., 1997. The Rio de la Plata - an environmental overview. Dalhousie University, Halifax, 248 pp.
Wilken, M. and Mienert, J., 2006. Submarine glacigenic debris flows, deep-sea channels and past ice-stream behaviour of the East Greenland continental margin. Quaternary Science Reviews, 25(7-8): 784-810.
Wilkinson, M.J., Marshall, L.G. and Lungberg, J.G., 2006. River behavior on megafans and potential influences on diversification and distribution of aquatic organisms. Journal of South American Earth Sciences, 21(1-2): 151-172.
Wright, L.D. and Friedrichs, C.T., 2006. Gravity-driven sediment transport on continental shelves: A status report. Continental Shelf Research, 26(17-18): 2092-2107
Wright, R. and Anderson, J.B., 1982. The importance of sediment gravity flow to sediment transport and sorting in a glacial marine environment: Eastern Weddell Sea, Antarctica. Geological Society of America Bulletin, 93(10): 951-963.
Yokokawa, M., 2001. 7. Sedimentary structures of contourites and turbidites observed by X-radiographic prints: Samples from Blake-Bahama outer Ridge and Sohm Abyssal Plain. In: L.D. Keigwin, D. Rio, G.D. Acton and E. Arnold (Editors), Proceedings of the Ocean Drilling Program, Scientific Results. Ocean Drilling Program, Volume 172, College Station, TX, pp. 1-37.
Zambrano, J.J. and Urien, C.M., 1970. Geological outline of the basins in southern Argentina and their continuation off the Atlantic shore. Journal of Geophysical Research, 75(8): 1363-1396.
Zavialov, P.O., Kostianoy, A.G. and Möller, O.O., 2003. SAFARI cruise: Mapping river discharge effects on Southern Brazilian shelf. Geophysical Research Letters, 30(21): 2126.
Zhou, J. and Lau, K.-M., 1998. Does a monsoon climate exist over South America? Journal of Climate, 11(5): 1020-1040.

6. Interaction of Pleistocene wave-supported sediment gravity flow deposits and contour current deposits on a slope terrace offshore the Rio de la Plata estuary, northern Argentine Slope

Citation: Huppertz, T.J., Piper, D.J.W. and Henrich, R., in preparation. Interaction of Pleistocene wave-supported sediment gravity flow deposits and contour current deposits on a slope terrace offshore the Rio de la Plata estuary, northern Argentine Slope. Journal of Sedimentary Research.

6.0. Abstract

Wave supported sediment gravity flows are widely recognized in Holocene strata on continental margins with high fine-grained sediment discharge. They represent an important process to transport fine-grained sediment across shelves. The flows are initiated and sustained by high turbulent suspended sediment load close to seabed. Similar flows were present on the Ewing terrace offshore northern Argentina during times in Marine Isotope Stage 2, when lowered sea level shifted the coastline seawards, thus lowering storm-wave base and facilitating sand mobilization.

Offshore the Rio de la Plata estuary in ~1200 m water depth is the northern part of the Ewing terrace, a slope subbasin stretching along the entire Argentine continental margin. Several sediment gravity cores, Parasound subbottom profiles and multibeam bathymetry data were used to interpret sedimentation processes on the northern part of the terrace. Using x-radiographs, grain size, color, petrology, and oxygen isotope data, the terrace sediments were characterized sedimentologically and dated. Hydroacoustic (Parasound) data was used to define the geometry of the terrace and the character of the deposits. Five different sedimentary facies are defined: (i) laminated facies, (ii) laminated and tilted facies, (iii) highly bioturbated facies, (iv) burrowed facies and (v) clast facies. The first is linked to wave-supported sediment gravity flows, facies ii has characters indicative of downslope and alongslope processes, facies iii is a reworked facies, facies iv is interpreted as a contourite facies and facies v is related to mass wasting processes. Using the occurrence of the different facies in the cores, a conceptual model of deposition could be developed for the northernmost Ewing terrace. The system is generally sediment-starved and forms a fine-grained contourite system. During infrequent (Pleistocene) storm events, sand is supplied to the terrace and may be subject to ocean current winnowing and thus contourite construction.

6.1. Introduction

Upper slope sands are generally shelf sediments transported to the shelf edge and across the shelf break. The shelf break is commonly characterized either by gullies and canyons, where the sand is directly transported into the canyon heads and forms turbidity currents within the canyons (Vittori et al., 2000; Mitchell, 2004; Jenner et al., 2007; Sultan et al., 2007; Henrich et al., 2010), or the slope shows few or no canyons or gullies, and the sand is transported over the shelf break and is deposited on the upper slope (Hill et al., 2007; Nittrouer et al., 2007). Reworking of these sands occurs either during wave action, possibly enhanced during storm events (Puig et al., 2003; Puig et al., 2004b), or by ocean currents (Viana and Faugères, 1998; Viana, 2002; Verdicchio and Trincardi, 2008).

Most cores from siliciclastic upper slope settings are sand-dominated with varying percentages of clay throughout. Bioturbation is generally high and the sediments have few structures preserved (Viana and Faugères, 1998; Rodriguez and Anderson, 2004). When sedimentary structures like cross bedding and laminations are preserved over large parts of the core, and bioturbation is minor within these layers, these deposits may be linked to short-term events (event beds) such as storms, flooding events or wave action forming rapidly accumulating tempestite or turbidite deposits (Wheatcroft, 1990; Einsele, 1996; Myrow and Southard, 1996; Wheatcroft et al., 1996).

Generally, turbidite deposits are frequently found in deep water, often bypassing large parts of the upper and mid-slope. On some margins, slope basins can prevent this process by preserving these storm or wave induced flows in relatively shallow water in slope basins including marine terraces (McAdoo et al., 1997; Beaubouef and Friedmann, 2000; Bouma, 2004).

Offshore Argentina, this is the case: several marine terraces characterize the slope (Hernández-Molina et al., 2009). The dominating terrace on the central and northern Argentine slope is the Ewing Terrace. Currently, little geological data is available from the northernmost part of this terrace. During 2009, the German research vessel RV METEOR collected several sediment cores on this part of the terrace. These cores are generally highly bioturbated, but in few instances, well laminated intervals with sharp depositional surfaces have been preserved. The main objectives of this paper are to (1) explore the Late Quaternary architecture of this continental slope basin (Ewing terrace) and (2) to investigate the types and timing of shelf sediment export on this slope system, especially during the last glacial cycle.

6.2. Regional setting

6.2.1. Physiography

The northern Argentine continental margin is a passive continental margin formed during initial rifting of the South Atlantic in Cretaceous times (Uliana et al., 1989). The dominant geomorphological feature is the Rio de la Plata estuary (Fig. 1), where the Parana and Uruguay rivers (also referred to as La Plata rivers), draining the second largest basin in South America, enter the ocean (Iriondo, 2007; Iriondo and Paira, 2007).

The continental shelf break occurs in 200 m water depth and is 400-500 km seawards of the coastline (Fig. 1) (Martins and Correa, 1996; Parker et al., 1996). The base of the slope occurs at 4500 m where it passes into the abyssal plain, termed the Argentine Basin (Ewing, 1965; Ewing and Lonardi, 1971). The slope is mainly characterized by the pronounced Ewing terrace, which occurs between 1000 and 1400 m water depth (Fig. 1). Offshore the Rio de la Plata estuary is another, shallower (400 to 500 m water depth) terrace found, the La Plata Terrace (Urien and Ewing, 1974; Perillo et al., 2005). Few canyons cut into the shelf break but start on the Ewing Terrace. Thus, there are few direct conduits connecting the shelf and the Ewing Terrace (Ewing and Lonardi, 1971; Urien and Ewing, 1974; Parker et al., 1996; Hernández-Molina et al., 2009).

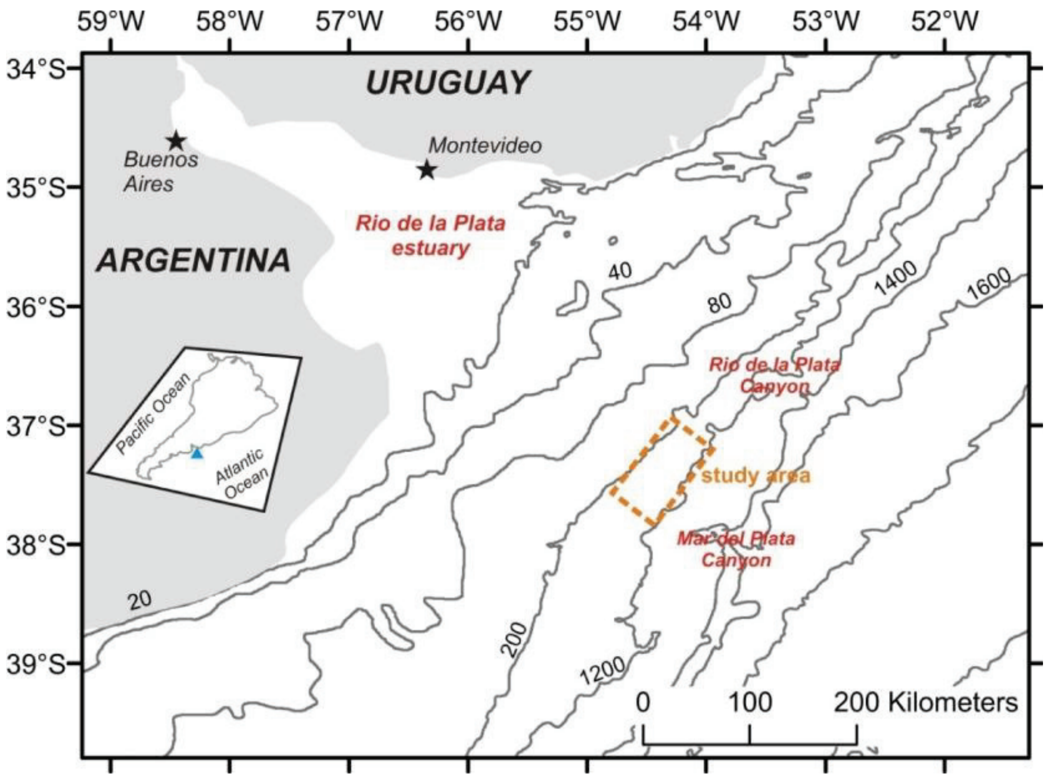

Figure 6.1: Overview of the northern Argentine and Uruguay continental margin in South America (see blue dot on small index map of South America). Bathymetry [in meters] from Gebco 2003 (www.gebco.net) and Martins and Correa (1996).

6.2.2. Geological setting

Few studies have focused on the northern Argentine margin. Most studies were either aiming at reconstructing the paleo-climatic setting (Chiessi et al., 2007) or used microfossils (Boltovskoy et al., 1996; Romero and Hensen, 2002) or surface sediment distribution patterns (Höppner and Henrich, 1999; Frenz et al., 2003) to understand today's and the paleoceanographic settings. Offshore Uruguay, due north of the study area, seismic studies have shown the presence of widespread mass wasting (Antobreh, 2005). On the Argentine slope, pollen studies (Groot et al., 1967) and variability of chemical elements downcore (Riedinger et al., 2005) enabled to preliminary define the termination 1 boundary at different water depths on mid and lower slope positions along this part of the Argentine margin.

6.2.3. Oceanographic setting

The oceanographic setting in the northern Argentine Slope is dominated by the Brazil Malvinas Confluence zone (BMC) (Stramma and England, 1999; Piola and Matano, 2001). In this zone, the surficial water masses (upper 600 m water column), the Antarctic-fed Falkland/Malvinas current and the southward-directed Brazil current, collide. Below these surface currents the Antarctic Intermediate Water and Circumpolar Deep Water is found. At a water depth of greater 1500 m, the Circumpolar Deep Water is split vertically by the southwards directed North Atlantic Deep Water (NADW). Below these water masses, the Argentine Basin is dominated by northwards flowing Antarctic Bottom Water (e.g. Gordon and Greengrove, 1986; Bianchi et al., 1993; Stramma and England, 1999; Piola and Matano, 2001).

During the Last Glacial Maximum (LGM), sea level was lowered by up to 120 m along the Argentine continental margin (Guilderson et al., 2000). Extensive sea ice coverage due to colder sea surface temperatures characterized the Circumpolar Ocean (Marchitto et al., 2002), resulting in a much steeper north to south thermal gradient during the LGM. The fate of the BMC remains unclear, but due to the strengthened Antarctic water masses, a northward shift was likely (Pahnke et al., 2008; Laprida et al., accepted). The intermediate and deep-water circulation changed also significantly during the LGM (Henrich et al., 2002; Gröger et al., 2003; Henrich et al., 2003), as it is in today’s ocean circulation the case (Viana and Faugères, 1998). Furthermore, the strength of the lower NADW was decreased (Came et al., 2003; Curry and Oppo, 2005; Marchitto and Broecker, 2006; Lynch-Stieglitz et al., 2007), whereas those of Upper NADW increased (Henrich et al. 2002, 2003).

6.2.4. Event beds on shelf and upper slope

When sedimentary structures of upper slope sands are preserved, these deposits are likely caused by short-term events, which can disrupt the hemipelagic sedimentation. These horizons are either turbidite deposits on the slope or tempestites on the shelf and uppermost slope (Einsele, 1991; Einsele and Seilacher, 1991). Rapid sedimentation will interfere with the biological community and bioturbation may be greatly reduced or halted (Dott, 1983). The preservation of event beds is usually poor due to rapid bioturbation or sediment reworking and winnowing (Wheatcroft, 1990; Wheatcroft et al., 2006), but in a few cases, rapid burial by a younger event bed will preserve an almost unbioturbated bed.

The sedimentary characteristics of storm events and turbidite deposits, as well as contourite beds, can be very similar (Dott and Bourgeois, 1982; Iseya, 1989; Héquette and Hill, 1995; Stow et al., 2002; Huppertz and Piper, 2010). Nevertheless, at least in Late Quaternary systems, the overall setting at the margin and changes due to sea level variations can be used to infer the most likely depositional process (Einsele and Seilacher, 1991; Lamb et al., 2008; Myrow et al., 2008).

Wave supported sediment gravity flows are generated when the thin sediment wave boundary layer is highly concentrated with sediment, allowing downslope driven movement (Traykovski et al., 2007). During present sea level highstands, these flows are generated seaward of rivers with high sediment discharge (Wheatcroft et al., 1997; Wheatcroft and Borgeld, 2000; Warrick and Milliman, 2003; Wright and Friedrichs, 2006). Such flows are stable until the flow cannot support its suspension anymore (Traykovski et al., 2007).

6.3. Methods

In 2009, the German research vessel Meteor collected several sediment gravity cores, multibeam data and ~100 km Parasound data throughout the northern Ewing Terrace at ~1200 m water depth seaward of the Rio de la Plata estuary (Figs. 2 and 3).

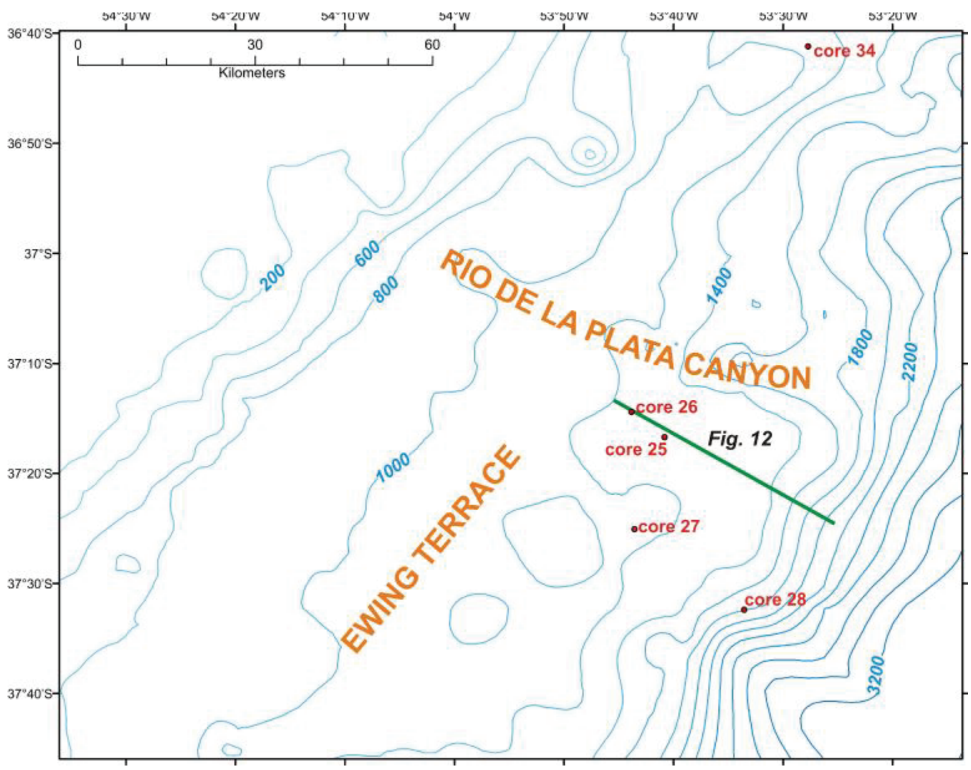

Figure 6.2: Map of the study area on the Ewing Terrace on the northern Argentine continental slope showing cores used in this study. Bathymetry in meters from Gebco 08 (www.gebco.net). Core 25: GeoB 13825-2, core 26: GeoB 13826-1, core 27: GeoB 13827-2, core 28: GeoB 13828-1, core 34: GeoB 6234-2; position of Figure 9 also indicated.

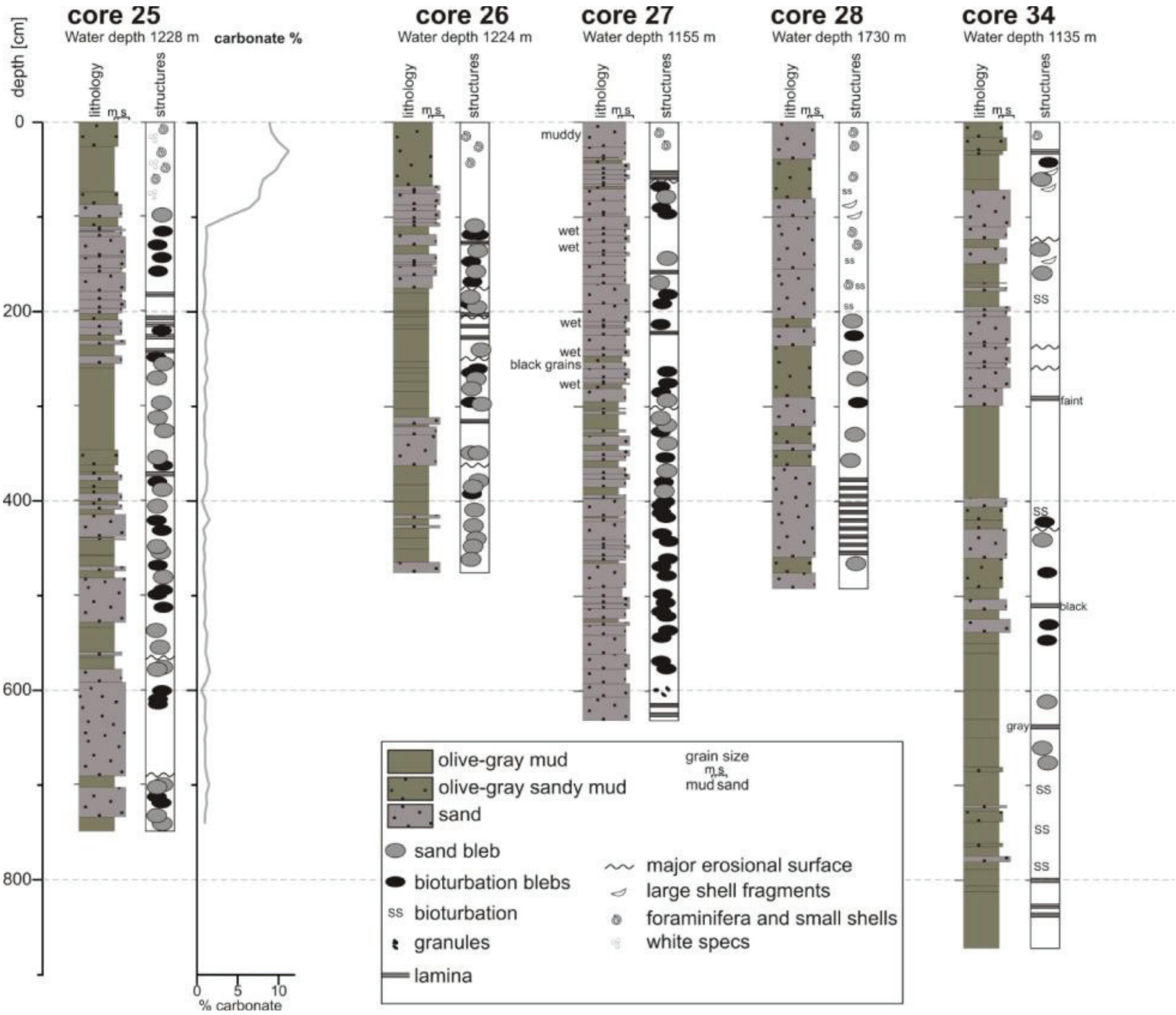

Figure 6.3: Core lithologies and macroscopic sedimentary structures of cores and the carbonate plot of core 25.

High-resolution Parasound data was used to image the upper hundred meters of seabed at ~0.5 m resolution; multibeam data collected using the ATLAS HydroSweep DS-2, imaged the bathymetry of the study area. Gravity cores with 6 or 12 m long barrels were collected throughout the terrace, split and described. Digital spectrophotometer data expressed in RGB (red-green-blue) color space and multi-sensor core logging data were collected with the GeoTEK MSCL-S bench, and were both used for core correlation. X-radiography slabs on all cores were further used for visualizing sedimentary structures and erosional surfaces.

Grain size analysis, typically at 10 cm spacing, was carried out on 2 cores (25 and 28, complete core numbers may be found in Fig. 2) to characterize the sandier intervals; muddier intervals were sampled every 30 cm. The samples were measured with the Beckmann Laser Coulter LS 230 with the Fraunhofer module. Grain size data were plotted as frequency curves downcore, as sand-silt-clay percentages downcore and as 3-D Golden Software Surfer™ maps following the methodology described by

Huppertz and Piper (2010) by plotting the bin size on the x-axis, the sampling interval on the y-axis and the percentages within each grain size class on the z-axis (Huppertz and Piper, 2010). Percentage sortable silt (% SS) was calculated from the Coulter Laser dataset and plotted downcore with no correction for carbonate necessary below 100 cm.

Age control relies on oxygen isotope data using the benthic foraminifera *A. angulosa* (Fig. 4) (Williamson et al., 1984). Low carbonate content in the cores greatly limited the use of radiocarbon dating; therefore the oxygen isotope curve of core 25 (sampling interval every 10 cm), was correlated to published benthic foraminifera $\delta^{18}O$ curves (Fig. 4) (Lisiecki and Raymo, 2005).

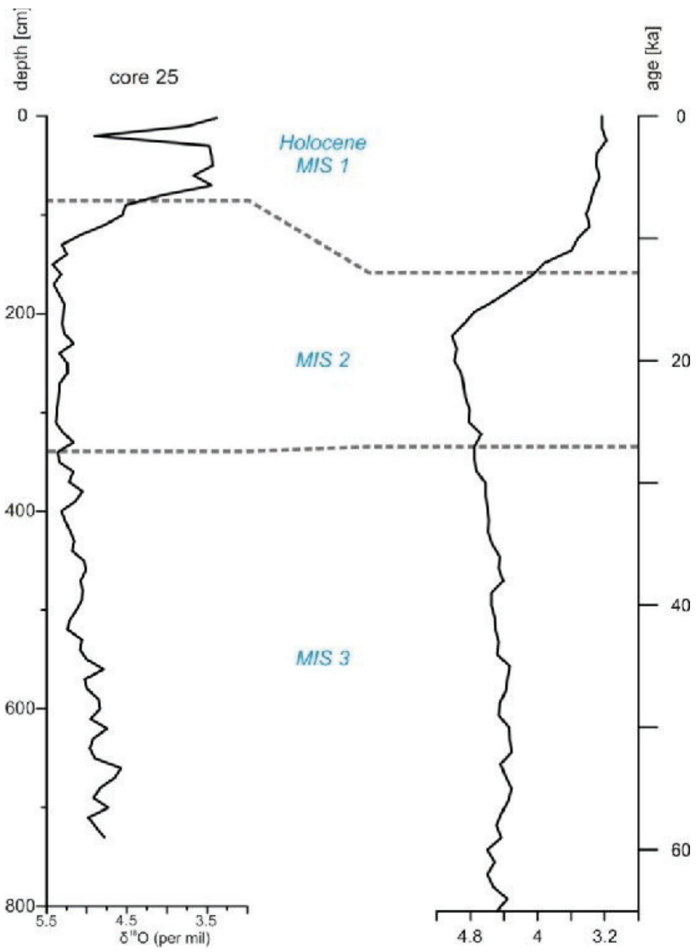

Figure 6.4: Oxygen isotope curve of core 25 (left curve) using the benthic foraminifera A. angulosa and its correlation to the interpreted oxygen isotope curve of Lisiecki and Raymo (2005) (right side panel).

Sand grain petrology of >400 grains per sample (from the 125-500 µm fraction) was counted using a reflected light microscope. The petrology samples were also sieved at 63 and 32 µm intervals. This weight data in addition to the coarser data were compared to laser analyzer data for grain size distribution estimates (Fig. 5).

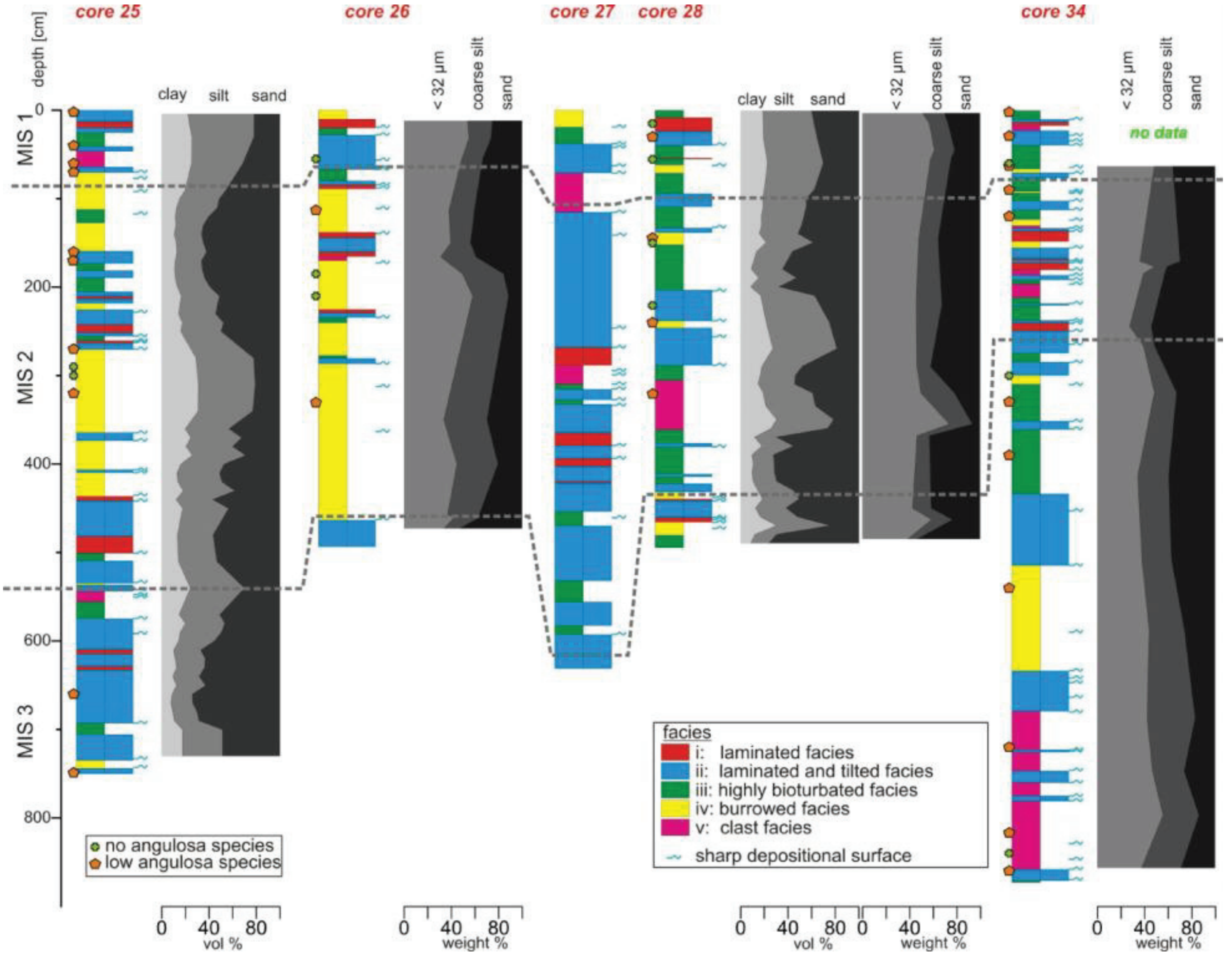

Figure 6.5: Core facies downcore in relationship to sand silt clay ratios (cores 25 and 28) and the sand coarse silt and <32 µm derived from the petrology data (cores 26, 28 and 34). As seen in core 28, this derivative grain size data agrees at least for the sand percentages well to the true grain size from the coulter laser data.

6.4. Results

6.4.1. Age model and core correlation

The age model relies mostly on the oxygen isotope curves of core 25, 27 and 34 and their correlation to a published isotope curve stack (Fig. 4) (Lisiecki and Raymo, 2005). Marine isotope stages (MIS) 1 and 2 are easily recognizable due to their well observable trends (Fig. 4) and its comparison to high resolution curves from the area (Chiessi et al., 2008); the boundary between stage 2 and 3 is less clear. The boundary was set at 330 cm (Fig. 4) following the downcore trends of several other isotope curve records, when a slight increase in values records lighter isotopic values (Lisiecki and Raymo, 2005). A radiocarbon date in core 25 at 709-712 cm depth returned beyond the limit of ^{14}C dating and therefore correlates well to the interpretation of the oxygen isotope data, indicating the base of 25 core to be ~60 ka (base of Marine Isotope Stage

3). Cores 26 and 28 have discontinuous $\delta^{18}O$ measurements, but the trends in the downcore plots were sufficient to match with the well-established curve of core 25, 27 and 34 (Fig. 6). In cores 28 and 34, few outliers may suggest reworking processes (e.g. in both cores at 200 cm depth).

Core correlation is mainly based on the RGB R value, and oxygen isotope data (Figs. 6 and 7). Lithological correlations (Figs. 3 and 7) and to a very limited extent correlations based on the Parasound data were used to support and improve correlations.

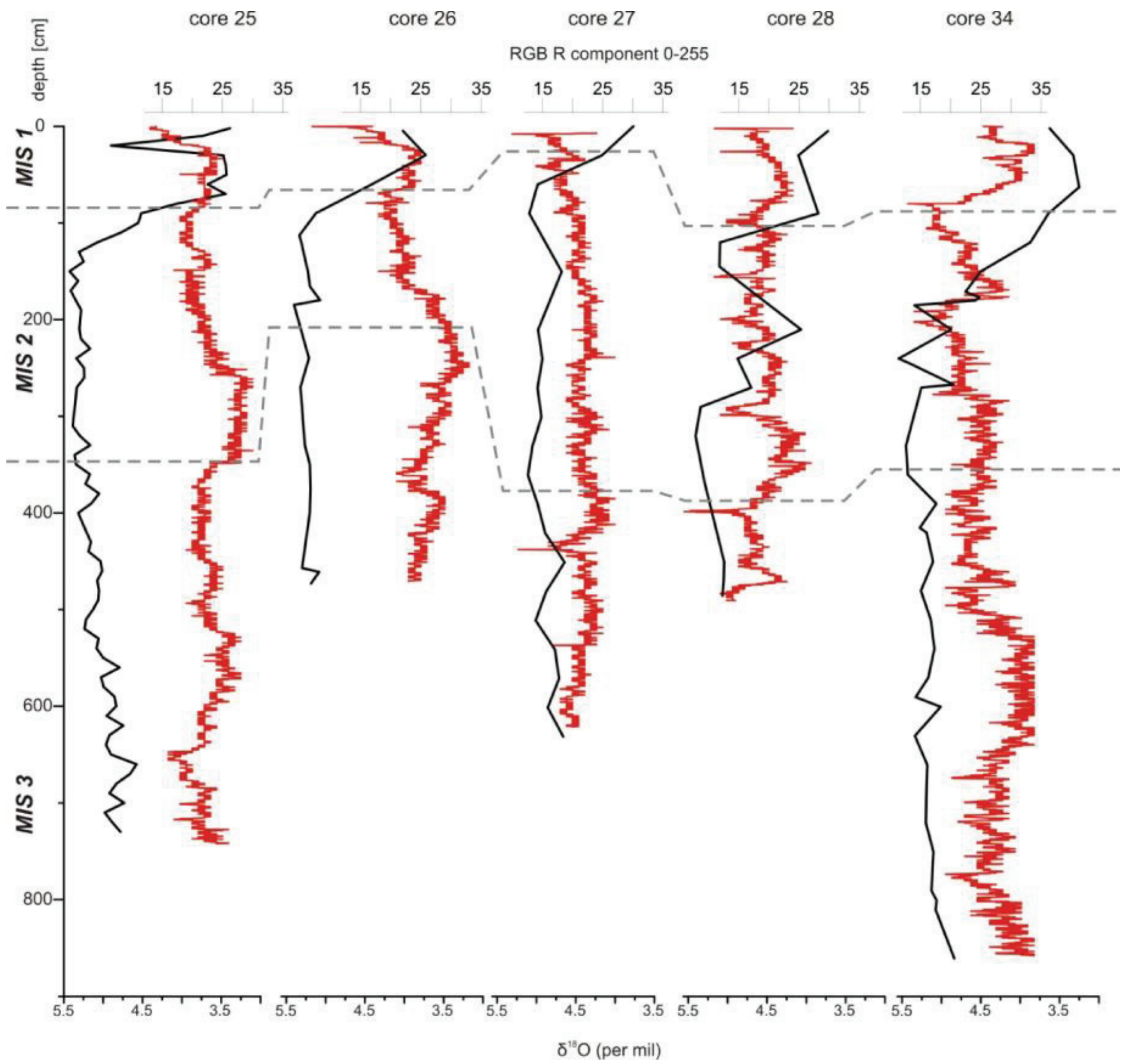

Figure 6.6: Core correlation and age control of cores from the northern Ewing Terrace using the RGB R component (red graph) and oxygen isotope data.

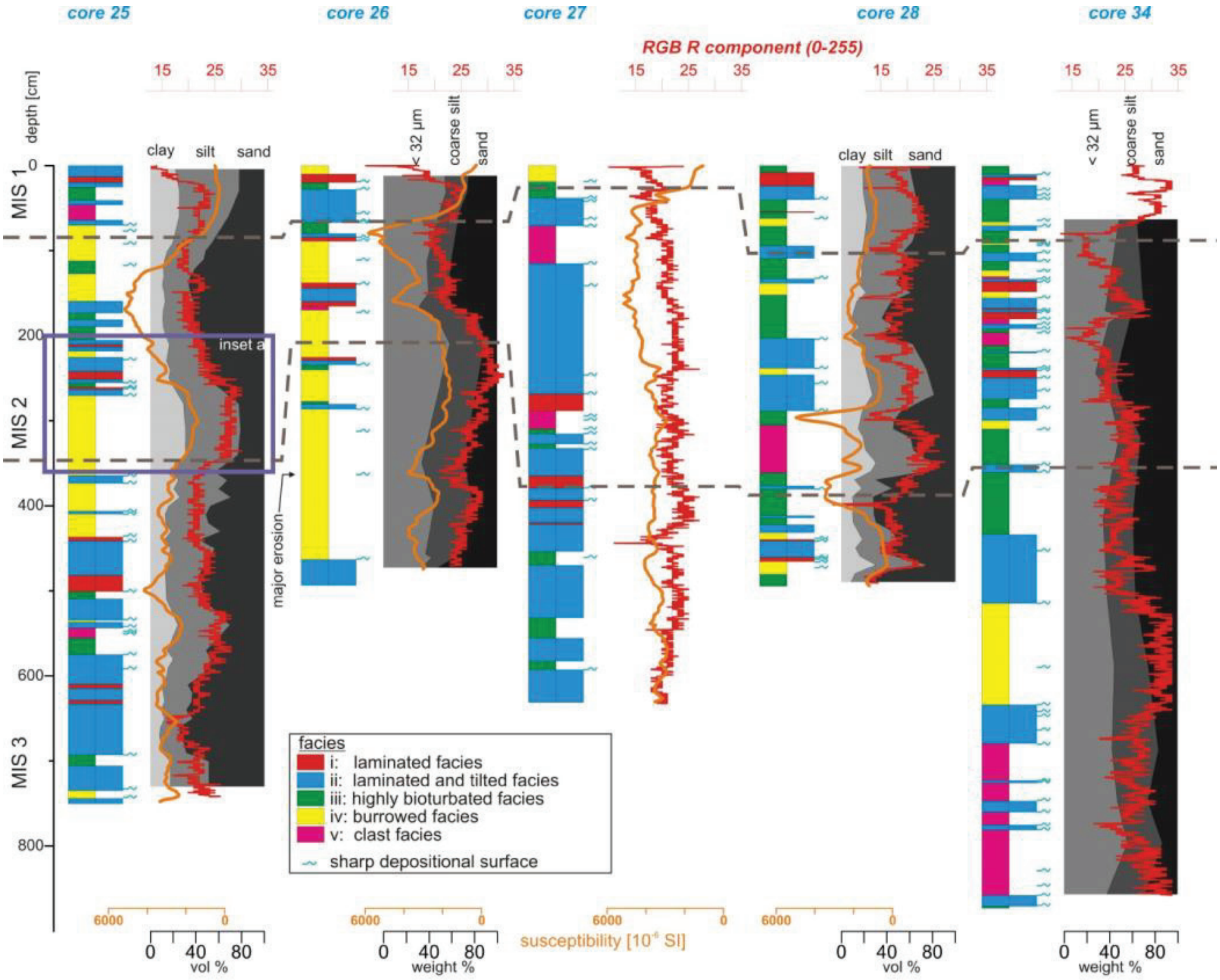

core 25
core 26
core 27
core 28
core 34
RGB R component (0-255)
depth [cm]
MIS 1
MIS 2
MIS 3
clay
silt
sand
< 32 µm
coarse silt
inset a
major erosion
facies
i: laminated facies
ii: laminated and tilted facies
iii: highly bioturbated facies
iv: burrowed facies
v: clast facies
sharp depositional surface
susceptibility [10⁻⁶ SI]
vol %
weight %

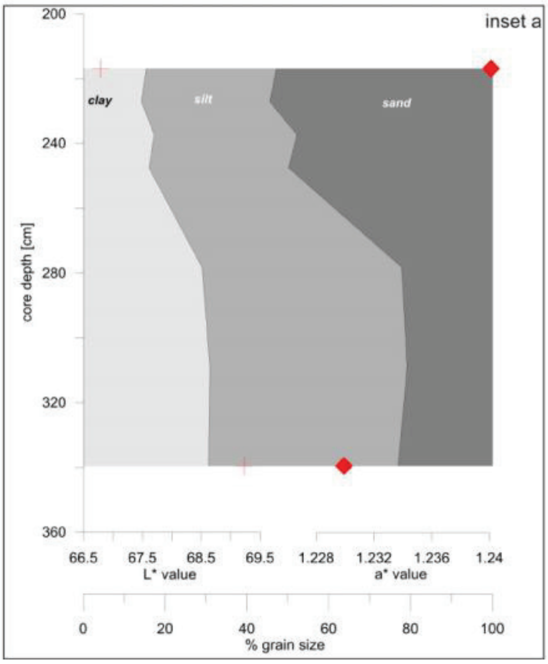

inset a
clay
silt
sand
core depth [cm]
L* value
a* value
% grain size

Figure 6.7 on previous page: Core facies and their relationship to RGB R-color and magnetic susceptibility data. Note that the magnetic susceptibility data increases to the left to match with the sand grain size data. The magnetic susceptibility data links to the sand percentages and anti-correlated to the red colors which are linked to the mud (mainly the silt fraction). Core 26 shows a major erosional surface at ~380 cm as shown also in Fig. 3. This surface is also nicely shown in the magnetic susceptibility data and grain size derivative, inset a shows the result of the color testing on the <53μm fraction. The increase of clay downcore results in a decrease of the CIELab a (red tracer) indicating that the red is not found within this fraction.*

6.4.2. Sedimentary facies

Characteristic sedimentary structures were used to define five different facies (Fig. 8, Table 2): (i) laminated facies (ii) laminated and tilted facies, (iii) highly bioturbated facies, (iv) burrowed facies and (v) clast facies. The facies are present in all cores and can be used to distinguish spatially and temporally between different depositional environments on the northern Ewing terrace. Sharp depositional surfaces are unrelated to facies and occur throughout the cores (Figs. 7 and 8).

The laminated facies (i) (Fig. 8) shows small-scale laminations (mostly sub-cm-scale) over several cm in the cores; locally faint wavy character may result in the appearance of flaser-bedding. Bioturbation is absent.

The laminated and tilted facies (ii) (Fig. 8) is very similar to the laminated facies, but the laminations are less well preserved due to bounding non-depositional surfaces, resulting locally in tilted units. Bioturbation is low and does not destroy the appearance of the laminations.

The highly bioturbated facies (iii) (Fig. 8) is dominated by bioturbation resulting in complete destruction of original depositional bedding. The degree of burrowing is also sufficient intense to prevent linking the bioturbation to a particular organism.

This is in contrast to the burrowed facies (iv) (Fig. 8), where the bioturbation is sufficient to destroy all depositional bedding (bio-deformational structures), but the burrows have been preserved enabling their link to specific organisms: these include amongst others *Scolicia*, *Zoophycos*, *Skolithos*, *Chondrites* and *Planolites*.

The clast facies (v) (Fig. 8) includes all sequences, in which muddy intraclasts of 0.5 to 5 cm diameter occur. Their occurrence is always linked to erosional surfaces above and below. Furthermore, these clasts may show faint internal laminations and small burrows, which resemble those of the laminated facies. This indicates reworking of locally deposited material.

The laminated intervals of Facies i and ii occur always stacked and bound by sharp depositional surfaces (Fig. 5). Contacts of Facies i and ii also show sharp depositional surfaces in stacked sequences. In few incidences, the laminated facies occurs interbedded with the clast facies v (Fig. 9). The grain size of the lamina suggests a coarse silt-fine sand fraction and shows little grain size variability downcore (Fig. 10).

In core 28, these units display inverse grading (Figs. 9 and 10). Nevertheless, a muddy tail is present throughout all of the cores (Figs. 9 and 10).

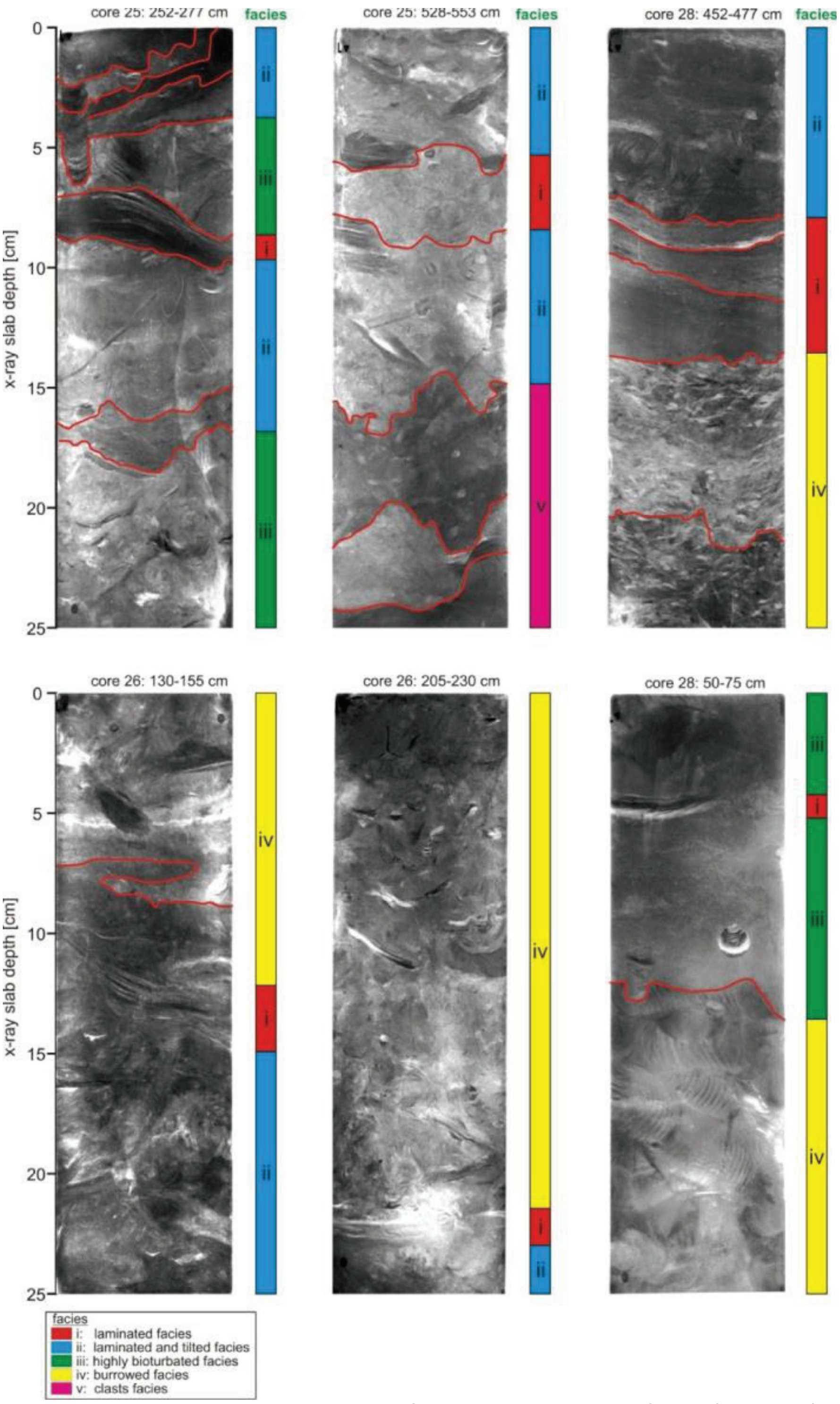

Figure 6.8: Representative X-radiographs showing frequent erosional surfaces (red lines) throughout the slabs; the sedimentological character of the different facies was defined in this study (see Table 2 and text for detailed descriptions of facies).

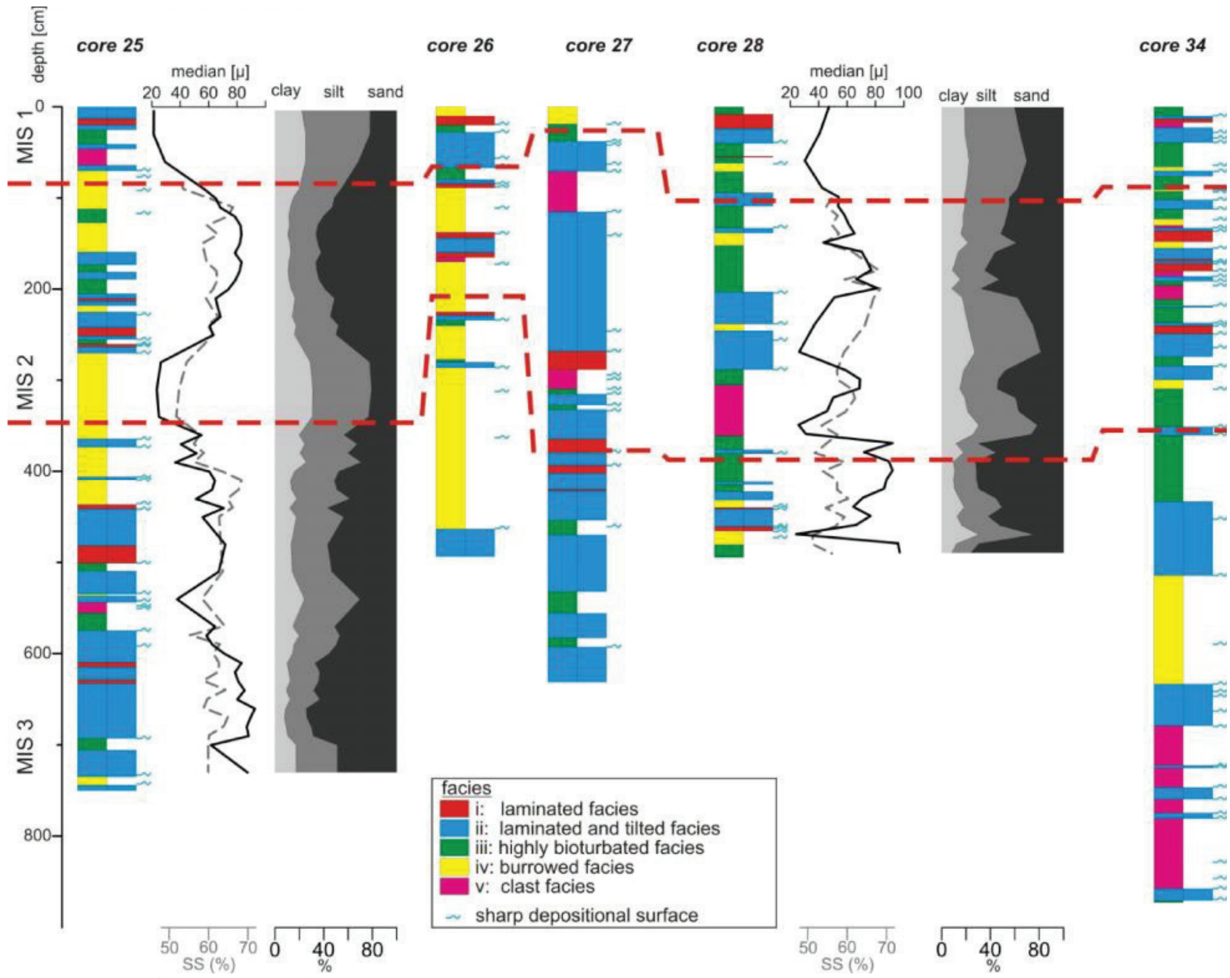

Figure 6.9: Sedimentary facies and grain size data including the mean and sortable silt data in the cores from the northern Ewing Terrace

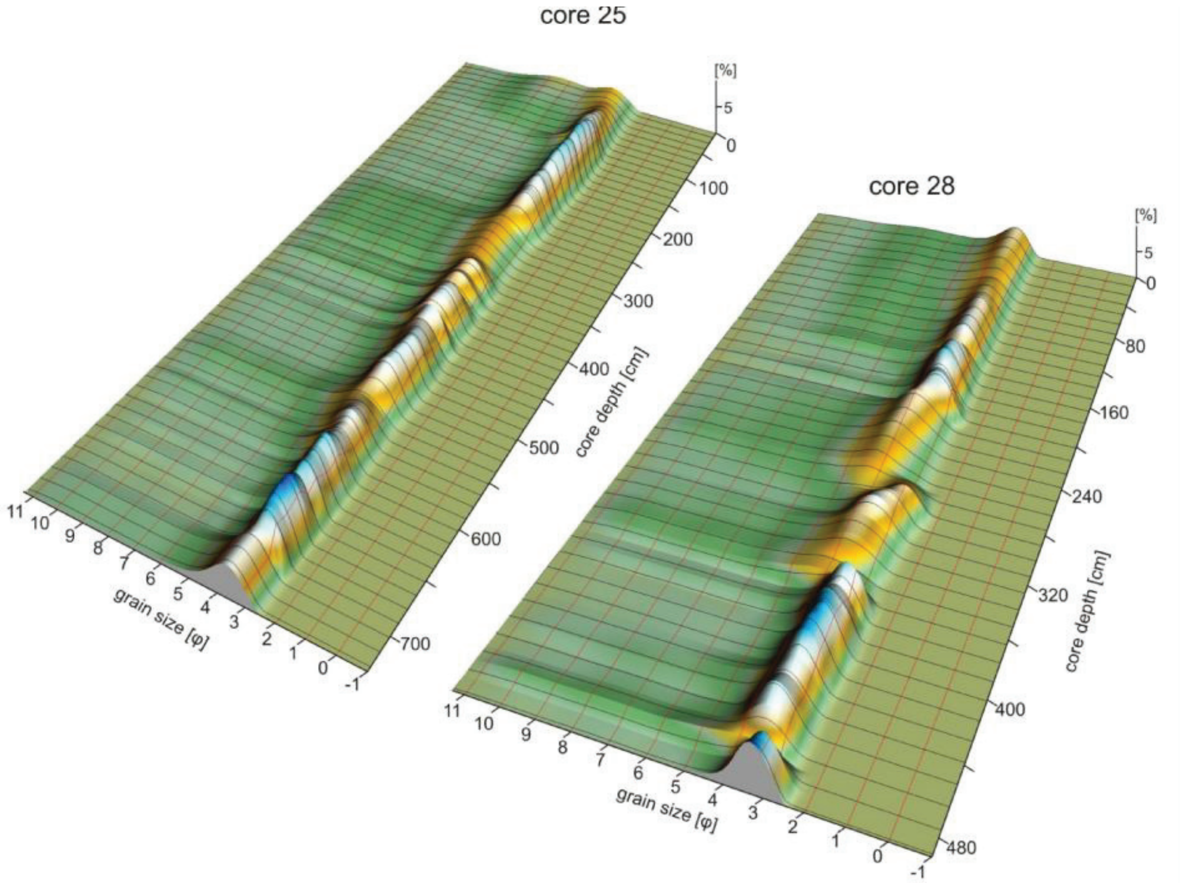

Figure 6.10: Grain size maps of core 25 and 28 following the methodology of Huppertz and Piper (2010), see text for details.

6.4.3. Grain size data and facies

Grain size data is available only from cores 25 and 28 (Figs. 9, 10 and 11). Both cores are dominated by fine sand to coarse silt (3-6 φ, Figs. 9 and 10) with ~20% clay throughout (Figs. 9 and 11). No coarse sand is present. Following the notation of Folk (1974), all of the facies are poorly to very poorly sorted (Fig. 12). Nevertheless, there are some facies which are less sorted (low µm and high Φ values, Fig. 12) than other facies. Facies i and ii are characterized by beds of coarse silt to sand. Facies iii shows a less sorted character than Facies i and ii, but is otherwise quite similar to i and ii. Facies iv is characterized by moderately sorted intervals with lower median values than facies i, ii, and iii (Fig 9, core 25 and Fig. 12). Facies v is characterized by inversely graded sequences and is only moderately sorted. The % SS data does not show any great variability downcore and does not correlate clearly to the different facies (Fig. 9). Core 28 displays inverse grading between 200-255 cm, where laminated facies i and ii occur, and at 280-350 cm depth, where facies v is present (Figs. 9 and 10). Erosional surfaces are absent in these two intervals.

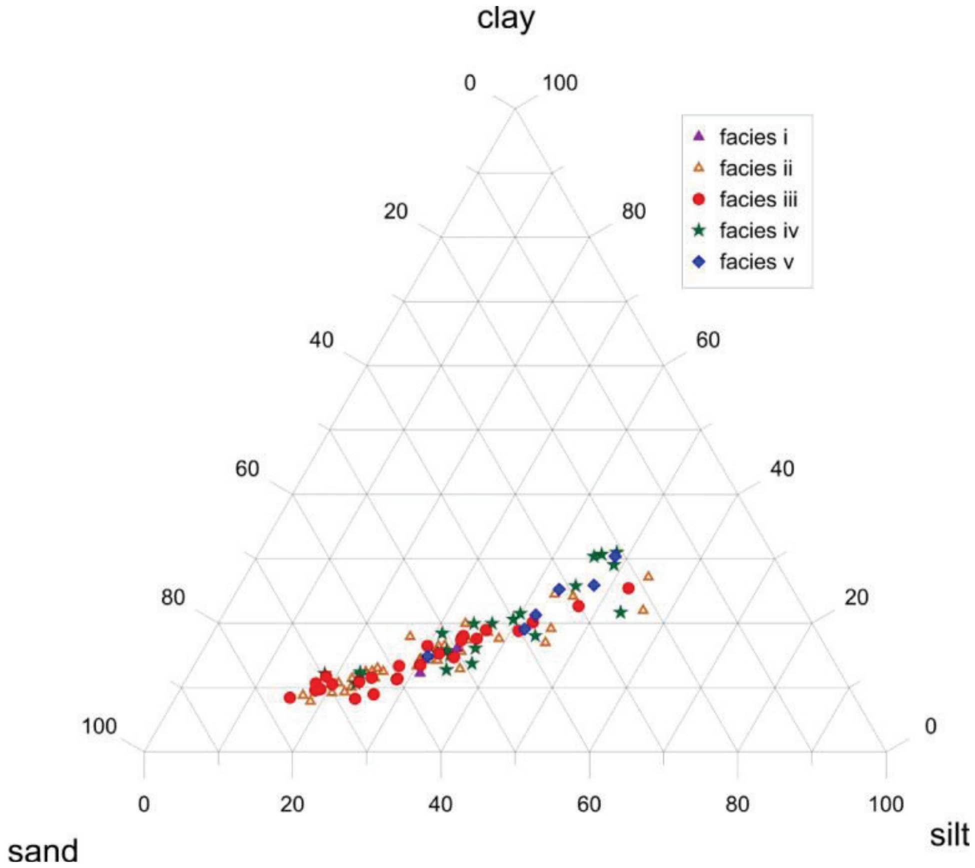

Figure 6.11: Ternary diagram showing the grain size data of the different facies in the cores. This highlights that the overall processes of deposition has not changed significantly over time resulting in homogenous grain size data distributions.

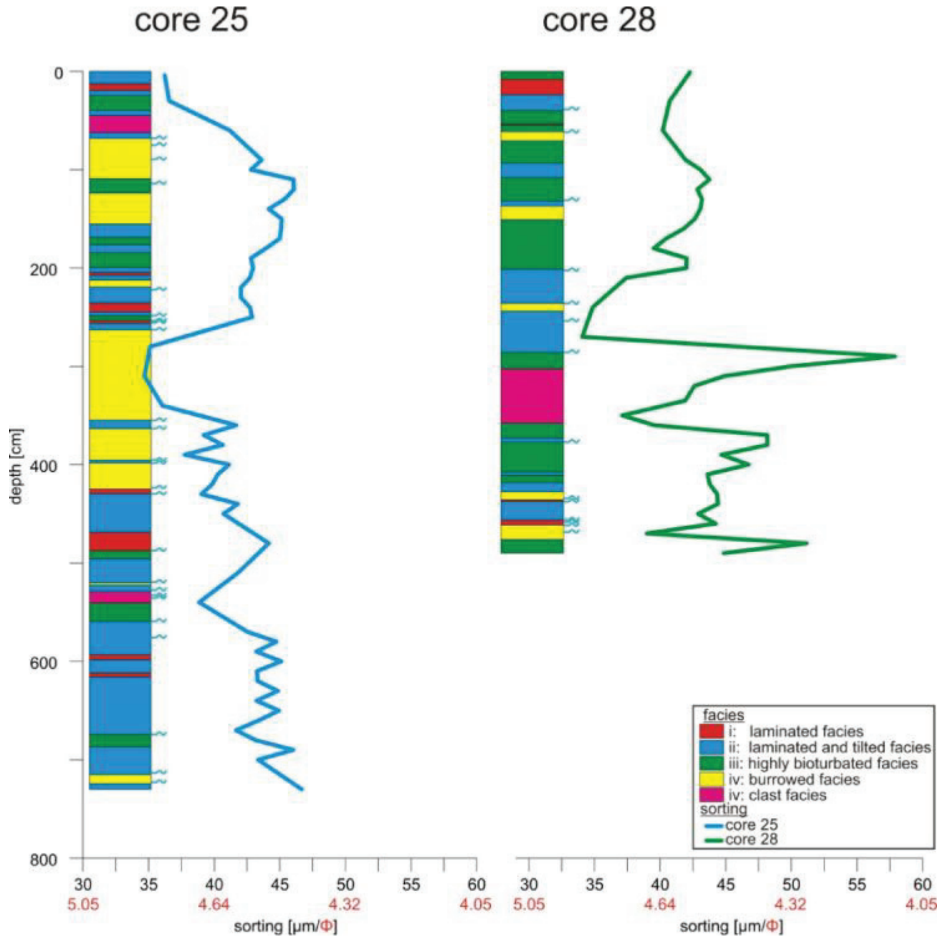

Figure 6.12: Sorting (in µm and Φ) of the grain size data in core 25 and 28 following notations of Folk (1974).

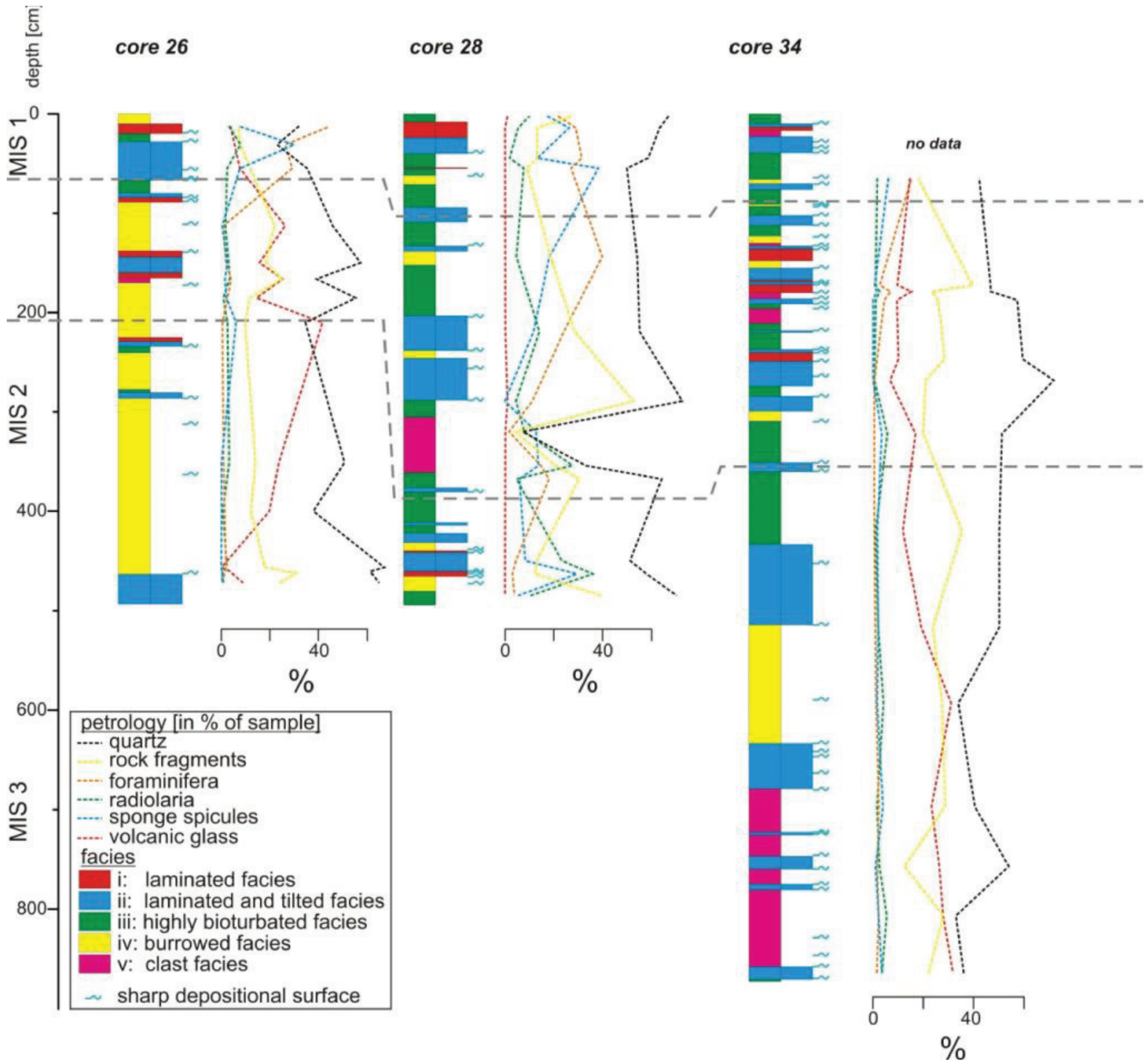

Figure 6.13: Variation of the petrology data (% data can be found in Table 1) downcore and its correlation to the core facies. This shows that the overall petrology does not change significantly downcore. Nevertheless, few levels show changes in the overall composition of the cores.

6.4.4. Petrology

The petrology data (visualized in Fig. 13) does not show strong variance through the different facies (Table 1 and Fig. 13). The dominant component is quartz, which varies between 50-80% downcore. Other important components include dispersed volcanic glass and other rock fragments. Biogenic components are generally low, but include benthic foraminifera, sponge spicules and radiolarians; planktonic foraminifera are only present in the upper ~70-90 cm of the cores (Table 1). Thus, the petrology data does indicate that the source of the material has not changed in a prominent manner over time.

Small shell fragments (>500 μm) and the occurrence of the benthic foraminifera *A. angulosa* throughout the cores may indicate the sources of the sediments from outer shelf areas, where these foraminifera most commonly occur (Harloff and Mackensen, 1997 and references therein). Few levels show independent of the facies very few or the lack of the *A. angulosa* foraminifera (Fig. 5).

Table 6-1: Petrology data of the cores from the La Plata Terrace, tr indicates trace or no occurrence; graphical display of petrology data can be found in Fig. 13 later on in this chapter.

		% sand fraction components					
core	depth	quartz	rock fragments	foraminifera	radiolaria	sponge spicules	volcanic glass
core 26	12 cm	32.12	7.08	44.56	3.11	6.74	3.80
	32 cm	22.61	7.99	26.32	7.99	28.65	5.65
	55 cm	35.71	11.58	29.34	2.51	7.53	7.72
	113 cm	45.98	22.30	0.92	1.84	0.46	26.44
	150 cm	57.74	18.18	1.97	2.95	2.46	15.72
	166 cm	38.32	24.80	4.10	3.48	1.64	25.20
	185 cm	56.01	11.59	2.58	0.86	2.15	14.38
	210 cm	34.45	9.77	0.51	2.57	6.17	41.90
	350 cm	50.89	14.00	0.99	3.16	tr	23.87
	400 cm	37.76	12.24	1.45	0.83	tr	19.92
	457 cm	67.46	17.99	2.12	2.38	tr	tr
	461 cm	61.17	31.94	1.46	0.63	tr	3.55
	473 cm	65.13	23.25	0.51	0.34	0.85	9.57
core 28	3 cm	42.02	17.15	13.55	6.35	10.81	0.69
	15 cm	39.71	8.23	18.16	3.39	16.46	tr
	45 cm	36.73	8.24	19.76	1.21	8.36	tr
	55 cm	31.32	5.55	16.97	4.89	23.98	tr
	145 cm	34.02	11.75	25.15	2.89	11.34	tr
	220 cm	34.54	17.84	15.18	8.92	7.40	tr
	290 cm	45.47	33.19	7.11	2.80	tr	0.65
	320 cm	3.47	2.55	0.93	5.09	8.10	tr
	355 cm	21.94	13.08	9.28	17.72	8.65	tr
	368 cm	40.04	19.21	11.49	2.87	3.59	tr
	450 cm	32.27	8.16	2.84	14.54	5.32	tr
	463 cm	36.57	7.62	1.90	22.86	19.43	tr
	485 cm	44.00	24.75	2.50	6.50	3.25	tr
core 34	63 cm	42.43	17.66	15.37	1.61	6.19	14.91
	171 cm	46.88	39.51	2.46	0.89	0.67	9.60
	177 cm	46.99	23.26	6.96	2.69	1.58	15.66
	185 cm	57.14	25.81	4.51	1.00	tr	9.52
	245 cm	59.26	28.86	1.02	0.26	tr	10.22
	267 cm	71.89	20.77	0.41	0.41	tr	6.52
	320 cm	51.19	19.93	0.55	5.85	3.47	16.82
	415 cm	49.82	35.54	0.54	0.89	1.61	11.61
	510 cm	50.90	23.55	1.20	1.80	1.80	18.76
	590 cm	33.79	27.57	1.17	4.08	1.36	31.26
	690 cm	40.48	28.67	2.17	1.69	3.86	23.13
	750 cm	54.09	12.37	1.68	2.52	1.05	26.42
	800 cm	32.71	27.76	2.12	5.41	2.12	27.76
	860 cm	35.92	21.84	1.46	3.40	3.40	32.04

6.4.5. Grain size, color and susceptibility data

When comparing the grain size data derived from the sieving for petrology to the coulter laser dataset, it shows that the overall trends can be imaged in the data, but the finest fraction is underestimated by the laser analyzer. Nevertheless, estimates of the overall percentage in the sand fraction seem to agree with the laser data (Fig. 5, core 28).

Similarly, the magnetic susceptibility data follows the general trend of the sand in the cores (Fig. 7). Thus, the magnetic minerals responsible for the magnetic susceptibility record are possibly within the sand fraction (Table 1). This is in contrast to the R color value, which anti-correlates to the sand content and thus the magnetic susceptibility data (Fig. 7). Nevertheless, color testing on the <53µm fraction did not support the idea that the red signal is found within the <53 µm fraction (Fig. 7, inset a).

6.4.6. Parasound data

Parasound and multibeam data on the northern Ewing terrace shows a mounded structure (Figs. 2, 14 and 15). Reflections A1-A5 were established locally to understand the local architecture of this part of the terrace (Figs. 14 and 15). The relief of the structure is ~30 m and drops to three sides into either canyons or the open slope (Fig. 2). Parasound data shows a major regional erosional surface at ~ 25 ms (~20 m) depth (Fig. 14), termed A5. Above the contact, the seismic character is poorly laminated and has units showing a chaotic appearance. These seem to mostly pinch out towards the shelf break (to the NW), whereas seawards they terminate abruptly on inclining slopes (Fig. 15). Erosional surfaces and onlap structures are frequently observed. Below the surface, well-stratified sequences dominate and little major erosion is observed.

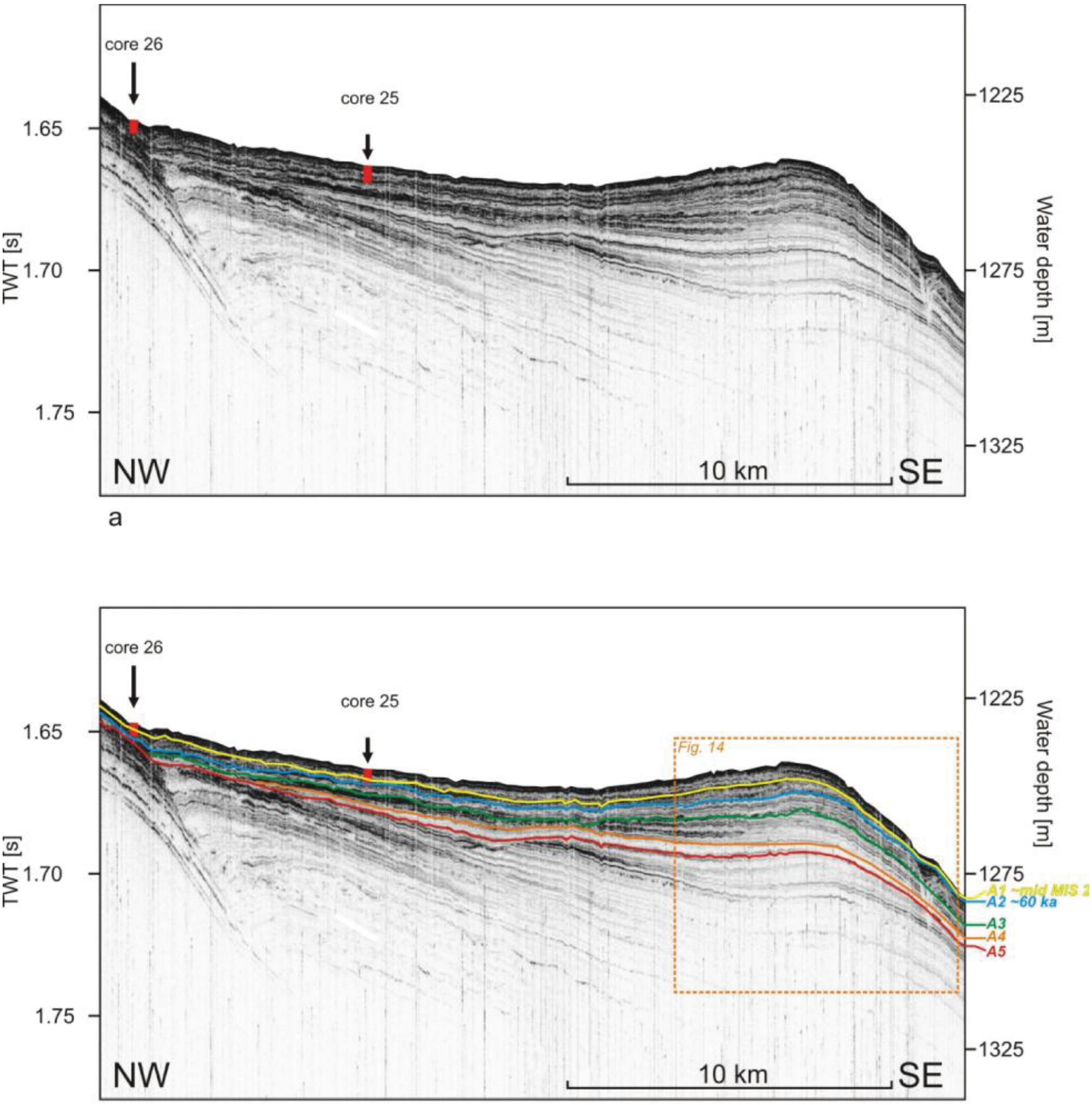

Figure 6.12 Parasound data from the Ewing terrace showing the core positions of core 25 and 26 and the very local seismic stratigraphy of reflections A1-A5. A5 represents a major change in style of sedimentation from a current dominated regime below A5 to a downslope-dominated regime above A3. The reflections of A1 and A2 could be dated by core 25 (see Fig. 15).

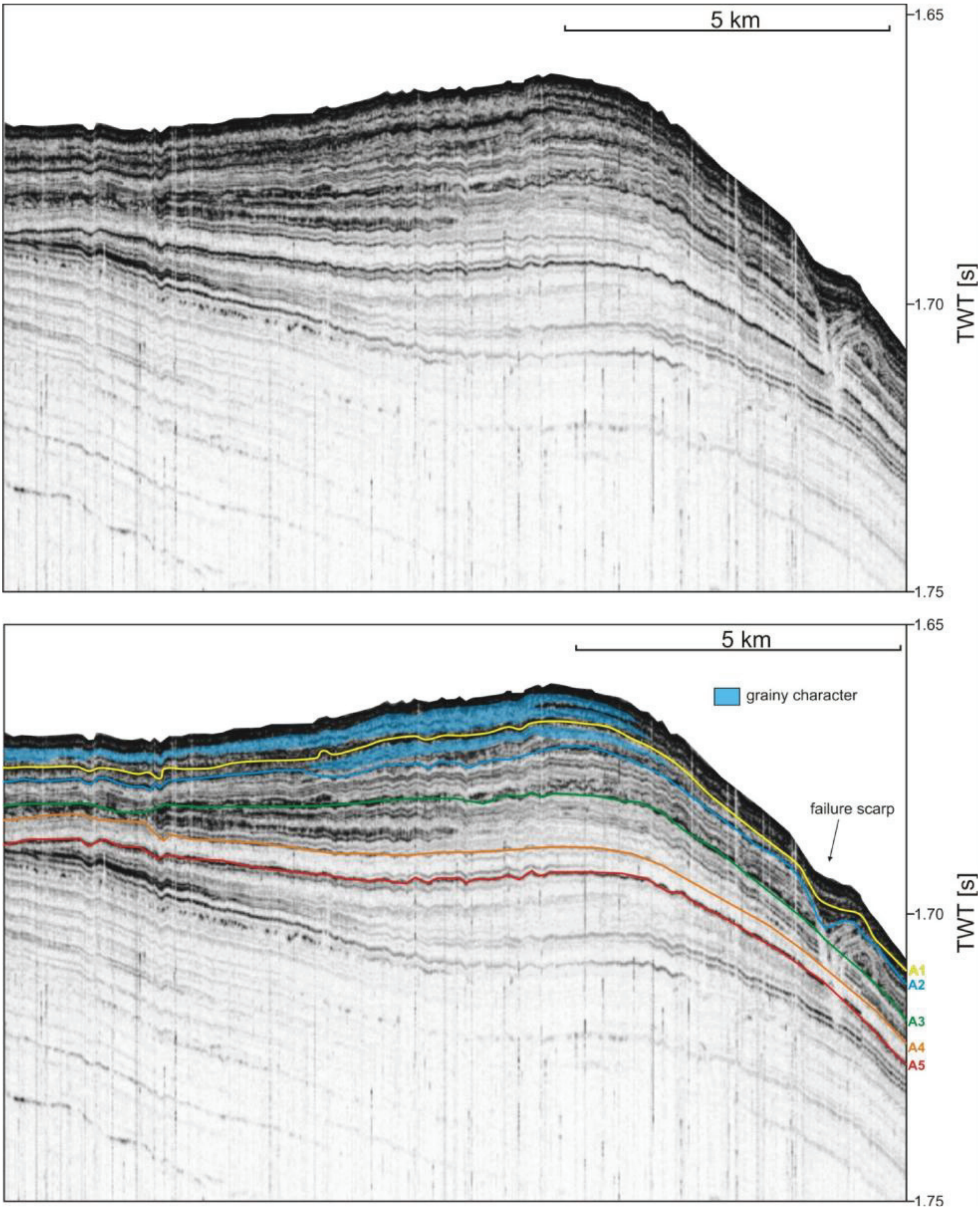

Figure 6.13: Enlarged Parasound image of the mound shown in Fig. 14. The seismic stratigraphy is shown again (see also Fig. 14); additionally, grainy appearing facies are shown in blue and a major scarp is annotated.

6.5. Discussion

6.5.1. Spatial and temporal distribution of facies

The spatial and temporal distribution of the different facies can be established from the regional age model presented earlier and summarized in Figs. 4 and 9. There is no obvious correlation of Pleistocene sea level variations to the different facies, which appear random in their occurrence (Fig. 16). The laminated intervals i and ii always occur in stacks and are in places inter-bedded with facies iii (e.g. Fig. 9, core 25 ~180-280 cm). This is in contrast to the other facies, which do not show such a clear stacking or repetitive occurrence downcore (Fig. 9). Facies iv is usually thick bedded (more than a meter is common (Fig. 9)), facies v occurs apparently randomly throughout the cores and has generally a thickness of 10-30 cm (Fig. 9).

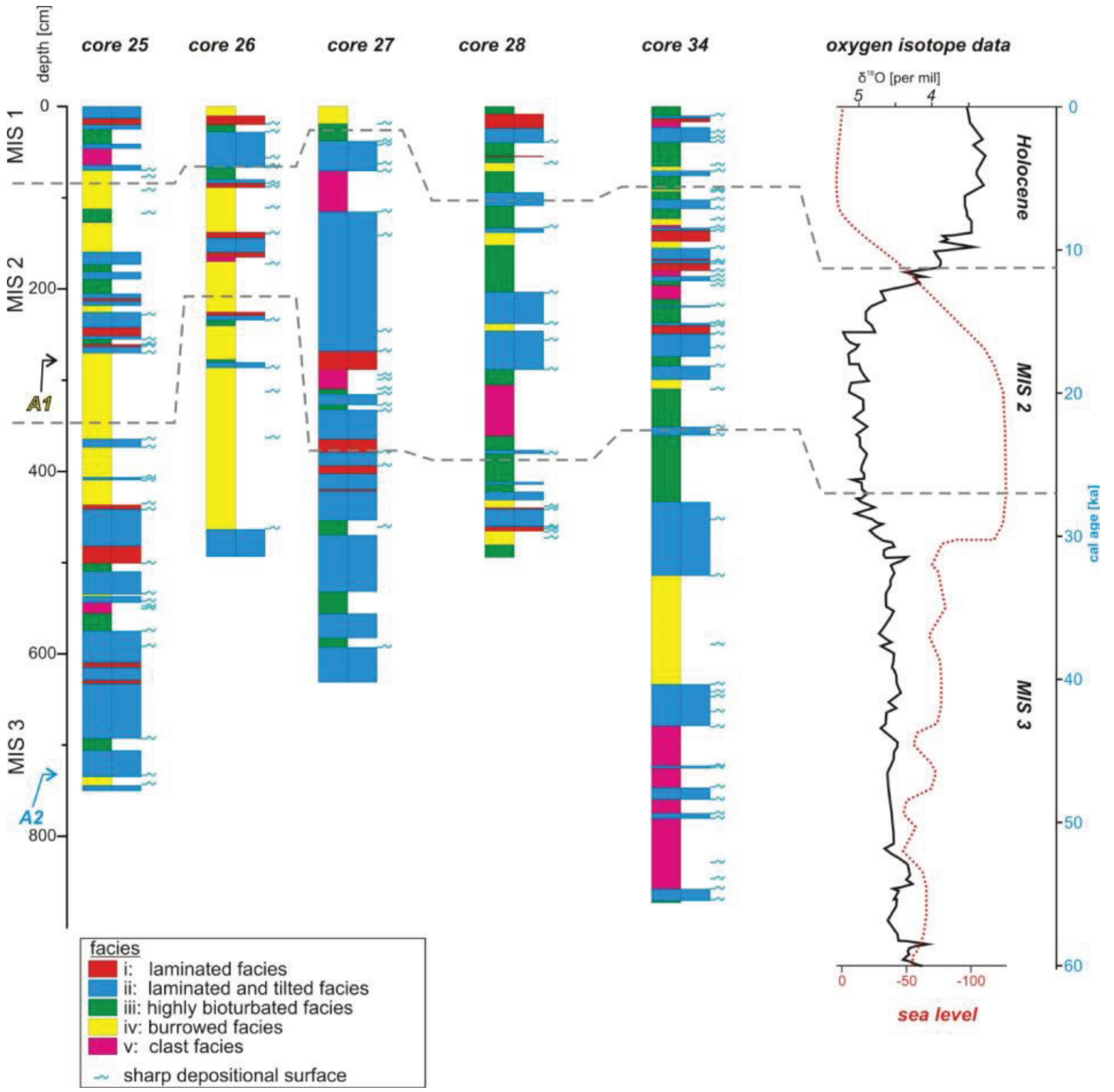

Figure 6.14: Sedimentary facies in cores and their relationship to sea level (Lambeck and Chappell, 2001) and the oxygen isotope data (Shackleton et al., 1983) and thus calibrated ages. Sea level is independent of the different facies that occur random in the cores. This agrees with their interpretation as storm event deposits (see text for details). The positions of the reflections A1 and A2 are also shown (see also Fig. 13).

6.5.2. Facies characterization

The different facies can be characterized by different parameters including petrology data, color data, grain size distribution and magnetic susceptibility data. The petrology data (125-500 μm) (Table 1) and the grain size data (Figs. 9 and 11) indicate no significant change in source material, as their overall distributions does not change greatly downcore. Nevertheless, the grain size data does show some downcore variability, suggesting that the process of deposition has differed over time. Source areas remained similar, as the oceanic circulation on the shelf south of the Brazil Malvinas confluence zone does not differ greatly from the setting of the upper slope (Stramma and England, 1999; Piola and Matano, 2001; Zavialov et al., 2003; Piola et al., 2008a).

Table 6-2.: Sedimentary facies and their depositional interpretation

facies	sedimentological character	depositional process	general depositional environment	interpretation
(i) well laminated facies	well laminated; locally subhorizontally bedding	wave-supported gravity flows/ tempestites	high energetic system	wave supported gravity flows
(ii) laminated and tilted facies	laminated sequences, frequently tilted	burrowed gravity flows	high energetic system	contourites and/or gravity flows
(iii) highly bioturbated facies	highly bioturbated sequences, destuction of all sedimentary structures	reworking of facies i, ii and iv	reworking in a quiescent environment with little down and alongslope movement	reworking of other facies present
(iv) burrowed facies	burrows dominate, can be linked to organism, presevation of bedding rarely observed	contourite in the sense of gentle alongslope movement	alongslope movement with low flow speeds typical for muddy contourites	sediment straved contourite
(v) clasts facies	laminated and un-laminated clasts in muddy matrix, erosional surfaces common	mass transport deposit	hmid-high energy forming small MTDs with low flow speeds and little spatial displacement	mass wasting

Facies i and ii are characterized by high sand content (up to 60%), higher magnetic susceptibility data (Fig. 7) and show generally smaller foraminifera compared to e.g. Facies iv. Facies i and ii also show less overall biogenic material and fewer counts of siliceous organisms. The red trace is low. Sharp depositional surfaces are mostly found within these two facies whereas they are relatively less common in the other facies (Fig. 7).

Facies iv is, in contrast, characterized by low sand content (~20%) and thus low magnetic susceptibility values (Fig. 7). Clay values can reach up to 30%. High red color values are characteristic. Petrology data shows overall more foraminifera specimen and more calcareous and siliceous biogenic fragments.

Facies iii and v do not show any clear trends in the grain size, magnetic susceptibility or color data (Fig. 7).

6.5.3. Facies interpretation

The temporal and spatial distribution of the different facies can be established from the regional stratigraphic framework, presented in section 4.1 and summarized in Figs. 9 and 15. There are generally two types of surfaces present in the cores. Few of these surfaces are truly erosional. These are shown in Fig. 3 and are characterized by the removal of material at their base. This is supported by jumps in the color and magnetic susceptibility data (Fig. 7). These true erosional surfaces are distinctly different from other sharp contacts in the cores, shown on e.g. Fig. 5. Little or no erosion has occurred at these surfaces, as the oxygen isotope curves (Fig. 4) do not show any significant jumps. Furthermore, only in few cases are structures truly cut (Fig. 8). Therefore, these surfaces are interpreted as sharp depositional surfaces over a highly bioturbated and thus irregular seafloor.

The spatial and temporal distribution of the laminated facies i and ii and its relationship to the other facies in the cores and its setting along the continental margin (Figs. 1, 2 and 9) suggests, that these sediments have been deposited rapidly, showing minor basal erosion or a rapid change in style of sedimentation, and lateral thinning (Fig. 14). There are four possible processes of forming such facies: (a) direct input of sediment from hyperpycnal flows (Mulder et al., 2003), (b) pro-delta slumping forming turbidity currents (Postma, 1984), (c) contour current activity (benthic storms, contourite deposition) (Weatherly and Kelley, 1985; Stow et al., 2008) or (d) wave supported sediment gravity flows (Wright and Friedrichs, 2006). All four possibilities will be evaluated in context of the data.

The (a) direct input of sediment by hyperpycnal flows can generally only be observed close to the source of the sediment discharge (Mulder et al., 2003), but on the Ewing terrace, this interpretation is not likely as some of the laminated intervals also occur during sea level highstands (Fig. 16). During these times, the possible sources of the hyperpycnal flows, the La Plata rivers, are (I) too far away, and (II) previous studies have suggested that it is unlikely that this river system is capable of forming frequently hyperpycnal flows (Mulder and Syvitski, 1995).

A similar case must be made for the (b) pro-delta slumping and resulting turbidity currents. The laminated facies i and ii do not only occur during lower and rising sea level but also during sea level highstands (Fig. 16), when the delta of the La Plata rivers is within the Rio de la Plata estuary (Fig. 1). During this time, only a small fraction of coarse-grained sediment reaches the shelf edge seawards of the Rio de la Plata estuary (Fig. 1) (Cavallotto et al., 2004; Violante and Parker, 2004). Additionally, during sea level lowstands in glacial times(Guilderson et al., 2000), the delta of the La Plata Rivers was to the north of the study area (Martins and Willwock, 1987).

Ocean currents are capable of winnowing slope sediments during deep-sea contour current storms (benthic storms) (Weatherly and Kelley, 1982; 1985). More persistent contour current flow having bed loads over long time scales may result in contourite deposition (Stow et al., 2008). During such events, mostly silt-sized sediments can be transported alongslope within an ocean current (Weatherly and Kelley, 1985; Faugères and Stow, 1993). Such sediments are generally thoroughly bioturbated sequences with few sedimentary structures remaining (McCave, 1985), unless high sedimentation rates enables preservation. Facies i and ii show low mud content throughout (Fig. 9). This mud would generally be winnowed out by the current (McCave, 1985; McCave and Hall, 2006) unless introduced later by bioturbation. This bioturbation, needed to explain the ~10% clay, is not observed in facies i (Figs.8 and 9), but possibly within facies ii. The % SS indicates flow speeds observed generally in sandy contourite systems (McCave, 2007), which would generally not allow mud sedimentation, even when taking flocculation processes into account (Fig. 9) (Stow et al., 2002). The repeatedly un-bioturbated beds (Facies i and ii) within the cores on the Ewing terrace are thus unlikely the product of neither typical turbidity currents (pro-delta slumping or due to hyperpycnal flows).

These facies can thus either be the result of (α) bottom current flow and related depositional processes or (β) the result of wave-supported sediment gravity flows. Facies i tends to be less likely the result of current induced deposition as it is (a) not bioturbated (Fig. 8), has (b) thicknesses of less than 5 cm (Figs. 7 and 8), (c) is frequently found between sharp depositional surfaces (Fig. 5) and (d) has mm-scale structures preserved. Such a setting is very unique in slope systems, and can only be preserved if rapid burial is assured (Wheatcroft, 1990). Thus, event-like deposition is more likely for these beds (facies i) rather than contouritic deposition as suggested by contour currents which are less likely to create such structures.

This is different for facies ii, which does not show structures that are clearly indicative of either (α) benthic storms and contourite deposits or (β) wave supported sediment gravity flows (event bed deposition). Instead, evidence of both processes may be observed within this facies. Therefore, the unambiguous interpretation of this facies is not possible. It is thus suggested that facies ii sequences display the interaction of both processes. This interaction results in very complex internal sedimentary structures (Fig. 8). The interaction of along and downslope processes may result mostly from the reworking of event beds by the contour current after deposition. Such interpretation is supported by the fact that the facies ii dominated core 27 is found on a small, mounded structure (Fig. 18) typical for contourite deposition (Stow et al., 2002). The intensity of contour current reworking, including net sediment export to areas down current, remains unclear.

The highly bioturbated facies iii has lost its original depositional signal and is characterized by intense bioturbation (Fig. 8). Petrology data (Fig. 13), color and magnetic susceptibility data (Fig. 7), and grain size data (Fig. 11) indicate in few cases, when stacked with facies i and ii, their depositional characters, but it can also have a very different character, more similar to Facies iv. Thus, this facies is interpreted as reworking all other facies and has therefore different characters depending on which facies is being reworked. It may also include hemipelagic background sedimentation during times of either no gravity flows or when no contour currents were active or not sufficient strong to rework bottom sediments: formation of coarser grained lags (sand-size) may result from this inability (Stow et al., 2002). This coarse lag would have been removed during current strengthening, and therefore has mostly not been preserved on the northern Ewing Terrace. Seabed photography does show locally the presence of such winnowed coarse lags on parts of the Ewing Terrace (Ewing and Lonardi, 1971).

The less intensely bioturbated Facies iv is characterized by burrows of larger organisms. These burrows can still be linked to the organism. Erosional or sharp depositional surfaces are lacking (Fig. 5). This facies is characterized by a smaller sand fraction compared to facies i and ii and shows reddish colors throughout (Fig. 7). Larger and overall more foraminifera and higher biogenic debris suggests a change in source material. This muddy facies is interpreted as a contourite deposit. This interpretation is supported by the presence of a small, mounded structure on the Ewing terrace (Figs. 14 and 15). The reason for the fine-grained sediment found within this facies may be two-fold: (a) the current is sediment starved or (b) the current is insufficient strong to transport sand. Within this setting, we favor case (a) due to the following reasons: (1) the contour current is of Antarctic sources which has the capability of forming sandy contourites to the south (Hernández-Molina et al., 2009), (2) the current has created facies ii deposits, which are sandy winnowed event-deposits, (3) the distribution of sand on the terrace is highly variable (Figs. 2 and 3) and (4) the study area is downcurrent of the Mar del Plata canyon (Fig. 1) which may act as a sediment trap (Voigt et al., 2011) or changes flow dynamics greatly, as it was shown on other margins in similar settings (Marchès et al., 2006; Marchès et al., 2007; Marchès et al., 2010).

The clast facies, Facies v, is characterized by clasts between 1-15 cm diameter (Fig. 8), displaying typical mud clast conglomerates described from mass transport deposits (Jenner et al., 2007). These clasts may show sub-cm-scale lamina and lithological contacts (Fig. 5). This indicates that these deposits have not been transported over large distances, which would destroy these clasts and result in major deformation (Tripsanas et al., 2008).

6.5.4. High resolution seismic architecture

When looking at the high resolution Parasound data, the major erosional surface A5 (Fig. 14) can be traced throughout the terrace. No age control is currently available for this erosional surface. Nevertheless, contour current activity has been responsible for the unit below A5 as it was shown on a regional scale on the Argentine margin

(Hernández-Molina et al., 2009). Since formation of the A5 reflection, the seismic expression has changed within the section (Figs. 14 and 15).

Core data suggests a sequence characterized by along and downslope driven processes (Fig. 17). Seismic data supports such an interpretation (Fig. 14), as elements indicative of alongslope and downslope driven processes can be found, e.g. a small mound (Fig. 15) on the terrace, which has a gentle slope on the shelf side and drops off steeply onto the slope is typical of contourite systems (Hernández-Molina et al., 2008b). Nevertheless, downslope driven flow deposits are intercalated and reworked within the mound as seen in e.g. few erosional surfaces, grainy (sandy) appearing units (Fig. 3) and in core data the presence of facies i and especially facies v indicative of downslope driven transport (Fig. 7 and Table 2).

6.5.5. Alongslope versus downslope sediment transport

It has previously been suggested, that the sediments on the Ewing Terrace were exclusively deposited through contour current activity dominating sedimentation patterns on this slope. This preliminary interpretation was based on sedimentary structures and on low resolution seismic data (Bozzano et al., 2010; Huppertz et al., 2010). Using the newer datasets including especially grain size data (Fig. 10) and high-resolution Parasound data (Fig. 14), this interpretation may need some modifications. This slope has alongslope components as well as downslope processes acting (Table 2). The downslope processes are in form of wave-supported gravity flows and are at times the dominating process on the slope (Fig. 5, Table 2).

The contour current processes were active throughout time along this slope, but were generally sediment-starved (Figs. 7, 15 and 17), due to lack of material available for take-up. This resulted in mud-dominated contour currents. Coarse material was supplied only randomly from the shelf during (Pleistocene) storm events as wave supported sediment gravity flows. Several flows were initiated preceding each other in short intervals (days to weeks) during times of storm tracking and occur thus frequently stacked (Fig. 5), allowing preservation of earlier (deeper) flows and allowing only the most recent flows to be reworked by the contour current forming facies ii deposits.

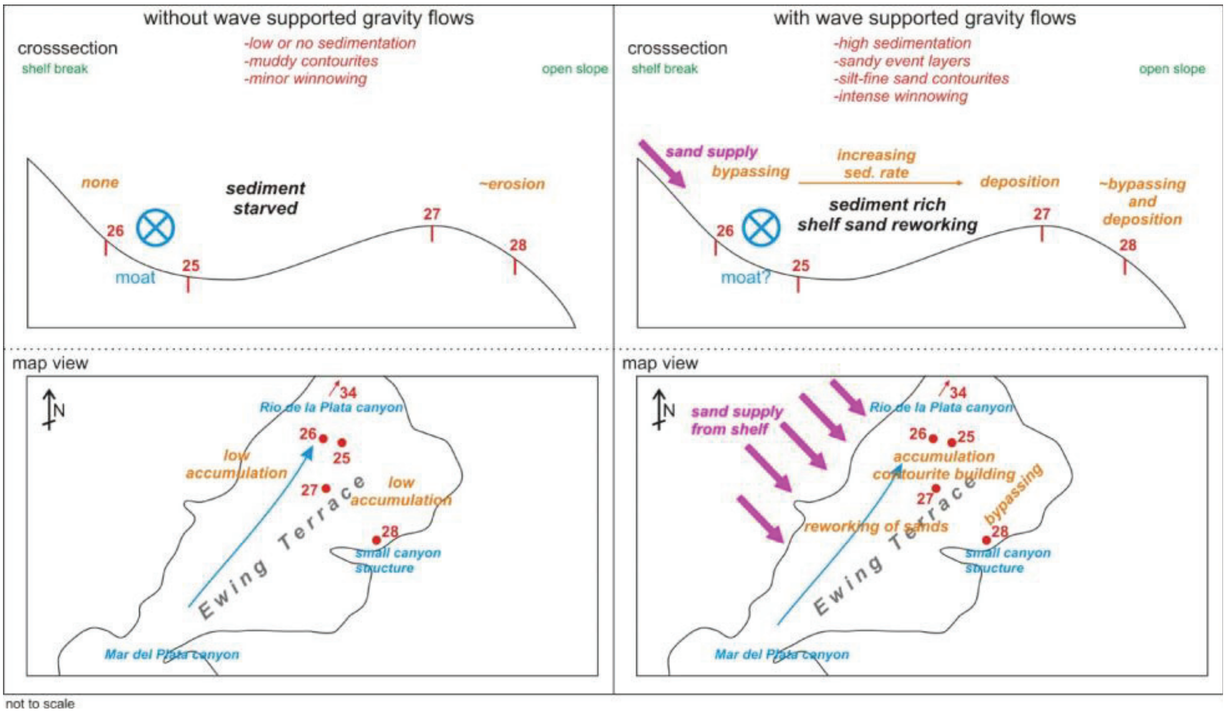

Figure 6.15: Schematic sketch showing the main two modes of sedimentation on the northernmost Ewing terrace on the Argentine slope. Deposition is highly dependent on the frequency and volume of wave-supported gravity flows, which supply sediment to the otherwise sediment-starved current, which generally only forms fine-grained contourites. After supply of sand to the system, this sand may be subject to reworking by the bottom current forming mounded structures on the terrace. This is only the case when the gravity flows are not rapidly buried and are thus being winnowed; the blue circle with the X indicates a possible position of the ocean current core related to a moat structure (Fig. 13).

6.5.6. General model of deposition for the northern Ewing Terrace

Using the sedimentological (Figs. 7 and 10) and acoustic (Fig. 14) results, a general model of sedimentation processes is developed for the northernmost Ewing Terrace on the northern Argentine slope (Fig. 17). The slope sedimentation is driven by two main processes: (1) wave-supported sediment gravity flows transport pre-sorted shelf sands to the terrace, and (2) contour currents. Thus, there can be two different modes of deposition occurring on the terrace (Fig. 17). During times of no wave supported gravity flows, the system is sediment-starved and therefore transports mud, which is the only grain size available to the current. This forms the observed facies iv. Additionally, reworking of underlying facies ii may occur and results in facies iii.

When wave-supported sediment gravity flows are present during storm events, the depositional processes on the Ewing terrace are greatly different (Fig. 17) and characterized by high sand supply from the shelf causing increased sedimentation rates throughout the terrace. Depending on the frequency between flows, these result in either facies i which represents well-preserved gravity flows, or facies ii and iii, which are facies modified to different extents by later reworking processes including winnowing and bioturbation. These gravity-driven flows also supply coarse sediment, which is then entrained onto the Antarctic-sourced ocean currents and used to construct coarser-grained contourite deposits.

6.6. Conclusion

The interaction of alongslope processes, namely benthic storms or contourites and downslope processes in the form of wave supported sediment gravity flows have been described from the northern-most Ewing terrace on the Argentine margin. Five different sedimentary facies could be detected on the terrace. Each facies describes a specific depositional environment linked to either alongslope processes or mass wasting or the interaction of both processes.

Using the spatial and temporal distribution of the different facies on the terrace, two different depositional modes could be observed: The contourite system is generally sediment starved. During intense (mostly Pleistocene) storm events, shelf material is mobilized and transported to the terrace. Here, the sediment is either rapidly buried and thus preserved as event beds, or is reworked by the ocean currents forming drift deposits. Other forms of mass wasting are only rarely observed.

6.7. References

Adams, E.A. and Schlager, W., 2000. Basic types of submarine slope curvature. Journal of Sedimentary Geology, 70(4): 814-828.

Aksu, A.E. and Hiscott, R.N., 1989. Slides and debris flows on the high-latitude continental slopes of Baffin Bay. Geology, 17(10): 885-888.

Anderson, J.B., Kurtz, D.D., Domack, E.W. and Balshaw, K.M., 1980. Glacial and glacial marine sediments of the Antarctic continental shelf. Journal of Geology, 88(4): 399-414.

Angulo, R.J., Lessa, G.C. and de Souza, M.C., 2006. A critical review of mid- to late-Holocene sea-level fluctuations on the eastern Brazilian coastline. Quaternary Science Reviews, 25(5-6): 486-506.

Antobreh, A.A., 2005. Channelised and open-slope processes of mass sediment transport: their morphological and seismic characterisation from selected Atlantic high productivity regions. Ph. D. Thesis, University of Bremen, Bremen, 130 pp.

Antonioli, F., Bard, E., Potter, E.-K., Silenzi, S. and Improta, S., 2004. 215-ka History of sea-level oscillations from marine and continental layers in Argentarola Cave speleothems (Italy). Global and Planetary Change, 43(1-2): 57-78.

Arhan, M., Naveira Garabato, A.C., Heywood, K.J. and Stevens, D.P., 2002. The Antarctic Circumpolar Current between the Falkland Islands and South Georgia. Journal of physical Oceanography, 32(6): 1914–1931.

Armishaw, J.E., Holmes, R.W. and Stow, D.A.V., 1998. Morphology and sedimentation on the Hebrides Slope and Barra Fan, NW UK continental margin. In: M.S. Stoker, D. Evans and A. Cramp (Editors), Geological processes on continetal margins: mass-wasting and stability. Geological Society, Special Publication 129, London, pp. 81-104.

Assumpcao, M., 1998. Seismicity and stresses in the Brazilian passive margin. Bulletin of the Seismological Society of America, 88(1): 160-169.

Baltzer, A., Cochonat, P. and Piper, D.J.W., 1994. In situ geotechnical characterization of sediments on the Nova Scotian Slope, eastern Canadian continental margin. Marine Geology, 120(3-4): 291-308.

Baltzer, A., Holmes, R. and Evans, D., 1998. Debris flows on the Sula Sgeir Fan, NW of Scotland. In: M.S. Stoker, D. Evans and A. Cramp (Editors), Geological processes on continental margins: sedimentation, mass-wasting and stability. Geological Society, 129, London, pp. 105-115.

Baracco, R., Garcia-Rodriguez, F., del Puerto, L., Inda, H. and Castineira, C., 2008. Holocene relative sea-level variation inferred from records in the basin of Castillos, Shallow Lakes Conference 2008: Structure and function of world shallow lakes, Punta del Este, Uruguay, pp. 75.

Beaubouef, R.T. and Friedmann, S.J., 2000. High resolution seismic/sequence stratigraphic framework for the evolution of Pleistocene intra slope basins, western Gulf of Mexico: depositional models and reservoir analogs, GCSSEPM Foundation 20th Annual Research Conference: Deep Water reservoirs of the World, Houstan, TX, pp. 40-60.

Benavídez Sosa, A., 1998. Sismicidad y sismotectónica en Uruguay. Fisica de la Tierra, 10: 167-186.

Benetti, S., 2006. Late Quaternary sedimentary processes along the western North Atlantic margin. Ph. D. Thesis, University of Southampton, Southampton, 188 pp.

Benthien, A. and Müller, P.J., 2000. Anomalously low alkenone temperatures caused by lateral particle and sediment transport in the Malvinas Current region, western Argentine Basin. Deep Sea Research Part I: Oceanographic Research Papers, 47(12): 2369-2393.

Berbery, E.H. and Barros, V.R., 2002. The hydrologic cycle of the La Plata Basin in South America. Journal of Hydrometeorology, 3(6): 630-645.

Berry, J.A. and Piper, D.J.W., 1993. Seismic stratigraphy of the central Scotian rise: a record of continental margin glaciation. Geo-Marine Letters, 13(4): 197-206.

Bianchi, A.A., Giulivi, C.F. and Piola, A.R., 1993. Mixing in the Brazil-Malvinas confluence. Deep Sea Research Part I: Oceanographic Research Papers, 40(7): 1345-1358.

Blanc, S., Goni, G. and Novarini, J., 1983. Surface mixed layer temperature and layer depth in water off the Argentinian coast. Journal of Geophysical Research, 88(C10): 5987–5996.

Blatt, H., Middleton, G. and Murry, R., 1980. Origin of sedimentary rocks. Prentice-Hall, Inc., Englewood Cliffs, New Jersey, 782 pp.

Blum, M.D. and Törnqvist, T.E., 2000. Fluvial responses to climate and sea-level change: a review and look forward. Sedimentology, 47: 2-48.

Boczar-Karakiewicz, B., Bona, J.L. and Pelchat, B., 1991. Interaction of internal waves with the seabed on continental shelves. Continental Shelf Research, 11(8-10): 1181-1197.

Boltovskoy, E., Boltovskoy, D., Correa, N. and Brandini, F., 1996. Planktic foraminifera from the southwestern Atlantic (30 °–60 °S): species-specific patterns in the upper 50 m. Marine Micropaleontology, 28(1): 53-72.

Bondevik, S., Mangerud, J., Birks, H.H., Gulliksen, S. and Reimer, P., 2006. Changes in North Atlantic radiocarbon reservoir ages during the Allerød and Younger Dryas. Science, 312(5779): 1514-1517.

Bouma, A.H., 1962. Sedimentology of some flysch deposits. Elsevier Publishing Company, Amsterdam, 168 pp.

Bouma, A.H., 2004. Key controls on the characteristics of turbidite systems. In: S.A. Lomas and P. Joseph (Editors), Confined turbidite systems. Geological Society, London, Special Publication 222, London, pp. 9-22.

Boyle, E.A., 1997. Characteristics of the deep ocean carbon system during the past 150,000 years: ΣCO_2 distributions, deep water flow patterns, and abrupt climate change. Proceedings of the National Academy of Sciences of the United States of America, 94(16): 8300-8307.

Bozzano, G., Violante, R.A., Paterlini, M., Hernández-Molina, F.J., Hanebuth, T.J.J., Huppertz, T.J., Strasser, M., Razik, S., Orgeira, M.J. and Krastel, S., 2010. The contourite drift over the Ewing Terrace (NE Argentina, SW Atlantic). Geo-Temas, 11: 25-26.

Brink, K.H., Bane, J.M., Church, T.M., Fairall, C.W., Geernaert, G.L., Hammond, D.E., Henrichs, S.M., Martens, C.S., Nittrouer, C.A., Rogers, D.P., Roman, M.R., Roughgarde, J.D., Smith, R.L., Wright, L.D. and Yoder, J.A., 1992. Coastal ocean processes: a science prospectus. Technical Report WHOI-92-18, Wood Hole Oceanographic Institute.

Bryn, P., Berg, K., Stoker, M.S., Haflidason, H. and Solheim, A., 2005a. Contourites and their relevance for mass wasting along the mid-Norwegian margin. Marine and Petroleum Geology, 22(1-2): 85-96.

Bryn, P., Berg, K., Forsberg, C.F., Solheim, A. and Kvalstad, T.J., 2005b. Explaining the Storegga Slide. Marine and Petroleum Geology, 22(1-2): 11-19.

Cacchione, D.A., Pratson, L.F. and Ogston, A.S., 2002. The shaping of continental slopes by internal tides. Science, 296: 724-727.

Came, R.E., Oppo, D.W. and Curry, W.B., 2003. Atlantic Ocean circulation during the Younger Dryas: Insights from a new Cd/Ca record from the western subtropical South Atlantic. Paleoceanography, 18(4): 1086.

Campbell, D.C., 2000. Relationship of sediment properties to failure horizons for a small area of the Scotian Slope. Current research 2000-D8, Geological Survey of Canada, Dartmouth.

Campbell, D.C., Shimeld, J.W., Mosher, D.C. and Piper, D.J.W., 2004. Relationships between sediment mass-failure modes and magnitudes in the evolution of the Scotian Slope, offshore Nova Scotia, Offshore Technology Conference, Houston, Texas, pp. OTC 16743.

Campbell, D.C. and MacDonald, A.W.A., 2006. Geohazard assessment of five deepwater pipeline scenarios on the Scotian Slope. Open File 5079, Geological Survey of Canada, Ottawa.

Cao, L., Fairbanks, R.G., Mortlock, R.A. and Risk, M.J., 2007. Radiocarbon reservoir age of high latitude North Atlantic surface water during the last deglacial. Quaternary Science Reviews, 26(5-6): 732-742.

Carter, L., 2007. The role of intermediate-depth currents in continental shelf-slope accretion: Canterbury Drifts, SW Pacific Ocean. In: A.R. Viana and M. Rebesco (Editors), Economic and palaeoceanographic significance of contourite deposits. Geological Society, Special Publication 276, London, pp. 129-154.

Cavallotto, J.L., Violante, R.A. and Parker, G., 2004. Sea-level fluctuations during the last 8600 years in the de la Plata river (Argentina). Quaternary International, 114(1): 155-165.

Chiessi, C.M., Ulrich, S., Mulitza, S., Pätzold, J. and Wefer, G., 2007. Signature of the Brazil-Malvinas Confluence (Argentine Basin) in the isotopic composition of planktonic foraminifera from surface sediments. Marine Micropaleontology, 64(1-2): 52-66.

Chiessi, C.M., Mulitza, S., Paul, A., Pätzold, J., Groeneveld, J. and Wefer, G., 2008. South Atlantic interocean exchange as the trigger for the Bølling warm event. Geology, 36(12): 919-922.

Chiessi, C.M., Mulitza, S., Pätzold, J. and Wefer, G., 2010. How different proxies record precipitation variability over southeastern South America. IOP Conference Series: Earth and Environmental Science, 9: 012007.

Chubbs, J.F., 2003. Geohazards at the proposed Weymouth wellsite, Central Scotian Slope, offshore eastern Canada. B.Sc. Thesis, Saint Mary's University, Halifax, 75 pp.

Clapperton, C.M., 1993. Quaternary geology and geomorphology of South America. Elsevier, Amsterdam, 780 pp.

Clark, P.U. and Mix, A.C., 2002. Ice sheets and sea level of the Last Glacial Maximum. Quaternary Science Reviews, 21(1-3): 1-7.

Clark, R. and Wilson, P., 1992. Occurrence and significance of ventifacts in the Falkland Islands, South Atlantic. Geografiska Annaler. Series A, Physical Geography, 74(1): 35-46.

Clausen, L., 1998. 1. Late Neogene and Quaternary sedimentation on the continental slope and upper rise offshore southeast Greenland: interplay of contour and turbidity processes. In: A.D. Saunders, H.C. Larsen and S.W. Wise (Editors), Proceedings of the Ocean Drilling Program, Scientific Results, 152, College Station, TX, pp. 3-18.

Coles, V.J., McCartney, M.S., Olson, D.B. and Smethie, W.M., 1996. Changes in Antarctic Bottom Water properties in the western South Atlantic in the late 1980s. Journal of Geophysical Research, 101(C4): 8957-8970.

Coward, M.P., Purdy, E.G., Ries, A.C. and Smith, D.G., 1999. The distribution of petroleum reserves in basins of the South Atlantic margins. In: N.R. Cameron, R.H. Bate and V.S. Clure (Editors), The oil and gas habitats of the South Atlantic. Geological Society, Special Publication 153, London, pp. 101-131.

Cruz, F.W., Burnsa, S.J., Jercinovic, M., Karmann, I., Sharp, W.D. and Vuille, M., 2007. Evidence of rainfall variations in Southern Brazil from trace element ratios (Mg/Ca and Sr/Ca) in a Late Pleistocene stalagmite. Geochimica et Cosmochimica Acta, 71(9): 2250-2263.

Cruz, F.W., Vuille, M., Burns, S.J., Wang, X., Cheng, H., Edwards, R.L., Karmann, I., Auler, A.S. and Nguyen, H., 2009. Orbitally driven east–west antiphasing of South American precipitation. Nature Geosciences, 2(3): 210-214.
Curry, W.B. and Oppo, D.W., 2005. Glacial water mass geometry and the distribution of $\delta^{13}C$ of CO_2 in the western Atlantic Ocean. Paleoceanography, 20: PA1017.
Darwin, C., 1846. Geological observations on South America. Smith, Elder and Co., London, 279 pp.
de Santa Ana, H., Latrónica, L., Tomasini, J., Morales, E., Ferro, S., Gristo, P., Machado, L., Veroslavsky, G. and Ucha, N., 2008. Economic and exploratory review of gas hydrates and other gas manifestations of the Uruguayan continental shelf, 6th International Conference on Gas Hydrates (ICGH 2008), Vancouver, BC , Canada.
Delaney, P.J.V. (Editor), 1966. Geology and geomorpholohy of the coastal plain of Rio Grande do Sul, Brazil and northern Uruguay. Coastal Studies Series, Coastal Studies Series 15. Lusiana State University Press, Baton Rouge, 58 pp.
Delmonte, B., Petit, J.R. and Maggi, V., 2002. Glacial to Holocene implications of the new 27000-year dust record from the EPICA Dome C (East Antarctica) ice core. Climate Dynamics, 18(8): 647-660.
Depetris, P.J. and Griffin, J.J., 1968. Suspended load in the Rio de la Plata drainage basin. Sedimentology, 11(1-2): 53-60.
Depetris, P.J., Kempe, S., Latif, M. and Mook, W.G., 1996. ENSO-controlled flooding in the Paraná River (1904–1991) Naturwissenschaften, 83(3): 127-129.
Depetris, P.J. and Pasquini, A.I., 2007. The geochemistry of the Paraná River: an overview. In: M.H. Iriondo, J.C. Paggi and A.R. Paira (Editors), The Middle Paraná River: Limnology of a Subtropical Wetland. Springer Verlag, Berlin, Heidelberg, pp. 143-174.
Dingle, R.V., 1980. Large allochthonous sediment masses and their role in the construction of the continental slope and rise off southwestern Africa. Marine Geology, 37(3-4): 333-354.
Dingle, R.V. and Robson, S., 1985. Slumps, canyons and related features on the continental margin off East London, SE Africa (SW Indian Ocean). Marine Geology, 67(1-2): 37-54.
Domack, E.W., Jacobson, E.A., Shipp, S. and Anderson, J.B., 1999. Late Pleistocene–Holocene retreat of the West Antarctic Ice-Sheet system in the Ross Sea: Part 2—Sedimentologic and stratigraphic signature. Geological Society of America Bulletin, 111(10): 1517-1536.
Dott, R.H. and Bourgeois, J., 1982. Hummocky stratification: significance of its variable bedding sequences. Geological Society of America Bulletin, 93: 663-680.
Dott, R.H., 1983. Episodic sedimentation-How normal is average? How rare is rare? Does it matter? Journal of Sedimentary Petrology, 53(1): 5-23.
Dowdeswell, J.A. and Murray, T., 1990. Modelling rates of sedimentation from icebergs. In: J.A. Dowdeswell and J.D. Scourse (Editors), Glacimarine Environments: Processes and Sediments. Geological Society, Special Publication 53, London, pp. 121-137.
Dowdeswell, J.A., Ó Cofaigh, C. and Pudsey, C.J., 2004. Continental slope morphology and sedimentary processes at the mouth of an Antarctic palaeo-ice stream. Marine Geology, 204(1-2): 203-214.

Dowdeswell, J.A., Evans, J., Ó Cofaigh, C. and Anderson, J.B., 2006. Morphology and sedimentary processes on the continental slope off Pine Island Bay, Amundsen Sea, West Antarctica. Geological Society of America Bulletin, 118(5-6): 606-619.
Drago, E.C. and Amsler, M.L., 1998. Suspended sediment at a cross section of the Middle Parana River: concentration, granulometry and influence of the main tributaries. In: M.P. Bordas and D.E. Walling (Editors), Sediment budgets. IAHS Publication, 174, Wallingford, pp. 381-396.
Ducassou, E., Mulder, T., Migeon, S., Gonthier, E., Murat, A., Revel, M., Capotondi, L., Bernasconi, S.M., Mascle, J. and Zaragosi, S., 2008. Nile floods recorded in deep Mediterranean sediments. Quaternary Research, 70(3): 382-391.
Einsele, G. and Seilacher, A., 1991. Distinction of tempestites and turbidites. In: G. Einsele, W. Ricken and A. Seilacher (Editors), Cycles and events in stratigraphy. Springer Verlag, Berlin, Heidelberg, New York, pp. 377-382.
Einsele, G., 1991. Submarine mass flow deposits and turbidites. In: G. Einsele, W. Ricken and A. Seilacher (Editors), Cycles and events in stratigraphy. Springer Verlag, Berlin, Heidelberg, New York, pp. 313-339.
Einsele, G., 1996. Event deposits: the role of sediment supply and relative sea-level changes - overview. Sedimentary Geology, 104(1-4): 11-37.
Ellwood, B.B., 1993. Magnetic properties of Argentine Basin Project MUDWAVE samples. Deep Sea Research Part II, 40(4/5): 921-937.
Esteves, L.S., Toldo, E.E., Dillenburg, S.R. and Tomazelli, L.J., 2002. Long- and short-term coastal erosion in southern Brazil. Journal of Coastal Research, Special Issue 36(ICS 2002 Proceedings): 273-282.
Ewing, M., Ludwig, W.J. and Ewing, J.I., 1964. Sediment distribution in the oceans: the Argentine Basin. Journal of Geophysical Research, 69(10): 2003-2032.
Ewing, M., 1965. The sediments of the Argentine Basin (Harold Jeffreys Lecture). Quarterly Journal of the Royal Astronomical Society, 6: 10-27.
Ewing, M., Eittreim, S.L., Ewing, J.I. and Le Pichon, X., 1971. Sediment transport and distribution in the Argentine Basin. 3. Nepheloid layer and processes of sedimentation. Physics and Chemistry of the Earth, 8: 49-77.
Ewing, M. and Lonardi, A.G., 1971. Sediment transport and distribution in the Argentine Basin. 5. Sedimentary structure of the Argentine margin, basin, and related provinces. Physics and Chemistry of the Earth, 8: 123-251.
Farinati, E.A., 1985. Radiocarbon dating of Holocene marine deposits, Bahía Blanca area, Buenos Aires province, Argentina. In: J. Rabassa (Editor), Quaternary of South America and Antarctic peninsula. A. A. Balkema, 3, Rotterdam, Boston, pp. 197-206.
Faugères, J.-C., Gonthier, E. and Stow, D.A.V., 1984. Contourite drift molded by deep Mediterranian outflow. Geology, 12(5): 296-300.
Faugères, J.-C. and Stow, D.A.V., 1993. Bottom-current-controlled sedimentation: a synthesis of the contourite problem. Sedimentary Geology, 82(1-4): 287-297.
Faugères, J.-C., Mézerais, M.L. and Stow, D.A.V., 1993. Contourite drift types and their distribution in the North and South Atlantic Ocean basins. Sedimentary Geology, 82(1-4): 189-203.
Figueiredo, A.G., 1980. Response of water column to strong wind forcing, southern Brazilian inner shelf: Implications for sand ridge formation. Marine Geology, 35(4): 367-376.

Figueiredo, A.G., Sanders, J.E. and Swift, D.J.P., 1982. Storm-graded layers on inner continental shelves: Examples from southern Brazil and the Atlantic coast of the Central United States. Sedimentary Geology, 31(3-4): 171-190.
Flood, R.D., Shor, A. and Manley, P.L., 1993. Morphology of abyssal mudwaves at Project MUDWAVES sites in the Argentine Basin. Deep Sea Research Part II: Topical Studies in Oceanography, 40(4/5): 859-888.
Folk, R.L., 1974. Petrology of sedimentary rocks. Hempwell Publishing Company, Austin, TX.
Framinan, M.B. and Brown, O.B., 1996. Study of the Río de la Plata turbidity front, Part 1: spatial and temporal distribution. Continental Shelf Research, 16(10): 1259-1282.
Franke, D., Neben, S., Ladage, S., Schreckenberger, B. and Hinz, K., 2007. Margin segmentation and volcano-tectonic architecture along the volcanic margin off Argentina/Uruguay, South Atlantic. Marine Geology, 244(1-4): 46-67.
Fray, C. and Ewing, M., 1963. Pleistocene sedimentation and fauna of the Argentine shelf: I. Wisconsin sea level as indicated in Argentine continental shelf sediments. Proceedings of the Academy of Natural Sciences of Philadelphia, 115: 113-126.
Frenz, M., Höppner, R., Stuut, J.-B.W., Wagner, T. and Henrich, R., 2003. Surface sediment bulk geochemistry and grain size composition related to the oceanic circulation along the South American continental margin in the southwest Atlantic. In: G. Wefer, S. Mulitza and V. Ratmeyer (Editors), The South Atlantic in the Late Quaternary: reconstruction of material budgets and current systems. Springer Verlag, Berlin, Heidelberg, pp. 347-373.
Friedrichs, C.T., 2004. Gravity-driven sediment transport on the continental shelf: implications for equilibrium profiles near river mouths. Coastal Engineering, 51(8-9): 795-811.
Gaiero, D.M., Probst, J.-L., Depetris, P.J., Bidart, S.M. and Leleyter, L., 2003. Iron and other transition metals in Patagonian riverborne and windborne materials: geochemical control and transport to the southern South Atlantic Ocean. Geochimica et Cosmochimica Acta, 67(19): 3603-3623.
Gaiero, D.M., Brunet, F., Probst, J.-L. and Depetris, P.J., 2007. A uniform isotopic and chemical signature of dust exported from Patagonia: Rock sources and occurrence in southern environments. Chemical Geology, 238(1-2): 107-120.
Gan, M.A., Kousky, V.E. and Ropelewaki, C.F., 2004. The South America monsoon circulation and its relationship to rainfall over west-central Brazil. Journal of Climate, 17(1): 47-66.
Garcia, N.O. and Vargas, W.M., 1996. The spatial variability of runoff and precipitation in the Rio de la Plata basin. Hydrological Sciences Journal, 41(3): 279-299.
Gauley, B.-J.L., 2001. Lithostratigraphy and sediment failure on the central Scotian Slope. M. Sc. Thesis, Dalhousie University, Halifax, 214 pp.
Gilberto, D.A., Bremec, C.S., Acha, E.M. and Mianzán, H.W., 2004. Large-scale spatial patterns of benthic assemblages in the SW Atlantic: the Río de la Plata estuary and adjacent shelf waters. Estuarine, Coastal and Shelf Science, 61(1): 1-13.
Gipp, M.R. and Piper, D.J.W., 1989. Chronology of Late Wisconsin glaciation, Emerald Basin, Scotian Shelf. Canadian Journal of Earth Sciences, 26: 333-335.
Gipp, M.R., 1994. Late Wisconsinan deglaciation of Emerald Basin, Scotian Shelf. Canadian Journal of Earth Sciences, 31(3): 554-566.

Gómez, E.A. and Perillo, G.M.E., 1991. Submarine outcrops underneath shoreface-connected sand ridges, outer Bahía Blanca estuary, Argentina. In: J. Rabassa (Editor), Quaternary of South America and Antarctic Peninsula. A. A. Balkema, 9, Rotterdam, Boston, pp. 23-37.
Gonthier, E., Faugères, J.-C. and Stow, D.A.V., 1984. Contourite facies of the Faro Drift, Gulf of Cadiz. In: D.A.V. Stow and D.J.W. Piper (Editors), Fine grained sediments: deep water processes and facies. Geological Society, Special Publication 15, London, pp. 275-292.
Gordon, A.L. and Greengrove, C.L., 1986. Geostrophic circulation of the Brazil-Falkland confluence. Deep Sea Research Part I: Oceanographic Research Papers, 33(5): 573-585.
Grimm, A.M., 2003. The El Niño impact on the summer monsoon in Brazil: regional processes versus remote influences. Journal of Climate, 16(2): 263-280.
Gröger, M., Henrich, R. and Bickert, T., 2003. Variability of silt grain size and planktonic foraminiferal preservation in Plio/Pleistocene sediments from the western equatorial Atlantic and Caribbean. Marine Geology, 201: 307-320.
Groot, J.J. and Groot, C.R., 1966. Pollen spectra from deep-sea sediments as indicators of climatic changes in southern South America. Marine Geology, 4(6): 525-537.
Groot, J.J., Groot, C.R., Ewing, M., Burckle, L. and Conolly, J.R., 1967. Spores, pollen, diatoms and provenance of the Argentine Basin sediments. In: M. Sears (Editor), Progress in Oceanography, Volume 4. Pergamon Press, pp. 179-217.
Gross, G.M., 1972. Oceanography: A View of the Earth. Prentice-Hall, Inc., Englewood Cliffs.
Guerrero, R.A. and Piola, A.R., 1997. Masas de agua en la plataforma continental. In: E.E. Boschi (Editor), Antecedentes históricos de las exploraciones en el mar y las características ambientales. Instituto Nacional de Investigación y Desarrollo Pesquero (INIDEP), Mar del Plata, pp. 107-118.
Guerrero, R.A., Acha, E.M., Framinan, M.B. and Lasta, C.A., 1997. Physical oceanography of the Río de la Plata Estuary, Argentina Continental Shelf Research, 17(7): 727-742.
Guilderson, T.P., Burckle, L., Hemming, S.R. and Peltier, W.R., 2000. Late Pleistocene sea level variations derived from the Argentine Shelf. Geochemistry, Geophysics, Geosystems, 1(12): 1055.
Hampton, M.A., Lee, H.J. and Locat, J., 1996. Submarine landslides. Reviews of Geophysics, 34(1): 33-59.
Han, G., 2004. Scotian Slope circulation and eddy variability from TOPEX//Poseidon and frontal analysis data. Journal of Geophysical Research, 109: C03028.
Harloff, J. and Mackensen, A., 1997. Recent benthic foraminiferal associations and ecology of the Scotia Sea and Argentine Basin. Marine Micropaleontology, 31(1-2): 1-29.
Hart, B.S., Prior, D.B., Barrie, J.V., Curry, R.G. and Luternauer, J.L., 1992. A river mouth submarine channel and failure complex, Fraser Delta, Canada. Sedimentary Geology, 81(1-2): 73-87.
Haughton, P.D.W., Davis, C., McCaffrey, W.D. and Barker, S., 2009. Hybrid sediment gravity flow deposits – Classification, origin and significance. Marine and Petroleum Geology, 26(10): 1900-1918.

Hemming, S.R., Van de Flierdt, T., Goldstein, S.L., Franzese, A.M., Roy, M., Gastineau, G. and Landrot, G., 2007. Strontium isotope tracing of terrigenous sediment dispersal in the Antarctic Circumpolar Current: Implications for constraining frontal positions. Geochemistry, Geophysics, Geosystems, 8: Q06N13.
Henrich, R., Baumann, K.-H., Huber, R. and Meggers, H., 2002. Carbonate preservation records of the past 3 Myr in the Norwegian–Greenland Sea and the northern North Atlantic: implications for the history of NADW production. Marine Geology, 184(1-2): 17-39.
Henrich, R., Baumann, K.-H., Gerhardt, S., Gröger, M. and Volbers, A.N.A., 2003. Carbonate preservation in deep and intermediate water masses in the South Atlantic: evaluation and geological record (a review). In: G. Wefer, S. Mulitza and V. Ratmeyer (Editors), The South Atlantic in the Late Quatenary: Reconstruction of material budgets and current systems. Springer Verlag, Berlin, pp. 645-670.
Henrich, R., Hanebuth, T.J.J., Krastel, S., Neubert, N. and Wynn, R.B., 2008. Architecture and sediment dynamics of the Mauritania Slide Complex. Marine and Petroleum Geology, 25(1): 17-33.
Henrich, R., Cherubini, Y. and Meggers, H., 2010. Climate and sea level induced turbidite activity in a canyon system offshore the hyperarid Western Sahara (Mauritania): the Timiris Canyon. Marine Geology, 275(1-4): 178-198.
Hensen, C., Zabel, M. and Schulz, H.D., 2000. A comparison of benthic nutrient fluxes from deep-sea sediments off Namibia and Argentina. Deep Sea Research Part II, 47(9-11): 2029-2050.
Hensen, C., Zabel, M., Pfeifer, K., Schwenk, T., Kasten, S., Riedinger, N., Schulz, H.D. and Boetius, A., 2003. Control of sulfate pore-water profiles by sedimentary events and the significance of anaerobic oxidation of methane for the burial of sulfur in marine sediments. Geochimica et Cosmochimica Acta, 67(14): 2631-2647.
Héquette, A. and Hill, P.R., 1995. Response of the seabed to storm-generated combined flows on a sandy Arctic shoreface, Canadian Beaufort Sea. Journal of Sedimentary Research, 65(3a): 461-471.
Héquette, A., Desrosiers, M., Hill, P.R. and Forbes, D.L., 2001. The influence of coastal morphology on shoreface sediment transport under storm-combined flows, Canadian Beaufort Sea. Journal of Coastal Research, 17(3): 507-516.
Hernández-Molina, F.J., Llave, E., Stow, D.A.V., García, M., Somoza, L., Vázquez, J.T., Lobo, F.J., Maestro, A., Dias-del-Rio, V., León, R., Medialdea, T. and Gardner, J., 2006. The contourite depositional system of the Gulf of Cádiz: A sedimentary model related to the bottom current activity of the Mediterranean outflow water and its interaction with the continental margin. Deep Sea Research Part II: Topical Studies in Oceanography, 53(11-13): 1420-1463.
Hernández-Molina, F.J., Malodonado, A. and Stow, D.A.V., 2008a. Abyssal plain contourites. In: M. Rebesco and A. Camerlenghi (Editors), Developments in Sedimentology 60. Elsevier, pp. 347-378.
Hernández-Molina, F.J., Llave, E. and Stow, D.A.V., 2008b. Continental slope contourites. In: M. Rebesco and A. Camerlenghi (Editors), Developments in Sedimentology 60. Elsevier, pp. 379-408.
Hernández-Molina, F.J., Paterlini, M., Violante, R.A., Marshall, P., de Isasi, M., Somoza, L. and Rebesco, M., 2009. Contourite depositional system on the Argentine

slope: an exceptional record of the influence of Antarctic water masses. Geology, 37(6): 507-510.
Hernández-Molina, F.J., Paterlini, C.M., Somoza, L., Violante, R.A., Arecco, M.A., de Isasi, M., Rebesco, M., Uenzelmann-Neben, G. and Mashall, P., 2010. Giant mounded drifts in the Argentine Continental Margin: Origins, and global implications for the history of thermohaline circulation. Marine and Petroleum Geology, 27(7): 1508-1530.
Hesse, R., Klauck, I., Khodabakhsh, S. and Piper, D.J.W., 1999. Continental slope sedimentation adjacent to an ice margin. III. The upper Labrador Slope. Marine Geology, 155(3-4): 249-276.
Hesse, R. and Khodabakhsh, S., 2006. Significance of fine-grained sediment lofting from melt-water generated turbidity currents for the timing of glaciomarine sediment transport into the deep sea. Sedimentary Geology, 186(1-2): 1-11.
Hieke, W., 2000. Transparent layers in seismic reflection records from the central Ionian Sea (Mediterranean)—evidence for repeated catastrophic turbidite sedimentation during the Quaternary. Sedimentary Geology, 135(1-4): 89-98.
Hill, P.R., 1983. Detailed morphology of a small area on the Nova Scotian continental slope. Marine Geology, 53(1-2): 55-76.
Hill, P.R., 1984a. Facies and sequence analysis of Nova Scotian slope muds: turbidites vs 'hemipelagic' deposition. In: D.A.V. Stow and D.J.W. Piper (Editors), Fine grained sediments: deep water processes and facies. Geological Society, Special Publication 15, London, pp. 311-318.
Hill, P.R., 1984b. Sedimentary facies of the Nova Scotian upper and middle continental slope, offshore eastern Canada. Sedimentology, 31(3): 293-309.
Hill, P.S., Fox, J.M., Crockett, J.S., Curran, K.J., Friedrichs, C.T., Geyer, W.R., Milligan, T.G., Ogston, A.S., Puig, P., Scully, M.E., Traykovski, P.A. and Wheatcroft, R.A., 2007. Sediment delivery to the seabed on continental margins. In: C.A. Nittrouer, J.A. Austin, M.E. Field, J.H. Kravitz, J.P.M. Syvitski and P.L. Wiberg (Editors), Continental margin sedimentation: from sediment transport to sequence stratigraphy. Blackwell Publishing, Oxford, UK, pp. 49-99.
Hjelstuen, B.O., Sejrup, H.P., Haflidason, H., Nygård, A., Berstad, I.M. and Knorr, G., 2004. Late Quaternary seismic stratigraphy and geological development of the south Vøring margin, Norwegian Sea. Quaternary Science Reviews, 23(16-17): 1847-1865.
Hogg, N.G., 1983. A note on the deep circulation of the western North Atlantic: its nature and causes. Deep Sea Research Part A. Oceanographic Research Papers, 30(9): 945-961.
Höppner, R. and Henrich, R., 1999. Kornsortierungsprozesse am Argentinischen Kontinentalhang an Hand von Siltkorn-Analysen. Zentralblatt für Geologie und Paläontologie, Teil I, 7-9: 897-905.
Horn, D.R., Ewing, M., Horn, B.M. and Delach, M.N., 1971. Turbidites of the Hatteras and Sohm Abyssal Plains, western North Atlantic. Marine Geology, 11(5): 287-323.
Howe, J.A., 1995. Sedimentary processes and variations in slope-current activity during the last Glacial-Interglacial episode on the Hebrides Slope, northern Rockall Trough, North Atlantic Ocean. Sedimentary Geology, 96(3-4): 201-230.

Hughes Clarke, J.E., O'Leary, D.W. and Piper, D.J.W., 1992. The relative importance of mass wasting and deep boundary current activity on the continental rise off western Nova Scotia. In: C.W. Poag and P.C. de Graciansky (Editors), Geologic evolution of Atlantic continental rises. van Nostrand Reinhold, New York, pp. 266-281.
Hundert, T. and Piper, D.J.W., 2008. Late Quaternary sedimentation on the southwestern Scotian Slope, eastern Canada: relationship to glaciation. Canadian Journal of Earth Sciences, 45(3): 267-285.
Huppertz, T.J., 2007. Late Quaternary history of Flemish Pass, southeast Canadian continental margin. M.Sc. Thesis, Dalhousie University, Halifax, 124 pp.
Huppertz, T.J. and Piper, D.J.W., 2009. The influence of shelf-crossing glaciation on continental slope sedimentation, Flemish Pass, eastern Canadian continental margin. Marine Geology, 265(1-2): 67-85.
Huppertz, T.J., Piper, D.J.W., Mosher, D.C. and Jenner, K.A., 2009. The significance of mass transport deposits for the evolution of a proglacial continental slope. In: D.C. Mosher, C.R. Shipp, L. Moscardelli, J.D. Chaytor, C.D.P. Baxter, H.J. Lee and R. Urgeles (Editors), Submarine mass movements and their consequences IV. Springer Verlag, Dordrect, Heidelberg, London, New York, pp. 631-641.
Huppertz, T.J., Hanebuth, T.J.J., Henrich, R., Preu, B.M., Schwenk, T. and Strasser, M., 2010. A contourite system offshore the Rio de la Plata estuary, Argentina. Geo-Temas, 11: 77-78.
Huppertz, T.J. and Piper, D.J.W., 2010. Interbedded Late Quaternary turbidites and contourites in Flemish Pass, off southeast Canada: their recognition, origin and temporal variation. Sedimentary Geology, 228(1-2): 46-60.
Husebyea, E.S. and Mäntyniemib, P., 2005. The Kaliningrad, West Russia earthquakes on the 21st of September 2004 - Surprise events in a very low-seismicity area. Physics of the Earth and Planetary Interiors, 153(4): 227-236.
Iriondo, M.H. and Garcia, N.O., 1993. Climatic variations in the Argentine plains during the last 18,000 years. Palaeogeography, Palaeoclimatology, Palaeoecology, 101: 209-220.
Iriondo, M.H., 2004. The littoral complex at the Paraná mouth. Quaternary International, 114(1): 143-154.
Iriondo, M.H., 2007. Geomorphology. In: M.H. Iriondo, J.C. Paggi and A.R. Paira (Editors), The Middle Paraná River: Limnology of a Subtropical Wetland. Springer Verlag, Berlin, Heidelberg, pp. 33-52.
Iriondo, M.H. and Paira, A.R., 2007. Physical geography of the basin. In: M.H. Iriondo, J.C. Paggi and A.R. Paira (Editors), The Middle Paraná River: Limnology of a Subtropical Wetland. Springer Verlag, Berlin, Heidelberg, pp. 7-31.
Iseya, F., 1989. Mechanism of inverse grading of suspended load deposits. In: A. Taira and F. Masuda (Editors), Sedimentary facies in the active plate margin. Terra Scientific Publishing Company, Tokyo, pp. 113-129.
Isla, F.I., Cortizo, L.C. and Schnack, E.J., 1996. Pleistocene and Holocene beaches and estuaries along the southern barrier of Buenos Aires, Argentina. Quaternary Science Reviews, 15(8-9): 833-841.
Isla, F.I., 1998. Holocene coastal evolution of Buenos Aires. In: J. Rabassa (Editor), Quaternary of South America and Antarctic Peninsula. A. A. Balkema, 11, Rotterdam, Boston, pp. 297-321.

Isla, F.I. and Schnack, E.J., 2009. The changing coastlines of South America. In: E.M. Latrubesse (Editor), Natural Hazards and Human-Exacerbated Disasters in Latin America. Elsevier, 13, Amsterdam, pp. 49-73.
Jackson, J.M., 1985. Uruguay. In: M.L. Schwartz and E.C.F. Bird (Editors), The world's coastline. van Nostrand Reinhold, New York, pp. 79-84.
Jenner, K.A., Piper, D.J.W., Campbell, D.C. and Mosher, D.C., 2007. Lithofacies and origin of Late Quaternary mass transport deposits in submarine canyons, central Scotian Slope, Canada. Sedimentology, 54(1): 19-38.
Jenner, K.A., Piper, D.J.W., Campbell, C.D. and Mosher, D.C., 2010. Piston cores and supporting high-resolution seismic data, Scotian Slope, Eastern Canada: data and interpretations. Open File 6558, Geological Survey of Canada, Ottawa.
Johnson, G.L., Sommerhoff, G. and Egloff, J., 1975. Structure and morphology of the West Reykjanes Basin and the southeast Greenland continental margin. Marine Geology, 18(4): 175-196.
Kaiser, J. and Lamy, F., 2010. Links between Patagonian Ice Sheet fluctuations and Antarctic dust variability during the last glacial period (MIS 4-2). Quaternary Science Reviews, 29(11-12): 1464-1471.
Keigwin, L.D., Rio, D. and Acton, G.D., 1997. LEG 172 Preliminary Report. Preliminary Report No. 72, Ocean Drilling Program, College Station TX.
Keigwin, L.D., 2001. 9. Data report: Late Pleistocene stable isotope studies of ODP sites 1054, 1055 and 1063. In: L.D. Keigwin, D. Rio, G.D. Acton and E. Arnold (Editors), Proceedings of the Ocean Drilling Program, Scientific Results. Ocean Drilling Program, Volume 172, College Station, TX, pp. 1-14.
King, E.L., Sejrup, H.P., Haflidason, H., Elverhøi, A. and Aarseth, I., 1996. Quaternary seismic stratigraphy of the North Sea Fan: glacially-fed gravity flow aprons, hemipelagic sediments, and large submarine slides. Marine Geology, 130(3-4): 293-315.
King, E.L., Haflidason, H., Sejrup, H.P. and Løvlie, R., 1998. Glacigenic debris flows on the North Sea Trough Mouth Fan during ice stream maxima. Marine Geology, 152(1-3): 217-246.
King, L.H. and Fader, G.B.J., 1986. Wisconsin glaciation of the Atlantic continental shelf of southeast Canada. Bulletin 363, Geological Survey of Canada, Ottawa.
King, L.H., Rokoengen, K., Fader, G.B.J. and Gunleiksrud, T., 1991. Till-tongue stratigraphy. Geological Society of America Bulletin, 103(5): 637-659.
King, L.H., 1993. Till in the marine environment. Journal of Quaternary Science, 8(4): 347-358.
King, L.H., 1996. Late Wisconsinan ice retreat from the Scotian Shelf. Geological Society of America Bulletin, 108(8): 1056-1067.
Krinsley, D., Biscaye, P.E. and Turekian, K.K., 1973. Argentine Basin sediment sources as indicated by quartz surface textures. Journal of Sedimentary Petrology, 43(1): 251-257.
Kuenen, P.H. and Menard, H.W., 1952. Turbidity currents, graded and non-graded deposits. Journal of Sedimentary Petrology, 22(2): 83-96.
Kuvaas, B., Kristoffersen, Y., Guseva, J., Leitchenkov, G., Gandjukhin, V. and Kudryavtsev, G., 2004. Input of glaciomarine sediments along the east Antarctic continental margin; depositional processes on the Cosmonaut Sea continental

slope and rise and a regional acoustic stratigraphic correlation from 40° W to 80° E. Marine Geophysical Researches, 25(3-4): 247-263.
Laberg, J.S. and Vorren, T.O., 1995. Late Weichselian submarine debris flow deposits on the Bear Island Trough Mouth Fan. Marine Geology, 127(1-4): 45-72.
Laberg, J.S. and Vorren, T.O., 2000. Flow behaviour of the submarine glacigenic debris flows on the Bear Island Trough Mouth Fan, western Barents Sea. Sedimentology, 47(6): 1105-1117.
Laberg, J.S. and Andreassen, K., 2007. Submarine paleo-failure morphology on a glaciated continental margin from 3D seismic data. In: V. Lykousis, D. Sakellariou and J. Locat (Editors), Submarine mass movements and their consequences. Springer Verlag, 3rd International Symposium, Dordrecht, pp. 11-18.
Lamb, M.P., Myrow, P.M., Lukens, C., Houck, K. and Strauss, J., 2008. Deposits from wave-influenced turbidity currents: Pennsylvanian Minturn Formation, Colorado, U.S.A. Journal of Sedimentary Research, 78(7): 480-498.
Lambeck, K. and Chappell, J., 2001. Sea level change through the last glacial cycle. Science, 292: 679-686.
Laprida, C., Chapori, N.G., Chiessi, C.M., Violante, R.A., Watanabe, S. and Totah, V., accepted. Middle Pleistocene sea surface temperature in the Brazil-Malvinas Confluence Zone: Paleoceanographic implications based on planktonic foraminifera. Micropaleontology.
Lastras, G., Acosta, J., Munoz, A. and Canals, M., 2011. Submarine canyon formation and evolution in the Argentine Continental Margin between 44°30'S and 48°S. Geomorphology, 128(3-4): 116-139.
Ledbetter, M.T. and Johnson, D.A., 1976. Increased transport of Antarctic Bottom Water in the Vema Channel during the last ice age. Science, 194(4267): 837-839.
Ledbetter, M.T. and Klaus, A., 1987. Influence of bottom currents on sediment texture and sea-floor morphology in the Argentine Basin. In: P.P.E. Weaver and J. Thomson (Editors), Geology and Geochemistry of Abyssal Plains. Geological Society, Special Publication 31, London, pp. 23-31.
Ledbetter, M.T., 1993. Late Pleistocene to Holocene fluctuations in bottom-current speed in the Argentine Basin mudwave field Deep Sea Research Part II, 40(4/5): 911-920.
Lemmen, D.S., 1990. Glaciomarine sedimentation in Disraeli Fiord, high Arctic Canada. Marine Geology, 94(1-2): 9-22.
Lisiecki, L.E. and Raymo, M.E., 2005. A Pliocene-Pleistocene stack of 57 globally distributed benthic δ18O records. Paleoceanography, 20: PA1003.
Lonardi, A.G. and Ewing, M., 1971. Sediment transport and distribution in the Argentine Basin. 4. Bathymetry of the continental margin, Argentine Basin and other related provinces. Canyons and sources of sediments. Physics and Chemistry of the Earth, 8: 79-121.
Loncke, L., Gaullier, V., Droz, L., Ducassou, E., Migeon, S. and Mascle, J., 2009. Multi-scale slope instabilities along the Nile deep-sea fan, Egyptian margin: A general overview. Marine and Petroleum Geology, 26(5): 633-646.
Lowe, D.R., 1976. Grain flow and grain flow deposits. Journal of Sedimentary Petrology, 46(1): 188-199.

Lowe, D.R., 1982. Sediment gravity flows: II. Depositional models with special reference to the deposits of high density turbidity currents. Journal of Sedimentary Petrology, 52(1): 279-297.
Lowe, D.R. and Guy, M., 2000. Slurry-flow deposits in the Britannia Formation (Lower Cretaceous), North Sea: a new perspective on the turbidity current and debris flow problem. Sedimentology, 47(1): 31-70.
Lynch-Stieglitz, J., Adkins, J.F., Curry, W.B., Dokken, T.M., Hall, I.R., Herguera, J.C., Hirschi, J.J.-P., Ivanova, E.V., Kissel, C., Marchal, O., Marchitto, T.M., McCave, I.N., McManus, J.F., Mulitza, S., Ninneman, U.S., Peeters, F., Yu, E.-F. and Zahn, R., 2007. Atlantic meridional overturning circulation during the Last Glacial Maximum. Science, 316(5821): 66-69.
Mahiques, M.M., Tassinardi, C.C.G., Marcolini, S., Violante, R.A., Figueira, R.C.L., da Silveira, I.C.A., Burone, L. and de Mello e Sousa, S.H., 2008. Nd and Pb isotope signatures on the southeastern South American upper margin: Implications for sediment transport and source rocks. Marine Geology, 250(1-2): 51-63.
Manley, P.L. and Flood, R.D., 1993a. Paleoflow history determined from mudwave migration: Argentine Basin. Deep-Sea Research II, 40(4/5): 1033-1055.
Manley, P.L. and Flood, R.D., 1993b. Project mudwaves. Deep-Sea Research II, 20(4/5): 851-857.
Marchès, E., Mulder, T., Cremer, M., Bonnel, C., Hanquiez, V., Gonthier, E. and Lecroart, P., 2006. Capture of a deep sea current by a canyon in the Gulf of Cadiz (Algarve margin, south Portugal), 5th symposium on the Iberian Atlantic Margin, Aveiro.
Marchès, E., Mulder, T., Cremer, M., Bonnel, C., Hanquiez, V., Gonthier, E. and Lecroart, P., 2007. Contourite drift construction influenced by capture of Mediterranean Outflow Water deep-sea current by the Portimão submarine canyon (Gulf of Cadiz, South Portugal). Marine Geology, 242(4): 247-260.
Marchès, E., Mulder, T., Gonthier, E., Cremer, M., Hanquiez, V., Garlan, T. and Lecroart, P., 2010. Perched lobe formation in the Gulf of Cadiz: Interactions between gravity processes and contour currents (Algarve Margin, Southern Portugal). Sedimentary Geology, 229(3): 81-94.
Marchitto, T.M., Oppo, D.W. and Curry, W.B., 2002. Paired benthic foraminiferal Cd/Ca and Zn/Ca evidence for a greatly increased presence of Southern Ocean Water in the glacial North Atlantic. Paleoceanography, 17(3): 1038.
Marchitto, T.M. and Broecker, W.S., 2006. Deep water mass geometry in the glacial Atlantic Ocean: A review of constraints from the paleonutrient proxy Cd/Ca. Geochemistry, Geophysics, Geosystems, 7: Q12003.
Martín-Chivelet, J., Fregenal-Martínez, M.A. and Chacón, B., 2008. Traction structures in contourites. In: M. Rebesco and A. Camerlenghi (Editors), Developments in Sedimentology 60. Elsevier, pp. 159-182.
Martin, L. and Suguio, K., 1992. Variation of coastal dynamics during the last 7000 years recorded in beach-ridge plains associated with river mouths: example from the central Brazilian coast. Palaeogeography, Palaeoclimatology, Palaeoecology, 99(1-2): 119-140.
Martins, L.R. and Willwock, J.A., 1987. Eastern South America Quaternary coastal and marine geology: a synthesis, Quaternary coastal geology of Western Africa and South America. Unesco Reports in Marine Sciences, 43, Dakar, pp. 28-96.

Martins, L.R. and Correa, I.C.S., 1996. Atlas morphology and sedimentology of the southwest Atlantic coastal zone and continental shelf from Cabo Frio (Brazil) and Peninsula Valdés (Argentina), Universidade Federal do Rio Grande do Sul, Rio Grande do Sul.
Martins, L.R., Martins, I.R. and Urien, C.M., 2003. Aspectos sedimentares da plataforma continental na área de influência do Rio de la Plata. Gravel, 1: 68-80.
Martins, L.R. and Urien, C.M., 2004. Areias da plataforma e a erosão costeira. Gravel, 2: 4-24.
Martins, L.R., Urien, C.M. and Martins, I.R., 2005a. Gênese dos sedimentos da plataforma continental Atlântica entre o Rio Grande do Sul (Brasil) e Tierra del Fuego (Argentina). Gravel, 3: 85-102.
Martins, L.R., Martins, I.R. and Urien, C.M., 2005b. Sand bodies of the Santa Catarina inner continental shelf, Brazil. Gravel, 3: 103-108.
Martins, L.R., Martins, I.R. and Martins, R.R., 2005c. Utilização de testemunhador livre na região dos Poços de Lama. Gravel, 3: 1-8.
Maslin, M.A., Owen, M., Day, S. and Long, D., 2004. Linking continental-slope failures and climate change: Testing the clathrate gun hypothesis. Geology, 32(1): 53-56.
Maslin, M.A. and Ridgwell, A.J., 2005. Mid-Pleistocene revolution and the ‘eccentricity myth’. In: M.J. Head and P.L. Gibbard (Editors), Early-Middle Pleistocene transitions: the land-ocean evidence. Geological Society, Special Publication 247, London, pp. 19-34.
Matsumoto, K., 1997. Modeled glacial North Atlantic ice-rafted debris pattern and its sensitivity to various boundary conditions. Paleoceanography, 12(2): 271-280.
McAdoo, B.G., Orange, D.L., Screaton, E., Lee, H.J. and Kayen, R., 1997. Slope basins, headless canyons, and submarine palaeoseismology of the Cascadia accretionary complex. Basin Research, 9(4): 313-324.
McCave, I.N., 1985. Sedimentology and stratigraphy of box cores from the HEBBLE site on the Nova Scotian continental rise. Marine Geology, 66(1-4): 59-89.
McCave, I.N. and Hall, I.R., 2006. Size sorting in marine muds: Processes, pitfalls, and prospects for paleoflow-speed proxies. Geochemistry, Geophysics, Geosystems, 7(10): Q10N05.
McCave, I.N., 2007. Deep-sea sediment deposits and properties controlled by currents In: C. Hillaire-Marcel and A. de Vernal (Editors), Developments in Marine Geology 1: Proxies in Late Cenozoic Paleoceanography. Elsevier, Amsterdam, pp. 19-62.
McHugh, C.M.G., Damuth, J.E. and Mountain, G.S., 2002. Cenozoic mass-transport facies and their correlation with relative sea-level change, New Jersey continental margin. Marine Geology, 184(3-4): 295-334.
Mémery, L., Arhan, M., Alvarez-Salgado, X.A., Mercier, H., Castro, C.G. and Rios, A.F., 2000. The water masses along the western boundary of the south and equatorial Atlantic. Progress In Oceanography, 47(1): 69-98.
Middleton, G. and Hampton, M.A., 1973. Sediment gravity flows: mechanics of flow and deposition. In: G. Middleton and A.H. Bouma (Editors), Turbidites and deep water sedimentation. Pacific Section S. E. P. M., Short Course 1, Los Angeles, pp. 1-38.
Middleton, G.V. and Hampton, M.A., 1976. Subaqueous sediment transport and deposition by sediment gravity flows. In: D.J. Stanley and D.J.P. Swift (Editors),

Marine sediment transport and environmental management. Wiley & sons, New York, London, Toronto, Sidney, pp. 197-218.
Middleton, G.V. and Neal, W.J., 1989. Experiments on the thickness of beds deposited by turbidity currents Journal of Sedimentary Research, 59(2): 297-307.
Middleton, G.V., 1993. Sediment deposition from turbidity currents. Annual Review of Earth and Planetary Sciences, 21: 89-114.
Mienert, J., Berndt, C., Laberg, J.S. and Vorren, T.O., 2002. Slope instability of continental margins. In: G. Wefer, D. Billett, D. Hebbeln, B.B. Jorgensen, M. Schlüter and T.C.E. van Weering (Editors), Ocean Margin Systems. Springer, Berlin, Heidelberg, pp. 179-193.
Migeon, S., Ducassou, E., Le Gonidec, Y., Rouillard, P., Mascle, J. and Revel-Rolland, M., 2010. Lobe construction and sand/mud segregation by turbidity currents and debris flows on the western Nile deep-sea fan (Eastern Mediterranean). Sedimentary Geology, 229(3): 124-143.
Mitchell, N.C., 2004. Form of submarine erosion from confluences in Atlantic USA continental slope canyons. American Journal of Science, 304: 590-611.
Mitchell, T.D. and Jones, P.D., 2005. An improved method of constructing a database of monthly climate observations and associated high-resolution grids. International Journal of Climatology, 25(6): 693-712.
Möller, O.O., Piola, A.R., Freitas, A.C. and Campos, E.J.D., 2008. The effects of river discharge and seasonal winds on the shelf off southeastern South America. Continental Shelf Research, 28(13): 1607-1624.
Mosher, D.C., Piper, D.J.W., Vilks, G.V., Aksu, A.E. and Fader, G.B.J., 1989. Evidence for Wisconsinan glaciation in the Verill canyon area, Scotian slope. Quaternary Research, 31(1): 27-40.
Mosher, D.C., Moran, K. and Hiscott, R.N., 1994. Late Quaternary sediment, sediment mass flow processes and slope stability on the Scotian slope, Canada. Sedimentology, 41(5): 1039-1061.
Mosher, D.C. and Simpkin, P.G., 1999. Environmental marine geosciences 1: status and trends of marine high-resolution seismic reflection profiling: data acquisition. Geoscience Canada, 26(4): 174-188.
Mosher, D.C., Piper, D.J.W., Campbell, D.C. and Jenner, K.A., 2004. Near-surface geology and sediment-failure geohazards of the central Scotian Slope. AAPG Bulletin, 88(6): 703-723.
Mosher, D.C. and Piper, D.J.W., 2007. Multibeam seafloor imagery of the Laurentian Fan and the 1929 Grand Banks landslide area. Open File 5638, Geological Survey of Canada, Ottawa.
Mosher, D.C., Xu, Z. and Shimeld, J., 2009. The Pliocene Shelburne mass-movement and consequent tsunami, western Scotian slope. In: D.C. Mosher, C.R. Shipp, L. Moscardelli, J.D. Chaytor, C.D.P. Baxter, H.J. Lee and R. Urgeles (Editors), Submarine mass movements and their consequences IV. Springer Verlag, Dordrect, Heidelberg, London, New York, pp. 765-775.
Mulder, T. and Moran, K., 1995. Relationship among submarine instabilities, sea level variations, and the presence of an ice sheet on the continental shelf: An example from the Verrill Canyon Area, Scotian Shelf. Paleoceanography, 10(1): 137-154.

Mulder, T. and Syvitski, J.P.M., 1995. Turbidity currents generated at river mouths during exceptional discharges to the world oceans. Journal of Geology, 103(3): 285-299.
Mulder, T., Migeon, S., Savoye, B. and Faugères, J.-C., 2001. Inversely graded turbidite sequences in the deep Mediterranean: a record of deposits from flood-generated turbidity currents? Geo-Marine Letters, 21(2): 86-93.
Mulder, T., Syvitski, J.P.M., Migeon, S., Faugères, J.-C. and Savoye, B., 2003. Marine hyperpycnal flows: initiation, behavior and related deposits. A review. Marine and Petroleum Geology, 20(6-8): 861-882.
Mulder, T., Lecroart, P., Hanquiez, V., Marches, E., Gonthier, E., Guedes, J.-C., Thiébot, E., Jaaidi, B., Kenyon, N.H., Voisset, M., Perez, C., Sayago, M., Fuchey, Y. and Bujan, S., 2006. The western part of the Gulf of Cadiz: contour currents and turbidity currents interactions. Geo-Marine Letters, 26(1): 31-41.
Mulder, T., Faugères, J.-C. and Gonthier, E., 2008. Mixed turbidite–contourite systems. In: M. Rebesco and A. Camerlenghi (Editors), Developments in Sedimentology 60. Elsevier, pp. 435-456.
Myrow, P.M. and Southard, J.B., 1996. Tempestite deposition. Journal of Sedimentary Research, 66(5): 875-887.
Myrow, P.M., Lukens, C., Lamb, M.P., Houck, K. and Strauss, J., 2008. Dynamics of a transgressive prodeltaic system: implications for geography and climate within a Pennsylvanian intracratonic basin, Colorado, U.S.A. Journal of Sedimentary Research, 78(8): 512-528.
National Geographic Society; Cartographic Division, 1990. World ocean floors [cartographic material] / produced by the Cartographic Division, National Geographic Society ; John B. Garver Jr., chief cartographer ; painting by Tibor G. Toth ; design, Allen Caroll. In: A. Carroll, J.B. Garver and T.G. Toth (Editors). The Society, Washington, D.C. .
Niedoroda, A.W., Reed, C., Das, H., Hatchett, L. and Perlet, A.B., 2006. Controls of the behaviour of marine debris flows. Norwegian Journal of Geology (Norsk Tidsskrift), 86(3): 256-274.
Niedoroda, A.W., Reed, C.W., Das, H. and Hatchett, L., 2007. The general behavior of mass gravity flows in the marine environment. In: V. Lykousis, D. Sakellariou and J. Locat (Editors), Submarine mass movements and their consequences. Springer Verlag, 3rd International Symposium, Dordrecht, pp. 111-118.
Nittrouer, C.A., Austin, J.A., Field, M.E., Kravitz, J.H., Syvitski, J.P.M. and Wiberg, P.L., 2007. Writing a Rosetta stone: insights into continental-margin sedimentary processes and strata. In: C.A. Nittrouer, J.A. Austin, M.E. Field, J.H. Kravitz, J.P.M. Syvitski and P.L. Wiberg (Editors), Continental margin sedimentation: from sediment transport to sequence stratigraphy. Blackwell Publishing, Oxford, UK, pp. 1-48.
Normark, W.R., Piper, D.J.W. and Stow, D.A.V., 1983. Quaternary development of channels, levees, and lobes on middle Laurentian Fan. AAPG Bulletin, 67(9): 1400-1409.
Normark, W.R. and Piper, D.J.W., 1991. Initiation processes and flow evolution of turbidity currents: implications for the depositional record. SEPM Special Publication, 46: 207-230.

Nygard, A., Sejrup, H.P., Haflidason, H. and King, E.L., 2002. Geometry and genesis of glacigenic debris fows on the North Sea Fan: TOBI imagery and deep-tow boomer evidence. Marine Geology, 188(1-2): 15-33.
O'Connor, W.P., 1991. A numerical model of tides and storm surges in the Rio de la Plata Estuary. Continental Shelf Research, 11(12): 1491-1508.
Owen, M., Day, S. and Maslin, M., 2007. Late Pleistocene submarine mass movements: occurrence and causes. Quaternary Science Reviews, 26(7-8): 958-978.
Pahnke, K., Goldstein, S.L. and Hemming, S.R., 2008. Abrupt changes in Antarctic Intermediate Water circulation over the past 25,000 years. Nature Geosciences, 1: 870-874.
Palma, E.D., Matano, R.P., Piola, A.R. and Sitz, L.E., 2004a. A comparison of the circulation patterns over the southwestern Atlantic shelf driven by different wind stress climatologies. Geophysical Research Letters, 31: L24303.
Palma, E.D., Matano, R.P. and Piola, A.R., 2004b. A numerical study of the southwestern Atlantic shelf circulation: barotropic response to tidal and wind forcing. Journal of Geophysical Research, 109: C08014.
Panario, D. and Gutiérrez, O., 1999. The continental Uruguayan Cenozoic: an overview. Quaternary International, 62(1): 75-84.
Parker, G., Paterlini, C.M. and Violante, R.A., 1994. Edad y génesis del Río de la Plata. Revista de la Asociación Geológica Argentina, 49(1-2): 11-18.
Parker, G., Violante, R.A. and Paterlini, M.C., 1996. Fisiografia de la plataforma continental. In: V.A. Ramos and M.A. Turic (Editors), Geologia y recursos naturales de la plataforma continental Argentina. Asociacion Geologica Argentina, Buenos Aires.
Parker, G., Paterlini, C.M. and Violante, R.A., 1997. El fondo marino. In: E. Boschi (Editor), El Mar Argentino y sus recursos pesqueros, Tomo 1: Antecedentes historicos de las exploraciones en el mar y las caracteristicas ambientaies. Instituto Nacional de Investigación y Desarrollo Pesquero Secretaría de Agricultura, Ganadería, Pesca y Allmentación, Mar del Plata, Argentina, pp. 65-87.
Parker, G., Violante, R.A., Paterlini, C.M., Costa, I.P., Marcolini, S. and Cavallotto, J.L., 2008. Las secuencias depositacionales del plioceno-cuaternario en la plataforma submarina adyacente al litoral del este Bonaerense. Latin American Journal of Sedimentology and Basin Analysis, 15(2): 105-124.
Peltier, W.R. and Drummond, R., 2002. A “broad-shelf effect” upon postglacial relative sea level history. Geophysical Research Letters, 29: 1169.
Pereyra, F.X., Baumann, V., Altinier, V., Ferrer, J. and Tchilinguirian, P., 2004. Génesis de suelos y evolución del paisaje en el delta del río Paraná. Revista de la Asociación Geológica Argentina, 59(2): 229-242.
Perillo, G.M.E. and Sequeira, M.E., 1989. Geomorphologic and sediment transport characteristics of the middle reach of the Bahia Blanca estuary (Argentina). Journal of Geophysical Research, 94(C10): 14351-14362.
Perillo, G.M.E., Piccolo, M.C. and Marcovecchio, J., 2005. Coastal oceanography of the western South Atlantic continental shelf (33 to 55°S). In: A.R. Robinson and K.H. Brink (Editors), The sea. Havard Collage, 14, Boston, pp. 295-327.

Pickerill, R.K., Piper, D.J.W., Collins, J., Kleiner, A. and Gee, L., 2001. Scotian slope mapping project: The benefits of an integrated regional high-resolution multibeam survey, Offshore Technology Conference, Houston, Texas, pp. OTC 12995.
Pierce, J.W. and Siegel, F.R., 1979. Supended particulate matter on the southern Argentine shelf. Marine Geology, 29(1-4): 73-91.
Pierson, T.C., 1981. Dominant particle support mechanisms in debris flows at Mt Thomas, New Zealand, and implications for flow mobility. Sedimentology, 28: 49-60.
Piola, A.R. and Rivas, A.L., 1997. Corrientes en la plataforma continental. In: E. Boschi (Editor), El mar Argentino y sus recursos pesqueros, Volume 1, pp. 119-132.
Piola, A.R., Campos, E.J.D., Möller, O.O., Charo, M. and Martinez, C., 2000. Subtropical shelf front off eastern South America. Journal of Geophysical Research, 105(C3): 6565-6578.
Piola, A.R. and Matano, R.P., 2001. Brazil and Falklands (Malvinas) currents. In: J.H. Steele and S.A. Thorpe (Editors), Encyclopedia of Ocean Sciences. Academic Press, San Diego, pp. 340-349.
Piola, A.R. and Romero, S.I., 2004. Analysis of space-time variability of the Plata river plume. Gayana (Concepción), 68(2): 482-486.
Piola, A.R., Matano, R.P., Palma, E.D., Möller, O.O. and Campos, E.J.D., 2005. The influence of the Plata River discharge on the western South Atlantic shelf. Geophysical Research Letters, 32: L01603.
Piola, A.R., 2006. Antarctic intermediate water. In: B. Riffenburgh (Editor), Encyclopedia of the Antarctic. Routledge, New York, pp. 62-65.
Piola, A.R., Romero, S.I. and Zyjaczkovski, U., 2008a. Space- time variability of the Plata plume inferred from ocean color. Continental Shelf Research, 28(13): 1556-1567.
Piola, A.R., Möller, O.O., Guerrero, R.A. and Campos, E.J.D., 2008b. Variability of the subtropical shelf front off eastern South America: Winter 2003 and summer 2004. Continental Shelf Research, 28(13): 1639-1648.
Piper, D.J.W., Mudie, P.J., Aksu, A.E. and Hill, P.R., 1978. Late Quatenary sedimentation, 50°N, north-east Newfoundland shelf. Géographie physique et Quaternaire, 32(4): 321-332.
Piper, D.J.W., 1978. Turbidite muds and silts on deep sea fans and abyssal plains. In: D.J. Stanley and G. Kelling (Editors), Sedimentation in submarine canyons, fans and trenches. Dowden, Hutchinson & Ross, Inc., Stroudsburg, pp. 163-176.
Piper, D.J.W., Normark, W.R. and Sparkes, R., 1987. Late Cenozoic stratigraphy of the central Scotian slope, eastern Canada. Bulletin of Canadian Petroleum Geology, 35(1): 1-11.
Piper, D.J.W. and Sparkes, R., 1987. Proglacial sediment instability features on the Scotian Slope at 63°W. Marine Geology, 76: 15-31.
Piper, D.J.W. and Aksu, A.E., 1987. The source and origin of the 1929 Grand Banks turbidity current inferred from sediment budgets. Geo-Marine Letters, 7: 177-182.
Piper, D.J.W. and Sparkes, R., 1990. Pliocene - Quaternary geology of the central Scotian Slope. Open File 2233, Geological Survey of Canada, Ottawa.
Piper, D.J.W. and Fehr, S.D., 1991. Radiocarbon chronology of late Quaternary sections on the inner and middle Scotian Shelf, south of Nova Scotia. Current Research Paper 91-1E, Geological Survey of Canada, Ottawa.

Piper, D.J.W., Mudie, P.J., Aksu, A.E. and Skene, K.I., 1994. A 1 Ma record of sediment flux south of the Grand Banks used to infer the development of glaciation in southeastern Canada. Quaternary Science Reviews, 13(1): 23-37.
Piper, D.J.W. and Deptuck, M., 1997. 5. Fine-grained turbidites of the Amazon Fan: facies characterization and interpretation. In: R.D. Flood, D.J.W. Piper, A. Klaus and L.C. Peterson (Editors), Proceedings of the Ocean Drilling Program, Scientific Results, Volume 155. Ocean Drilling Program, College Station, TX, pp. 79-108.
Piper, D.J.W., Pirmez, C., Manley, P.L., Long, D., Flood, R.D., Normark, W.R. and Showers, W., 1997. 6. Mass transport deposits of the Amazon fan. In: R.D. Flood, D.J.W. Piper, A. Klaus and L.C. Peterson (Editors), Proceedings of the Ocean Drilling Program, Scientific Results, Volume 155, College Station, TX, pp. 109-146.
Piper, D.J.W. and Skene, K.I., 1998. Latest Pleistocene ice-rafting events on the Scotian Margin (eastern Canada) and their relationship to Heinrich events. Paleoceanography, 13(2): 205-214.
Piper, D.J.W., Skene, K.I. and Morash, N., 1999. History of major debris flows on the Scotian Rise, offshore Nova Scotia. Current research 1999-E, Geological Survey of Canada, Ottawa.
Piper, D.J.W., 2000. Pleistocene ice outlets on the central Scotian Slope, offshore Nova Scotia. Current research 2000-D7, Geological Survey of Canada, Dartmouth.
Piper, D.J.W., 2001. The geological framework of sediment instability on the Scotian Slope: studies to 1999. Open File 3920, Geological Survey of Canada, Ottawa.
Piper, D.J.W. and Normark, W.R., 2001. Sandy fans—from Amazon to Hueneme and beyond. AAPG Bulletin, 85(8): 1407-1438.
Piper, D.J.W. and MacDonald, A., 2001. Timing and position of late Wisconsinan ice margins on the upper slope seaward of Laurentian channel. Géographie physique et Quaternaire, 55(2): 131-140.
Piper, D.J.W., Mosher, D.C. and Newton, S., 2002. Ice-margin seismic stratigraphy of the central Scotian Slope, eastern Canada. Current Research 2002-E16, Geological Survey of Canada, Dartmouth.
Piper, D.J.W. and Hundert, T., 2002. Provenance of distal Sohm Abyssal Plain sediments: history of supply from the Wisconsinan glaciation in eastern Canada. Geo-Marine Letters, 22(2): 75-85.
Piper, D.J.W. and Campbell, D.C., 2002. Surficial geology of the Scotian Slope, eastern Canada. Current Research 2002-E15, Geological Survey of Canada, Dartmouth.
Piper, D.J.W., Mosher, D.C., Gauley, B.-J., Jenner, K.A. and Campbell, D.C., 2003. The chronology and recurrence of submarine mass movements on the continental slope off southeastern Canada. In: J. Locat and J. Mienert (Editors), Submarine mass movements and their consequences: First international symposium. Kluwer Academic Publishers, pp. 299-306.
Piper, D.J.W. and Ingram, S., 2003. Major Quaternary sediment failures on the east Scotian Rise, eastern Canada. Current Research 2003-D1, Geological Survey of Canada (Atlantic), Dartmouth.
Piper, D.J.W. and DeWolfe, M., 2003. Petrographic evidence from the eastern Canadian margin of shelf-crossing glaciations. Quaternary International, 99-100: 99-113.

Piper, D.J.W. and McCall, C., 2003. A synthesis of the distribution of submarine mass movements on the eastern Canadian margin. In: J. Locat and J. Mienert (Editors), Submarine mass movements and their consequences: First international symposium. Kluwer Academic Publishers, pp. 291-298.
Piper, D.J.W., Adam, W.A.M., Stephen, I., Williams, G.L. and McCall, C., 2005. Late Cenozoic architecture of the St. Pierre Slope. Canadian Journal of Earth Sciences, 42(11): 1967-1985.
Piper, D.J.W., 2005. Late Cenozoic evolution of the continental margin of eastern Canada. Norwegian Journal of Geology (Norsk Tidsskrift), 85: 305-318.
Piper, D.J.W. and Brunt, R.A., 2006. High-resolution seismic transects of the upper continental slope off southeastern Canada. Open File 5310, Geological Survey of Canada, Ottawa.
Piper, D.J.W., Shaw, J. and Skene, K.I., 2007. Stratigraphic and sedimentological evidence for late Wisconsinan sub-glacial outburst floods to Laurentian Fan. Paleogeography, Paleoclimatology, Paleoecology, 246(1): 101-119.
Piper, D.J.W. and Normark, W.R., 2009. Processes that initiate turbidity currents and their influence on turbidites: a marine geology perspective. Journal of Sedimentary Research, 79(6): 347-362.
Piper, D.J.W., Deptuck, M., Mosher, D.C., Hughes Clarke, J.E. and Migeon, S., 2011. Erosional and depositional features of glacial meltwater discharges on the eastern Canadian continental margin, SEPM Special Publication
Popescu, I., Lericolais, G., Panin, N., Normand, A., Dinu, C. and Le Drezen, E., 2004. The Danube submarine canyon (Black Sea): morphology and sedimentary processes. Marine Geology, 206(1-4): 249-265
Porebski, S.J., Meischner, D. and Görlich, K., 1991. Quaternary mud turbidites from the South Shetland Trench (West Antarctica): recognition and implications for turbidite facies modelling. Sedimentology, 38(4): 691-715.
Postma, G., 1984. Slumps and their deposits in fan delta front and slope. Geology, 12(1): 27-30.
Postma, G. and Roep, T.B., 1985. Resedimented conglomerates in the bottomsets of Gilbert-type gravel deltas. Journal of Sedimentary Research, 55(6): 874-885.
Powell, R.D. and Molnia, B.F., 1989. Glacimarine sedimentary processes, facies and morphology of the south-southeast Alaska shelf and fjords. Marine Geology, 85(2-4): 359-390.
Pratson, L.F., Ryan, W.B.F., Mountain, G.S. and Twichell, D.C., 1994. Submarine canyon initiation by downslope-eroding sediment flows: Evidence in late Cenozoic strata on the New Jersey continental slope. Geological Society of America Bulletin, 106(3): 395-412.
Pratson, L.F. and Coakley, B.J., 1996. A model for the headward erosion of submarine canyons induced by downslope-eroding sediment flows. Geological Society of America Bulletin, 108(2): 225-234.
Pratson, L.F. and Haxby, W.F., 1996. What is the slope of the U.S. continental slope? Geology, 24(1): 3-6.
Pratson, L.F., Nittrouer, C.A., Wiberg, P.L., Steckler, M.S., Swenson, J.B., Cacchione, D.A., Karson, J.A., Murray, A.B., Wolinsky, M.A., Gerber, T.P., Mullenbach, B.L., Spinelli, G.A., Fulthorpe, C.S., O'Grady, D.B., Parker, G., Driscoll, N.W., Burger, R.L., Paola, C., Orange, D.L., Field, M.E., Friedrichs, C.T. and Fedele, J.J., 2007.

Seascape evolution on clastic continental shelves and slopes. In: C.A. Nittrouer, J.A. Austin, M.E. Field, J.H. Kravitz, J.P.M. Syvitski and P.L. Wiberg (Editors), Continental margin sedimentation: from sediment transport to sequence stratigraphy. Blackwell Publishing, Oxford, UK, pp. 339-380.

Prior, D.B., Coleman, J.L. and Garrison, L.E., 1979. Digitally acquired undistorted side-scan sonar images of submarine landslides, Mississippi River delta. Geology, 7(9): 423-425.

Prior, D.B. and Doyle, E.H., 1985. Intra-slope canyon morphology and its modification by rockfall processes, U.S. Atlantic continental margin. Marine Geology, 67(1-2): 177-196.

Puig, P., Ogston, A.S., Mullenbach, B.L., Nittrouer, C.A. and Sternberg, R.W., 2003. Shelf-to-canyon sediment-transport processes on the Eel continental margin (northern California). Marine Geology, 193(1-2): 129-149.

Puig, P., Palanques, A., Guillen, J. and El Khatab, M., 2004a. Role of internal waves in the generation of nepheloid layers on the northwestern Alboran slope: Implications for continental margin shaping. Journal of Geophysical Research, 109: C09011.

Puig, P., Ogston, A.S., Mullenbach, B.L., Nittrouer, C.A., Parsons, J.D. and Sternberg, R.W., 2004b. Storm-induced sediment gravity flows at the head of the Eel submarine canyon, northern California margin. Journal of Geophysical Research, 109(C): C03019.

Rasmussen, T.L., Oppo, D.W., Thomsen, E. and Lehman, S.J., 2003. Deep sea records from the southeast Labrador Sea: Ocean circulation changes and ice-rafting events during the last 160,000 years. Paleoceanography, 18(1): 1018.

Rebesco, M., Camerlenghi, A., Volpi, V., Neagu, C., Accettella, D., Lindberg, B., Cova, A., Zgur, F. and Magico Party, 2007. Interaction of processes and importance of contourites: insights from the detailed morphology of sediment Drift 7, Antarctica. In: A.R. Viana and M. Rebesco (Editors), Economic and palaeoceanographic significance of contourite deposits. Geological Society, Special Publication 276, London, pp. 95-110.

Reynolds, T., 2000. Reservoir architecture in the Mars field, deepwater Gulf of Mexico, USA: the implications of production, seismic, core and well-log data, GCSSEPM Foundation 20th Annual Research Conference: Deep Water reservoirs of the World, Houston, TX, pp. 877-893.

Riedinger, N., Pfeifer, K., Kasten, S., Garming, J.F.L., Vogt, C. and Hensen, C., 2005. Diagenetic alteration of magnetic signals by anaerobic oxidation of methane related to a change in sedimentation rate. Geochimica et Cosmochimica Acta, 69(16): 4117-4126.

Rivas, A.L. and Langer, A.F., 1996. Mass and heat transport in the Argentine continental shelf. Continental Shelf Research, 16(10): 1283-1295.

Rivas, A.L., 1997. Current-meter observations in the Argentine continental shelf. Continental Shelf Research, 17(4): 391-406.

Robichaud, M., 2006. Late Quaternary evolution of the Northeast Fan, offshore Nova Scotia. B.Sc. Thesis, Dalhousie University, Halifax, 98 pp.

Rodriguez, A.N. and Anderson, J.B., 2004. Contourite origin for shelf and upper slope sand sheet, offshore Antarctica. Sedimentology, 51(4): 699-711.

Romero, O.E. and Hensen, C., 2002. Oceanographic control of biogenic opal and diatoms in surface sediments of the Southwestern Atlantic. Marine Geology, 186(3-4): 263-280.
Rose, L.E. and Kuehl, S.A., 2010. Recent sedimentation patterns and facies distribution on the Poverty Shelf, New Zealand. Marine Geology, 270(1-4): 160-174.
Rostamini, K., Peltier, W.R. and Mangini, A., 2000. Quaternary marine terraces, sea-level changes and uplift history of Patagonia, Argentina: comparisons with predictions of the ICE-4G (VM2) model of the global process of glacial isostatic adjustment Quaternary Science Reviews, 19(14-15): 1495-1525.
Sadler, P.M., 1982. Bed-thickness and grain size of turbidites. Sedimentology, 29(1): 37-51.
Schaaf, A., 1996. Sea level changes, continental shelf morphology, and global paleoecological constraints in the shallow benthic realm: a theoretical approach. Palaeogeography, Palaeoclimatology, Palaeoecology, 121(3-4): 259-271.
Schlager, W. and Camber, O., 1986. Submarine slope angles, drowning unconformities, and self-erosion of limestone escarpments. Geology, 14(9): 762-765.
Schmid, C., Siedler, G. and Zenk, W., 2000. Dynamics of Intermediate Water Circulation in the subtropical South Atlantic. Journal of Physical Oceanography, 30(12): 3191-3211.
Schnack, E.J., 2009. The vulnerability of the east coast of South America to sea level rise and possible adjustment strategies. In: R.A. Warrick, E.M. Barrow and T.M.L. Wigley (Editors), Climate and sea level change: observations, projections and implications. Cambridge University Press, Cambridge, pp. 336-348.
Schnitker, D., Belknap, D.F., Bacchus, T.S., Friez, J.K., Lusardi, B.A. and Popek, D.M., 2001. Deglaciation of the Gulf of Maine. In: T.K. Weddle and M.J. Retelle (Editors), Deglacial history and relative sea level changes, northern New England and adjacent Canada. Geological Society of America, Special Paper 351, Boulder, pp. 9-34.
Segl, M. and Shipboard Scientific Party, 1994. Meteor Berichte Geo Bremen South Atlantic 1994, Cruise No. 29/1, 17 June - 5 September 1994. 95-2, Leitstelle Meteor, Institut für Meereskunde der Universität Hamburg.
Sejrup, H.P., Larsen, E., Haflidason, H., Berstad, I.M., Hjelstuen, B.O., Jonsdottir, H.E., King, E.L., Landvik, J., Longva, O., Nygård, A., Ottesen, D., Raunholm, S., Rise, L. and Knut, S., 2003. Configuration, history and impact of the Norwegian Channel Ice Stream. Boreas, 32(1): 18-36.
Sejrup, H.P., Hjelstuen, B.O., Dahlgren, K.I.T., Haflidason, H., Kuijpers, A.H., Nygård, A., Praeg, D., Stoker, M.S. and Vorren, T.O., 2005. Pleistocene glacial history of the NW European continental margin. Marine and Petroleum Geology, 22(9-10): 1111-1129.
Shackleton, N.J., Imbrie, J. and Hall, M.A., 1983. Oxygen and carbon isotope record of East Pacific core V19-30: implications for the formation of deep water in the late Pleistocene North Atlantic. Earth and Planetary Science Letters, 65(2): 233-244.
Shanmugam, G. and Moiola, R.J., 1982. Eustatic control of turbidites and winnowed turbidites. Geology, 10(5): 231-235.
Shanmugam, G., 2008. Deep-water bottom currents and their deposits. In: M. Rebesco and A. Camerlenghi (Editors), Developments in Sedimentology 60. Elsevier, pp. 59-81.

Shaw, J., Piper, D.J.W., Fader, G.B.J., King, E.L., Todd, B.J., Bell, T., Batterson, M.J. and Liverman, D.G.E., 2006. A conceptual model of the deglaciation of Atlantic Canada. Quaternary Science Reviews, 25(17-18): 2059-2081.
Shepard, F.P., 1981. Submarine canyons: multiple causes and long-time persistence. AAPG Bulletin, 65(6): 1062-1077.
Shipboard Scientific Party, 2001. 6. Bermuda Rise and Sohm Abyssal Plain, sites 1063 and 1064. In: L.D. Keigwin, D. Rio, G.D. Acton, G.G. Bianchi, W. Borowski, N. Cagatay, W.P. Chaisson, B.M. Clement, E. Cortijo, G.B. Dunbar, R.D. Flood, S.-O. Franz, L. Giosan, J. Gruetzner, S. Hagen, B. Haskell, M.J. Horowitz, E.P. Laine, S.P. Lund, M. Okada, M.-S. Poli, I. Raffi, M.K. Reuer, Y.G. Ternois, T. Williams, D.M. Winter, M.E. Yokokawa and S.E. Swanson (Editors), Proceedings of the Ocean Drilling Program, Part A: Initial Reports 172. Ocean Drilling Program, 172, College Station, TX, pp. 251-308.
Shor, A.N. and Piper, D.J.W., 1989. A large Late Pleistocene blocky debris flow on the central Scotian slope. Geo-Marine Letters, 9: 153-160.
Sijp, W.P. and England, M.H., 2008. The effect of a northward shift in the southern hemisphere westerlies on the global ocean. Progress In Oceanography, 79(1): 1-19.
Sivkov, V., Gorbatskiy, V., Kuleshov, A. and Zhurov, Y., 2002. Muddy contourites in the Baltic Sea: an example of a shallow-water contourite system. In: D.A.V. Stow, C.J. Pudsey, J.-C. Faugères and A.R. Viana (Editors), Deep-water contourite systems: modern drifts and ancient series, seismic and sedimentary characteristics. Geological Society, Memoir 22, London, pp. 121-136.
Skene, K.I. and Piper, D.J.W., 2003. Late Quaternary stratigraphy of Laurentian Fan: a record of events off the eastern Canadian continental margin during the last deglacial period. Quaternary International, 99-100: 135-152.
Skene, K.I. and Piper, D.J.W., 2006. Late Cenozoic evolution of Laurentian Fan: development of a glacially-fed submarine fan. Marine Geology, 227(1-2): 67-92.
Smith, R.U., 2004. Silled sub-basins to connected tortuous corridors: sediment distribution systems on topographically complex sub-aqueous slopes. In: S.A. Lomas and P. Joseph (Editors), Confined turbidite systems. Geological Society, London, Special Publication 222, London, pp. 23-43.
So, L.C., Pierce, J.W. and Siegel, F.R., 1974. Sand waves in the Gulf of San Matias, Argentina. Geografiska Annaler. Series A, Physical Geography, 56(3-4): 227-235.
Solheim, A., Faleide, J.I., Andersen, E.S., Elverhøi, A., Forsberg, C.F., Vanneste, K., Uenzelmann-Neben, G. and Channell, J.E.T., 1998. Late Cenozoic seismic stratigraphy and glacial geological development of the East Greenland and Svalbard-Barents Sea continental margins. Quaternary Science Reviews, 17(1-3): 155-184.
Spieß, V. and Shipboard Scientific Party, 2002. ODP Südatlantik 2001, Cruise No. 49, Leg 2, 13 February – 7 March 2001, Montevideo – Montevideo. 02-1, Leitstelle Meteor, Institut für Meereskunde der Universität Hamburg.
Stanley, D.J., 1981. Unifites: structureless muds of gravity-flow origin in Mediterranean basins. Geo-Marine Letters, 1(2): 77-83.
Stea, R.R., Piper, D.J.W., Fader, G.B.J. and Boyd, R., 1998. Wisconsinan glacial and sea-level history of Maritime Canada and the adjacent continental shelf: A

correlation of land and sea events. Geological Society of America Bulletin, 110(7): 821-845.
Stea, R.R., Fader, G.B.J., Scott, D.B. and Wu, P., 2001. Glaciation and relative sea level change in Maritime Canada. In: T.K. Weddle and M.J. Retelle (Editors), Deglacial history and relative sea level changes. Geological Society of America, Special Paper 351, Boulder, pp. 35-49.
Stevenson, F.J. and Cheng, C.-N., 1969. Amino acid levels in the Argentine Basin sediments; correlation with Quaternary climatic changes. Journal of Sedimentary Research, 39(1): 345-349.
Stevenson, M.R., Dias-Brito, D., Stech, J.L. and Kampel, M., 1998. How do cold water biota arrive in a tropical bay near Rio de Janeiro, Brazil? Continental Shelf Research, 18(13): 1595-1612.
Stow, D.A.V. and Lovell, J.P.B., 1979. Contourites: their recognition in modern and ancient sediments. Earth-Science Reviews, 14(3): 251-291.
Stow, D.A.V., 1979. Distinguishing between fine-grained turbidites and contourites on the Nova Scotian deep water margin. Sedimentology, 26(3): 371-387.
Stow, D.A.V., 1982. Bottom currents and contourites in the North Atlantic. Bulletin de l'Institut de Geologie du Bassin d'Aquitaine, 31: 151-166.
Stow, D.A.V. and Piper, D.J.W., 1984. Deep-water fine-grained sediments: facies models. In: D.A.V. Stow and D.J.W. Piper (Editors), Fine grained sediments: deep water processes and facies. Geological Society, Special Publication 15, London, pp. 611-646.
Stow, D.A.V. and Holbrook, J.A., 1984. North Atlantic contourites: an overview. In: D.A.V. Stow and D.J.W. Piper (Editors), Fine grained sediments: deep water processes and facies. Geological Society, Special Publication 15, London, pp. 245-256.
Stow, D.A.V., 1985. Fine-grained sediments in deep water: An overview of processes and facies models. Geo-Marine Letters, 5(1): 17-23.
Stow, D.A.V. and Wetzel, A., 1990. Hemiturbidite: a new type of deep water sediment. In: J.R. Cochran and D.A.V. Stow (Editors), Proceedings Ocean Drilling Program Scientific Results, 116, College Station, TX, pp. 25-34.
Stow, D.A.V., Faugères, J.-C., Howe, J.A., Pudsey, C.J. and Viana, A.R., 2002. Bottom currents, contourites and deep-sea sediment drifts: current state of the art. In: D.A.V. Stow, C.J. Pudsey, J.A. Howe, J.-C. Faugères and A.R. Viana (Editors), Deep-water contourite systems: modern drifts and ancient series, seismic and sedimentary characteristics. The Geological Society, Memoir 22, London, pp. 7-20.
Stow, D.A.V. and Faugères, J.-C., 2008. Contourite facies and the facies model. In: M. Rebesco and A. Camerlenghi (Editors), Developments in Sedimentology 60. Elsevier, pp. 223-256.
Stow, D.A.V., Hunter, S.E., Wilkinson, D. and Hernández-Molina, F.J., 2008. The nature of contourite deposition. In: M. Rebesco and A. Camerlenghi (Editors), Developments in Sedimentology 60. Elsevier, pp. 143-156.
Stow, D.A.V., Hernández-Molina, F.J., Llave, E., Sayago-Gil, M., Díaz del Río, V. and Branson, A., 2009. Bedform-velocity matrix: The estimation of bottom current velocity from bedform observations. Geology, 37(4): 327-330.

Stramma, L., 1989. The Brazil current transport south of 23°S. Deep Sea Research Part A. Oceanographic Research Papers, 36(4): 639-646.
Stramma, L. and England, M.H., 1999. On the water masses and mean circulation of the South Atlantic Ocean. Journal of Geophysical Research, 104(C9): 20863-20883.
Sultan, N., Cochonat, P., Canals, M., Cattaneo, A., Dennielou, B., Haflidason, H., Laberg, J.S., Long, D., Mienert, J., Trincardi, F., Urgeles, R., Vorren, T.O. and Wilson, C., 2004. Triggering mechanisms of slope instability processes and sediment failures on continental margins: a geotechnical approach. Marine Geology, 213(1-4): 291-321.
Sultan, N., Gaudin, M., Berne, S., Canals, M., Urgeles, R. and Lafuerza, S., 2007. Analysis of slope failures in submarine canyon heads: An example from the Gulf of Lions. Journal of Geophysical Research, 112: F01009.
Swift, D.J.P., Parker, G., Lanfredi, N.W., Perillo, G.M.E. and Figge, K., 1978. Shoreface-connected sand ridges on American and European shelves: A comparison. Estuarine and Coastal Marine Science, 7(3): 257-273.
Syvitski, J.P.M., Alexander, C.R., Field, M.E., Gardner, J.V., Orange, D.L. and Yun, J.W., 1996a. Continental-slope sedimentation: the view from northern California. Oceanography, 9(3): 163-167.
Syvitski, J.P.M., Andrews, J.T. and Dowdeswell, J.A., 1996b. Sediment deposition in an iceberg-dominated glacimarine environment, East Greenland: basin fill implications. Global and Planetary Change, 12(1-4): 251-270.
Takahashi, T., 1981. Debris flow. Annual Review of Fluid Mechanics, 13(1): 57-77.
Talling, P.J., Lawrence, A.A. and Wynn, R.B., 2007. New insights into the evolution of large-volume turbidity currents: comparison of turbidite shape and previous modelling results. Sedimentology, 54(4): 737-769.
Taylor, J., Dowdeswell, J.A., Kenyon, N.H., Whittington, R.J., van Weering, T.C.E. and Mienert, J., 2000. Morphology and Late Quaternary sedimentation on the North Faeroes slope and abyssal plain, North Atlantic. Marine Geology, 168(1-4): 1-24.
Taylor, J., Dowdeswell, J.A. and Siegert, M.J., 2002. Late Weichselian depositional processes, fuxes, and sediment volumes on the margins of the Norwegian Sea (62-75°N). Marine Geology, 188(1-2): 61-77.
Toggweiler, J.R. and Russell, J., 2008. Ocean circulation in a warming climate. Nature, 451: 286-288.
Tonni, E.P., Cione, A.L. and Figini, A.J., 1999. Predominance of arid climates indicated by mammals in the pampas of Argentina during the Late Pleistocene and Holocene. Palaeogeography, Palaeoclimatology, Palaeoecology, 147(3-4): 257-281.
Traykovski, P.A., Geyer, W.R., Irish, J.D. and Lynch, J.F., 2000. The role of wave-induced density-driven fluid mud flows for cross-shelf transport on the Eel River continental shelf. Continental Shelf Research, 20(16): 2113-2140.
Traykovski, P.A., Wiberg, P.L. and Geyer, W.R., 2007. Observations and modeling of wave-supported sediment gravity flows on the Po prodelta and comparison to prior observations from the Eel shelf. Continental Shelf Research, 27(3-4): 375-399.
Tripsanas, E.K., Bryant, W.R. and Prior, D.B., 2003. Structural characteristics of cohesive gravity-flow deposits, and a sedimentological approach on their flow mechanisms. In: J. Locat and J. Mienert (Editors), Submarine mass movements

and their consequences. Springer Verlag, 1st International Symposium, Dordrecht, pp. 129-136.
Tripsanas, E.K., Piper, D.J.W. and Campbell, D.C., 2008. Evolution and depositional structure of earthquake-induced mass movements and gravity flows: southwest Orphan Basin, Labrador Sea. Marine and Petroleum Geology, 25(7): 645-662.
Tripsanas, E.K. and Piper, D.J.W., 2008. Late Quaternary stratigraphy and sedimentology of Orphan Basin: implications for meltwater dispersal in the southern Labrador Sea. Paleogeography, Paleoclimatology, Paleoecology, 260(3-4): 521-539.
Tripsanas, E.K., Piper, D.J.W., Jenner, K.A. and Bryant, W., 2009. Submarine mass-transport facies: new perspectives on flow processes from cores on the eastern North American margin. Sedimentology, 55(1): 97-136.
Trowbridge, J.H. and Kinecke, G.C., 1994. Structure and dynamics of fluid muds on the Amazon continental shelf. Journal of Geophysical Research, 99(C1): 865-874.
Tucholke, B.E., Hollister, C.D., Biscaye, P.E. and Gardner, W.D., 1985. Abyssal current character determined from sediment bedforms on the Nova Scotian continental rise. Marine Geology, 66(1-4): 43-57.
Turekian, K.K. and Stuvier, M., 1964. Clay- and carbonate-accumulation rates in three South Atlantic deep-sea cores. Science, 146: 55-56.
Uliana, M.A., Biddle, K.T. and Cerdan, J., 1989. Mesozoic extension and the formation of Argentine sedimentary basins. In: A.J. Tankard and H.R. Balkwill (Editors), Extensional tectonics and stratigraphy of the North Atlantic margins. American Association of Petroleum Geologists, AAPG Memoir 46, Tulsa, Oklahoma, pp. 599-614.
Urien, C.M., 1967. Los sedimentos modernos del Rio de la Plata exterior. Boletín del Servicio de Hidrografía Naval, 6(2): 113-213.
Urien, C.M. and Zambrano, J.J., 1973. The geology of the basins of the Argentine continental margin and Malvinas Plateau. In: A.E.M. Nairn and F.G. Stehli (Editors), The ocean basins and margins. Plenum Press, 1, New York, pp. 135-170.
Urien, C.M. and Ewing, M., 1974. Recent sediments and environments of southern Brazil, Uruguay, Buenos Aires and Rio Negro continental shelf. In: C.A. Burke and C.L. Drake (Editors), The geology of continental margins. Springer Verlag, Berlin, pp. 157-177.
Urien, C.M., Martins, L.R. and Martins, I.R., 2003. Paleoplataformas e progradação deltaica do neógeno na margem continental do Uruguai e norte da Argentina. Gravel, 1: 40-46.
van Weering, T.C.E. and van Iperen, J., 1984. Fine-grained sediments of the Zaire deep-sea fan, southern Atlantic Ocean. In: D.A.V. Stow and D.J.W. Piper (Editors), Fine grained sediments: deep water processes and facies. Geological Society, Special Publication 15, London, pp. 95-113.
Vanney, J.-R. and Stanley, D.J., 1983. Shelf break physiography: an overview. In: D.J. Stanley and G.T. Moore (Editors), The Shelfbreak : critical interface on continental margins. Society of Economic Paleontologists and Mineralogists, Special Publication 33, Tulsa, pp. 1-24.
Vera, C.S., Baez, J., Douglas, M., Emmanuel, C.B., Marengo, J., Meitin, J., Nicolini, M., Nogues-Paegle, J., Paegle, J., Penalba, O., Salio, P., Saulo, C., Silva Dias, M.A.,

Silva Dias, P. and Zipser, E., 2006. The South American low-level jet experiment. Bulletin of the American Meteorological Society, 87(1): 63-77.
Verdicchio, G. and Trincardi, F., 2008. Mediterranean shelf-edge muddy contourites: examples from the Gela and South Adriatic basins. Geo-Marine Letters, 28(3): 137-151.
Viana, A., 2002. Seismic expression of shallow- to deep-water contourites along the south-eastern Brazilian margin. Marine Geophysical Researches, 22(5-6): 509-521.
Viana, A.R., Faugères, J.-C. and Stow, D.A.V., 1998a. Bottom-current-controlled sand deposits — a review of modern shallow- to deep-water environments. Sedimentary Geology, 115(1-4): 53-80.
Viana, A.R., Faugères, J.-C., Kowsmann, R.O., Lima, J.A.M., Caddah, L.F.G. and Rizzo, J.G., 1998b. Hydrology, morphology and sedimentology of the Campos continental margin, offshore Brazil. Sedimentary Geology, 115(1-4): 133-157.
Viana, A.R. and Faugères, J.-C., 1998. Upper slope sand deposits: the example of Campos Basin, a latest Pleistocene-Holocene record of the interaction between alongslope and downslope currents. In: M.S. Stoker and D. Evans (Editors), Geological processes on continental margins: sedimentation, mass-wasting and stability. Geological Society, London, Special Publication 129, London, pp. 287-316.
Violante, R.A. and Parker, G., 2004. The post-last glacial maximum transgression in the de la Plata River and adjacent inner continental shelf, Argentina. Quaternary International, 114(1): 167-181.
Vittori, J., Morash, A., Savoye, B., Marsset, T., Lopez, M., Droz, L. and Cremer, M., 2000. The Quaternary Congo deep-sea fan: preliminary results on reservoir complexity in turbiditic systems using 2D high resolution seismic and multibeam data, GCSSEPM Foundation 20th Annual Research Conference: Deep Water reservoirs of the World, Houstan, TX, pp. 1045-1058.
Voigt, I., Hanebuth, T.J.J., Preu, B.M., Schwenk, T., Krastel, S. and Henrich, R., 2011. A submarine canyon as sink in the interplay of down-slope and along-slope processes – The Mar del Plata Canyon offshore Argentina, AGU Chapman Source to Sink. American Geophysical Union, Oxnard, CA.
Volbers, A.N.A. and Henrich, R., 2004. Calcium carbonate corrosiveness in the South Atlantic during the Last Glacial Maximum as inferred from changes in the preservation of Globigerina bulloides: A proxy to determine deep-water circulation patterns? Marine Geology, 204(1-2): 43-57.
von Lom-Keil, H., Spieß, V. and Hopfauf, V., 2002. Fine-grained sediment waves on the western flank of the Zapiola Drift, Argentine Basin: evidence for variations in Late Quaternary bottom flow activity. Marine Geology, 192(1-3): 239-258.
von Lom-Keil, H., Schlacht, R. and Spieß, V., 2003. Bottom current influenced sedimentation in the Argentine Basin and on the Argentine continental margin reflected in high resolution seismic data, EGS-AGU-EUG Joint Assembly. European Geophysical Society, pp. 11459.
Vorren, T.O., Lebesbye, E., Andreassen, K. and Larsen, K.B., 1989. Glacigenic sediments on a passive continental margin as exemplified by the Barents Sea. Marine Geology, 85(2-4): 251-272.

Vorren, T.O. and Laberg, J.S., 1997. Trough mouth fans — palaeoclimate and ice-sheet monitors. Quaternary Science Reviews, 16(8): 865-881.
Vorren, T.O., Laberg, J.S., Blaume, F., Dowdeswell, J.A., Kenyon, N.H., Mienert, J., Rumohr, J. and Werner, F., 1998. The Norwegian-Greenland Sea continental margins: morphology and late Quaternary sedimentary processes and environment. Quaternary Science Reviews, 17(1-3): 273-302.
Wade, J.A. and MacLean, B.C., 1990. The geology of the southeastern margin of Canada, Part 2: Aspects of the geology of the Scotian Basin from recent seismic and well data. In: M.J. Keen and G.L. Williams (Editors), Geology of the continental margin of eastern Canada. Geological Survey of Canada, Ottawa, pp. 190-238.
Waelbroeck, C., Labeyrie, L., Michel, E., Duplessy, J.-C., McManus, J.F., Lambeck, K., Balbon, E. and Labracherie, M., 2002. Sea level and deep water temperature changes derived from benthic foraminifera isotopic records. Quaternary Science Reviews, 21(1-3): 295-305.
Walker, R.G., 1967. Turbidite sedimentary structures and their relationship to proximal and distal depositional environments. Journal of Sedimentary Research, 37(1): 25-43.
Warrick, J.A. and Milliman, J.D., 2003. Hyperpycnal sediment discharge from semiarid southern California rivers: Implications for coastal sediment budgets. Geology, 31(9): 781-784.
Weatherly, G.L. and Kelley, E.A., 1982. “Too cold” bottom layers at the base of the Scotian Rise. Journal of Marine Research, 40: 985-1012.
Weatherly, G.L. and Kelley, E.A., 1985. Storms and flow reversals at the HEBBLE site. Marine Geology, 66(1-4): 205-218.
Wells, P.G. and Daborn, G.R., 1997. The Rio de la Plata - an environmental overview. Dalhousie University, Halifax, 248 pp.
Wheatcroft, R.A., 1990. Preservation potential of sedimentary event layers. Geology, 18(9): 843-845.
Wheatcroft, R.A., Borgeld, J.C., Born, R.S., Drake, D.E., Leithold, E.L. and Sommerfield, C.K., 1996. The anatomy of an oceanic flood deposit. Oceanography, 9(3): 158-162.
Wheatcroft, R.A., Sommerfield, C.K., Drake, D.E., Borgeld, J.C. and Nittrouer, C.A., 1997. Rapid and widespread dispersal of flood sediment on the northern California margin. Geology, 25(2): 163-166.
Wheatcroft, R.A. and Borgeld, J.C., 2000. Oceanic flood deposits on the northern California shelf: large-scale distribution and small-scale physical properties. Continental Shelf Research, 20(16): 2163-2190.
Wheatcroft, R.A., Stevens, A.W., Hunt, L.M. and Milligan, T.G., 2006. The large-scale distribution and internal geometry of the fall 2000 Po River flood deposit: Evidence from digital X-radiography. Continental Shelf Research, 26(4): 499-516.
Wilken, M. and Mienert, J., 2006. Submarine glacigenic debris flows, deep-sea channels and past ice-stream behaviour of the East Greenland continental margin. Quaternary Science Reviews, 25(7-8): 784-810.
Wilkinson, M.J., Marshall, L.G. and Lungberg, J.G., 2006. River behavior on megafans and potential influences on diversification and distribution of aquatic organisms. Journal of South American Earth Sciences, 21(1-2): 151-172.

Williamson, M.A., Keen, C.E. and Mudie, P.J., 1984. Foraminiferal distribution on the continental margin off Nova Scotia. Marine Micropaleontology, 9(3): 219-239.
Wright, L.D. and Friedrichs, C.T., 2006. Gravity-driven sediment transport on continental shelves: A status report. Continental Shelf Research, 26(17-18): 2092-2107
Wright, R. and Anderson, J.B., 1982. The importance of sediment gravity flow to sediment transport and sorting in a glacial marine environment: Eastern Weddell Sea, Antarctica. Geological Society of America Bulletin, 93(10): 951-963.
Yokokawa, M., 2001. 7. Sedimentary structures of contourites and turbidites observed by X-radiographic prints: Samples from Blake-Bahama outer Ridge and Sohm Abyssal Plain. In: L.D. Keigwin, D. Rio, G.D. Acton and E. Arnold (Editors), Proceedings of the Ocean Drilling Program, Scientific Results. Ocean Drilling Program, Volume 172, College Station, TX, pp. 1-37.
Zambrano, J.J. and Urien, C.M., 1970. Geological outline of the basins in southern Argentina and their continuation off the Atlantic shore. Journal of Geophysical Research, 75(8): 1363-1396.
Zavialov, P.O., Kostianoy, A.G. and Möller, O.O., 2003. SAFARI cruise: Mapping river discharge effects on Southern Brazilian shelf. Geophysical Research Letters, 30(21): 2126.
Zhou, J. and Lau, K.-M., 1998. Does a monsoon climate exist over South America? Journal of Climate, 11(5): 1020-1040.

7. Conclusions and outlook

Continental margins are the interface between the land and the ocean, where eroded sediment is transported to by various processes including fluvial and eolian sediment transport. During this study, sedimentary processes have been studied on two contrasting margins: the highly studied mid-latitude glaciated Scotian Slope on the southeast Canadian continental margin and the poorly understood non-glaciated northern Argentine and Uruguay Slope on the east coast of South America seawards of the Rio de la Plata estuary. In both study areas, a similar methodological approach and similar research focus improved the understanding of continental margin sedimentation in such contrasting environments greatly and ensured data comparability.

7.1. Scotian Slope

A new regional seismic stratigraphy has been established for the Scotian Slope from St. Pierre Bank in the northeast to Northeast Fan in the southwest. The stratigraphy is based on high-resolution Huntec data and low-resolution airgun data. Other seismic stratigraphic approaches with a more local scope have been integrated into the stratigraphic framework. This enabled to not only understand better the timing of mass transport failures and resulting deposits (MTDs) but also to see how different types of MTDs vary temporally and spatially along the margin. On the Scotian slope, slope sedimentation is highly governed by the shelf ice sheet dynamics; highest sedimentation rates occur, when the ice sheet was at the shelf break forming upper slope till tongues. Seawards of these more stagnant ice sheet areas, well-laminated plume sedimentation occurs, whereas in areas where the ice sheet showed higher dynamics, slope sedimentation is limited to interglacial climatic stages, when no ice sheet is present. During the ice sheet presence, different types of small and large MTDs characterize slope sedimentation. Seawards of trough mouth fans (Scotian Gulf) glacigenic debris flows indicate the direct impact of ice sheets. Major slope erosion is observable. Seawards of Northeast Channel and the Laurentian Channel slope angles are too high to form glacial fans as it is observed e.g. on the Norwegian margin. Most of the sediments are bypassing in these areas and deposition occurs only on the lower rise and abyssal plain where highest sedimentation rates since MIS 12 in the slope system are oberved.

The key results from the Scotian Slope are:

I. Ice sheets terminating at the shelf break have a major impact on slope dynamics and sedimentation: thus during glaciations when ice did not reach the margin (e.g. in marine isotope stage 4), slope sedimentation is characterized by plume sedimentation and few minor MTDs. This is in contrast to glacial stages with ice at the margin (e.g. during marine isotope stage 2 and 6) when major MTDs characterize the sedimentary sequence.

II. Ice sheet processes are directly related to slope sedimentation: stagnant ice indicated by the presence of till tongues results in plume sedimentation on the slope with few turbidites and thin MTDs. Fast flowing ice offshore shelf troughs result in widespread slope failures and in areas of high slope angles in sediment bypassing the slope.
III. MTDs usually occur in similar areas along the slope: the presence of a slope failure indicates a high likeliness of a preceding failure: this enabled to classify the Scotian Slope in different MTD zones: each zone is characterized by a specific failure reoccurrence time and specific types of MTDs occur within each zone.
IV. During OIS 6, major widespread erosion affected the slope eroding 100s meters of sediment: widespread failures can be especially observed on the eastern and western Scotian Slope.
V. Long-term slope evolution results in almost complete removal of slope sequence by failure, the deposits are found on the abyssal plain (Sohm Abyssal Plain)
VI. Plume sedimentation is the most significant process for building glaciated continental slopes
VII. Slope sedimentation is greatly reduced when ice was not present in the region, e.g. during the early Quaternary, and deposition occurs mostly on the slope and upper rise

7.2. Northern Argentine and Uruguay Slope

The northern Argentine and Uruguay slope is characterized by different alongslope processes (e.g. contourites and benthic storm events) and downslope processes (e.g. debris flows and turbidite deposits). Slope sedimentation changes significantly at ~37°S when the Ewing Terrace terminates and the slope to the north shows no terraces. This significant change is directly related to the influx of fluvial sediment and to a lesser extent (but possibly dominating in the Holocene) the oceanic circulation. To the south of this boundary, slope sedimentation is characterized by the interaction of alongslope processes in the form of contourite drifts and rare shelf export during storm events. A more detailed study on the northernmost part of the Ewing Terrace (Chapter 6) suggests that the Antarctic sourced ocean currents may at times be sediment-starved. During rare times of sediment export from the shelf to the terrace, coarse material may be supplied building coarser grained contourite deposits on this part of the Ewing Terrace.

The key results from the northern Argentine and Uruguay Slope are:

I. Slope sedimentation is driven by the oceanographic setting (mainly by the presence of the Brazil Malvinas Confluence), at times of rare storm events shelf sediment export may occur supplying sandier sediments to the terrace.
II. Along- and downslope driven processes are shaping the margin currently, during glacial more shelf-sourced sediment has reached the upper slope compared to the interglacial setting (Holocene).
III. Preliminary work on the Uruguay continental slope may suggest that during glacial times the fluvial discharge from the La Plata Rivers may have a much greater impact on slope depositional processes compared to Holocene times.
IV. The northern Ewing Terrace is likely a sediment-starved area characterized by rare Pleistocene wave supported gravity flows and muddy or sandy contourite deposits related to sediment availability.

7.3. General results of study considering both continental slope systems

The key results from both slopes are:

1. Slope seabed classification, based on slope morphology and dominant sedimentation processes and their deposits, is a very valuable tool to understand process interaction within a slope system and to get an idea of process variability on very different slopes over short and long time spans.
2. Slope systems are independent of their latitude, and thus climatic history, highly influenced by processes acting on the shelf and thereby at the shelf break.
3. Ice sheets have a major impact on styles of slope sedimentation by eroding enormous volumes of sediment over several glacial cycles: therefore, not only are sedimentation rates higher on glacial margins, but also rates of erosion are significantly larger.
4. The processes acting on glaciated and non-glaciated margins are very similar: mass wasting and other downslope-driven processes occur in both slope systems more frequent during glacial stages with ice sheet build-up at the earth’s poles. However, the volumes and affected areas are significantly higher in glaciated slope systems where the ice sheet has a direct influence on sedimentation, whereas slopes where ice sheets did not terminate at the shelf break show lower erosion rates and deposition.
5. During sea level lowstands, sedimentation patterns change greatly on continental margins and outer shelf processes can easily affect upper slope sedimentation.

6. During interglacial periods, shelves act as sediment traps: in glacial stages with a seaward migration of the coastline due to continental ice sheet build-up more dynamic sediment-processes affect slope deposition by supplying vast amounts of sediment to the shelf break.
7. Oceanic circulation has a significant impact on the styles of (Quaternary) sedimentation, nevertheless downslope driven processes are always present. Upper slope sands should not be prematurely linked to contourite deposition: in complex slope systems, multi-proxy datasets need consideration before interpreting datasets and arriving at conclusion (e.g. the identification of depositional modes of mid-slope sand beds may require detailed analyses).
8. Slope sediment budgets can only be achieved when sedimentation processes on the abyssal plains of margins are included, because frequently most of the sediment is transported and deposited in these areas. Consider the observed shift of depositional centers on Scotian Slope from the Early Quaternary (lower slope) to the Late Quaternary (Sohm Abyssal Plain).

7.4. Future perspectives and needed work

A. More work is needed on the upper Argentine Slope to understand if the recognized shelf sediment export can also be recorded in cores from other areas along this margin. Possible methodical approaches may include detailed analyses of outer shelf and upper slope sediments in stratigraphically long sediment cores. Required and most useful datasets include detailed cm-scale resolution grain size data, neodymium isotopes to evaluate and define source areas for the sand beds and possibly the laminated muds. Furthermore, to give the slope a geological and seismo-stratigraphic framework, high resolution acoustic data and possibly extensive multibeam coverage will be needed to compare slope failures and modes of deposition regionally.
B. On the Argentine and Uruguay Margin, a regional seismic stratigraphy needs to be established for the whole study area to link the timing of different along- and downslope driven processes along the margin to each other and to understand the true nature of the observed change in sedimentation at ~37°S, especially at times when the oceanic circulation differed greatly from today's (e.g. last glacial). Detailed sediment transport studies, including possibly seabed monitoring at the shelf break, will be needed to decipher the Argentine Slope contourite system and its interaction with downslope driven processes as well as its fate northwards offshore Uruguay.

C. On the Scotian Slope, a link of the new regional slope seismic stratigraphy to the shelf area would improve greatly the timing of shelf processes and to understand processes of sediment transport across the shelf break: this would similarly be needed on the Argentine margin once the driving slope processes have been identified in more detail. On the Scotian Slope, such shelf to slope correlation may either be based on direct traces using Airgun and Huntec seismic data, or, when the geological setting prevents direct tracing, e.g. due to till tongues, jump-correlations based on seismic character or age control in cores may be needed to cross this critical interface.
D. More general, the styles and timing of sedimentation close to the shelf break and on the upper slope need to be evaluated at much higher spatial resolution. A new effort to link shelf and slope depositional modes together needs to be made. Very few research studies have addressed the question concerning how shelf and slope processes interact raising the possibility that some shelf break crossing processes may have been underestimated.

Acknowledgements

I would like to thank my supervisor in Canada, David Piper, for his endless wisdom and especially patience with looking at my drafts over and over again. I want to equally thank my German supervisor, Rüdiger Henrich, for making it possible to come to Bremen and work on the Argentine Slope, Additionally, you helped me not only to understand the Argentine Slope system but also to get used to the German way of research, where I sometimes had my troubles understanding how things work over here in “old Europe”, as most of my other research career was spent overseas.
An enormous thank you also to Ned King from GSCA, who was always there for me, when something went wrong again. This includes not only things in the lab or during writing but also more in general anything related to frustrations linked to PhD work – and everyone has those once a while. Also great thanks to Gordon Cameron from GSCA who was always challenging my research ideas and asked the tough Qs. You, Gordon and Ned helped me greatly to keep my research on track and not to drift into ‘geo-poetry’: it may have saved me from trouble a few times. Thanks!!!!
Additionally, I would like to thank Till Hanebuth for fruitful discussions on processes affecting sedimentation on the Argentine and Uruguayan Slope, and to prepare me for several conference talks by taking time looking at presentations and playing advocates devil. Thanks so much!
Similarly, I would like to thank Cristiano Chiessi for helping me approach the Argentine Margin from the oceanographic and climatic point of view and ensuring that I do finally understand ocean circulation down there: thanks so much!
I would also like to thank all members of the two research groups where I was based out of: GSCA and sedimentology group in Bremen. A special thanks goes to Owen Brown (GSCA) for running grain size data and to Susan Lemerchant (GSCA) and Claudia Currie (GSCA) for pulling out 1000s of line-km of seismic data and digitizing it all. I would also like to thank Helga Heilmann and Brit Kockisch (both Uni Bremen) to help me get my research done in the labs here at school.
Great thanks also to the entire M78/3a cruise participants and boat crew, especially Sebastian Krastel, who co-wrote my unforeseen proposal for Bremen, making it also possible for me to go to Bremen.
Finally I would like to thank the entire GSCA and Marum staff and my Marum lunch group who supported me morally throughout my PhD time. This was an awesome 3 years, where I met a whole lot of interesting new people, some of who have become close friends by now and who I will have contact to my entire life. This project has been funded by NSERC and a MARUM Unforeseen Proposal. Thank you for making this project possible and for being part of my academic career!
At last I would like to also thank my wife and family for moral support getting this work done!

N a m e : Tammo Jan Huppertz Datum 27. 4. 2011

Anschrift : Carl-Friedrich Gauss Strasse 8, 28357 Bremen

E r k l ä r u n g

Hiermit versichere ich, dass ich

1. die Arbeit ohne unerlaubte fremde Hilfe angefertigt habe,

2. keine anderen als die von mir angegebenen Quellen und Hilfsmittel benutzt habe und

3. die den benutzten Werken wörtlich oder inhaltlich entnommenen Stellen als solche kenntlich gemacht habe.

Bremen , den 27. 4. 2011 .

(Unterschrift)

Dieses ist die überarbeitete Version gemäß den Auflagen der Prüfungskommission, erstellt im Dezember 2011, in der alle benötigten Korrekturen angewendet wurden.